Imperial College London

Assessing Disease Activity in Multiple Sclerosis:

Biomarkers and Clinical Measures

Dr Joel Benjamin Raffel

A thesis submitted for the degree of
Doctor of Philosophy

Division of Brain Sciences

Faculty of Medicine

Imperial College London

December 2019

ACKNOWLEDGMENTS

Foremost, I would like to thank the individuals who volunteered to take part in these research studies, without whom this work would not be possible. Thank you for all your time, patience, and generosity.

I would also like to express my sincere gratitude to Fast Forward LLC (National Multiple Sclerosis Society), GE Healthcare Ltd, and the Multiple Sclerosis Trials Collaboration for providing me with funding to carry out this work.

My primary supervisor Professor Richard Nicholas gave me continuous support throughout my clinical fellowship. His enthusiasm, guidance, creativity and knowledge were a constant source of inspiration and motivation. He was always available to talk and made me feel very welcome as part of the Imperial MS Team. Thank you very much Richard!

Thank you also to all those who have made scientific contributions to the studies reported in this thesis, especially Sujata Sridharan, James Cole, Arie Gafson, Alison Wallace, Olga Ciccarelli, and Tim Friede. Individual contributions to each study are detailed in Chapters 2-5.

Finally, to Elsa, Louis, and Maya – thank you for bringing me joy on a daily basis! This thesis is dedicated to you.

DECLARATION OF ORIGINALITY

Scientific contributions of colleagues and collaborators are acknowledged in each results chapter. The work of others is appropriately referenced. All other work in this thesis is my own and conforms to the rules and guidelines set out for PhD theses by Imperial College London.

COPYRIGHT DECLARATION

The copyright of this thesis rests with the author. Unless otherwise indicated, its contents are licensed under a Creative Commons Attribution - Non-Commercial 4.0 International Licence (CC BY-NC).

Under this licence, you may copy and redistribute the material in any medium or format. You may also create and distribute modified versions of the work. This is on the condition that: you credit the author and do not use it, or any derivative works, for a commercial purpose.

When reusing or sharing this work, ensure you make the licence terms clear to others by naming the licence and linking to the licence text. Where a work has been adapted, you should indicate that the work has been changed and describe those changes.

Please seek permission from the copyright holder for uses of this work that are not included in this licence or permitted under UK Copyright Law.

ABSTRACT

Background: Multiple sclerosis (MS) is the commonest cause of non-traumatic neurological disability in young adults. Disease-modifying therapies are available which vary in their overall efficacy and safety profiles, with the most effective treatments reserved for those with the most active disease. People with MS (PwMS) who show lack of response to initial treatment may also switch to more effective treatments.

Outcome measures are required in MS, for example to inform clinical decisions regarding initiation and switching of disease-modifying therapies. Outcome measures are required both to guide decision-making at an individual level, and to test research questions in large cohorts at a group level.

Objectives:

i) To evaluate whether relapses or MRI activity after starting the disease-modifying therapy natalizumab predict long-term disability progression.

ii) To investigate 18 kDa translocator protein (TSPO) positron emission tomography (PET) with the novel ligand ^{18}F-GE180 as a marker for neuroinflammation, to assess disease activity in MS and response to natalizumab treatment.

iii) To investigate whether the machine-learning model 'Brain Predicted Age', which estimates chronological age based upon T1-weighted brain MRIs, can assess disease severity in MS.

iv) To assess the prognostic value of the patient reported outcome 'Multiple Sclerosis Impact Scale–29' (MSIS-29) on hard clinical endpoints including 'survival time' in people with MS.

Methods:

i) Observational cohort of 161 PwMS initiating natalizumab, with up to 7 years of follow-up.

ii) Cohort of 16 PwMS starting natalizumab, with ^{18}F-GE180 PET at baseline, 10 weeks after, and 58 weeks after treatment initiation. 11 healthy controls (HCs) had one ^{18}F-GE180 PET scan. In addition, a 'blocking study' investigated whether ^{18}F-GE180 PET is labelling TSPO: 6 PwMS had a baseline ^{18}F-GE180 PET followed by repeat PET after administration of the TSPO ligand XBD-173.

iii) Observational cohort of 541 subjects with clinically isolated syndrome, MS or HCs, with 1,652 T1-weighted MRI scans and up to 15 years follow-up.

iv) Observational cohort of 2,126 PwMS that completed the MSIS-29 questionnaires, with up to 10 years of follow-up.

Results:

i) Relapses and MRI activity after natalizumab initiation predicted disability progression at years 1 and 2. However, this effect disappeared with longer follow-up. Instead there was a paradoxical trend towards inflammatory activity on treatment predicting a lower risk of disability progression.

ii) ^{18}F-GE180 had lower extraction over the blood-brain barrier than expected from preclinical studies, although did show some specific binding. ^{18}F-GE180 signal was increased in MS lesions, and decreased after natalizumab treatment. ^{18}F-GE180 signal was not increased in other regions of interest.

iii) Brain Predicted Age was substantially greater than chronological age in all disease subgroups. Brain Predicted Age correlated with disease characteristics and predicted future disability progression. Longitudinal

change in Brain Predicted Age increased at a rate ~46% faster in subjects with MS than in HCs. The model compared favourably with conventional univariate measures of brain atrophy.

iv) 264 PwMS died over the follow-up period. Higher MSIS-29 physical and psychological scores predicted reduced survival time, independently of other risk factors.

Conclusions: **i)** While relapses and MRI activity remain useful markers of disease activity, there is a need for additional outcome measures which can predict long-term disability progression in PwMS on disease-modifying therapy.

ii) ^{18}F-GE180 has low brain extraction (~1%) and poor signal-to-noise ratio. Results should be interpreted with caution, given the unexpected pharmacokinetic characteristics of the tracer.

iii) The Brain Predicted Age model could provide conceptually simple and clinically meaningful quantitative data in MS from a standard T1-weighted MRI scan, and will be further evaluated using the MAGNIMS multi-centre cohort.

iv) MSIS-29 scores can be prognostic for hard clinical endpoints in MS. This is the first study to associate PROs with survival in any neurological disease. PROs are cheap and easy to administer, and could allow the collection of clinically meaningful outcome data in large MS cohorts.

CV AND LIST OF PUBLICATIONS

Name: Joel Benjamin Raffel
GMC No: 7040692
Qualifications: BM BCh, BA, MRCP

EDUCATION AND QUALIFICATIONS:

MRCP, 2012.

- **Part 2 PACES –** Sitting 2012/03
- **Part 2 Written –**Sitting 2011/02
- **Part 1 –** Sitting 2010/03

Clinical Medicine, Green College, Oxford University, 2006-2009

- '**Distinction'** for academic performance throughout clinical school.
- '**Merit'** in Final Year BM BCh exam, and **nomination** for George Pickering Prize (award given to single top student; top 12 students of the year received a nomination).
- Other awards during clinical school: Psychiatry exam - **top mark** in year; Neurology written exam - **2nd top mark** in year; Emergency, Orthopaedics and Musculoskeletal Medicine exam – **merit**; Year 4 OSCE – **merit**; Laboratory medicine – **merit**. ***Proxime accessit*** in Hobson Mann scholarship for academic performance throughout 4th year (scholarship awarded to the top six students).

Pre-Clinical Medicine, St. Anne's College, Oxford University, 2003-2006

- **1st class honours** - BA in Medical Sciences, specialising in neuroscience. Dissertation on the 'Role of the NR2B subunit for the induction of LTP in GluRA-/- mice' also received **1st class honours**. Awarded **scholarship** for outstanding academic achievement at St Anne's College, Oxford.
- **'Merit'** in 'the nervous system' examination - **top mark** of the year.

CAREER HISTORY:

2018 – Present:	**Medical Assessor; Licensing Division; Medicines and Healthcare products Regulatory Agency, UK.** Responsible for assessment of marketing authorisation applications for new and generic medicinal products proposed for the UK or EU market. Responsible primarily for medicinal products in areas of neurology and psychiatry. Also provide scientific advice to applicants, relating to clinical trial design and regulatory requirements.
2014-2018:	**Clinical Research Fellow, Imperial College London**. Investigated clinical, radiological, and patient-reported outcomes in multiple sclerosis, using several different study designs and cohorts.
2011-2013:	**ST1-ST2,** Imperial College Healthcare NHS Trust. NIHR Academic Clinical Fellowship Scheme.
6 months	Clinical neurology, Charing Cross Hospital
6 months	Academic neurology, Multiple sclerosis research group, under supervision of Professor Richard Reynolds and Dr Richard Nicholas
6 months	Cardiology, Hammersmith Hospital
6 months	Acute Medicine, and A&E, Hammersmith Hospital
2010-2011	**FY2**, Royal London Hospital, London. NIHR Academic FY2 Scheme
2 months	Clinical psychiatry. On acute stroke thrombolysis rota.
6 months	Academic and clinical neurology, under supervision of Professor Gavin Giovannoni. On acute stroke thrombolysis rota.
4 months	Medical Assessment Unit, and A&E

2009-2010	**FY1,** Whittington Hospital, Archway, London.	
4 months	General Surgery	
2 months	Acute Medicine	
2 months	Care of Older Patients / General Medicine	
4 months	Cardiology	

RESEARCH UNDERTAKEN DURING CLINICAL FELLOWSHIP:

Main research projects undertaken as a clinical research fellow and described in this thesis:

- Completed observational study on clinical markers of response to treatment (relapses, new MRI lesions, worsening disability), and correlation with disability progression in MS, using long-term real-world data. Published in *PLOS One*. (**Chapter 2**).
- Acquisition and analysis of translocation protein positron emission tomography (TSPO-PET) before and after treatment in multiple sclerosis (MS). Papers published in *Molecular Imaging and Biology* and *European Journal of Nuclear Medicine and Molecular Imaging*. (**Chapter 3**).
- Investigated a novel machine-learning model for quantifying 'brain age' based upon T1 MRI, and its performance as an outcome measure in MS. Granted access to large multicentre *MAGNIMS* imaging datasets, results of which have been submitted for publication. (**Chapter 4**).
- Investigation of patient-reported outcomes (PROs) and their role in predicting hard clinical outcomes such as 10-year mortality. First study to show that PROs can help predict survival time in neurological disease. Published in *PLOS Medicine* (Impact Factor 13.5). (**Chapter 5**).

Other projects, not within the remit of this thesis, undertaken during clinical research fellowship:

- Completed study on longitudinal changes in anti-JC virus antibody titres after natalizumab treatment in MS, and the implications for managing the risk of progressive multifocal leukoencephalopathy. Published with editorial comment, *Multiple Sclerosis Journal*.
- Completed a commentary article regarding the efficacy of dalfampridine on walking speed as reported in randomised controlled trials, and how this translates to assessing drug efficacy in individual patients in the working neurology clinic. Published in *Multiple Sclerosis Journal*.
- Contributed to design and implementation of custom-made software platform for collection of both clinical and patient-centred data in MS, as part of OPTIMISE consortium. Vision is for a clinical registry to store, curate, and analyse data for research purposes (for example comparative clinical efficacy data), with patient-facing and clinician-facing interfaces to enhance the clinical consultation.
- Contributed to systematic review of therapies evaluated in secondary progressive MS. Published in *Drugs* journal.
- Performed meta-analysis of randomised controlled trials in primary progressive and secondary progressive MS, following Cochrane guidelines. Focusing on change in placebo cohorts over time, and relevance to comparative clinical efficacy studies. Published in *Multiple Sclerosis Journal*.
- Acquisition and analysis of other innovative imaging modalities as markers of treatment response, including arterial spin labelling (ASL) and magnetic resonance spectroscopy (MRS).
- Supervised MPhil student investigating computerised tests of cognitive impairment to be used longitudinally from home environment.
- Supervised medical student investigating association between deprivation in childhood and severity of MS in later life.
- Supervised medical student conducting research into cause of death in MS and pathways for palliative care. Published in *PLOS One*.
- Created resource at Imperial College NHS Trust whereby cerebrospinal fluid samples collected for clinical reasons are also processed and stored in research facility for future research.

PUBLICATIONS:

1) Sridharan S*, **Raffel J***, Nandoskar A, Record C, Brooks DJ, Owen D, Sharp D, Muraro PA, Gunn R, Nicholas R. Confirmation of specific binding of the 18-kDa Translocator Protein (TSPO) radioligand [18F]GE-180: a blocking study using XBD173 in multiple sclerosis normal appearing white and grey matter. *Mol Imaging Biol.* 2019;21(5):935-944

   (*joint first authors)

2) Nicholas RS, Han E, **Raffel J**, Chataway J, Friede T. Over three decades study populations in progressive multiple sclerosis have become older and more disabled, but have lower on-trial progression rates: A systematic review and meta-analysis of 43 randomised placebo-controlled trials. *Multiple Sclerosis Journal.* 2019;25(11):1462-1471.

3) **Raffel J**, Wallace A, Gveric D, Reynolds R, Friede T, Nicholas R. Patient-reported outcomes and survival in multiple sclerosis: A 10-year retrospective cohort study using the Multiple Sclerosis Impact Scale-29. *PLOS Medicine* (Impact Factor 13.5). 2017;14(7):e1002346.

4) Kamourieh S, Gananandan K, **Raffel J**, Nicholas R. Natalizumab Granule Cell Neuronopathy: FDG-PET in diagnosis and immune reconstitution with G-CSF. *Neuroimmunology and Neuroinflammation*. 2017;4(5):e384.

5) Puentes F, van der Star B, Lidster K, Boomkamp S, Kipp M, Boon L, Bosca I, **Raffel J**, Gnanapavan S, van der Valk P, Barnett SC, Baker D, Amor S. Neurofilament Light as an immune target for pathogenic antibodies. *Immunology*. 2017;152(4):580-588.

6) Nandoskar A, **Raffel J**, Scalfari AS, Friede T, Nicholas RS. Pharmacological approaches to the management of secondary progressive multiple sclerosis. *Drugs*. 2017;77(8):885-910. Review.

7) **Raffel J**, Sridharan S, Nicholas R. [11C]PBR28 PET in multiple sclerosis: neuroinflammation or otherwise? *Annals of Neurology.* 2017;81:323-324.

8) **Raffel J**, Gafson AR, Dahdaleh S, Malik O, Jones B, Nicholas R. Inflammatory activity on natalizumab predicts short-term but not long-term disability in multiple sclerosis. *PLOS One*. 2017;12(1):e0169546.

9) **Raffel J**, Wakerley B, Nicholas R. Multiple sclerosis. *Medicine*. 2016; 44(9):537–541

10) Martin J*, **Raffel J***, Nicholas R. Progressive dwindling in multiple sclerosis: An opportunity to improve care. *PLOS One.* 2016;11(7):e0159210

    (*joint first authors)

11) Feeney C, Scott G, **Raffel J**, Roberts S, Coello C, Jolly A, Searle G, Goldstone AP, Brooks DJ, Nicholas RS, Trigg W, Gunn RN, Sharp DJ. Kinetic analysis of the translocator protein positron emission tomography ligand [18F]GE-180 in the human brain. *Eur J Nucl Med Mol Imaging.* 2016;43(12):2201-2210.

12) **Raffel J**, Gafson AR; Malik O; Nicholas R. Anti-JC virus antibody titres increase over time with natalizumab treatment. *Multiple Sclerosis Journal.* 2015;21(14):1833-8.

13) Amor S, van der Star BJ, Bosca I, **Raffel J**, Gnanapavan S, Watchorn J, Kuhle J, Giovannoni G, Baker D, Malaspina A, Puentes F. Neurofilament light antibodies in serum reflect response to natalizumab treatment in multiple sclerosis. *Multiple Sclerosis Journal.* 2014;20(10):1355-62

14) **Raffel J**, Dobson R, Gafson A, Mattoscio M, Muraro P, Giovannoni G. Multiple sclerosis therapy and Epstein-Barr virus antibody titres. *Mult Scler Relat Disord*. 2014;3:372-4

15) Stansfeld S, Dinos S, **Raffel J.** Environmental influences: the workplace and mental health – models, vulnerability factors, and interventions. In: Sloboda Z, Petras H. (eds.) *Defining Prevention Science.* New York, USA: Springer; 2014. p. 219-250. ISBN 978-1-4899-7424-2

16) **Raffel JB**, Malik O, Nicholas R. Assessing dalfampridine efficacy in the physician's office. *Multiple Sclerosis Journal*. 2014;20(1):24-6

17) **Raffel JB**, Thompson J. Carbon monoxide from domestic coffee roasting. *Annals of Internal Medicine.* 2013 159(11):795-6.

18) **Raffel JB**, Hunt D, Topping J, Bremner J, Brown K, Giovannoni G. Assay selection affects John Cunningham virus serostatus classification in multiple sclerosis. *Annals of Neurology*. 2012;72(2):295-6

19) Sharrief AZ, **Raffel J**, Zee DS. Vitamin B12 deficiency with bilateral globus pallidus abnormalities. *Arch Neurol.* 2012;69(6):769-772.

20) **Raffel JB**, Al-Lawati A, Murch N. Rash and dyspnoea in a 39 year old man. *BMJ*. 2011;29:343.

21) Romberg C, **Raffel J**, Martin L, Sprengel R, Seeburg PH, Rawlins JN, Bannerman DM, Paulsen O. Induction and expression of GluA1 (GluRA)-independent LTP in the hippocampus. *Eur J Neurosci*. 2009;29(6):1141-52.

CONFERENCE ABSTRACTS:

First author

1) **Raffel J**, Cole J, Record C, Sridharan S, Sharp D, Nicholas R. Brain Age: A novel approach to quantify the impact of multiple sclerosis on the brain. American Academy of Neurology annual meeting, Boston, April 2017.

2) **Raffel J**, Gafson A, Malik O, Nicholas R. Longitudinal anti-JCV antibody titres increase with natalizumab treatment. ECTRIMS annual conference. Barcelona, Spain. October, 2015.

3) **Raffel J**, Gafson A, Dahdaleh S, Malik O, Nicholas R. Post-natalizumab relapses and MRI activity do not predict long-term disability outcomes. ECTRIMS annual conference. Barcelona, Spain. October, 2015.

4) **Raffel J**, Gafson A, Malik O, Nicholas R. Anti-JCV titres increase over time with natalizumab treatment natalizumab. Association of British Neurologists. Harrogate, UK. May, 2015.

5) **Raffel J**, Gafson A, Dahdaleh S, Malik O, Nicholas R. Early prediction of long-term response to natalizumab in multiple sclerosis. Association of British Neurologists. Harrogate, UK. May, 2015.

6) **Raffel J**, Nicholas R, Roncaroli F, Reynolds R. Astrocytes upregulate interleukin-17 receptor expression in white matter lesions in multiple sclerosis. Joint ACTRIMS / ECTRIMS meeting. Boston, USA. September 2014.

7) **Raffel JB**, Guo YK, Matthews PM. OPTIMISE: A vision for personalised medicine in multiple sclerosis. Launch of Data Science Institute by Imperial College London and Huawei Technologies Co. April 2014.

8) **Raffel JB**, Hunt D, Topping J, Bremner J, Brown K, Giovannoni G. Classification of JC virus serostatus depends upon assay selection: a comparison of Biogen and HPA assays. Association of British Neurologists. Brighton, UK. May, 2012.

9) **Raffel J**, Dobson R, Giovannoni G. The effect of natalizumab and beta interferon on urinary free light chains and anti-EBV nuclear antigen-1 antibodies in relapsing remitting multiple sclerosis. Association of British Neurologists. Newcastle, UK. October 2011.

10) **Raffel J**, Romberg C, Rawlins N, Paulsen O. 'Memories are made of this? The role of NMDA receptors in the induction of long-term potentiation (LTP) in wildtype and GluRA knockout mice.' Prize-winning poster presentation. Meeting for Clinician Scientists in Training, Medical Research Society, Royal College of Physicians, London. February 2011.

11) **Raffel J**. When the picture doesn't fit – Psychogenic non-epileptiform seizures on the background of domestic abuse in pregnancy. *The Royal College of Obstetricians and Gynaecologists* National Medical Students and Young Doctors Evening. Jan 2010.

'Senior' author

12) Record C, De Simoni S, Feeney C, Sharp D, Nicholas R, **Raffel J**. Improved cerebral blood flow after natalizumab treatment in multiple sclerosis. ECTRIMS annual conference. London, UK. October, 2016.

13) Peress L, Ribeiro Violante I, Scott G, Zimmerman K, Sharp D, Nicholas R, **Raffel J**. Thalamic magnetic resonance spectroscopy in highly active multiple sclerosis. ECTRIMS annual conference. London, UK. October, 2016.

14) Connell L, Daws R, Hampshire A, Nicholas R, **Raffel J**. Validating a participant-led computerised cognitive battery in people with multiple sclerosis. ECTRIMS annual conference. London, UK. October, 2016.

15) Sridharan S, Hinz R, Trigg W, Buckley C, Brooks D, Nicholas R, **Raffel J**. Kinetic analysis of brain TSPO-PET data using [18F]GE-180 in relapsing-remitting multiple sclerosis patients pre and post-treatment. NRM conference, Boston, 2016.

Other

16) Mallas E, Simoni S, Scott G, Zentar M, Jolly A, Li L, Ross E, Zimmerman K, Feeney C, **Raffel J**, Roberts S, Gorgoraptis N, Sharp DJ. Abnormal activation of the dorsal attentional network in memory impairment after traumatic brain injury. Organization for Human Brain Mapping, Vancouver, Canada. June 2017.

17) Yong M, Yang L, **Raffel J**, Craner M, Hemmingway C, Giovanonni G, Overell J, Hyde R, van Beek J, Thomas F, Guo Y, Matthews P. OPTIMISE: User-guided solutions for harmonized clinical and patient-centred data capture. ECTRIMS annual conference. London, UK. October, 2016.

18) Mitchell B, **Raffel J**, Nicholas R. Increasing area level deprivation in England impacts age of progression and wheelchair use in multiple sclerosis. ECTRIMS annual conference. London, UK. October, 2016.

19) Wallace A, **Raffel J**, Reynolds R, Friede T, Nicholas R. Increased multiple sclerosis impact scale-29 score is associated with reduced survival in multiple sclerosis. ECTRIMS annual conference. London, UK. October, 2016.

20) Yong M, Yang L, **Raffel J**, Craner M, Hemingway C, Giovanonni G, Overell J, Hyde R, van Beek J, Thomas F, Guo Y, Matthews PM. OPTIMISE – A web-based solution for recording and analyzing longitudinal multiple sclerosis data. AAN annual conference, Vancouver, 2016.

21) Yong M, He S, **Raffel J**, Oehmichien A, Guitton F, Emam I, Pandis I, Guo Y, Matthews P. Standing on the Shoulders of Giants: A plugin to provide medical imaging support for tranSMART. 2015 tranSMART Foundation Annual Meeting – Amsterdam.

22) Nicholas R, **Raffel J**, Malik O. Progressive multifocal leukoencephalopathy presenting with posterior fossa radiological features in the context of natalizumab therapy in relapsing-remitting multiple sclerosis. . ECTRIMS annual conference. Barcelona, Spain. October, 2015.

23) Feeney C, Scott G, **Raffel J**, Coello C, Searle G, Gunn R, Sharp D. Kinetic analysis of the translocator protein positron emission tomography ligand 18[F]-GE180 in the human brain. Society for Neuroscience Annual Meeting. Chicago, USA. October 2015.

ACADEMIC TEACHING:

2014-2017 Primary supervisor for medical students undertaking 10-week BSc projects, on five occasions over this period.

2016-2017 Supervised MPhil student, investigating computerised tests of cognitive impairment in MS, to be used longitudinally from home environment.

2015 Supervised Masters student for 8-week internship on immunohistochemistry project.

OTHER RELEVANT EXPERIENCE:

2010-2017 Listed as sub-investigator on 8 commercial CTIMP studies, with responsibilities for participant consent, first-dose administration, blinded assessment, and sign-off of clinical records.

2014-2017 Peer review of articles for journals *Expert Opinion on Drug Metabolism and Toxicology*, and *European Journal of Neurology*.

ABBREVIATIONS

ANOVA	One-way analysis of variance
Brain-PAD	Brain Predicted Age Difference
BVMT-R	Brief Visuospatial Memory Test - Revised
CI	Confidence intervals
CIS	Clinically isolated syndrome
CVLT-II	California Verbal Learning Test II
Df	Degrees of freedom
DMT	Disease-modifying therapy
EDSS	Expanded Disability Status Scale
GM	Grey matter
HAB	High affinity binders
HC	Healthy controls
HR	Hazard ratio
LAB	Low affinity binders
MAB	Mixed affinity binders
MS	Multiple sclerosis
MSIS-29	Multiple Sclerosis Impact Scale–29
MSIS-29-PHYS	MSIS-29 physical
MSIS-29-PSYCH	MSIS-29 psychological
MSSTB	MS Society Tissue Bank
NAWM	Normal-appearing white matter
NS	Not statistically significant.
OR	Odds ratio

PET	Positron emission tomography
PPMS	Primary progressive multiple sclerosis
prEDSS	Patient-reported Expanded Disability Status Scale
PRO	Patient-reported outcome
PwMS	People with multiple sclerosis
RRMS	Relapsing-remitting multiple sclerosis
SD	Standard deviation
SDMT	Symbol Digit Modalities Test
SPMS	Secondary progressive multiple sclerosis
TSPO	18 kDa translocator protein
UCL	University College London
V_{ND}	Non-displaceable distribution volume
V_S	Specific distribution volume
V_T	Volume of distribution
WM	White matter

TABLE OF CONTENTS

TITLE PAGE ..... **- 1 -**
ACKNOWLEDGMENTS ..... **- 2 -**
DECLARATION OF ORIGINALITY ..... **- 3 -**
COPYRIGHT DECLARATION ..... **- 3 -**
ABSTRACT ..... **- 4 -**
CV AND LIST OF PUBLICATIONS ..... **- 7 -**
ABBREVIATIONS ..... **- 12 -**
TABLE OF CONTENTS ..... **- 14 -**
LIST OF TABLES ..... **- 20 -**
LIST OF FIGURES ..... **- 21 -**

CHAPTER 1 - INTRODUCTION ..... **- 23 -**
I.1 ABBREVIATIONS ..... - 24 -
I.2 BACKGROUND ..... - 25 -
I.2.1 The burden of multiple sclerosis ..... - 25 -
I.2.2 Disease course in MS ..... - 25 -
I.2.3 The pathophysiology of MS ..... - 26 -
I.2.4 Disease-modifying therapy in MS ..... - 28 -
I.2.5 Personalised medicine in MS ..... - 29 -
I.2.6 Outcome measures for personalised medicine in MS ..... - 30 -
I.3 THESIS OVERVIEW ..... - 31 -
I.3.1 Chapter 2 - Relapses and MRI Activity on Natalizumab Predict Short-term but not Long-term Disability Progression ..... - 32 -
I.3.2 Chapter 3 - 18 kDa Translocator Protein Radioligand ^{18}F-GE180 as a Marker of Neuroinflammatory Activity in Multiple Sclerosis ..... - 34 -
I.3.3 Chapter 4 - Brain Predicted Age in Multiple Sclerosis: A Model using Machine Learning Analysis of MRI ..... - 36 -
I.3.4 Chapter 5 - Patient-Reported Outcomes can Predict Survival Time in Multiple Sclerosis: A Cohort Study using the Multiple Sclerosis Impact Scale–29 ..... - 38 -
I.4 REFERENCES ..... - 41 -

CHAPTER 2: RELAPSES AND MRI ACTIVITY ON NATALIZUMAB PREDICT SHORT-TERM BUT NOT LONG-TERM DISABILITY PROGRESSION ..... **- 49 -**

II.1 ABSTRACT ..... - 50 -
II.2 ABBREVIATIONS ..... - 52 -
II.3 INTRODUCTION ..... - 53 -
II.4 METHODOLOGY ..... - 54 -
II.4.1 Data collection ..... - 54 -
II.4.2 Early markers of inflammatory disease activity ..... - 55 -
II.4.3 Disease progression ..... - 56 -
II.4.4 Statistical analysis ..... - 56 -
II.4.5 Contribution to work ..... - 57 -
II.5 RESULTS ..... - 57 -
II.5.1 Study population ..... - 57 -
II.5.2 Markers of inflammatory disease do not affect disability progression ..... - 60 -
II.5.3 Modified Rio Score predicts short-term but not medium-term disability progression ..... - 61 -
II.5.4 Relapses and MRI activity predict short-term but not medium-term disability progression ..... - 64 -
II.5.5 Results are not affected by change in medication, baseline disability, or neutralising antibodies ..... - 66 -
II.5.6 Relapses in the first year of treatment with natalizumab predict further relapses ... - 67 -
II.6 DISCUSSION ..... - 67 -
II.7 ACKNOWLEDGEMENTS ..... - 71 -
II.8 CONFLICTS OF INTEREST ..... - 71 -
II.9 REFERENCES ..... - 72 -

CHAPTER 3: 18 KDA TRANSLOCATOR PROTEIN RADIOLIGAND 18F-GE180 AS A MARKER OF NEUROINFLAMMATORY ACTIVITY IN MULTIPLE SCLEROSIS ..... - 74 -

III.1 ABSTRACT ..... - 75 -
III.2 ABBREVIATIONS ..... - 78 -
III.3 INTRODUCTION ..... - 79 -
III.3.1 Microglia as a marker of disease activity in MS ..... - 80 -
III.3.2 TSPO PET to measure neuroinflammation in MS ..... - 81 -
III.3.3 TSPO PET for treatment efficacy in MS ..... - 82 -
III.3.4 ^{18}F-GE180: a novel TSPO PET radiotracer ..... - 83 -
III.3.5 ^{18}F-GE180 *in vivo* characteristics: necessity for an ^{18}F-GE180 'blocking study' ..... - 84 -
III.3.6 Study overview ..... - 85 -
III.4 METHODOLOGY ..... - 86 -
III.4.1 Study administration ..... - 86 -
III.4.2 Objectives ..... - 86 -
III.4.3 Study hypotheses ..... - 87 -

III.4.4 'Natalizumab cohort' overview ..... - 87 -
III.4.5 'Blocking study' overview ..... - 88 -
III.4.6 Subject recruitment ..... - 89 -
III.4.7 Inclusion and exclusion criteria ..... - 90 -
III.4.8 Sample size considerations ..... - 92 -
III.4.9 Scanning protocol ..... - 93 -
III.4.10 Arterial plasma measurement ..... - 94 -
III.4.11 Image analysis ..... - 95 -
III.4.12 Kinetic analysis ..... - 96 -
III.4.13 Calculating the non-displaceable component of V_T [blocking study] ..... - 97 -
III.4.14 Clinical outcome measures ..... - 98 -
III.4.15 Statistical analysis ..... - 99 -
III.4.16 Contribution to work ..... - 100 -
III.5 RESULTS OF KINETIC ANALYSIS OF ^{18}F-GE180 FROM HEALTHY CONTROLS ..... - 101 -
III.6 'BLOCKING STUDY' RESULTS ..... - 104 -
III.6.1 Subject characteristics ..... - 104 -
III.6.2 ^{18}F-GE180 V_T does not differ between regions of interest or between TSPO HABs and MABs ..... - 105 -
III.6.3 Visual assessment of blockade of TSPO ..... - 106 -
III.6.4 Calculation of V_{ND} suggests that ^{18}F-GE180 binds specifically to TSPO ..... - 107 -
III.6.5 Specific binding to TSPO is ubiquitous in the MS brain ..... - 109 -
III.7 'NATALIZUMAB COHORT' RESULTS ..... - 109 -
III.7.1 Study procedures ..... - 110 -
III.7.2 Subject characteristics ..... - 110 -
III.7.3 Visual inspection of ^{18}F-GE180 signal ..... - 113 -
III.7.4 ^{18}F-GE180 V_T does not differ between TSPO HABs and MABs ..... - 115 -
III.7.5 ^{18}F-GE180 V_T is increased in MS lesions at baseline ..... - 117 -
III.7.6 ^{18}F-GE180 V_T decreases after natalizumab in white matter lesions, but not in other regions of interest ..... - 118 -
III.7.7 ^{18}F-GE180 V_T increases prior to the development of new white matter lesions on MRI ..... - 120 -
III.7.8 ^{18}F-GE180 V_T does not predict response to natalizumab treatment ..... - 122 -
III.8 DISCUSSION ..... - 123 -
III.8.1 Blocking study ..... - 124 -
III.8.2 Natalizumab cohort ..... - 127 -
III.8.3 Conclusion ..... - 131 -
III.9 ACKNOWLEDGEMENTS ..... - 132 -
III.10 CONFLICTS OF INTEREST ..... - 132 -
III.11 REFERENCES ..... - 133 -

CHAPTER 4: BRAIN PREDICTED AGE IN MULTIPLE SCLEROSIS: A MODEL USING MACHINE LEARNING ANALYSIS OF MRI .... - 143 -

IV.1 ABSTRACT ..... - 144 -

IV.2 ABBREVIATIONS ..... - 146 -

IV.3 INTRODUCTION ..... - 147 -

IV.3.1 Brain ageing ..... - 148 -

IV.3.2 Quantifying brain ageing ..... - 149 -

IV.3.3 Applicability to multiple sclerosis ..... - 151 -

IV.4 METHODOLOGY ..... - 153 -

IV.4.1 Study population ..... - 153 -

IV.4.2 MRI acquisition ..... - 154 -

IV.4.3 Clinical outcomes ..... - 155 -

IV.4.4 Brain Predicted Age analysis ..... - 155 -

IV.4.5 Lesion filling ..... - 158 -

IV.4.6 Statistical analysis ..... - 159 -

IV.4.7 Contribution to work ..... - 160 -

IV.5 NATALIZUMAB COHORT RESULTS ..... - 161 -

IV.5.1 Study procedures ..... - 162 -

IV.5.2 Subject characteristics ..... - 162 -

IV.5.3 Brain-PAD is increased in subjects with MS, and correlates with radiological markers of disease severity ..... - 163 -

IV.5.4 Results consistent after lesion filling ..... - 166 -

IV.5.5 Brain-PAD decreases after natalizumab in those responding to treatment ..... - 168 -

IV.6 UCL COHORT RESULTS ..... - 169 -

IV.6.1 Study procedures ..... - 169 -

IV.6.2 Subject characteristics ..... - 170 -

IV.6.3 Brain-PAD is increased in people with MS and CIS ..... - 172 -

IV.6.4 Brain Predicted Age and Brain-PAD at baseline scan correlate with disease characteristics ..... - 173 -

IV.6.5 Baseline Brain Predicted Age and Brain-PAD are associated with risk of future disability progression ..... - 176 -

IV.6.6 Longitudinal Brain Predicted Age analysis shows ‘faster ageing’ in people with MS ..... - 177 -

IV.6.7 Brain-PAD is increased in CIS, but may normalise in those who do not develop MS ..... - 179 -

IV.7 FACTORS WHICH CONTRIBUTE TO BRAIN PREDICTED AGE ..... - 181 -

IV.7.1 MRI magnetic field has no effect on Brain-PAD ..... - 182 -

IV.7.2 ‘Filling MS lesions’ has minimal effect on Brain-PAD ..... - 183 -

IV.7.3 Brain Predicted Age is driven by a variety of known and unknown variables ..... - 184 -

IV.7.4 Brain Predicted Age is more closely associated with disability outcomes than existing univariate measures of brain atrophy ..... - 185 -
IV.8 DISCUSSION ..... - 187 -
IV.9 CONFLICTS OF INTEREST ..... - 192 -
IV.10 REFERENCES ..... - 192 -

CHAPTER 5: PATIENT-REPORTED OUTCOMES CAN PREDICT SURVIVAL TIME IN MULTIPLE SCLEROSIS: A COHORT STUDY USING THE MULTIPLE SCLEROSIS IMPACT SCALE–29 ..... - 200 -

V.1 ABSTRACT ..... - 201 -
V.2 ABBREVIATIONS ..... - 203 -
V.3 INTRODUCTION ..... - 204 -
V.3.1 Surrogates for prognosis: capturing the patient experience ..... - 204 -
V.3.2 Patient reported outcomes in other disease areas ..... - 205 -
V.3.3 The Multiple Sclerosis Impact Scale–29 ..... - 206 -
V.4 METHODOLOGY ..... - 207 -
V.4.1 Study population ..... - 207 -
V.4.2 Outcome measures ..... - 208 -
V.4.3 Statistical analysis ..... - 209 -
V.4.4 Analysis history ..... - 210 -
V.4.5 Contribution to work ..... - 211 -
V.5 NATALIZUMAB COHORT RESULTS ..... - 212 -
V.5.1 Study procedures ..... - 212 -
V.5.2 Subject characteristics ..... - 213 -
V.5.3 MSIS-29 score is increased in subjects with MS ..... - 214 -
V.5.4 MSIS-29 scores improve after natalizumab in those responding to treatment ..... - 215 -
V.6 MSSTB STUDY RESULTS ..... - 218 -
V.6.1 Study participants ..... - 218 -
V.6.2 A higher MSIS-29-PHYS score is associated with reduced survival time ..... - 220 -
V.6.3 A higher MSIS-29-PSYCH score is associated with reduced survival time ..... - 224 -
V.6.4 MSIS-29-PHYS score is correlated with prEDSS score but is independently associated with survival time ..... - 226 -
V.6.5 Increase in the MSIS-29-PHYS score over one year is associated with reduced survival time ..... - 228 -
V.7 DISCUSSION ..... - 230 -
V.8 ACKNOWLEDGEMENTS ..... - 235 -
V.9 CONFLICTS OF INTEREST ..... - 235 -
V.10 REFERENCES ..... - 235 -
V.11 APPENDIX - MULTIPLE SCLEROSIS IMPACT SCALE (MSIS-29) ..... - 240 -

CHAPTER 6: CONCLUSIONS ..... - 244 -

VI.1 ABBREVIATIONS ..... - 245 -

VI.2 CONCLUSIONS ..... - 246 -

VI.3 REFERENCES ..... - 250 -

APPENDIX A – PUBLICATIONS BY THE THESIS AUTHOR DIRECTLY RELATED TO THE WORK PRESENTED IN THE THESIS ..... - 254 -

Inflammatory activity on natalizumab predicts short-term but not long-term disability in multiple sclerosis. *PLOS One*. 2017 ..... - 256 -

Kinetic analysis of the translocator protein positron emission tomography ligand [18F]GE-180 in the human brain. Eur J Nucl Med Mol Imaging. 2016 ..... - 269 -

Confirmation of specific binding of the 18-kDa Translocator Protein (TSPO) radioligand [18F]GE-180: a blocking study using XBD173 in multiple sclerosis normal appearing white and grey matter. Mol Imaging Biol. 2019..... - 280 -

Patient-reported outcomes and survival in multiple sclerosis: A 10-year retrospective cohort study using the Multiple Sclerosis Impact Scale-29. PLOS Medicine. 2017 ..... - 291 -

APPENDIX B – LIST OF PUBLICATIONS BY THE THESIS AUTHOR RELATED TO WORK CONDUCTED DURING CLINICAL FELLOWSHIP BUT NOT OTHERWISE DISCUSSED IN THESIS - 307 -

APPENDIX C – PERMISSIONS TO REPRODUCE, IN THIS THESIS, PUBLICATIONS OF THE THESIS AUTHOR AND PUBLISHED FIGURES FROM THIRD PARTY COPYRIGHT WORKS ..... - 309 -

Permissions to reproduce, in this thesis, publications of the thesis author ..... - 310 -

Permissions to reproduce, in this thesis, published figures from third party copyright works ..... - 311 -

LIST OF TABLES

Chapter 2 - Relapses and MRI Activity on Natalizumab Predict Short-term but not Long-term Disability Progression

Table 1: Modified Rio Score ..... - 55 -
Table 2: Characteristics of study cohort ..... - 59 -

Chapter 3 - 18 kDa Translocator Protein Radioligand 18F-GE180 as a Marker of Neuroinflammatory Activity in Multiple Sclerosis

Table 3: Summary of participant demographics ..... - 105 -
Table 4: Regional V_T estimates for regions of interest in individual participants ..... - 106 -
Table 5: Baseline characteristics of PwMS and HCs ..... - 111 -
Table 6: Clinical and patient-reported outcomes in PwMS and HCs at baseline ..... - 112 -

Chapter 4 - Brain Predicted Age in Multiple Sclerosis: A Model using Machine Learning Analysis of MRI

Table 7: MRI acquisition protocols ..... - 155 -
Table 8: Baseline characteristics of PwMS and HCs ..... - 162 -
Table 9: Clinical and patient-reported outcomes in PwMS and HCs at baseline ..... - 163 -
Table 10: Baseline characteristics of PwMS and HCs ..... - 171 -
Table 11: Ordinary least squares linear regression with hierarchical partitioning, to predict Brain Age. ..... - 185 -
Table 12: Ordinary least squares linear regression with hierarchical partitioning, to predict cross-sectional EDSS score ..... - 186 -

Chapter 5 - Patient-Reported Outcomes can Predict Survival Time in Multiple Sclerosis: A Cohort Study using the Multiple Sclerosis Impact Scale–29

Table 13: Baseline characteristics of PwMS and HCs ..... - 213 -
Table 14: Clinical and patient-reported outcomes in PwMS and HCs at baseline ..... - 214 -
Table 15: Differences in baseline characteristics between those included and those not included in the study, those with and without imputed data, those with and without prEDSS data, and those with and without longitudinal MSIS-29 data ..... - 219 -
Table 16: Variation in characteristics between those with different baseline MSIS-29 scores ..... - 223 -
Table 17: Reduced survival time (greater hazard ratio for death) was associated with older age, higher prEDSS score, and higher MSIS-29-PHYS score in the limited cohort with prEDSS score available (n = 625) ..... - 227 -

LIST OF FIGURES

Chapter 1 – Introduction

Figure 1: The typical course of relapsing-remitting and secondary progressive multiple sclerosis..... - 26 -
Figure 2: Typical evolution of multiple sclerosis disability, radiographic changes, and pathophysiology, over time. ..... - 27 -
Figure 3: On-treatment inflammatory disease activity does not affect long-term disability progression, tested as survival analysis. ..... - 33 -
Figure 4: V_T in selected regions of interest in HCs and PwMS at baseline..... - 36 -
Figure 5: 'Brain predicted age difference' (Brain-PAD) = Brain-predicted age minus chronological age ..... - 37 -
Figure 6: Brain-PAD is increased in MS, correlates with disability, and increases longitudinally ..... - 38 -
Figure 7: Higher MSIS-29-PHYS scores are associated with reduced survival time ..... - 40 -

Chapter 2 - Relapses and MRI Activity on Natalizumab Predict Short-term but not Long-term Disability Progression

Figure 8: Flowchart of participants..... - 58 -
Figure 9: On-treatment inflammatory disease activity does not affect long-term disability progression, tested as survival analysis. ..... - 61 -
Figure 10: On-treatment inflammatory disease activity predicts short-term but not long-term disability outcomes. ..... - 63 -
Figure 11: Results remain consistent after exclusion of those who switched from natalizumab to other disease-modifying therapies ..... - 67 -

Chapter 3 - 18 kDa Translocator Protein Radioligand 18F-GE180 as a Marker of Neuroinflammatory Activity in Multiple Sclerosis

Figure 12: Immunofluorescent stain in white matter lesion of post-mortem human MS brain ..... - 80 -
Figure 13: Biomarkers of *in vivo* rate of neurodegeneration should be able to detect treatment effect at earlier time point than biomarkers of *in vivo* extent of neurodegeneration..... - 83 -
Figure 14: 'Natalizumab cohort' design ..... - 88 -
Figure 15: 'Blocking study' design ..... - 89 -
Figure 16: Method for lesion segmentation in T1 space..... - 96 -
Figure 17: ^{18}F-GE180 Standardised uptake values and volume of distribution (V_T) in healthy controls..... - 103 -
Figure 18: Sum 60-90 minute PET images (kBq.ml^{-3}) before and after XBD-173 ..... - 107 -
Figure 19: Occupancy and polymorphism plots. ..... - 108 -
Figure 20: Reduction in uptake post-XBD-173 administration. ..... - 109 -
Figure 21: Increased 60–90 minute SUVs in a gadolinium-enhancing lesion..... - 114 -
Figure 22: No effect of TSPO genetic polymorphism on ^{18}F-GE180 V_T..... - 116 -
Figure 23: V_T in selected regions of interest in healthy controls and PwMS at baseline ..... - 118 -
Figure 24: ^{18}F-GE180 V_T is increased in MS lesions compared to other regions of interest at baseline and 10 weeks after initiation of natalizumab, but not at 58 weeks after initiation of natalizumab..... - 119 -
Figure 25: ^{18}F-GE180 V_T after 58 weeks of natalizumab reduces in white matter lesions but grey matter lesions ..... - 120 -
Figure 26: New lesions and 'pre-lesions' have increased V_T..... - 122 -

Chapter 4 - Brain Predicted Age in Multiple Sclerosis: A Model using Machine Learning Analysis of MRI

Figure 27: Model of premature brain ageing after environmental insult ..... - 149 -

Figure 28: 'Brain Predicted Age Difference' (Brain-PAD) = Brain Predicted Age minus chronological age ..... - 151 -
Figure 29: Overview of Brain Predicted Age model methodology. ..... - 157 -
Figure 30: Lesion segmentation methodology ..... - 159 -
Figure 31: Brain Predicted Age and Brain-PAD in multiple sclerosis and healthy controls ..... - 165 -
Figure 32. Lesion-Filled scans ..... - 167 -
Figure 33: Longitudinal Brain-PAD after natalizumab treatment ..... - 169 -
Figure 34: Flowchart of exclusions for UCL cohort ..... - 170 -
Figure 35: Baseline scans by disease subtype ..... - 173 -
Figure 36: Brain Predicted Age and Brain-PAD correlate with disease characteristics. ..... - 175 -
Figure 37: Survival from disability milestones and EDSS progression as a function of Brain Predicted Age and Brain-PAD ..... - 177 -
Figure 38: Longitudinal change in Brain Predicted Age in people with multiple sclerosis and healthy controls. ..... - 179 -
Figure 39: Brain-PAD in those with 'long-term CIS' (no RRMS diagnosed and > 10 years follow-up), and those who converted from 'CIS to RRMS'. ..... - 181 -
Figure 40: There was no difference in healthy control Brain-PAD between scans acquired using a 1.5 Tesla MRI scan and scans acquired using a 3.0 Tesla MRI scan ..... - 183 -
Figure 41: Unfilled Brain-PAD at baseline correlates strongly with lesion-filled Brain-PAD at baseline in those with CIS or MS ..... - 184 -

Chapter 5 - Patient-Reported Outcomes can Predict Survival Time in Multiple Sclerosis: A Cohort Study using the Multiple Sclerosis Impact Scale–29

Figure 42: MSIS-29 scores are higher in subjects with MS than HCs ..... - 215 -
Figure 43: Change in MSIS-29 scores are associated with response to treatment ..... - 217 -
Figure 44: Higher MSIS-29-PHYS scores are associated with reduced survival time ..... - 222 -
Figure 45: Higher MSIS-29-PSYCH scores are associated with reduced survival time. ..... - 225 -
Figure 46: Correlation between different outcome measures ..... - 227 -
Figure 47: Longitudinally increase in MSIS-29-PHYS score is associated with reduced survival time. ..... - 229 -

Chapter 6 – Conclusions

Figure 48: Biomarkers of *in vivo* rate of neurodegeneration ('Biomarker 1') should be able to detect treatment effect at earlier time point than those of *in vivo* extent of neurodegeneration ('Biomarker 2'). ..... - 247 -

Chapter 1

Introduction

I.1 ABBREVIATIONS

Brain-PAD	Brain predicted age difference.
CIS	Clinically isolated syndrome
DMT	Disease-modifying therapy
EDSS	Expanded disability status scale
HC	Healthy control
MS	Multiple sclerosis
MSIS-29	Multiple Sclerosis Impact Scale–29
MSIS-29-PHYS	MSIS-29 physical
MSIS-29-PSYCH	MSIS-29 psychological
PET	Positron emission tomography
PPMS	Primary progressive multiple sclerosis
PwMS	People with multiple sclerosis
RRMS	Relapsing-remitting multiple sclerosis
SPMS	Secondary progressive multiple sclerosis
TSPO	18 kDa translocator protein
V_T	Volume of distribution

I.2 BACKGROUND

I.2.1 The burden of multiple sclerosis

Multiple sclerosis (MS) affects approximately 1 in 1000 people in temperate countries including the UK, and 2.5 million individuals worldwide.[1] It is the commonest cause of non-traumatic neurological disability in young adults.[2] Clinical severity ranges from so-called 'benign MS', in which the patient remains fully functional in all neurological systems 15 years after disease onset, to 'malignant MS', characterised by an aggressive course with accumulation of severe disability within 5 years of diagnosis.[3-7] Based on historical cohorts, the average time from MS onset to wheelchair use is 30 years.[8-11] Average life expectancy is reduced by 5 to 10 years.[12, 13] MS is associated with cognitive impairment, high rates of unemployment, and in the UK has a cost-of-illness of approximately £10,000 per patient per year in the early stages of the disease to £35,000/year for those who are restricted to a wheelchair.[14-16]

I.2.2 Disease course in MS

Approximately 85-90% of people with MS (PwMS) initially experience a 'relapsing-remitting' course where symptoms arise acutely or subacutely in a 'relapse', and then resolve completely or partially.[3] Other pwMS have a disease course characterised by progressive disease from onset independent of clinical relapses, termed primary progressive MS (PPMS).[17] The majority of those with relapsing-remitting MS (RRMS) eventually develop secondary progressive MS (SPMS), where irreversible disability gradually accrues over time, with or without acute exacerbations during the progressive course (Figure 1).[3, 17] Clinically isolated syndrome (CIS) is a term to describe those who have had a first clinical relapse, but do not yet meet diagnostic

criteria for RRMS.[17] 60-70% of people with CIS will have further demyelinating events within 20 years and so will be diagnosed with MS.[18, 19]

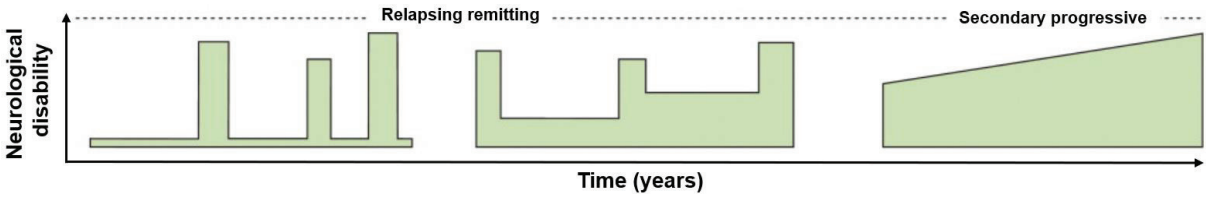


Figure 1: The typical course of relapsing-remitting and secondary progressive multiple sclerosis. Adapted from Compston and Coles, 2008.[20] Image adapted with permission of the rights holder, Elsevier

I.2.3 The pathophysiology of MS

The pathophysiology of MS is complex, and is still not fully understood.[21, 22] It has both focal neuroinflammatory and neurodegenerative components, which in a simplified model can be considered as the pathological substrates of clinical relapses and gradual progression of disability, respectively.[23, 24]

Focal white matter inflammation is driven, in part, by the peripheral activation of lymphocytes followed by acute influx across the blood-brain barrier.[25] An immune cascade leads to massive activation of macrophage/microglial cells, and phagocytosis of myelin.[26] These white matter lesions present clinically as relapses, and lesions visible on MRI which are gadolinium-enhancing in their early stages.[23, 24]

The typical evolution of relapsing MS over time is depicted in Figure 2.[25] Axonal loss begins at disease onset, but progressive disease presents clinically once axon loss surpasses central nervous system capacity to compensate for loss of function.[25] MRI lesions and relapses generally become less prominent as the disease enters the secondary progressive phase. Brain

atrophy continues in the grey matter and white matter, as does diffuse axonal loss within the normal appearing white matter.[27-30] This neurodegeneration is accompanied by a different type of inflammation, compartmentalised within the central nervous system and located behind a relatively intact blood-brain barrier.[23, 31-33] The interdependency between the focal inflammatory and neurodegenerative components of disease is a matter of debate; it remains uncertain whether decreasing focal inflammatory activity with treatment necessarily causes a downstream slowing of neurodegeneration.[23, 25, 34]

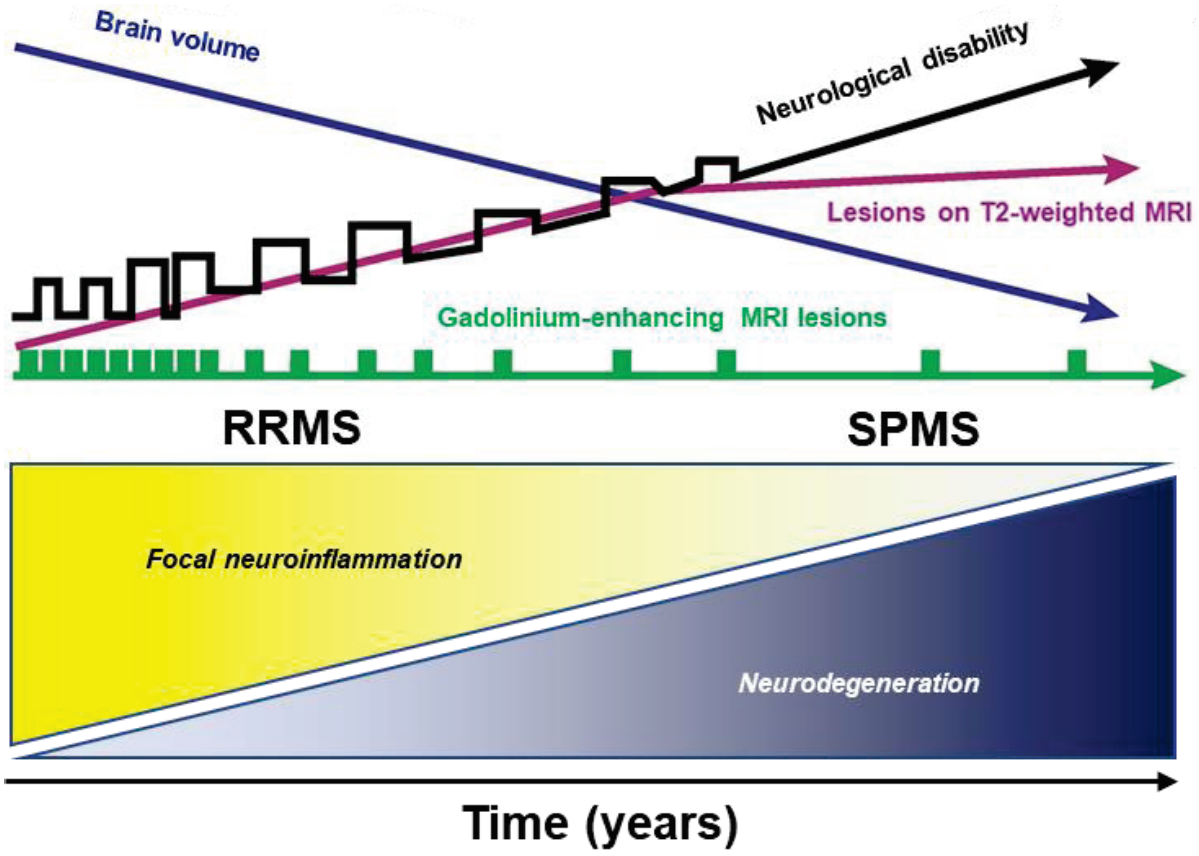


Figure 2: Typical evolution of multiple sclerosis disability, radiographic changes, and pathophysiology, over time. Black line: neurological disability. Green line: gadolinium enhancing lesions on MRI. Pink line: accumulated lesions on T2-weighted MRI. Blue line: Brain volume. RRMS = relapsing remitting multiple sclerosis. SPMS = secondary progressive multiple sclerosis. Adapted from Hauser and Oksenberg, 2006.[25] Image reproduced with permission of the rights holder, Elsevier.

I.2.4 Disease-modifying therapy in MS

No curative therapies exist for MS. Immunomodulatory disease-modifying therapies (DMTs) for MS include β-interferons, glatiramer acetate, dimethyl fumarate, teriflunomide, fingolimod, cladribine, alemtuzumab, natalizumab and ocrelizumab.[35] For subjects with relapsing MS, these DMTs are effective in reducing relapse rate and new MRI lesions, and are somewhat effective at slowing the gradual progression of disability.[36, 37] DMTs vary in their overall efficacy and safety profile.[36] A common approach is for the most effective and least safe DMTs to be reserved for patients with the most active disease, or patients who do not respond to first-line DMTs.[35, 36]

These therapies are thought to be less effective in SPMS and PPMS, especially in those without focal inflammatory activity.[35, 38] Even ocrelizumab, the first DMT to gain a license in PPMS, appears to exert its effect mostly in those with evidence of active focal inflammation.[39, 40]

One of the more effective DMTs in relapsing MS is natalizumab, which was granted a marketing authorisation throughout the European Union in 2006.[41-43] Natalizumab is a humanized antibody against the alpha-4 integrin that blocks the adhesion of lymphocytes and monocytes to endothelial cells of the blood-brain barrier, interfering with the subsequent passage of inflammatory cells into the central nervous system and therefore reducing focal white matter inflammation. It is effective at reducing relapse rate, by 68% compared to placebo, and new or enlarging lesions on T2-weighted MRI, by 83% compared to placebo.[42] In RRMS it decreases the likelihood of progression of disability by 42% over a 2-year period. Its use is complicated by the risk of progressive multifocal leukoencephalopathy, which can result in severe disability or death.[44, 45] It is administered as a monthly intravenous infusion, usually in

a hospital setting. As of June 2019, over 200,000 pwMS have received natalizumab worldwide.[46]

I.2.5 Personalised medicine in MS

Personalised medicine can be described as a pursuit of 'the right treatment for the right patient at the right time'.[47] The term 'personalised medicine' is often associated with genomic medicine, for example in oncology care.[48] Taken more broadly, 'personalised medicine' describes any attempt to deconstruct the heterogeneity of a disease so as to allow benefits and risks to be balanced optimally when making decisions for individuals.[48, 49]

There is marked heterogeneity in the clinical presentation, disease course, and response to treatment in MS.[50-52] Drug efficacy in individual pwMS is determined by factors that remain largely undefined. Given the number of available DMTs, physicians are faced with increasingly complex decisions when treating individuals, for example:

- What is this patient's prognosis? Should treatment be initiated, and at what point?
- Which DMT is likely to provide the optimal benefit-risk ratio for this individual?
- How should one decide whether to continue, switch or cease treatments?

Randomised-controlled trials support the overall benefit-risk of licensed DMTs in MS, but provide minimal information relating to specific questions as above, including the comparative clinical benefit of different DMTs and how this differs according to patient characteristics. At present, decision-making is mostly based on imprecise estimations of disease severity and prognosis in individuals, and balancing this against the perceived overall hierarchy of efficacy and safety of DMTs. Such decisions have a weak evidence base, and mostly have not been

directly tested.[52] Personalised medicine should therefore be considered as a priority for future care in MS.[52, 53]

I.2.6 Outcome measures for personalised medicine in MS

Due to the relapsing-remitting nature of MS, it can take months to years to assess whether DMTs have been successful in reducing or stopping MS relapses and new MRI lesions. It takes longer still to assess whether patients continue to accumulate irreversible disability. If a patient continues to take an ineffective treatment, this person loses time in the fight against disability while still being exposed to the risks of treatment.[52] To move towards personalised medicine in MS, clinicians will require tools for the early empirical assessment of therapy response in individuals, which can indicate whether the individual is likely to benefit long-term from continued treatment.[52, 54] This may require a biomarker that is sensitive to neurodegenerative activity, rather than only focal white matter inflammation.[55, 56] Such a biomarker could also be useful in the therapeutic pipeline as an early surrogate for a medication's efficacy. A prefatory study is reported in Chapter 2 of this thesis, investigating whether early relapses and new MRI lesions after initiation of natalizumab treatment predict long-term disability outcomes. In Chapter 3, a novel positron emission tomography (PET) ligand is investigated as a marker of disease activity before and after natalizumab treatment.

In addition to outcome measures which can guide clinical decision-making in individuals, personalised medicine will require the collection and analysis of 'big data': large datasets from clinical registry tools, which collect and codify patient characteristics, disease events, therapies, and outcome measures.[57-60] With data of sufficient quality and quantity, such databases could eventually strive to answer questions in personalised medicine such as:

'*for a 25-year-old female patient recently diagnosed with MS, with three motor-system relapses and 15 lesions on MRI, how does Drug X, Drug Y, and Drug Z affect the prognosis*?'

or

'for a 30-year-old male patient receiving treatment with Drug X for 2 years, with five new lesions on MRI since commencing treatment, how does continuing on Drug X versus switching to Drug Y affect the prognosis?'

A desirable database may have both clinician-facing and patient-facing interfaces, and be able to integrate clinician-reported, patient-reported, laboratory-based and radiological outcomes. One of many challenges is to develop outcome measures which are compatible with large multicentre cohorts, and which can be tracked over time to capture meaningful data related to the impact of disease on PwMS. Outcomes should have adequate psychometric properties, be clinically meaningfully, and should be robust to differences in methodology between centres.[59, 61] Chapters 4 and 5 of this thesis investigate respectively the clinical relevance of a novel MRI outcome and a well-established patient-reported outcome, both of which have potential for use in large multicentre cohorts.

I.3 THESIS OVERVIEW

Chapters 2 to 5 each report studies investigating different outcome measures for potential use in MS. These chapters include introduction, methodology, results, and discussion sections relevant to the studies investigated in that chapter. Therefore, the introductory Chapter 1 and the concluding Chapter 6 are kept brief. Summaries of Chapters 2 to 5 are presented below.

I.3.1 Chapter 2 - Relapses and MRI Activity on Natalizumab Predict Short-term but not Long-term Disability Progression

Observational studies of β-interferons and glatiramer acetate therapy have concluded that patients with relapses or new MRI lesions in the first year after initiation of treatment are more likely to have disability progression after medium-term follow-up.[62-68] This supports the practice, common among neurologists, of switching medications if patients experience significant on-treatment breakthrough inflammatory activity.[69] However, the above studies are limited by follow-up periods of less than 3 years. Their applicability to other therapies such as natalizumab is also uncertain.

In this chapter, a study is reported which evaluates whether on-treatment relapses or MRI activity after initiating natalizumab treatment predicts future disability progression, as measured with the expanded disability status scale (EDSS).[70] Data were retrospectively collated from an observational cohort of PwMS initiating natalizumab, with up to 7 years of follow-up. Data on relapse rate and EDSS were prospectively documented at routine 6-monthly clinic visits. MRI was routinely performed before treatment and at one year. A combined score of MRI and relapse activity – the Modified Rio Score – was also calculated (0 = low, 1 = medium, 2 = high inflammatory activity).[64] Disability progression was defined as an increase of 1 EDSS point in those with EDSS <5.5, or an increase of 0.5 EDSS point in those with EDSS ≥5.5.

46 of 161 PwMS had a relapse in the first year of treatment, and 28 of 161 had new MRI activity. Markers of inflammatory disease in the first year (Modified Rio Score, relapses, MRI activity) and second year (relapses) had no significant effect on disability progression when tested as a survival analysis (Modified Rio Score year 0-1: risk ratio 1.15, log-rank p = 0.74,

Cox regression $p = 0.44$; Relapses year 0-1: risk ratio 1.3, log-rank $p = 0.31$, Cox regression $p = 0.31$; MRI activity year 0-1: risk ratio 0.64, log-rank $p = 0.21$, Cox regression $p = 0.24$; Relapses year 1-2: risk ratio 1.17, log-rank $p = 0.51$, Cox regression $p = 0.51$; Figure 3A-D).

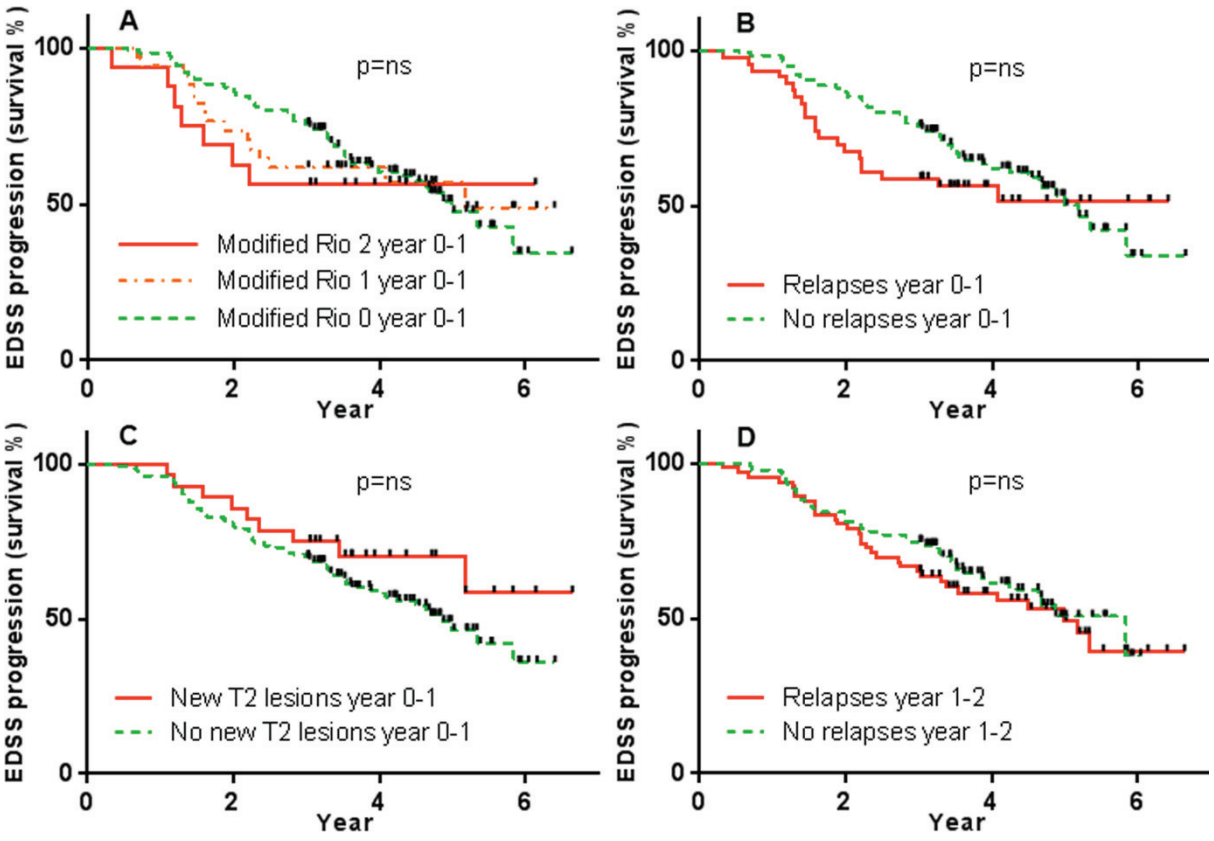


Figure 3: On-treatment inflammatory disease activity does not affect long-term disability progression, tested as survival analysis. First year after natalizumab initiation Modified Rio Score (A), relapses (B), and MRI activity (C), and second year after natalizumab initiation relapses (D), versus survival from EDSS progression over time. Black markers on survival lines represent the duration of follow-up data for those participants who have not undergone EDSS progression (i.e. the time of subject censorship in survival analysis). EDSS = Expanded Disability Status Scale. ns = not statistically significant.

Given that EDSS progression can be a reversible event and, further, since Kaplan-Meier curves were observed to cross, results were also analysed at different time points using Chi-squared test for trend. Here, relapses and Modified Rio Score in the first year of treatment did predict EDSS progression at year 1 and 2 after treatment initiation. However, this effect disappeared

with longer follow-up. Instead, there was a paradoxical trend towards inflammatory activity on treatment predicting a *lower* risk of EDSS progression by years 3-7.

In conclusion, on-treatment relapses and MRI activity do not predict long-term disability outcomes after natalizumab. This study confirms the need for improved biomarkers, including those that can better quantify neuroinflammation and neurodegeneration. This supports the rationale for the study reported in Chapter 3.

I.3.2 Chapter 3 - 18 kDa Translocator Protein Radioligand ^{18}F-GE180 as a Marker of Neuroinflammatory Activity in Multiple Sclerosis

Activated microglia are observed in focal inflammatory lesions and cortical grey matter pathology.[33, 71] In recent years, the case has grown for microglia playing a key role in neuroaxonal degeneration and progressive disease.[71-73] 18kDa translocator protein (TSPO) is expressed on microglia and other cells at sites of active CNS pathology.[74-76] $^{[18F]}$GE180 is a novel PET molecular imaging radiotracer that targets the TSPO receptor.[77] A genetic polymorphism is known to affect TSPO tracer binding. [78]

In this chapter, a study is reported which evaluates $^{[18F]}$GE180 PET as a biomarker for focal inflammatory and neurodegenerative disease activity in MS, and as a surrogate for response to natalizumab treatment. A cohort of 16 PwMS starting natalizumab had ^{18}F-GE180 PET at baseline, 10 weeks after, and 58 weeks after treatment initiation. 11 healthy controls (HCs) had one ^{18}F-GE180 PET scan. In addition, a 'blocking study' investigated whether ^{18}F-GE180 PET is labelling TSPO: 6 PwMS had a baseline ^{18}F-GE180 PET followed by repeat PET after

administration of the TSPO ligand XBD-173. A variety of methodological approaches were evaluated, including the gold-standard volume of distribution (V_T).

Administration of [18F]GE180 PET was safe, and well-tolerated by participants. In total, 71 PET scans were completed. A reversible two-tissue compartment model best fitted the data. The mean regional delivery rate constant K_1 was unexpectedly low (~0.01 mL/cm^3 min−1), suggesting poor extraction (~1%) across the blood-brain barrier. V_T values were correspondingly low, with a whole brain mean of 0.29 ± 0.17 mL/cm^3 in subjects with MS.

The MS 'blocking study' suggested that ^{18}F-GE180 V_T does include some specific signal, even if absolute V_T values are low. This allowed cautious exploration of the 'natalizumab cohort' data. V_T was increased in MS lesions at baseline (Figure 4), which decreased after 58 weeks of natalizumab treatment, although again differences relating to the TSPO polymorphism were not observed. ^{18}F-GE180 was not able to detect increased TSPO in MS in the grey matter or normal-appearing white matter as previously reported with other tracers, or differences in TSPO binding affinity as expected.[79-85] There were no associations between PET outcomes and clinical outcomes.

This was the first study to characterise the performance of ^{18}F-GE180 in humans and suggests that [18F]GE180 is limited by its low extraction over the blood-brain barrier. Positive results in MS lesions may reflect changes in blood-brain barrier permeability rather than changes in TSPO expression. The results of the 'blocking study' have broader implications on how novel TSPO tracers should be validated and compared.

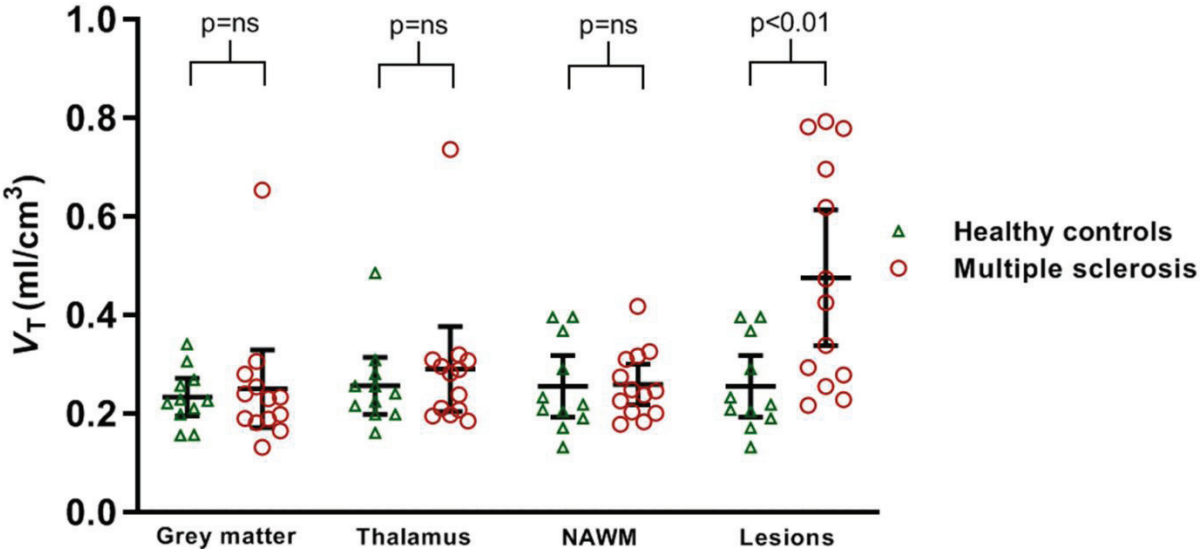


Figure 4: V_T in selected regions of interest in HCs and PwMS at baseline. There was no difference between HCs (green triangles) and PwMS (red circles) in the grey matter, thalamus, or NAWM. V_T in MS lesions was greater than V_T in HC white matter. In the above figure HC white matter is graphically represented as both 'HC NAWM' and 'HC lesions' for ease of comparison. *p*-values generated using unpaired *t* test. Error bars represent mean +/- 95% confidence intervals. NAWM = normal-appearing white matter; V_T = Volume of distribution. ns = not statistically significant.

I.3.3 Chapter 4 - Brain Predicted Age in Multiple Sclerosis: A Model using Machine Learning Analysis of MRI

Brain structure alters throughout life, and brain atrophy that occurs as part of normal ageing is non-linear and spatially variable.[86] Using machine-learning analysis of brain MRIs from 2,001 HCs of different chronological age, a Brain Age model has been developed at Imperial College London which can accurately predict chronological age based solely upon T1 MRI data (r * 0.96, mean absolute error * 4.4 years), and correlates with clinical outcome measures in the general population.[87, 88] This model can then be used to identify individuals whose 'brain age' appears younger or older than their chronological age, as illustrated in Figure 5. This 'Brain

Predicted Age' model has potential applicability to MS research, to quantify damage and accelerated ageing-like changes in the MS brain.

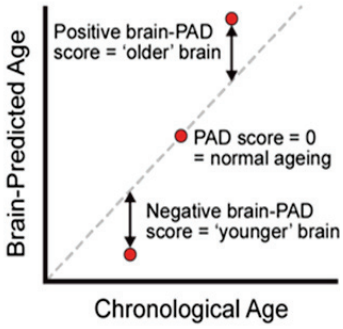


Figure 5: 'Brain predicted age difference' (Brain-PAD) = Brain-predicted age minus chronological age. For example, if brain-predicted age is identical to chronological age, Brain-PAD is 0. If brain-predicted age is 5 years older than true chronological age, Brain-PAD is +5. In healthy control populations, the mean Brain-PAD is expected to be 0

In this chapter, a study is reported which investigates Brain Predicted Age as a marker of disease severity in MS. Brain Predicted Age was investigated in the 'natalizumab cohort' described in Chapter 3. Subsequently, a larger observational cohort of 1,599 T1-weighted MRI scans from 541 participants were analysed and correlated with clinical data.

In the natalizumab cohort, Brain-PAD was increased in PwMS, correlated with markers of disease severity, and appeared to improve in responders to treatment. In the larger cohort, HCs had mean Brain-PAD close to zero, as expected. All disease subgroups had substantially older-appearing brains than their chronological age (CIS: mean Brain-PAD +4.0 years; RRMS: mean Brain-PAD +10.3 years, SPMS: mean Brain-PAD +17.4 years; PPMS: mean Brain-PAD +11.5 years; $p < 0.0001$; Figure 6A). Brain Predicted Age correlated strongly with EDSS (Figure 6B). Brain-PAD increased longitudinally in PwMS at a rate ~46% faster than in HCs (Figure 6C). The model compared favourably with conventional univariate measures of brain atrophy.

The Brain Predicted Age model could provide conceptually simple and clinically meaningful quantitative data from a standard T1-weighted MRI scan, which could be used across large imaging cohorts. This will be further evaluated using the MAGNIMS multi-centre cohort.

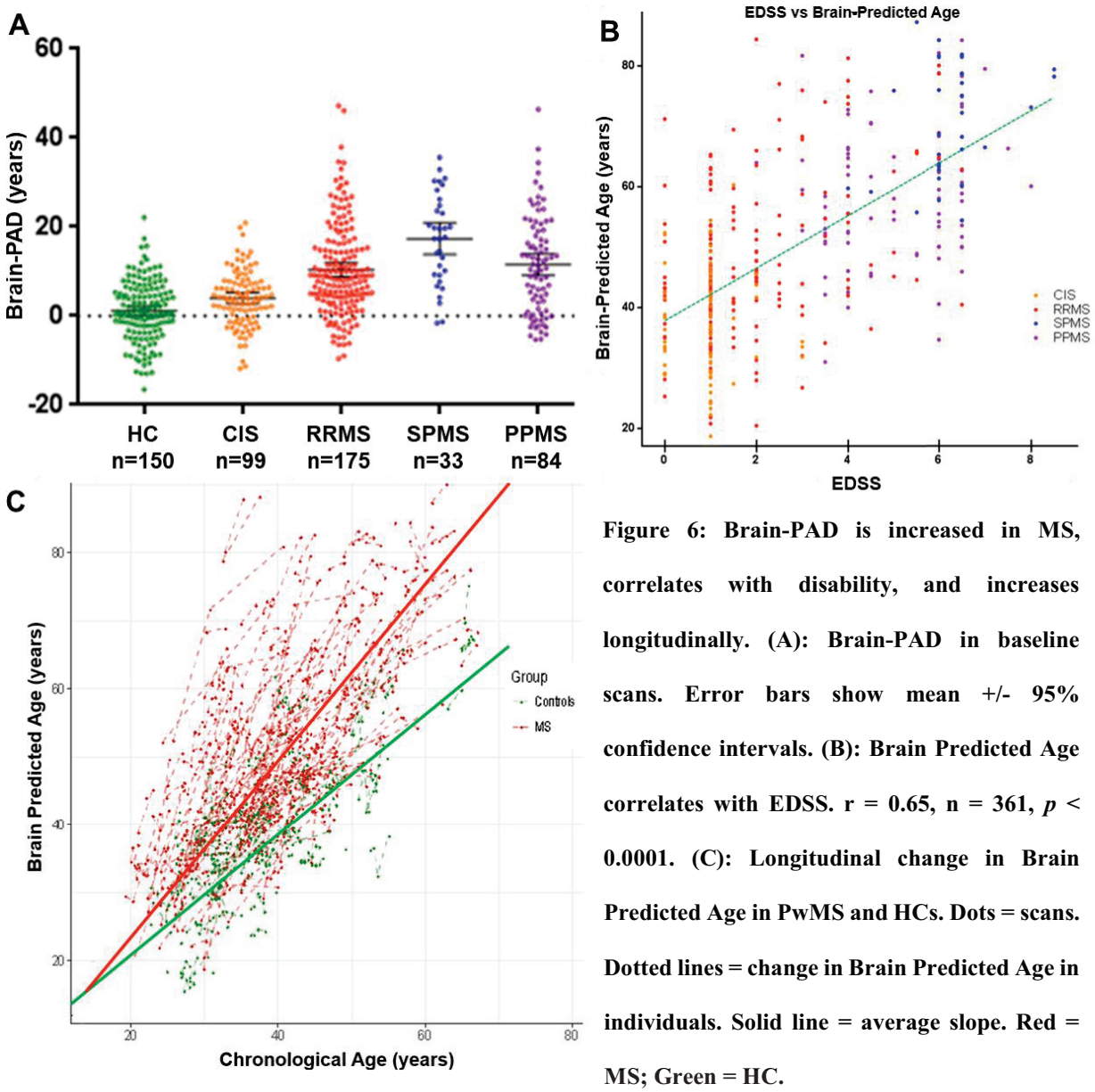


Figure 6: Brain-PAD is increased in MS, correlates with disability, and increases longitudinally. (A): Brain-PAD in baseline scans. Error bars show mean +/- 95% confidence intervals. (B): Brain Predicted Age correlates with EDSS. r = 0.65, n = 361, p < 0.0001. (C): Longitudinal change in Brain Predicted Age in PwMS and HCs. Dots = scans. Dotted lines = change in Brain Predicted Age in individuals. Solid line = average slope. Red = MS; Green = HC.

I.3.4 Chapter 5 - Patient-Reported Outcomes can Predict Survival Time in Multiple Sclerosis: A Cohort Study using the Multiple Sclerosis Impact Scale–29

Patient-reported outcomes (PROs) are increasingly used to complement traditional clinical outcomes in medical research, including in MS. In oncology and heart failure, PROs have been shown to predict hard clinical endpoints including those related to survival.[89-91] It is unknown whether PROs can be predictive of hard clinical endpoints in MS. If they were, they could be

developed for use in large clinical registry datasets to quantify the impact of disease on PwMS, for example.[92] The Multiple Sclerosis Impact Scale-29 (MSIS-29) is a patient-reported outcome that assesses physical (PHYS subscale) and psychological (PSYCH subscale) quality of life.

In this chapter, it is investigated whether MSIS-29 scores can predict survival time in a large observational cohort of PwMS. From 2004, the MSIS-29 was completed by PwMS registered with the MS Society Tissue Bank (n = 2,126; repeated one year later in n = 872). Survival time was defined using date of first MSIS-29 questionnaire as entry point, date of death as endpoint, and date of study completion as censorship date for those still alive.

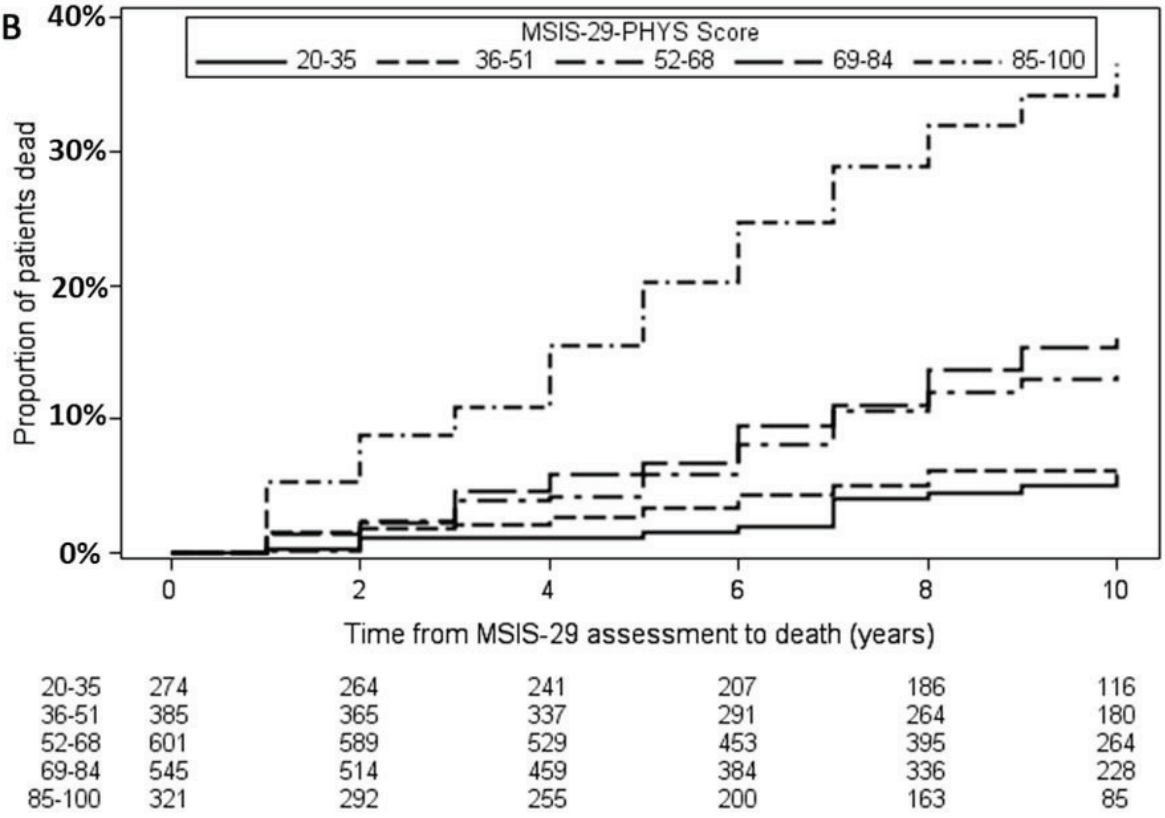
Median follow-up time was 9 years. At study completion, 264 (12.4%) of PwMS had died. Higher MSIS-29-PHYS score predicted reduced survival time independently of age and sex (Wald chi-square, [degrees of freedom = 4, n = 2,126] = 98.5; e.g. subgroup with highest scores vs subgroup with lowest scores: hazard ratio 5.7, 95% CI 3.1–10.5, $p < 0.001$; Figure 7). The MSIS-29-PSYCH score also predicted reduced survival time, although the effect was less strong (e.g. subgroup with highest scores versus subgroup with lowest scores: hazard ratio 2.8, 95% CI 1.8–4.4, $p < 0.001$). In those with high baseline MSIS-29-PHYS scores, mortality risk was even greater if the MSIS-29-PHYS score increased over one year. MSIS-29-PHYS scores were associated with survival time independent of age, sex, and patient-reported EDSS score.

This is the first study to associate PROs with survival outcomes in any neurological disease. The study supports the further development of PROs for incorporation into MS clinical registry databases, as clinically meaningful outcome measures which can track the impact of MS on individuals.

A

Parameter		Hazard Ratio	95% Hazard Ratio Confidence Limits		p-value	p-value factor
MSIS-29-PHYS score (compared to 20-35)	**36-51**	0.995	0.486	2.038	0.989	<0.001
	52-68	1.853	0.998	3.438	0.051	
	69-84	2.140	1.155	3.966	0.016	
	85-100	5.728	3.131	10.479	<0.001	
Age	per year	1.051	1.041	1.063		<0.001
Sex	male vs. female	1.906	1.479	2.457		<0.001

B



20-35	274	264	241	207	186	116
36-51	385	365	337	291	264	180
52-68	601	589	529	453	395	264
69-84	545	514	459	384	336	228
85-100	321	292	255	200	163	85

Figure 7: Higher MSIS-29-PHYS scores are associated with reduced survival time. (A) Table: Higher MSIS-29-PHYS score was associated with reduced survival time (greater hazard ratio for death), as were older age at first MSIS-29 completion and male sex. (B) Kaplan–Meier failure curves (*n* = 2,126). Note that Kaplan–Meier curves do not account for the effect of age and sex on survival time. Data at bottom of figure show number of data points at each time point for each MSIS-29-PHYS subgroup. MSIS-29 = Multiple Sclerosis Impact Scale–29; MSIS-29-PHYS = MSIS-29 physical.

I.4 REFERENCES

1. Milo R, Kahana E. Multiple sclerosis: geoepidemiology, genetics and the environment. Autoimmunity reviews. 2010;9(5):A387-94. doi: 10.1016/j.autrev.2009.11.010. PubMed PMID: 19932200.

2. Global Economic Impact of Multiple Sclerosis. Multiple Sclerosis International Federation, 2010. Available from https://www.msif.org/wp-content/uploads/2014/09/Global_economic_impact_of_MS.pdf . Last accessed October 2019.

3. Lublin FD, Reingold SC, Cohen JA, Cutter GR, Sorensen PS, Thompson AJ, Wolinsky JS, Balcer LJ, Banwell B, Barkhof F, Bebo B, Jr., Calabresi PA, Clanet M, Comi G, Fox RJ, Freedman MS, Goodman AD, Inglese M, Kappos L, Kieseier BC, Lincoln JA, Lubetzki C, Miller AE, Montalban X, O'Connor PW, Petkau J, Pozzilli C, Rudick RA, Sormani MP, Stuve O, Waubant E, Polman CH. Defining the clinical course of multiple sclerosis: the 2013 revisions. Neurology. 2014;83(3):278-86. Epub 2014/05/30. doi: 10.1212/WNL.0000000000000560. PubMed PMID: 24871874; PubMed Central PMCID: PMCPMC4117366.

4. Gholipour T, Healy B, Baruch NF, Weiner HL, Chitnis T. Demographic and clinical characteristics of malignant multiple sclerosis. Neurology. 2011;76(23):1996-2001. Epub 2011/06/08. doi: 10.1212/WNL.0b013e31821e559d. PubMed PMID: 21646626.

5. Hawkins SA, McDonnell GV. Benign multiple sclerosis? Clinical course, long term follow up, and assessment of prognostic factors. J Neurol Neurosurg Psychiatry. 1999;67(2):148-52. Epub 1999/07/17. doi: 10.1136/jnnp.67.2.148. PubMed PMID: 10406979; PubMed Central PMCID: PMCPMC1736487.

6. Amato MP, Zipoli V, Goretti B, Portaccio E, De Caro MF, Ricchiuti L, Siracusa G, Masini M, Sorbi S, Trojano M. Benign multiple sclerosis: cognitive, psychological and social aspects in a clinical cohort. J Neurol. 2006;253(8):1054-9. Epub 2006/04/13. doi: 10.1007/s00415-006-0161-8. PubMed PMID: 16609810.

7. Skoog B, Runmarker B, Winblad S, Ekholm S, Andersen O. A representative cohort of patients with non-progressive multiple sclerosis at the age of normal life expectancy. Brain : a journal of neurology. 2012;135(Pt 3):900-11. Epub 2012/03/01. doi: 10.1093/brain/awr336. PubMed PMID: 22366800.

8. Confavreux C, Vukusic S. Age at disability milestones in multiple sclerosis. Brain : a journal of neurology. 2006;129:595-605. doi: Doi 10.1093/Brain/Awh714. PubMed PMID: WOS:000235433800005.

9. Confavreux C, Aimard G, Devic M. Course and prognosis of multiple sclerosis assessed by the computerized data processing of 349 patients. Brain : a journal of neurology. 1980;103(2):281-300. Epub 1980/06/01. doi: 10.1093/brain/103.2.281. PubMed PMID: 7397479.

10. Runmarker B, Andersen O. Prognostic factors in a multiple sclerosis incidence cohort with twenty-five years of follow-up. Brain : a journal of neurology. 1993;116 (Pt 1):117-34. Epub 1993/02/01. doi: 10.1093/brain/116.1.117. PubMed PMID: 8453453.

11. Weinshenker BG, Bass B, Rice GP, Noseworthy J, Carriere W, Baskerville J, Ebers GC. The natural history of multiple sclerosis: a geographically based study. I. Clinical course and disability. Brain : a journal of neurology. 1989;112 (Pt 1):133-46. Epub 1989/02/01. doi: 10.1093/brain/112.1.133. PubMed PMID: 2917275.

12. Ragonese P, Aridon P, Salemi G, D'Amelio M, Savettieri G. Mortality in multiple sclerosis: a review. European journal of neurology : the official journal of the European Federation of Neurological Societies. 2008;15(2):123-7. Epub 2008/01/26. doi: 10.1111/j.1468-1331.2007.02019.x. PubMed PMID: 18217882.

13. Bronnum-Hansen H, Koch-Henriksen N, Stenager E. Trends in survival and cause of death in Danish patients with multiple sclerosis. Brain : a journal of neurology. 2004;127(Pt 4):844-50. Epub 2004/02/13. doi: 10.1093/brain/awh104. PubMed PMID: 14960501.

14. Rao SM, Leo GJ, Ellington L, Nauertz T, Bernardin L, Unverzagt F. Cognitive dysfunction in multiple sclerosis. II. Impact on employment and social functioning. Neurology. 1991;41(5):692-6. Epub 1991/05/01. doi: 10.1212/wnl.41.5.692. PubMed PMID: 1823781.

15. Kobelt G, Eriksson J, Phillips G, Berg J. The burden of multiple sclerosis 2015: Methods of data collection, assessment and analysis of costs, quality of life and symptoms. Multiple sclerosis. 2017;23(2_suppl):4-16. Epub 2017/06/24. doi: 10.1177/1352458517708097. PubMed PMID: 28643592.

16. Julian LJ, Vella L, Vollmer T, Hadjimichael O, Mohr DC. Employment in multiple sclerosis. Exiting and re-entering the work force. J Neurol. 2008;255(9):1354-60. Epub 2008/08/05. doi: 10.1007/s00415-008-0910-y. PubMed PMID: 18677639; PubMed Central PMCID: PMCPMC3057081.

17. Thompson AJ, Banwell BL, Barkhof F, Carroll WM, Coetzee T, Comi G, Correale J, Fazekas F, Filippi M, Freedman MS, Fujihara K, Galetta SL, Hartung HP, Kappos L, Lublin FD, Marrie RA, Miller AE, Miller DH, Montalban X, Mowry EM, Sorensen PS, Tintore M, Traboulsee AL, Trojano M, Uitdehaag BMJ, Vukusic S, Waubant E, Weinshenker BG, Reingold SC, Cohen JA. Diagnosis of multiple sclerosis: 2017 revisions of the McDonald criteria. Lancet Neurol. 2018;17(2):162-73. Epub 2017/12/26. doi: 10.1016/S1474-4422(17)30470-2. PubMed PMID: 29275977.

18. Miller DH, Chard DT, Ciccarelli O. Clinically isolated syndromes. Lancet Neurol. 2012;11(2):157-69. Epub 2012/01/24. doi: 10.1016/S1474-4422(11)70274-5. PubMed PMID: 22265211.

19. Fisniku LK, Brex PA, Altmann DR, Miszkiel KA, Benton CE, Lanyon R, Thompson AJ, Miller DH. Disability and T2 MRI lesions: a 20-year follow-up of patients with relapse onset of multiple sclerosis. Brain : a journal of neurology. 2008;131(Pt 3):808-17. Epub 2008/02/01. doi: 10.1093/brain/awm329. PubMed PMID: 18234696.

20. Compston A, Coles A. Multiple sclerosis. Lancet. 2008;372(9648):1502-17. doi: 10.1016/S0140-6736(08)61620-7. PubMed PMID: 18970977.

21. Korn T. Pathophysiology of multiple sclerosis. J Neurol. 2008;255 Suppl 6:2-6. Epub 2009/03/28. doi: 10.1007/s00415-008-6001-2. PubMed PMID: 19300953.

22. Grigoriadis N, van Pesch V, Paradig MSG. A basic overview of multiple sclerosis immunopathology. European journal of neurology : the official journal of the European Federation of Neurological Societies. 2015;22 Suppl 2:3-13. Epub 2015/09/17. doi: 10.1111/ene.12798. PubMed PMID: 26374508.

23. Lassmann H. Multiple sclerosis: Is there neurodegeneration independent from inflammation? J Neurol Sci. 2007;259(1-2):3-6. doi: DOI 10.1016/j.jns.2006.08.016. PubMed PMID: WOS:000248617400002.

24. Frischer JM, Weigand SD, Guo Y, Kale N, Parisi JE, Pirko I, Mandrekar J, Bramow S, Metz I, Bruck W, Lassmann H, Lucchinetti CF. Clinical and pathological insights into the dynamic nature of the white matter multiple sclerosis plaque. Annals of neurology. 2015;78(5):710-21. Epub 2015/08/05. doi: 10.1002/ana.24497. PubMed PMID: 26239536; PubMed Central PMCID: PMCPMC4623970.

25. Hauser SL, Oksenberg JR. The neurobiology of multiple sclerosis: Genes, inflammation, and neurodegeneration. Neuron. 2006;52(1):61-76. doi: DOI 10.1016/j.neuron.2006.09.011. PubMed PMID: WOS:000241408100005.

26. van der Valk P, De Groot CJA. Staging of multiple sclerosis (MS) lesions: pathology of the time frame of MS. Neuropath Appl Neuro. 2000;26(1):2-10. doi: DOI 10.1046/j.1365-2990.2000.00217.x. PubMed PMID: WOS:000085846200002.

27. De Stefano N, Matthews PM, Filippi M, Agosta F, De Luca M, Bartolozzi ML, Guidi L, Ghezzi A, Montanari E, Cifelli A, Federico A, Smith SM. Evidence of early cortical atrophy in MS: relevance to white matter changes and disability. Neurology. 2003;60(7):1157-62. Epub 2003/04/12. doi: 10.1212/01.wnl.0000055926.69643.03. PubMed PMID: 12682324.

28. Fu L, Matthews PM, De Stefano N, Worsley KJ, Narayanan S, Francis GS, Antel JP, Wolfson C, Arnold DL. Imaging axonal damage of normal-appearing white matter in multiple sclerosis. Brain : a journal of neurology. 1998;121:103-13. doi: DOI 10.1093/brain/121.1.103. PubMed PMID: WOS:000071727300008.

29. Ge Y, Grossman RI, Udupa JK, Wei L, Mannon LJ, Polansky M, Kolson DL. Brain atrophy in relapsing-remitting multiple sclerosis and secondary progressive multiple sclerosis: longitudinal quantitative analysis. Radiology. 2000;214(3):665-70. Epub 2000/03/14. doi: 10.1148/radiology.214.3.r00mr30665. PubMed PMID: 10715027.

30. De Stefano N, Giorgio A, Battaglini M, Rovaris M, Sormani MP, Barkhof F, Korteweg T, Enzinger C, Fazekas F, Calabrese M, Dinacci D, Tedeschi G, Gass A, Montalban X, Rovira A, Thompson A, Comi G, Miller DH, Filippi M. Assessing brain atrophy rates in a large population of untreated multiple sclerosis subtypes. Neurology. 2010;74(23):1868-76. Epub 2010/06/10. doi: 10.1212/WNL.0b013e3181e24136. PubMed PMID: 20530323.

31. Magliozzi R, Howell O, Vora A, Serafini B, Nicholas R, Puopolo M, Reynolds R, Aloisi F. Meningeal B-cell follicles in secondary progressive multiple sclerosis associate with early onset of disease and severe cortical pathology. Brain : a journal of neurology. 2007;130:1089-104. doi: Doi 10.1093/Brain/Awm038. PubMed PMID: WOS:000246293300019.

32. Bevan RJ, Evans R, Griffiths L, Watkins LM, Rees MI, Magliozzi R, Allen I, McDonnell G, Kee R, Naughton M, Fitzgerald DC, Reynolds R, Neal JW, Howell OW. Meningeal inflammation and cortical demyelination in acute multiple sclerosis. Annals of neurology. 2018;84(6):829-42. Epub 2018/10/27. doi: 10.1002/ana.25365. PubMed PMID: 30362156.

33. Howell OW, Reeves CA, Nicholas R, Carassiti D, Radotra B, Gentleman SM, Serafini B, Aloisi F, Roncaroli F, Magliozzi R, Reynolds R. Meningeal inflammation is widespread and linked to cortical pathology in multiple sclerosis. Brain : a journal of neurology. 2011;134:2755-71. doi: Doi 10.1093/Brain/Awr182. PubMed PMID: WOS:000294959800028.

34. Confavreux C, Vukusic S, Moreau T, Adeleine P. Relapses and progression of disability in multiple sclerosis. The New England journal of medicine. 2000;343(20):1430-8. Epub 2000/11/18. doi: 10.1056/NEJM200011163432001. PubMed PMID: 11078767.

35. Rae-Grant A, Day GS, Marrie RA, Rabinstein A, Cree BAC, Gronseth GS, Haboubi M, Halper J, Hosey JP, Jones DE, Lisak R, Pelletier D, Potrebic S, Sitcov C, Sommers R, Stachowiak J, Getchius TSD, Merillat SA, Pringsheim T. Comprehensive systematic review summary: Disease-modifying therapies for adults with multiple sclerosis: Report of the Guideline Development, Dissemination, and Implementation Subcommittee of the American Academy of Neurology. Neurology. 2018;90(17):789-800. Epub 2018/04/25. doi: 10.1212/WNL.0000000000005345. PubMed PMID: 29686117.

36. Fogarty E, Schmitz S, Tubridy N, Walsh C, Barry M. Comparative efficacy of disease-modifying therapies for patients with relapsing remitting multiple sclerosis: Systematic review and network meta-analysis. Mult Scler Relat Disord. 2016;9:23-30. Epub 2016/09/21. doi: 10.1016/j.msard.2016.06.001. PubMed PMID: 27645339.

37. Rubin SM. Management of multiple sclerosis: an overview. Dis Mon. 2013;59(7):253-60. Epub 2013/06/22. doi: 10.1016/j.disamonth.2013.03.012. PubMed PMID: 23786659.

38. D'Amico E, Ziemssen T, Cottone S. To stop or not to stop disease modifying therapies in secondary progressive multiple sclerosis, that is the question. Expert Rev Neurother. 2017;17(9):847-9. Epub 2017/06/09. doi: 10.1080/14737175.2017.1340831. PubMed PMID: 28594298.

39. Wolinsky JS, Arnold DL, Bar-Or A, de Seze J, Giovannoni G, Hemmer B, Rammohan K, Chin P, Fontoura P, Garren H, Masterman D, Sauter A, Montalban X, Porter A. Efficacy of ocrelizumab in patients with PPMS with and without T1 gadolinium-enhancing lesions at baseline in a phase III placebo-controlled trial (LB148). Mult Scler J, 22 (2016), pp. 67-68.

40. Montalban X, Hauser SL, Kappos L, Arnold DL, Bar-Or A, Comi G, de Seze J, Giovannoni G, Hartung HP, Hemmer B, Lublin F, Rammohan KW, Selmaj K, Traboulsee A, Sauter A, Masterman D, Fontoura P, Belachew S, Garren H, Mairon N, Chin P, Wolinsky JS, Investigators OC. Ocrelizumab versus Placebo in Primary Progressive Multiple Sclerosis. The New England journal of medicine. 2017;376(3):209-20. Epub 2016/12/22. doi: 10.1056/NEJMoa1606468. PubMed PMID: 28002688.

41. Rudick R, Polman C, Clifford D, Miller D, Steinman L. Natalizumab: bench to bedside and beyond. Jama Neurol. 2013;70(2):172-82. Epub 2012/11/07. doi: 10.1001/jamaneurol.2013.598. PubMed PMID: 23128399.

42. Polman CH, O'Connor PW, Havrdova E, Hutchinson M, Kappos L, Miller DH, Phillips JT, Lublin FD, Giovannoni G, Wajgt A, Toal M, Lynn F, Panzara MA, Sandrock AW, Investigators A. A randomized, placebo-controlled trial of natalizumab for relapsing multiple sclerosis. The New England journal of medicine. 2006;354(9):899-910. Epub 2006/03/03. doi: 10.1056/NEJMoa044397. PubMed PMID: 16510744.

43. Miller DH, Khan OA, Sheremata WA, Blumhardt LD, Rice GP, Libonati MA, Willmer-Hulme AJ, Dalton CM, Miszkiel KA, O'Connor PW, International Natalizumab Multiple Sclerosis Trial G. A controlled trial of natalizumab for relapsing multiple sclerosis. The New England journal of medicine. 2003;348(1):15-23. Epub 2003/01/03. doi: 10.1056/NEJMoa020696. PubMed PMID: 12510038.

44. Kleinschmidt-DeMasters BK, Tyler KL. Progressive multifocal leukoencephalopathy complicating treatment with natalizumab and interferon beta-1a for multiple sclerosis. The New England journal of medicine. 2005;353(4):369-74. Epub 2005/06/11. doi: 10.1056/NEJMoa051782. PubMed PMID: 15947079.

45. Kleinschmidt-DeMasters BK, Miravalle A, Schowinsky J, Corboy J, Vollmer T. Update on PML and PML-IRIS occurring in multiple sclerosis patients treated with natalizumab. J Neuropathol Exp Neurol. 2012;71(7):604-17. Epub 2012/06/20. doi: 10.1097/NEN.0b013e31825caf2c. PubMed PMID: 22710964.

46. Post-marketing data from Biogen. URL: https://www.globenewswire.com/news-release/2019/09/12/1914566/0/en/New-Research-Demonstrate-Biogen-s-Continued-Commitment-to-Improve-Care-of-Patients-with-Multiple-Sclerosis-Across-Treatment-Spectrum.html. Website visited October 2019.

47. Abrahams E. Right drug-right patient-right time: personalized medicine coalition. Clin Transl Sci. 2008;1(1):11-2. Epub 2008/05/01. doi: 10.1111/j.1752-8062.2008.00003.x. PubMed PMID: 20443813; PubMed Central PMCID: PMCPMC5439586.

48. Redekop WK, Mladsi D. The faces of personalized medicine: a framework for understanding its meaning and scope. Value Health. 2013;16(6 Suppl):S4-9. Epub 2013/09/27. doi: 10.1016/j.jval.2013.06.005. PubMed PMID: 24034312.

49. Yeh RW, Kramer DB. Decision Tools to Improve Personalized Care in Cardiovascular Disease: Moving the Art of Medicine Toward Science. Circulation. 2017;135(12):1097-100. Epub 2017/03/23. doi: 10.1161/CIRCULATIONAHA.116.024247. PubMed PMID: 28320801; PubMed Central PMCID: PMCPMC5363276.

50. Lassmann H, Bruck W, Lucchinetti C. Heterogeneity of multiple sclerosis pathogenesis: implications for diagnosis and therapy. Trends Mol Med. 2001;7(3):115-21. Epub 2001/04/05. PubMed PMID: 11286782.

51. Disanto G, Berlanga AJ, Handel AE, Para AE, Burrell AM, Fries A, Handunnetthi L, De Luca GC, Morahan JM. Heterogeneity in multiple sclerosis: scratching the surface of a complex disease. Autoimmune Dis. 2010;2011:932351. Epub 2011/01/05. doi: 10.4061/2011/932351. PubMed PMID: 21197462; PubMed Central PMCID: PMCPMC3005811.

52. Derfuss T. Personalized medicine in multiple sclerosis: hope or reality? Bmc Med. 2012;10:116. Epub 2012/10/06. doi: 10.1186/1741-7015-10-116. PubMed PMID: 23035757; PubMed Central PMCID: PMCPMC3523020.

53. Gafson A, Craner MJ, Matthews PM. Personalised medicine for multiple sclerosis care. Multiple sclerosis. 2017;23(3):362-9. Epub 2016/09/28. doi: 10.1177/1352458516672017. PubMed PMID: 27672137.

54. Buck D, Hemmer B. Biomarkers of treatment response in multiple sclerosis. Expert Rev Neurother. 2014;14(2):165-72. Epub 2014/01/07. doi: 10.1586/14737175.2014.874289. PubMed PMID: 24386967.

55. Miller DH. Biomarkers and surrogate outcomes in neurodegenerative disease: lessons from multiple sclerosis. NeuroRx. 2004;1(2):284-94. Epub 2005/02/18. doi: 10.1602/neurorx.1.2.284. PubMed PMID: 15717029; PubMed Central PMCID: PMCPMC534945.

56. Ziemann U, Wahl M, Hattingen E, Tumani H. Development of biomarkers for multiple sclerosis as a neurodegenerative disorder. Prog Neurobiol. 2011;95(4):670-85. Epub 2011/04/29. doi: 10.1016/j.pneurobio.2011.04.007. PubMed PMID: 21524682.

57. Kalincik T, Butzkueven H. The MSBase registry: Informing clinical practice. Multiple sclerosis. 2019:1352458519848965. Epub 2019/05/24. doi: 10.1177/1352458519848965. PubMed PMID: 31120376.

58. Butzkueven H, Chapman J, Cristiano E, Grand'Maison F, Hoffmann M, Izquierdo G, Jolley D, Kappos L, Leist T, Pohlau D, Rivera V, Trojano M, Verheul F, Malkowski JP. MSBase: an international, online registry and platform for collaborative outcomes research in multiple sclerosis. Multiple sclerosis. 2006;12(6):769-74. Epub 2007/02/01. doi: 10.1177/1352458506070775. PubMed PMID: 17263005.

59. Bebo BF, Jr., Fox RJ, Lee K, Utz U, Thompson AJ. Landscape of MS patient cohorts and registries: Recommendations for maximizing impact. Multiple sclerosis. 2018;24(5):579-86. Epub 2017/03/11. doi: 10.1177/1352458517698250. PubMed PMID: 28279128; PubMed Central PMCID: PMCPMC5987851.

60. Nickerson M, Marrie RA. The multiple sclerosis relapse experience: patient-reported outcomes from the North American Research Committee on Multiple Sclerosis (NARCOMS) Registry. BMC Neurol. 2013;13:119.

Epub 2013/09/11. doi: 10.1186/1471-2377-13-119. PubMed PMID: 24016260; PubMed Central PMCID: PMCPMC3848753.

61. Amato MP, Portaccio E. Clinical outcome measures in multiple sclerosis. J Neurol Sci. 2007;259(1-2):118-22. Epub 2007/03/23. doi: 10.1016/j.jns.2006.06.031. PubMed PMID: 17376487.

62. Prosperini L, Gallo V, Petsas N, Borriello G, Pozzilli C. One-year MRI scan predicts clinical response to interferon beta in multiple sclerosis. European Journal of Neurology. 2009;16(11):1202-9. doi: DOI 10.1111/j.1468-1331.2009.02708.x. PubMed PMID: WOS:000270900700009.

63. Rio J, Rovira A, Tintore M, Sastre-Garriga J, Castillo J, Auger C, Nos C, Comabella M, Tur C, Vidal A, Montalban X. Evaluating the response to glatiramer acetate in relapsing-remitting multiple sclerosis (RRMS) patients. Mult Scler J. 2014;20(12):1602-8. doi: 10.1177/1352458514527863. PubMed PMID: WOS:000344136400009.

64. Sormani MP, Rio J, Tintore M, Signori A, Li D, Cornelisse P, Stubinski B, Stromillo ML, Montalban X, De Stefano N. Scoring treatment response in patients with relapsing multiple sclerosis. Mult Scler J. 2013;19(5):605-12. doi: 10.1177/1352458512460605. PubMed PMID: WOS:000318253100014.

65. Sormani MP, Li DK, Bruzzi P, Stubinski B, Cornelisse P, Rocak S, De Stefano N. Combined MRI lesions and relapses as a surrogate for disability in multiple sclerosis. Neurology. 2011;77(18):1684-90. doi: 10.1212/WNL.0b013e31823648b9. PubMed PMID: 21975200.

66. Rio J, Castillo J, Rovira A, Tintore M, Sastre-Garriga J, Horga A, Nos C, Comabella M, Aymerich X, Montalban X. Measures in the first year of therapy predict the response to interferon beta in MS. Multiple sclerosis. 2009;15(7):848-53. doi: 10.1177/1352458509104591. PubMed PMID: WOS:000267186300010.

67. Rio J, Rovira A, Tintore M, Huerga E, Nos C, Tellez N, Tur C, Comabella M, Montalban X. Relationship between MRI lesion activity and response to IFN-beta in relapsing-remitting multiple sclerosis patients. Multiple sclerosis. 2008;14(4):479-84. doi: 10.1177/1352458507085555. PubMed PMID: WOS:000256882100007.

68. Hyun JW, Kim SH, Jeong IH, Ahn SW, Huh SY, Park MS, Eom YI, Joo IS, Cho JY, Cho EB, Min JH, Kim BJ, Kim NH, Oh J, Park KD, Kim HJ. Utility of the rio score and modified rio score in korean patients with multiple sclerosis. PLoS One. 2015;10(5):e0129243. doi: 10.1371/journal.pone.0129243. PubMed PMID: 26010897; PubMed Central PMCID: PMCPMC4444088.

69. Rio J, Comabella M, Montalban X. Multiple sclerosis: current treatment algorithms. Curr Opin Neurol. 2011;24(3):230-7. doi: 10.1097/WCO.0b013e328346bf66. PubMed PMID: 21499098.

70. Kurtzke JF. Rating neurologic impairment in multiple sclerosis: an expanded disability status scale (EDSS). Neurology. 1983;33(11):1444-52. PubMed PMID: 6685237.

71. Muzio L, Martino G, Furlan R. Multifaceted aspects of inflammation in multiple sclerosis: The role of microglia. Journal of neuroimmunology. 2007;191(1-2):39-44. doi: DOI 10.1016/j.jneuroim.2007.09.016. PubMed PMID: WOS:000251521900006.

72. Sriram S, Rodriguez M. Indictment of the microglia as the villain in multiple sclerosis. Neurology. 1997;48(2):464-70. PubMed PMID: WOS:A1997WH53500031.

73. Lassmann H, van Horssen J. The molecular basis of neurodegeneration in multiple sclerosis. Febs Lett. 2011;585(23):3715-23. doi: DOI 10.1016/j.febslet.2011.08.004. PubMed PMID: WOS:000297318000016.

74. Cosenza-Nashat M, Zhao ML, Suh HS, Morgan J, Natividad R, Morgello S, Lee SC. Expression of the translocator protein of 18 kDa by microglia, macrophages and astrocytes based on immunohistochemical

localization in abnormal human brain. Neuropath Appl Neuro. 2009;35(3):306-28. doi: DOI 10.1111/j.1365-2990.2008.01006.x. PubMed PMID: WOS:000265556600007.

75. Banati RB, Newcombe J, Gunn RN, Cagnin A, Turkheimer F, Heppner F, Price G, Wegner F, Giovannoni G, Miller DH, Perkin GD, Smith T, Hewson AK, Bydder G, Kreutzberg GW, Jones T, Cuzner ML, Myers R. The peripheral benzodiazepine binding site in the brain in multiple sclerosis - Quantitative in vivo imaging of microglia as a measure of disease activity. Brain : a journal of neurology. 2000;123:2321-37. doi: DOI 10.1093/brain/123.11.2321. PubMed PMID: WOS:000165413200014.

76. Venneti S, Lopresti BJ, Wiley CA. The peripheral benzodiazepine receptor (Translocator protein 18kDa) in microglia: from pathology to imaging. Prog Neurobiol. 2006;80(6):308-22. Epub 2006/12/13. doi: 10.1016/j.pneurobio.2006.10.002. PubMed PMID: 17156911; PubMed Central PMCID: PMCPMC1849976.

77. Wadsworth H, Jones PA, Chau WF, Durrant C, Fouladi N, Passmore J, O'Shea D, Wynn D, Morisson-Iveson V, Ewan A, Thaning M, Mantzilas D, Gausemel I, Khan I, Black A, Avory M, Trigg W. [F-18]GE-180: A novel fluorine-18 labelled PET tracer for imaging Translocator protein 18 kDa (TSPO). Bioorg Med Chem Lett. 2012;22(3):1308-13. doi: DOI 10.1016/j.bmcl.2011.12.084. PubMed PMID: WOS:000300404200002.

78. Owen DR, Yeo AJ, Gunn RN, Song K, Wadsworth G, Lewis A, Rhodes C, Pulford DJ, Bennacef I, Parker CA, StJean PL, Cardon LR, Mooser VE, Matthews PM, Rabiner EA, Rubio JP. An 18-kDa Translocator Protein (TSPO) polymorphism explains differences in binding affinity of the PET radioligand PBR28. J Cerebr Blood F Met. 2012;32(1):1-5. doi: DOI 10.1038/jcbfm.2011.147. PubMed PMID: WOS:000299010000002.

79. Colasanti A, Guo Q, Muhlert N, Giannetti P, Onega M, Newbould RD, Ciccarelli O, Rison S, Thomas C, Nicholas R, Muraro PA, Malik O, Owen DR, Piccini P, Gunn RN, Rabiner EA, Matthews PM. In Vivo Assessment of Brain White Matter Inflammation in Multiple Sclerosis with (18)F-PBR111 PET. Journal of nuclear medicine : official publication, Society of Nuclear Medicine. 2014;55(7):1112-8. Epub 2014/06/07. doi: 10.2967/jnumed.113.135129. PubMed PMID: 24904112.

80. Datta G, Colasanti A, Kalk N, Owen D, Scott G, Rabiner EA, Gunn RN, Lingford-Hughes A, Malik O, Ciccarelli O, Nicholas R, Nei L, Battaglini M, Stefano ND, Matthews PM. (11)C-PBR28 and (18)F-PBR111 Detect White Matter Inflammatory Heterogeneity in Multiple Sclerosis. Journal of nuclear medicine : official publication, Society of Nuclear Medicine. 2017;58(9):1477-82. Epub 2017/03/18. doi: 10.2967/jnumed.116.187161. PubMed PMID: 28302760.

81. Sucksdorff M, Rissanen E, Tuisku J, Nuutinen S, Paavilainen T, Rokka J, Rinne J, Airas L. Evaluation of the Effect of Fingolimod Treatment on Microglial Activation Using Serial PET Imaging in Multiple Sclerosis. Journal of nuclear medicine : official publication, Society of Nuclear Medicine. 2017;58(10):1646-51. Epub 2017/03/25. doi: 10.2967/jnumed.116.183020. PubMed PMID: 28336784.

82. Versijpt J, Debruyne JC, Van Laere KJ, De Vos F, Keppens J, Strijckmans K, Achten E, Slegers G, Dierckx RA, Korf J, De Reuck JL. Microglial imaging with positron emission tomography and atrophy measurements with magnetic resonance imaging in multiple sclerosis: a correlative study. Mult Scler J. 2005;11(2):127-34. doi: Doi 10.1191/1352458505ms1140oa. PubMed PMID: WOS:000227717400001.

83. Debruyne JC, Versijpt J, Van Laere KJ, De Vos F, Keppens J, Strijckmans K, Achten E, Slegers G, Dierckx RA, Korf J, De Reuck JL. PET visualization of microglia in multiple sclerosis patients using [C-11]PK11195. European Journal of Neurology. 2003;10(3):257-64. doi: DOI 10.1046/j.1468-1331.2003.00571.x. PubMed PMID: WOS:000182651000009.

84. Politis M, Giannetti P, Su P, Turkheimer F, Keihaninejad S, Wu K, Waldman A, Malik O, Matthews PM, Reynolds R, Nicholas R, Piccini P. Increased PK11195 PET binding in the cortex of patients with MS correlates with disability. Neurology. 2012;79(6):523-30. PubMed PMID: WOS:000307458800011.

85. Feeney C, Scott G, Raffel J, Roberts S, Coello C, Jolly A, Searle G, Goldstone AP, Brooks DJ, Nicholas RS, Trigg W, Gunn RN, Sharp DJ. Kinetic analysis of the translocator protein positron emission tomography ligand [(18)F]GE-180 in the human brain. Eur J Nucl Med Mol Imaging. 2016;43(12):2201-10. Epub 2016/06/29. doi: 10.1007/s00259-016-3444-z. PubMed PMID: 27349244; PubMed Central PMCID: PMCPMC5047949.

86. Raz N, Rodrigue KM. Differential aging of the brain: Patterns, cognitive correlates and modifiers. Neurosci Biobehav R. 2006;30(6):730-48. doi: 10.1016/j.neubiorev.2006.07.001. PubMed PMID: WOS:000241208800003.

87. Cole JH, Ritchie SJ, Bastin ME, Valdes Hernandez MC, Munoz Maniega S, Royle N, Corley J, Pattie A, Harris SE, Zhang Q, Wray NR, Redmond P, Marioni RE, Starr JM, Cox SR, Wardlaw JM, Sharp DJ, Deary IJ. Brain age predicts mortality. Mol Psychiatry. 2017. doi: 10.1038/mp.2017.62. PubMed PMID: 28439103.

88. Cole JH, Leech R, Sharp DJ, Init AsDN. Prediction of Brain Age Suggests Accelerated Atrophy after Traumatic Brain Injury. Annals of neurology. 2015;77(4):571-81. doi: 10.1002/ana.24367. PubMed PMID: WOS:000352102500004.

89. Secord AA, Coleman RL, Havrilesky LJ, Abernethy AP, Samsa GP, Cella D. Patient-reported outcomes as end points and outcome indicators in solid tumours. Nat Rev Clin Oncol. 2015;12(6):358-70. doi: 10.1038/nrclinonc.2015.29. PubMed PMID: WOS:000355253200008.

90. Lipscomb J, Gotay CC, Snyder CF. Patient-reported outcomes in cancer: a review of recent research and policy initiatives. CA Cancer J Clin. 2007;57(5):278-300. doi: 10.3322/CA.57.5.278. PubMed PMID: 17855485.

91. Heidenreich PA, Spertus JA, Jones PG, Weintraub WS, Rumsfeld JS, Rathore SS, Peterson ED, Masoudi FA, Krumholz HM, Havranek EP, Conard MW, Williams RE, Cons COR. Health status identifies heart failure outpatients at risk for hospitalization or death. J Am Coll Cardiol. 2006;47(4):752-6. doi: 10.1016/j.jacc.2005.11.021. PubMed PMID: WOS:000235422900011.

92. Derfuss T. Personalized medicine in multiple sclerosis: hope or reality? Bmc Med. 2012;10. doi: Artn 116, 10.1186/1741-7015-10-116. PubMed PMID: WOS:000312393100001.

Chapter 2

Relapses and MRI Activity on Natalizumab Predict Short-term but not Long-term Disability Progression

II.1 ABSTRACT

Background: In people with multiple sclerosis treated with β-interferons or glatiramer acetate, new MRI lesions and relapses during the first year of treatment predicts a poor prognosis. This supports the practice, common among neurologists, of switching medications if patients experience significant breakthrough inflammatory activity. However, the studies associating new MRI lesions and relapses with poor prognosis are often limited by short follow-up duration. The association has also not been studied in those receiving natalizumab.

Objective: To evaluate whether relapses or MRI activity after starting natalizumab treatment predicts long-term disability progression.

Methods: Data were collected on relapses, new MRI activity, and Modified Rio Score (composite measure of relapses and MRI activity) after initiation of natalizumab in an observational cohort of 161 people with multiple sclerosis. These were correlated with Expanded Disability Status Scale (EDSS) progression at years 1, 2, 3, and 3-7 after treatment initiation, versus pre-treatment baseline.

Results: The cohort had high baseline disability, with a mean pre-treatment EDSS of 4.2 ± 1.8. 46/161 patients had a relapse in the first year after natalizumab initiation and 44/161 had EDSS progression by year 2. Relapses and Modified Rio Score in the first year of treatment predicted EDSS progression at year 1 and 2 after treatment initiation. However, this effect disappeared with longer follow-up. Instead there was a paradoxical trend towards inflammatory activity on treatment predicting a *lower* risk of EDSS progression by years 3-7, although this did not reach statistical significance. Those with and without EDSS progression did not differ in baseline

age, EDSS, or pre-treatment relapse rate. Relapses in year 0-1 predicted further relapses in years 1-3.

Conclusions: Breakthrough inflammatory activity after natalizumab treatment is predictive of short-term outcome measures of relapses or EDSS progression but not longer-term EDSS progression in this cohort of people with multiple sclerosis.

Publication outcome: Study published in *PLOS One* with the thesis author as first author.[1]

II.2 ABBREVIATIONS

CI	Confidence interval
EDSS	Expanded Disability Status Scale
MS	Multiple sclerosis
NS	Not statistically significant.
OR	Odds ratio
SD	Standard deviation

II.3 INTRODUCTION

In recent years, a number of new disease-modifying therapies have emerged for patients with multiple sclerosis (MS) with relapsing disease.[2] Most disease-modifying therapies demonstrated reductions in MRI activity in phase 2 studies, and reductions in relapse frequency in phase 3 studies along with a variable effect on time to disability progression. The principal argument for their long term use is that treatments that target inflammatory activity are expected to improve long term disability outcomes, at least at a population level.[3, 4]

These principles have been extended to the clinical management of MS patients at an individual level, where it is hypothesised that on-treatment breakthrough inflammatory activity is a prognostic marker for poor long-term disability outcomes.[5] This is supported by observational studies on therapies interferon-beta and glatiramer acetate, where early on-treatment relapses, MRI activity, and Kurtzke Expanded Disability Status Scale (EDSS) disability progression have been shown to predict poor medium-term clinical outcomes of relapses and/or EDSS progression in individuals.[6-12] For example, Rio and colleagues showed that combined scores of MRI lesions, relapses, and/or EDSS progression after interferon-beta initiation predicted further EDSS progression at two years.[10] Similarly, combined scores of MRI lesions and relapses after glatiramer acetate predict 'clinical activity' (defined as relapses or EDSS progression) after 2 years.[7] Most of these studies are limited in that their follow-up periods were between 2-3 years.[7-12] The applicability of these results to other therapies such as dimethyl fumarate, teriflunomide, fingolimod, cladribine, alemtuzumab, natalizumab and ocrelizumab is also uncertain.

If on-treatment breakthrough inflammatory activity does predict poor long-term disability outcomes, the next step would be to evaluate whether switching treatments can improve long-term prognosis, as proposed by the 'no evidence of disease activity' approach.[13] However, for the treating physician, it is currently unclear whether on-treatment inflammatory breakthrough activity should trigger a change in medication, or not.

Natalizumab is a highly active therapy that is widely used in patients with relapsing MS. It is effective in reducing relapses, MRI activity, and time to EDSS progression with a higher efficacy than interferon-beta.[14, 15] The objective of this observational study was to evaluate whether early relapses or MRI activity after starting natalizumab treatment predicts EDSS progression at later time points.

II.4 METHODOLOGY

II.4.1 Data collection

Data were collected from an observational cohort of 204 patients initiating natalizumab between March 2007 and October 2010 at Imperial College Healthcare NHS Trust, with up to 7 years of follow-up. Data on relapse rate and EDSS were prospectively documented at routine 6-monthly clinic visits. EDSS data were collected until December 2014. MRI was routinely performed prior to initiation of natalizumab treatment and at one year after natalizumab initiation. Data were retrospectively collated for the purpose of this study by examining patient healthcare records. Patients were excluded if they had less than three years follow-up or were treated with natalizumab for less than one year.

Data were analysed as part of a clinical audit, registered and ethically approved at Imperial College Healthcare NHS Trust, for which written informed consent was not required (Audit registration number 1987-2015).

II.4.2 Early markers of inflammatory disease activity

Relapses were defined as '*a new symptom or worsening of an old symptom accompanied by a new neurologic abnormality, lasting at least 24 hours in the absence of fever and preceded by stability or improvement for at least 30 days*'.[16] MRI activity was defined as the presence of 1 or more new or enlarging lesions on T2-weighted MRI, relative to the baseline MRI scan, and was assessed by a consultant neuroradiologist with experience in MS. A previously published scoring system which combines MRI and relapse activity was also applied to this first year after natalizumab therapy, which employs more stringent criteria to define new MRI activity (Modified Rio Score; Table 1).[8]

Modified Rio Score scoring criteria		
	Change over 1st year	**Score**
MRI	≤ 4 new T2 lesions	0
	> 4 new T2 lesions	1
Relapse	No relapses	0
	1 relapse	1
	≥ 2 relapses	2
Score = MRI criterion + relapse criterion		

Table 1: Modified Rio Score[8]. Minimum score is 0 (≤ 4 new T2 lesions and no relapses). Maximum score is 3 (> 4 new T2 lesions and ≥ 2 relapses).

II.4.3 Disease progression

Disability progression was defined as an increase of 1 EDSS point in those with EDSS <5.5, or an increase of 0.5 EDSS points in those with EDSS ≥5.5. EDSS progression was confirmed over 6 months at repeat clinic visits. Patients were labelled as disability progression responders and non-responders after 1 year of treatment ('Year 1 EDSS Progression'). This was repeated after 2 years, 3 years, and 3-7 years, by comparing the latest available EDSS rating (up to 7 years after treatment initiation) with the pre-natalizumab EDSS.

II.4.4 Statistical analysis

Demographic data are presented as mean +/- standard deviation (SD). Difference between means was assessed using unpaired *t* test after testing for normality of the data. To investigate the association between early markers of disease activity and disability progression, data were analysed in Kaplan-Meier curves using Log-Rank test and Cox regression, and also in 2x2 contingency tables using Fisher's exact test with odds ratios (OR) and 95% confidence intervals (CI) calculated. Chi-squared test for trend was used for 3x2 contingency tables of the Modified Rio Score and for analysis of change in categorical data over time. Corrections for multiple comparisons were not made, since comparisons were complementary and a consistency of results was apparent between different groups.[17, 18] For the purpose of displaying results in graphical format, results were converted to percentages. A logical regression multivariable model was also used to investigate for multivariate associations that predict disability outcomes. SPSS and R statistical package were used for these analyses.

II.4.5 Contribution to work

Joel Raffel[1, 2]	Led on overall scientific direction of project. Collated data, performed data analysis and interpretation of results. Supervised Arie Gafson during data collection. Wrote the manuscript published in *PLOS One*, adapted for thesis chapter.[1]
Arie Gafson[1, 2]	Contributed to data collection from 2014 onwards.
Samer Dahdaleh[2]	Contributed to data collection prior to 2014.
Omar Malik[2]	Consultant responsible for significant number of patients included in this cohort. Reviewed text prior to submission of *PLOS One* paper.
Brynmor Jones[2]	Radiologist responsible for categorising number of new MRI lesions for each participant. Reviewed text prior to submission of *PLOS One* paper.
Richard Nicholas[1, 2]	Consultant responsible for significant number of patients included in this cohort. Initial conceptualisation of this project. Overall responsibility and supervision of the project throughout.

1 Division of Brain Sciences, Faculty of Medicine, Imperial College London, London, United Kingdom.

2 Imperial College Healthcare NHS Trust, London, United Kingdom.

II.5 RESULTS

II.5.1 Study population

During the study period, 204 patients started natalizumab treatment. Subjects were excluded from analysis if they had discontinued natalizumab within 1 year (n = 16), if there were less than 3 years of clinical follow-up data (n = 20), or if there were insufficient clinical or radiological data (n = 7), leaving 161 patients for analysis. Of these, 127 received natalizumab

throughout the study period, 9 stopped natalizumab after 1+ year of treatment and switched to a new disease-modifying therapy, and 25 stopped natalizumab after 1+ year of treatment but did not receive new disease-modifying therapy (Figure 8). No differences existed in demographic, clinical and MRI data between those included in and excluded from the study. There were no differences between Year 3-7 EDSS Progression Responder and Year 3-7 EDSS Progression Non-Responder cohorts, other than the expected difference in most recent EDSS (Table 2). Logistic regression multivariable analysis that included age, sex, disease duration, number of previous treatments, pre-natalizumab relapse rate, and pre-natalizumab EDSS confirmed that none of these baseline measures predicted response to treatment (see Section II.5.5).

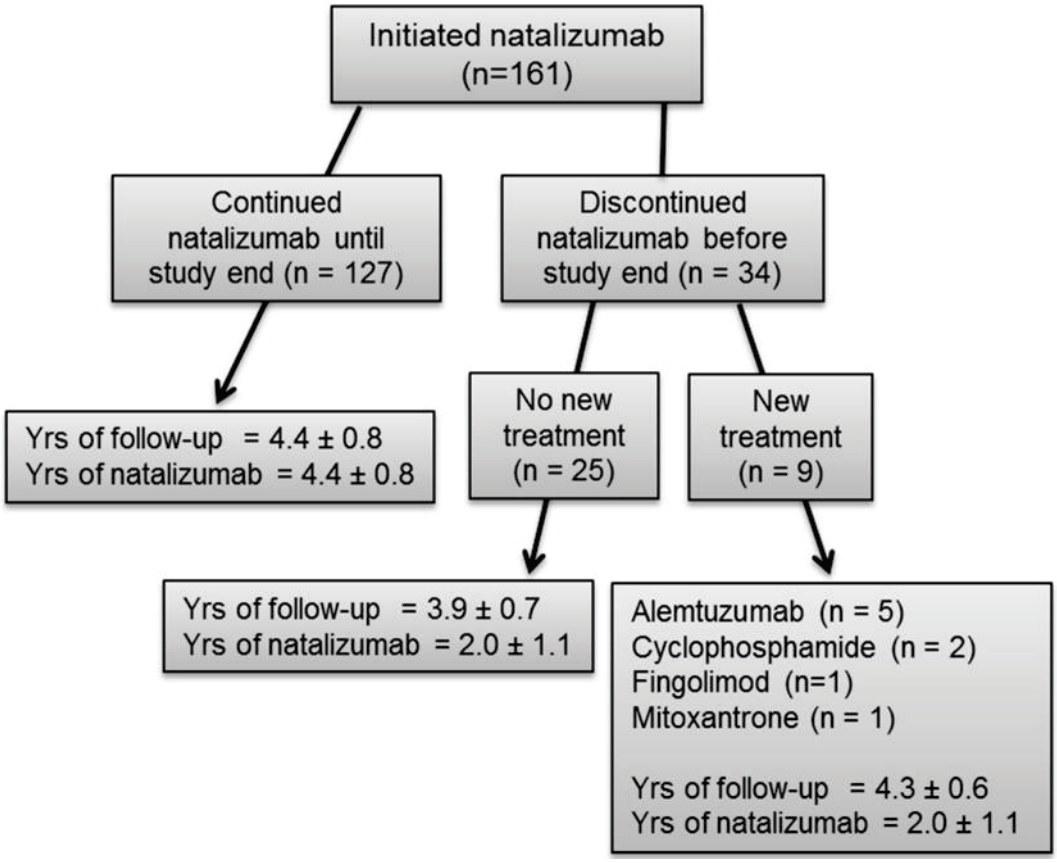


Figure 8: Flowchart of participants. 161 participants were included in all analyses. The treatment pathway and mean follow-up time (years ± SD).

	Full Cohort	Year 3-7 EDSS Progression Responders	Year 3-7 EDSS Progression Non-Responders
Sample size (n)	161	101	60
Mean age (years)	40.6 ± 10.2	39.7 ± 10.8	42.1 ± 9.1
Sex			
Female	101 (63%)	67 (66%)	34 (57%)
Male	60 (37%)	34 (34%)	26 (43%)
Disease duration (years)	8.9 ± 6.1	8.7 ± 6.0	9.4 ± 6.2
Number of previous treatments			
0	42 (26%)	30 (30%)	12 (20%)
1	89 (55%)	52 (51%)	37 (62%)
2	21 (13%)	14 (14%)	7 (12%)
3	8 (5%)	4 (4%)	4 (7%)
4	1 (1%)	1 (1%)	0
Relapses 2 years prior to natalizumab	3.0 ± 1.3	3.0 ± 1.3	2.9 ± 1.2
Pre natalizumab EDSS	4.2 ± 1.8	4.1 ± 1.9	4.4 ± 1.6
Most recent EDSS	4.5 ± 2.0	3.7 ± 2.0	5.8 ± 1.4 ****
Years of follow-up after natalizumab	4.3 ± 0.8	4.3 ± 0.8	4.3 ± 0.9

Table 2: Characteristics of study cohort. When divided into Year 3-7 EDSS Progression Responders and Non-Responders, there were no significant differences between characteristics, other than the expected difference in 'most recent EDSS' (** = $p < 0.0001$). Values presented as mean ± SD unless otherwise stated. Percentages are rounded to the nearest integer. EDSS = Expanded Disability Status Scale**

II.5.2 **Markers of inflammatory disease do not affect disability progression**

46 of 161 patients had a relapse in the first year, and 28 of 161 had new MRI activity. Modified Rio Score was '0' in 116 patients, '1' in 34 patients, and '2' in 16 patients. Markers of inflammatory disease in the first year (Modified Rio Score, relapses, MRI activity) and second year (relapses) had no significant effect on disability progression when tested as a survival analysis (**Modified Rio Score year 0-1**: risk ratio 1.15, log-rank $p = 0.74$, Cox regression $p = 0.44$; **Relapses year 0-1**: risk ratio 1.3, log-rank $p = 0.31$, Cox regression $p = 0.31$; **MRI activity year 0-1**: risk ratio 0.64, log-rank $p = 0.21$, Cox regression $p = 0.24$; **Relapses year 1-2:** risk ratio 1.17, log-rank $p = 0.51$, Cox regression $p = 0.51$; Figure 9A-D). On visual inspection of Kaplan-Meier curves, those with low Modified Rio Scores and those without relapses in year 0-1 appeared to have lower risk of disability progression in the first two years, but not after longer follow-up (Figure 9A-B).

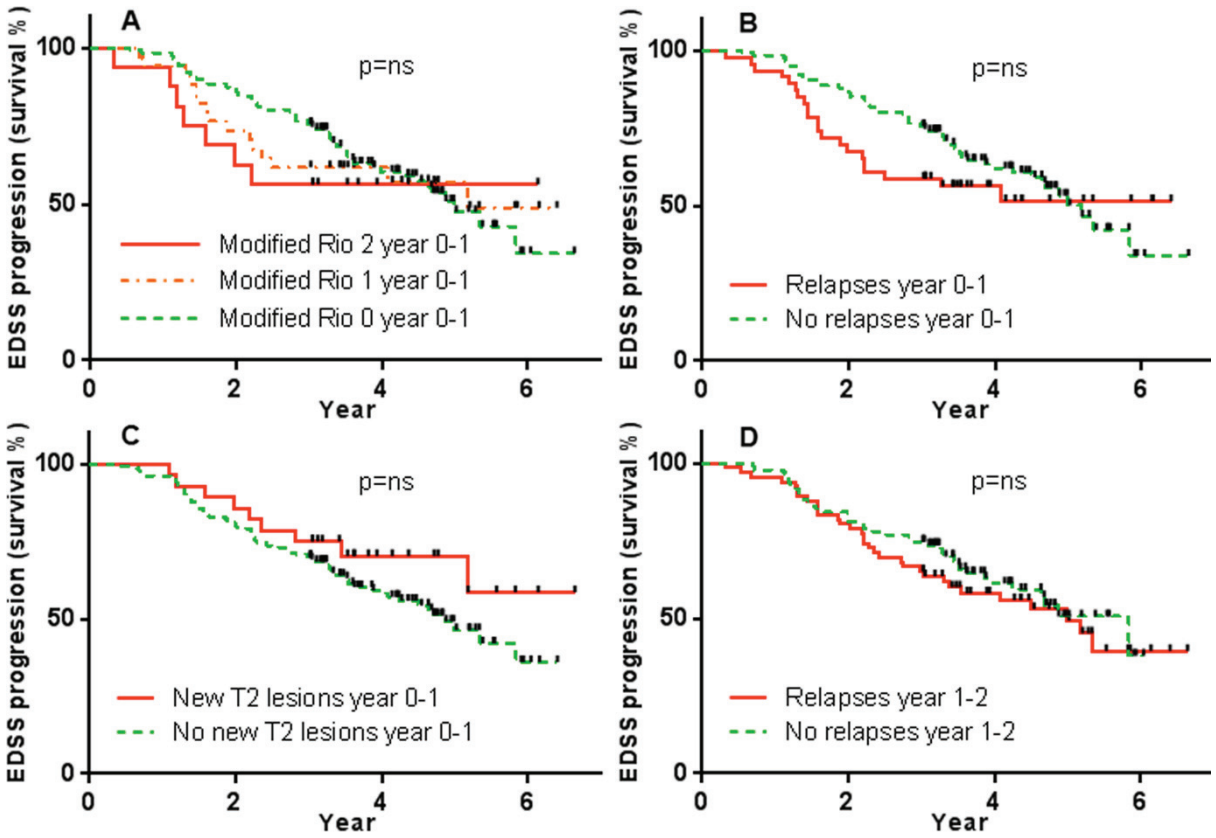


Figure 9: On-treatment inflammatory disease activity does not affect long-term disability progression, tested as survival analysis. First year after natalizumab initiation Modified Rio Score (A), relapses (B), and MRI activity (C), and second year after natalizumab initiation relapses (D), versus survival from EDSS progression over time. Black markers on survival lines represent the duration of follow-up data for those participants who have not undergone EDSS progression (i.e. the time of subject censorship in survival analysis). EDSS = Expanded Disability Status Scale. ns = not statistically significant.

II.5.3 Modified Rio Score predicts short-term but not medium-term disability progression

A limitation of Kaplan-Meier curves is that events (in this case disability progression) are treated as irreversible, which is inappropriate given that EDSS can improve with treatment. In addition, it was observed that curves converge and cross in both the Modified Rio Score and relapses survival analyses (Figure 9A-B), suggesting that any association between inflammatory biomarkers and disability progression may change over time. Therefore,

contingency tables were used to investigate the relationship between inflammatory biomarkers and EDSS progression at specific time points of years 1, 2, 3, and 3-7.

Modified Rio Score in the first year of treatment predicted EDSS progression at year 1 and 2 (**Year 1**: 15/111 vs 9/34 vs 5/16 EDSS progression for those with Modified Rio Score of 0, 1, 2 respectively. Modified Rio Score 1, OR 2.3, 95% CI 0.9 - 5.9; Modified Rio Score 2, OR 2.9, 95% CI 0.9 - 9.6; $p < 0.05$. **Year 2**: 25/111 vs 12/34 vs 7/16 EDSS progression for those with Modified Rio Score of 0, 1, 2 respectively. Modified Rio Score 1, OR 1.9, 95% CI 0.8 - 4.3; Modified Rio Score 2, OR 2.7, 95% CI 0.9 - 7.9; $p < 0.05$; Figure 10A to B). However, it did not predict EDSS progression at year 3, or year 3-7 (**Year 3**: 35/111 vs 12/34 vs 6/16 EDSS progression for those with Modified Rio Score of 0, 1, 2 respectively. Modified Rio Score 1, OR 1.2, 95% CI 0.4 - 2.7; Modified Rio Score 2, OR 1.3, 95% CI 0.4 - 3.9; $p = 0.57$; **Year 3-7**: 45/111 vs 12/34 vs 3/16 EDSS progression for those with Modified Rio Score of 0, 1, 2 respectively. Modified Rio Score 1, OR 0.8, 95% CI 0.4 - 1.8; Modified Rio Score 2, OR 0.3, 95% CI 0.1 - 1.3; $p = 0.11$; Figure 10C-D). If anything, there was a paradoxical trend towards *lower* Modified Rio Score predicting EDSS progression in years 3-7, although this was not statistically significant (Figure 10D). This shift over time in the polarity of the predictive value of Modified Rio Score on disability was caused by year-on-year increases in the proportion of non-responders within the Modified Rio Score 0 group ($p < 0.0001$), versus no significant year-on-year change in the proportion of non-responders within the Modified Rio Score 1-2 group ($p = 0.90$).

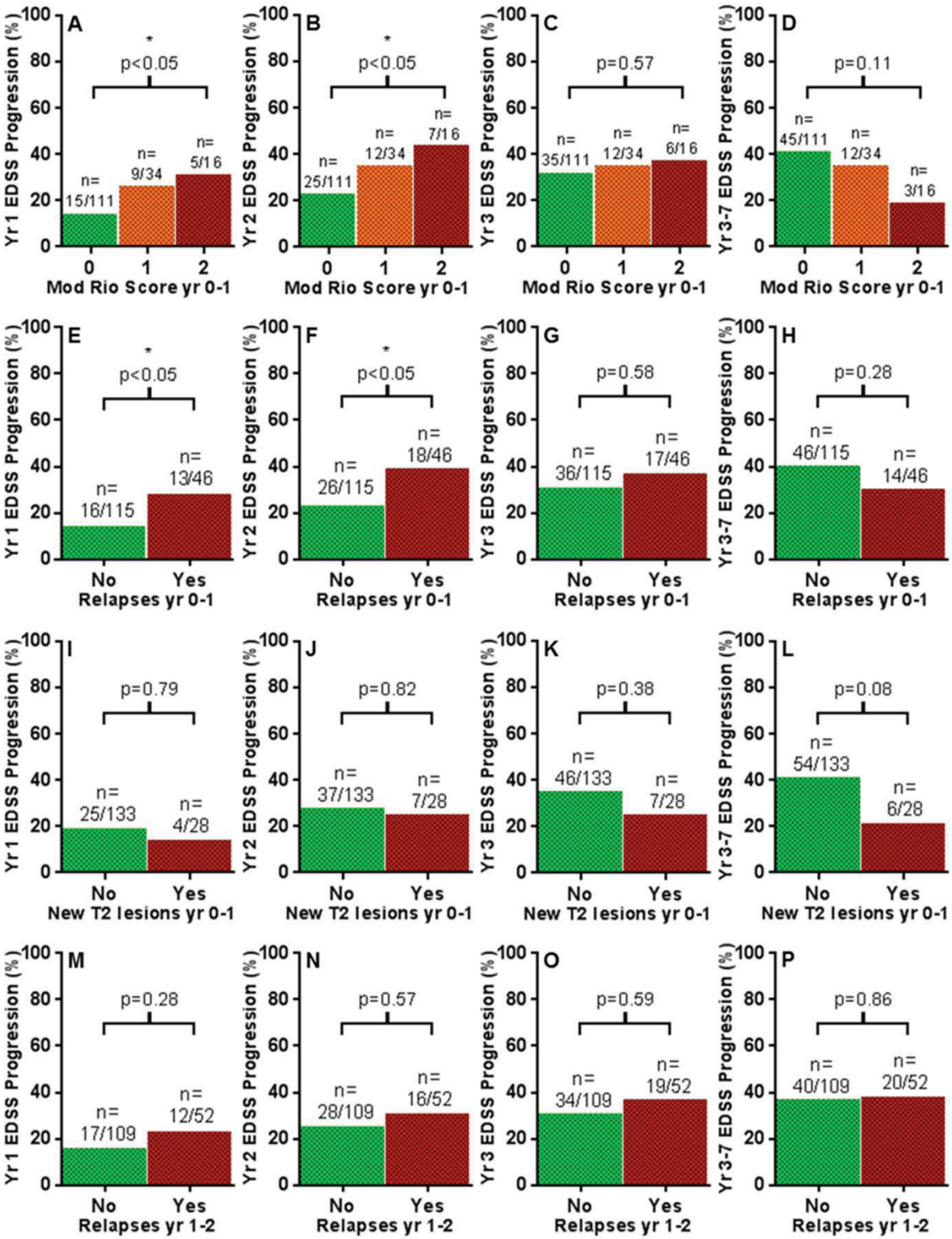


Figure 10: On-treatment inflammatory disease activity predicts short-term but not long-term disability outcomes. Early measures of on-treatment inflammatory disease in first year (A-L) and second year (M-P) after treatment initiation, versus percentage of future EDSS Progression in year 1 (A, E, I, M), year 2 (B,

F, J, N), year 3 (C, G, K, O), and years 3-7 (D, H, L, P). * denotes $p < 0.05$. 'Modified Rio Score' = Modified Rio Score. EDSS = Expanded Disability Status Scale.

II.5.4 Relapses and MRI activity predict short-term but not medium-term disability progression

Similar trends were observed when studying on-treatment relapses and MRI activity in isolation. Relapses in the first year of treatment predicted EDSS progression at year 1 and 2 (**Year 1**: 16/115 vs 13/48 EDSS progression for those without and with relapses respectively. OR 2.4, 95% CI 1.1 - 5.6, $p < 0.05$. **Year 2**: 26/115 vs 18/48 EDSS progression for those without and with relapses respectively. OR 2.2, 95% CI 1.1 - 4.6, $p < 0.05$; Figure 10E-F). However, they did not predict EDSS progression at year 3, or years 3-7 (**Year 3**: 36/115 vs 17/48 EDSS progression for those without and with relapses respectively. OR 1.3, 95% CI 0.6 - 2.6, $p = 0.58$. **Year 3-7**: 46/115 vs 14/48 EDSS progression for those without and with relapses respectively. OR 0.7, 95% CI 0.3 - 1.4, $p = 0.28$; Figure 10G-H). Again, if anything there was a paradoxical trend towards *lack* of relapses predicting EDSS progression at years 3-7, although this was not statistically significant (Figure 10H). New MRI activity in the first year of treatment did not predict EDSS progression at any future time point (**Year 1**: 25/113 vs 4/28 EDSS progression for those without and with new MRI activity respectively. OR 0.7, 95% CI 0.2 - 2.3, $p = 0.78$ **Year 2**: 37/113 vs 7/28 EDSS progression for those without and with new MRI activity respectively. OR 0.86, 95% CI 0.3 - 2.2, $p = 0.82$. **Year 3**: 46/113 vs 7/28 EDSS progression for those without and with new MRI activity respectively. OR 0.6, 95% CI 0.2 - 1.6, $p = 0.38$. **Year 3-7**: 54/113 vs 6/28 EDSS progression for those without and with new MRI activity respectively. OR 0.4, 95% CI 0.2 - 1.0, $p = 0.08$; Figure 10I-L). Again, there was a paradoxical trend towards *lack* of new MRI activity predicting EDSS progression at years 3-7, although this was not statistically significant (Figure 10L). As before, this shift over time in the

polarity of the predictive value of relapses and MRI activity on disability was caused by year-on-year increases in the proportion of non-responders within the 'no relapses group' ($p < 0.0001$) and 'no new MRI activity group' ($p < 0.0001$), versus no significant year-on-year change in the proportion of non-responders within the 'relapses group' ($p = 0.89$) and the 'new MRI activity group' ($p = 0.54$).

Similarly, the subgroup of patients with new gadolinium-enhancing MRI lesions in the first year of treatment (n = 14) had no difference in EDSS progression in future years (**Year 1:** 25/147 vs 4/14 EDSS progression for those without and with new gadolinium enhancing lesions respectively. OR 2.0, 95% CI 0.6 - 6.7, $p = 0.28$. **Year 2**: 40/147 vs 4/14 EDSS progression for those without and with new gadolinium enhancing lesions respectively. OR 1.1, 95% CI 0.3 - 3.6, $p = 1.0$. **Year 3**: 48/147 vs 4/14 EDSS progression for those without and with new gadolinium enhancing lesions respectively. OR 0.8, 95% CI 0.2 - 2.8, $p = 1.0$. **Year 3-7**: 56/147 vs 4/14 EDSS progression for those without and with new gadolinium enhancing lesions respectively. OR 0.65, 95% CI 0.2 - 2.2, $p = 0.57$). Relapses in the second year of treatment were also unable to predict EDSS progress at future time points (**Year 1**: 17/109 vs 12/52 EDSS progression for those without and with relapses respectively. OR 1.6, 95% CI 0.7 - 3.7, $p = 0.28$. **Year 2**: 28/109 vs 16/52 EDSS progression for those without and with relapses respectively. OR 1.3, 95% CI 0.6 - 2.7, $p = 0.57$. **Year 3**: 34/109 vs 19/52 EDSS progression for those without and with relapses respectively. OR 1.3, 95% CI 0.6 - 2.5, $p = 0.59$. **Year 3-7**: 40/109 vs 20/52 EDSS progression for those without and with relapses respectively. OR 1.1, 95% CI 0.5 - 2.1, $p = 0.86$; Figure 10M-P).

II.5.5 **Results are not affected by change in medication, baseline disability, or neutralising antibodies**

As may be expected, patients with inflammatory activity on natalizumab treatment were more likely to switch to other disease-modifying therapies, such as alemtuzumab, fingolimod, or cyclophosphamide. 8/46 of those with relapses in year 0-1 switched to an alternative treatment at some point during the 3-7 year follow-up period of this study, versus 1/115 of those with no relapses. However, the trends observed in this study remained consistent with subgroup analyses after exclusion of those that switched to other medications (for example as represented in Figure 11). Trends also remained consistent with subgroup analysis restricted to those with baseline EDSS scores <4 (n = 68) or ≥4 (n = 93), and also after exclusion of those with known neutralising antibodies (n = 6). There was no significant difference in mean follow-up time between those with different Modified Rio Scores, or indeed any of the other individual inflammatory measures.

Logistic regression multivariable model considered variables relating to demographics, disease history, and markers of inflammatory disease (age at natalizumab initiation, sex, pre-natalizumab relapse rate, pre-natalizumab MRI lesion count, pre-natalizumab MRI enhancing lesion count, number of previous treatments, post-natalizumab relapse rate, and post-natalizumab new MRI lesions), and found no further predictive relationships for disability outcomes (multiple r-squared: 0.051, $p = 0.46$).

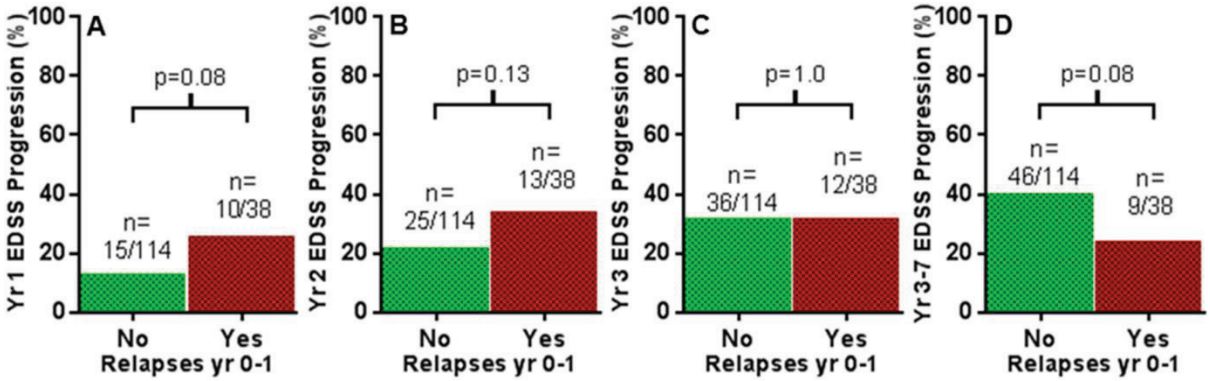


Figure 11: Results remain consistent after exclusion of those who switched from natalizumab to other disease-modifying therapies. On-treatment relapses in first year after treatment initiation versus percentage of future EDSS Progression in year 1 (A), year 2 (B), year 3 (C), and years 3-7 (D). EDSS = Expanded Disability Status Scale.

II.5.6 **Relapses in the first year of treatment with natalizumab predict further relapses**

Relapses in year 0-1 of treatment were correlated with the risk of further relapses in years 1-3. 35 of 115 (30%) with no relapses in year 0-1 reported relapses in years 1-3. In contrast, 31 out of 46 (67%) with relapses in year 0-1 reported relapses in years 1-3 (OR 4.7, 95% CI 2.3 - 9.8, $p < 0.0001$).

II.6 DISCUSSION

This was the first study to report on-treatment predictive measures of long-term disability outcomes in a cohort of patients on natalizumab, and has been published in *PLOS One*.[1] The study finds that relapses and Modified Rio Score in the first year of natalizumab treatment predict year 1 and year 2 EDSS progression. However, this effect disappears after three years of follow-up. If anything, there is a consistent paradoxical trend towards on-treatment relapses, MRI activity, and high Modified Rio Score predicting *better* 3-7 year disability outcomes,

versus pre-treatment baseline EDSS, although this did not reach statistical significance. This shift over time was driven by highly significant year-on-year increases in disability progression specifically in those *without* on-treatment inflammatory activity. In this group it was less likely for the EDSS to worsen in the first 1-2 years, but far more likely for the EDSS to worsen over each subsequent year. Results were consistent when restricted to those who remained on natalizumab throughout the follow-up period. Given this, these data could suggest a disconnect between natalizumab's ability to suppress focal inflammatory activity underlying relapses and new T2 MRI lesions, and its putative effect on the progression of long-term disability.

Previous studies looking at predictive measures of treatment response have tended to focus on earlier generation MS treatments such as β-interferons and glatiramer acetate. Like ours, these studies identified on-treatment MRI activity and relapses as medium-term (≤3 years) prognostic markers of EDSS progression and/or further relapses.[6-12] However, the majority had limited follow up and thus conclusions on long term disability could not be made.[7-12] It would be of interest whether long-term follow-up data from the above studies would find results consistent with ours. Alternatively, it could be that the prognostic importance of relapses and MRI activity differs between β-interferons, glatiramer acetate, and natalizumab treatment.

One should consider why on-treatment inflammatory activity predicts medium-term disability outcomes but may not predict long-term disability outcomes. It is possible that the predictive effect of relapses and MRI activity on short-term EDSS outcomes could reflect a predictive effect on relapse-mediated worsening of disability, which may be fully or partially reversible with sufficient follow-up.[19, 20] Related to this is a potential reporting bias, especially in studies based in the working neurology clinic, where it can be challenging to distinguish relapses from a true worsening of EDSS, and so both may be reported interdependently. This reporting bias

is likely to decrease with long-term follow-up. In addition, the study found that relapses in year 0-1 predict further relapses in years 1-3, in common with several of the above studies, which could again partly reflect a patient reporting bias.[7, 8, 10, 12] Future studies should use long-term disability progression as the preferred primary outcome.

Year 0-1 on-treatment MRI activity did not predict poor disability outcomes at any time point. This supports a post hoc analysis of randomized controlled trial data which showed that natalizumab is clinically effective even in those with on-treatment MRI activity.[21] Of course, some new T2 lesions might have developed before natalizumab became effective, which would dilute the predictive power of this outcome.[22] Future datasets could aim to 're-baseline' the patients with MRI scans performed 6 months after natalizumab initiation.[22] However, since gadolinium enhancing MRI also did not predict poor disability outcomes in the study reported in this chapter, this supports the lack of correlation between new MRI activity and long-term prognosis. Similarly, some relapses in years 0-1 may have developed before natalizumab became effective, but the data on year 1-2 relapses supports the lack of correlation between relapses and long-term prognosis.

Several caveats should be considered for this study. The cohort size is modest, and results should be replicated in larger cohorts. Importantly, the cohort had a high baseline EDSS (mean baseline EDSS 4.2) in comparison to β-interferon and glatiramer acetate studies (mean baseline EDSS 2 to 3), reflecting the fact that at the time of data collection there were limited treatment options available for highly active relapsing-remitting and relapsing-progressive MS. The cohort also had poorer outcomes - 46 of 161 patients had a relapse in the first year and 44/161 had EDSS progression by year 2 - than previously described natalizumab cohorts with less baseline disability such as those in the pivotal randomised controlled trials.[14, 15] It is likely that

some patients had already entered the predominantly progressive stage of disease which is less responsive to treatment.[23, 24] Therefore, within this cohort, it could be that on-treatment breakthrough inflammatory activity is not a poor prognostic marker for long-term disability since it signifies that the patient does have an ongoing treatable focal inflammatory disease component, as opposed to others in the cohort who may have entered a predominantly irreversible neurodegenerative progressive stage of disease. That said, those with on-treatment inflammatory activity had equivalent baseline age and EDSS to those without on-treatment inflammatory activity. In addition, results remained consistent when restricted to those with baseline EDSS <4.

Other caveats arise from the retrospective method of data collation, the potential bias caused by exclusion of those with <1 year of natalizumab treatment, and that follow-up time was variable although always greater than 3 years. Kaplan-Meier curves tended to converge after this 3-year time point, bringing about the possibility that associations were affected by selection bias related to duration of follow-up, although this seems unlikely since follow-up duration was consistent between groups. The observational nature of this study means one cannot speculate whether patients might have gained greater benefit from other treatments. Randomised controlled interventional studies are required to investigate whether those with breakthrough inflammatory activity would benefit from switching to other highly active treatments.

The data presented in this chapter suggest that neither decrease in relapse rate, MRI activity, nor short-term stability of EDSS can be assumed to equate with better long-term prognosis. There is a need for improved biomarkers to predict long-term response to treatment in MS. This supports the rationale for the study reported in Chapter 3, which investigates 18 kDa translocator protein (TSPO) positron emission tomography with the novel radiotracer ^{18}F-

GE180 as a possible biomarker for central nervous system inflammation in MS, and as a possible tool for predicting long-term response to disease-modifying therapy.

II.7 ACKNOWLEDGEMENTS

Thank you to the nurses and administrators at the natalizumab infusion clinic at Charing Cross Hospital for their assistance in collecting the data.

II.8 CONFLICTS OF INTEREST

The thesis author has no conflicts of interest relevant to this chapter.

Dr. Malik has received travel grants to educational meetings from Biogen Idec and honoraria from Biogen Idec, which have been used exclusively for clinical research, outside the submitted work.

Dr Nicholas received funding from GE Healthcare. Dr Nicholas has received outside the submitted work: grants, personal fees and non-financial support from Novartis; grants, personal fees and non-financial support from Biogen Idec; personal fees from Genzyme; and personal fees from Roche.

Other authors declare no conflicts of interest related to this chapter.

II.9 REFERENCES

1. Raffel J, Gafson AR, Dandaleh S, Malik O, Jones B, Nicholas R. Inflammatory Activity on Natalizumab Predicts Short-Term but Not Long-Term Disability in Multiple Sclerosis. Plos One. 2017;12(1). doi: ARTN e0169546, 10.1371/journal.pone.0169546. PubMed PMID: WOS:000391949500051.

2. Ransohoff RM, Hafler DA, Lucchinetti CF. Multiple sclerosis-a quiet revolution. Nat Rev Neurol. 2015;11(3). doi: 10.1038/nrneurol.2015.14. PubMed PMID: WOS:000350771000005.

3. Sormani MP, Bonzano L, Roccatagliata L, Mancardi GL, Uccelli A, Bruzzi P. Surrogate endpoints for EDSS worsening in multiple sclerosis. A meta-analytic approach. Neurology. 2010;75(4):302-9. doi: 10.1212/WNL.0b013e3181ea15aa. PubMed PMID: 20574036.

4. Goodin DS, Reder AT, Ebers GC, Cutter G, Kremenchutzky M, Oger J, Langdon D, Rametta M, Beckmann K, DeSimone TM, Knappertz V. Survival in MS: a randomized cohort study 21 years after the start of the pivotal IFNbeta-1b trial. Neurology. 2012;78(17):1315-22. doi: 10.1212/WNL.0b013e3182535cf6. PubMed PMID: 22496198; PubMed Central PMCID: PMCPMC3335454.

5. Rio J, Comabella M, Montalban X. Multiple sclerosis: current treatment algorithms. Curr Opin Neurol. 2011;24(3):230-7. doi: 10.1097/WCO.0b013e328346bf66. PubMed PMID: 21499098.

6. Prosperini L, Gallo V, Petsas N, Borriello G, Pozzilli C. One-year MRI scan predicts clinical response to interferon beta in multiple sclerosis. European Journal of Neurology. 2009;16(11):1202-9. doi: 10.1111/j.1468-1331.2009.02708.x. PubMed PMID: WOS:000270900700009.

7. Rio J, Rovira A, Tintore M, Sastre-Garriga J, Castillo J, Auger C, Nos C, Comabella M, Tur C, Vidal A, Montalban X. Evaluating the response to glatiramer acetate in relapsing-remitting multiple sclerosis (RRMS) patients. Mult Scler J. 2014;20(12):1602-8. doi: 10.1177/1352458514527863. PubMed PMID: WOS:000344136400009.

8. Sormani MP, Rio J, Tintore M, Signori A, Li D, Cornelisse P, Stubinski B, Stromillo ML, Montalban X, De Stefano N. Scoring treatment response in patients with relapsing multiple sclerosis. Mult Scler J. 2013;19(5):605-12. doi: 10.1177/1352458512460605. PubMed PMID: WOS:000318253100014.

9. Sormani MP, Li DK, Bruzzi P, Stubinski B, Cornelisse P, Rocak S, De Stefano N. Combined MRI lesions and relapses as a surrogate for disability in multiple sclerosis. Neurology. 2011;77(18):1684-90. doi: 10.1212/WNL.0b013e31823648b9. PubMed PMID: WOS:000296590800009.

10. Rio J, Castillo J, Rovira A, Tintore M, Sastre-Garriga J, Horga A, Nos C, Comabella M, Aymerich X, Montalban X. Measures in the first year of therapy predict the response to interferon beta in MS. Multiple sclerosis. 2009;15(7):848-53. doi: 10.1177/1352458509104591. PubMed PMID: WOS:000267186300010.

11. Rio J, Rovira A, Tintore M, Huerga E, Nos C, Tellez N, Tur C, Comabella M, Montalban X. Relationship between MRI lesion activity and response to IFN-beta in relapsing-remitting multiple sclerosis patients. Multiple sclerosis. 2008;14(4):479-84. doi: 10.1177/1352458507085555. PubMed PMID: WOS:000256882100007.

12. Hyun JW, Kim SH, Jeong IH, Ahn SW, Huh SY, Park MS, Eom YI, Joo IS, Cho JY, Cho EB, Min JH, Kim BJ, Kim NH, Oh J, Park KD, Kim HJ. Utility of the rio score and modified rio score in korean patients with multiple sclerosis. PLoS One. 2015;10(5):e0129243. doi: 10.1371/journal.pone.0129243. PubMed PMID: 26010897; PubMed Central PMCID: PMCPMC4444088.

13. Imitola J, Racke MK. Is No Evidence of Disease Activity a Realistic Goal for Patients With Multiple Sclerosis? Jama Neurol. 2015;72(2):145-7. doi: 10.1001/jamaneurol.2014.3860. PubMed PMID: WOS:000349619200003.

14. Polman CH, O'Connor PW, Havrdova E, Hutchinson M, Kappos L, Miller DH, Phillips JT, Lublin FD, Giovannoni G, Wajgt A, Toal M, Lynn F, Panzara MA, Sandrock AW, Investigators A. A randomized, placebo-controlled trial of natalizumab for relapsing multiple sclerosis. New Engl J Med. 2006;354(9):899-910. doi: Doi 10.1056/Nejmoa044397. PubMed PMID: WOS:000235679600003.

15. Rudick RA, Stuart WH, Calabresi PA, Confavreux C, Galetta SL, Radue EW, Lublin FD, Weinstock-Guttman B, Wynn DR, Lynn F, Panzara MA, Sandrock AW, Investigators S. Natalizumab plus interferon beta-1a for relapsing multiple sclerosis. New Engl J Med. 2006;354(9):911-23. doi: Doi 10.1056/Nejmoa044396. PubMed PMID: WOS:000235679600004.

16. Schumacher GA. Problems of experimental trials of therapy in MS: report of the panel on evaluation of experimental trials in MS. Annals of the New York Academy of Sciences, vol. 122, p. 552–68., 1968.

17. Feise RJ. Do multiple outcome measures require p-value adjustment? BMC medical research methodology. 2002;2:8. PubMed PMID: 12069695; PubMed Central PMCID: PMC117123.

18. Saville DJ. Multiple Comparison Procedures - the Practical Solution. Am Stat. 1990;44(2):174-80. doi: Doi 10.2307/2684163. PubMed PMID: WOS:A1990DK47300034.

19. Hirst C, Ingram G, Pearson O, Pickersgill T, Scolding N, Robertson N. Contribution of relapses to disability in multiple sclerosis. J Neurol. 2008;255(2):280-7. Epub 2008/01/22. doi: 10.1007/s00415-008-0743-8. PubMed PMID: 18204919.

20. Lublin FD, Baier M, Cutter G. Effect of relapses on development of residual deficit in multiple sclerosis. Neurology. 2003;61(11):1528-32. Epub 2003/12/10. doi: 10.1212/01.wnl.0000096175.39831.21. PubMed PMID: 14663037.

21. Bates D, Bartholome E. Treatment effect of natalizumab on relapse outcomes in multiple sclerosis patients despite ongoing MRI activity. J Neurol Neurosurg Psychiatry. 2012;83(1):55-60. doi: 10.1136/jnnp-2011-300279. PubMed PMID: 21865211.

22. Dobson R, Rudick RA, Turner B, Schmierer K, Giovannoni G. Assessing treatment response to interferon-beta: is there a role for MRI? Neurology. 2014;82(3):248-54. doi: 10.1212/WNL.0000000000000036. PubMed PMID: 24336144; PubMed Central PMCID: PMCPMC3902760.

23. Leray E, Yaouanq J, Le Page E, Coustans M, Laplaud D, Oger J, Edan G. Evidence for a two-stage disability progression in multiple sclerosis. Brain : a journal of neurology. 2010;133(Pt 7):1900-13. doi: 10.1093/brain/awq076. PubMed PMID: 20423930; PubMed Central PMCID: PMCPMC2892936.

24. Feinstein A, Freeman J, Lo AC. Progressive multiple sclerosis 2 Treatment of progressive multiple sclerosis: what works, what does not, and what is needed. Lancet Neurol. 2015;14(2):194-207. PubMed PMID: WOS:000347869400016.

Chapter 3

18 kDa Translocator Protein Radioligand ^{18}F-GE180 as a Marker of Neuroinflammatory Activity in Multiple Sclerosis

III.1 ABSTRACT

Background: Activated microglia are observed in focal inflammatory lesions and cortical grey matter pathology, and may play a key role in both inflammatory and neurodegenerative disease in multiple sclerosis (MS). ^{18}F-GE180 is a newly developed positron emission tomography (PET) molecular imaging radiotracer that targets the 18 kDa translocator protein (TSPO) receptor on microglia and other cells, and could be used as a marker of response to disease-modifying therapy. At the time at which it was conducted, this was the first study to characterise the performance of ^{18}F-GE180 in humans.

Objective: To investigate the kinetics of the ^{18}F-GE180 ligand and whether it labels its target receptor in the target organ. To evaluate ^{18}F-GE180 PET as a marker for disease activity in MS, and as a surrogate for response to natalizumab treatment.

Methods: 16 subjects with MS completed ^{18}F-GE180 PET at three time points: before, 10 weeks after, and 58 weeks after initiation of natalizumab. 11 healthy controls had one ^{18}F-GE180 PET scan. In addition, a 'blocking study' investigated whether ^{18}F-GE180 PET is actually labelling TSPO: 6 subjects with MS had a baseline ^{18}F-GE180 PET, followed two weeks later by a repeat PET after administration of the potent TSPO ligand XBD-173. A variety of methodological approaches were evaluated, including the gold-standard volume of distribution (V_T).

Results: Administration of ^{18}F-GE180 PET was safe, and well-tolerated by all participants. In total, 71 PET scans were completed, making this the largest study of TSPO PET in MS to date.

A reversible two-tissue compartment model best fitted the data. Unfortunately, the mean regional delivery rate constant K_1 was unexpectedly low (~0.01 mL/cm^3 min−1), suggesting poor extraction (~1%) across the blood-brain barrier. V_T values were correspondingly low – with a whole brain mean of 0.29 ± 0.17 mL/cm^3 in subjects with MS. ^{18}F-GE180 V_T was not able to detect differences in binding affinity relating to a known single nucleotide polymorphism in TSPO.

The MS 'blocking study' suggested that ^{18}F-GE180 V_T does include some specific signal, even if absolute V_T values are low. The non-displaceable distribution volume (V_{ND}) was 0.18 ± 0.05 mL/cm^3 or 0.11 ml/cm^3 using the occupancy plot (not constraining or constraining V_{ND} to be the same for all participants, respectively) and 0.20 ml/cm^3 using the polymorphism plot. On average, V_{ND} accounted for 55% of V_T in the whole brain, suggesting that 45% of V_T represents specific binding.

This allowed cautious exploration of the 'natalizumab cohort' data. V_T was increased in MS lesions at baseline. There was no difference in V_T between MS and healthy controls in other regions of interest. By 58 weeks after natalizumab initiation, V_T had decreased in MS lesions, but not in other regions of interest. There were no associations between PET outcomes and clinical outcomes. The increased ^{18}F-GE180 V_T in lesions was not affected by TSPO binding affinity.

Conclusions: ^{18}F-GE180 has considerably lower extraction across the blood-brain barrier than expected from animal studies and compared to other TSPO tracers. The 'blocking study' suggests that ^{18}F-GE180 does exhibit some specific binding. However, the tracer is still limited by poor signal-to-noise ratio. ^{18}F-GE180 V_T was not able to detect increased TSPO in MS in

the grey matter or normal-appearing white matter as previously reported with other tracers, or differences in TSPO binding affinity as expected. The 'natalizumab cohort' showed increased ^{18}F-GE180 V_T in MS lesions, which is responsive to natalizumab treatment, although these results are considered most likely to reflect changes in blood-brain barrier permeability rather than changes in TSPO expression. Overall, these results lend support to the conclusion that ^{18}F-GE180 is not a useful marker of TSPO expression in healthy controls or people with MS. Other TSPO tracers with improved performance may be useful in evaluating early response to disease-modifying therapy in MS.

Publication outcomes: Results of kinetic analysis in healthy controls published in *The European Journal of Nuclear Medicine and Molecular Imaging* with thesis author as co-author.[1]

Results from the 'blocking cohort' published in *Molecular Imaging and Biology* with the thesis author as 'joint first author'.[2]

^{18}F-GE180 PET results from the 'natalizumab cohort' were initially intended to be the main focus of this thesis. However, given the disappointing pharmacokinetic characteristics of ^{18}F-GE180 as reported in the above two papers, the results of the 'natalizumab cohort' have not been submitted for publication. Additional studies as described in Chapter 4 and Chapter 5 were undertaken by the thesis author *in lieu* of the ^{18}F-GE180 PET analysis from the 'natalizumab cohort'.

III.2 ABBREVIATIONS

ANOVA	One-way analysis of variance
BVMT-R	Brief Visuospatial Memory Test - Revised
CI	Confidence interval
CVLT-II	California Verbal Learning Test II
DMT	Disease-modifying therapy
EDSS	Expanded Disability Status Scale
GM	Grey matter
HAB	High affinity binders
HC	Healthy control
LAB	Low affinity binders
MAB	Mixed affinity binders
MS	Multiple sclerosis
NAWM	Normal-appearing white matter
NS	Not statistically significant
PET	Positron emission tomography
PwMS	People with multiple sclerosis
SD	Standard deviation
SDMT	Symbol Digit Modalities Test
TSPO	18 kDa translocator protein
V_{ND}	Non-displaceable distribution volume
V_S	Specific distribution volume
V_T	Volume of distribution
WM	White matter

III.3 INTRODUCTION

In the previous chapter, data were presented to conclude that clinical relapses and new MRI lesions did not predict long-term disability progression in people with multiple sclerosis (PwMS) on natalizumab treatment. It is still possible that neuroinflammatory activity after treatment is related to long-term prognosis, but that 'relapses' and 'new MRI lesions' are limited as outcome measures in multiple sclerosis (MS), for possible reasons including the following:

- Clinical relapses and new MRI lesions are both somewhat 'blunt instruments' for the quantification of neuroinflammatory activity. They are mostly used as binary outcomes (yes/no), and do not capture the complexity of *in vivo* neuroinflammation, for example the change in inflammatory activity within an individual lesion. The detection of a new relapse or new MRI lesion is also dependent on the location of neuroinflammation.[3-7] The reporting of relapses by patients is subjective and variably reported, and subject to inter-rater variability.[8, 9]

- The time course to develop a new MRI lesion is problematic for assessing the efficacy of a medication. If a subject is assessed 6-months after initiating treatment for example, a 'new' lesion on MRI may reflect disease activity from the first few months of treatment or even preceding treatment.[10]

- More fundamentally, it is possible that 'focal white matter inflammation' is not directly related to the neurodegeneration which accompanies the gradual accumulation of disability in the progressive phase of disease. This neurodegeneration may be

accompanied by a different type of inflammation, compartmentalised within the central nervous system, and located behind a relatively intact blood-brain barrier.[7, 11-15]

This chapter introduces 18 kDa translocator protein (TSPO) PET, which could address some or all of the above issues. The TSPO PET radioligand ^{18}F-GE180 is evaluated as a marker for disease activity in MS, and as a surrogate for response to natalizumab treatment.

III.3.1 Microglia as a marker of disease activity in MS

It is likely that focal white matter inflammation is instigated, in part, by T and B lymphocytes. However, it is activated macrophage/microglial cells that execute the downstream event of myelin phagocytosis.[16] Activated microglia are observed in all established lesions showing active demyelination, and so the presence of microglia is seen as a good indicator of active focal neuroinflammation.[17] An example of microglia in an active white matter lesion is shown in Figure 12.

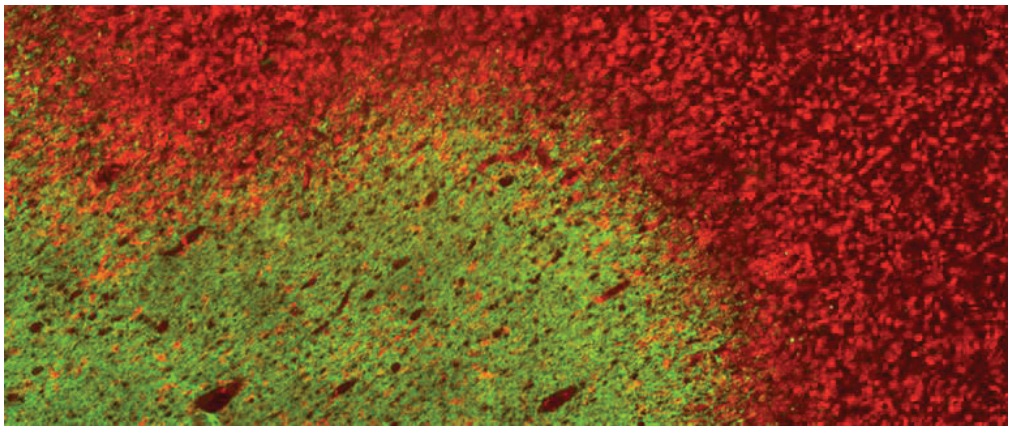


Figure 12: Immunofluorescent stain in white matter lesion of post-mortem human MS brain. Performed by the thesis author using antibody to ionised calcium-binding adapter molecule 1 (which labels activated microglia, red) and antibody to myelin oligodendrocyte glycoprotein (MOG, which labels myelin sheath, green), as previously described.[18]

Activated microglia are also observed in cortical grey matter pathology, and correlate with the degree of meningeal inflammation and cortical demyelination.[14] In recent years, the case for microglia/macrophages playing a key role in neuroaxonal degeneration and progressive disease in MS has grown.[17, 19, 20]

III.3.2 TSPO PET to measure neuroinflammation in MS

Positron emission tomography (PET) is a nuclear medical imaging technique that produces a three-dimensional image of biologically active functional processes in the body. A radiotracer is selected that binds to a specific molecule of choice, and the levels of this molecule can then be visualised. The advent of PET offers advantages over conventional MRI, which produces detailed images of structure, but cannot image biologically active functional processes.

One such molecule that can be visualised by PET imaging is the 18kDa translocator protein (TSPO). TSPO is an outer mitochondrial membrane protein, expressed in the brain and many other tissues, and thought to be involved in mitochondrial 'household' functions such as cholesterol transportation.[21] TSPO PET is considered an *in* vivo marker of neuroinflammation, since TSPO is expressed on microglia and other cells at sites of active CNS pathology.[22-24] TSPO PET signal is upregulated in a variety of neuroinflammatory and neurodegenerative diseases, including Alzheimer's disease,[25, 26] frontotemporal dementia,[27] Parkinson's disease,[28] amyotrophic lateral sclerosis,[29] Huntington's disease,[30] and viral encephalitis.[31, 32]

In tissue studies in MS, TSPO expression is increased in active lesions and at the edges of chronic active lesions, due to the increased density of TSPO-expressing microglia, including

microglia which do not have a traditional 'activated phenotype', and to a lesser extent in astrocytes and occasional B cells.[22, 33, 34]

Clinical TSPO PET studies in MS have shown increased signal within lesions, and in peri-lesional white matter, normal-appearing white matter, and cortical grey matter, with the strength and pattern of TSPO PET signal correlating with clinical outcomes.[23, 35-40] TSPO PET is therefore a promising biomarker for neuroinflammation and neurodegeneration in MS.[41]

III.3.3 TSPO PET for treatment efficacy in MS

TSPO PET signal may be expected to decrease after treatment with any effective disease-modifying therapy (DMT), since microglia are key downstream effector cells in MS.[16] Histological evaluation of microglia activity is used routinely in the assessment of DMT efficacy in animal models of MS. In humans, there is evidence of decreased microglial activity after natalizumab, using a cerebrospinal fluid biomarker.[42] In an animal model of MS, TSPO PET was able to quantitate microglial activation, which diminished after treatment with DMTs.[43] In humans, TSPO PET signal was found to decrease after treatment with glatiramer acetate and fingolimod, although these studies were limited by the low number of participants, and there was no attempt to correlate TSPO PET signal with individual response to treatment.[44, 45] Since TSPO PET could quantify the *rate* of neurodegeneration, it may be able to assess treatment efficacy at a far earlier time point than biomarkers which quantify the *extent* of neurodegeneration such as MRI brain atrophy or optical coherence tomography, as depicted in Figure 13.

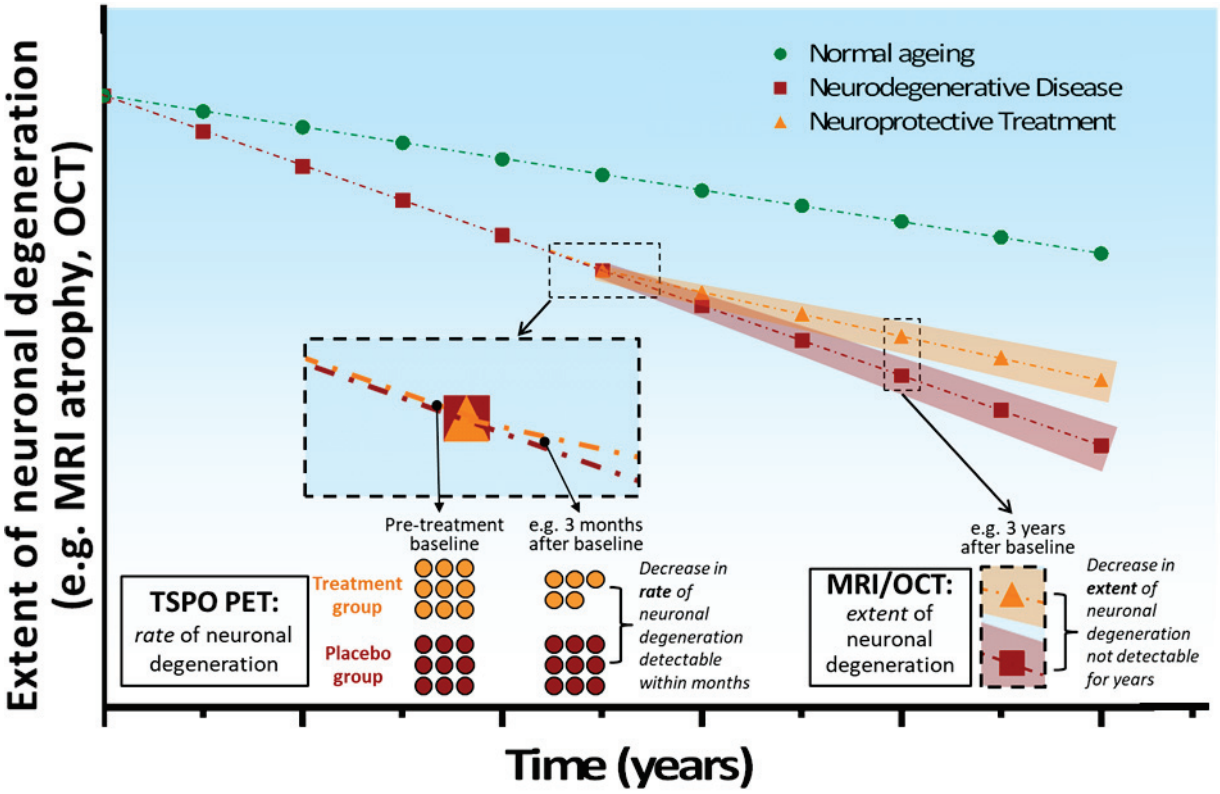


Figure 13: Biomarkers of *in vivo* rate of neurodegeneration should be able to detect treatment effect at earlier time point than biomarkers of *in vivo* extent of neurodegeneration. OCT = optical coherence tomography

TSPO PET is therefore a possible biomarker which could empirically assess disease activity – both inflammatory and neurodegenerative - and therefore could predict long-term response to DMTs in MS. TSPO PET could also be used in the therapeutic pipeline as an early biomarker of a medication's efficacy in MS, and in clinical trials as an early clinical endpoint, especially if it is sensitive to changes in neurodegenerative activity.

III.3.4 ^{18}F-GE180: a novel TSPO PET radiotracer

The aforementioned TSPO PET clinical studies in MS mostly used the TSPO radiotracer [^{11}C]-PK11195. However, [^{11}C]PK-11195 has high nonspecific signal, and requires nonstandard approaches to data analysis.[46-48] In addition, because ^{11}C has a short half-life (20.3 minutes),

[^{11}C]PK-11195 can be used only in locations with on-site cyclotrons.[49]

Several TSPO ligands have recently been developed, with the aim of greater specific binding and improved signal-to-noise ratio. ^{18}F-GE180 (GEH120714) is one such radiotracer. It has several theoretical advantages over [^{11}C]-PK11195, including higher binding potential.[50-52] In rats, the pharmacokinetic profile of ^{18}F-GE180 has higher level of specific binding in TSPO rich organs and brain regions. There is no marked binding of ^{18}F-GE180 in rat brain regions where TSPO is not found such as the striatum. ^{18}F-GE180 also has improved performance over [^{11}C]-PK11195 in regards to brain uptake in animals.[50-52] In addition, it is possible for ^{18}F-GE180 to be manufactured and then transported to hospital sites for use, unlike [^{11}C]-based ligands, thus increasing its clinical and commercial application.

There is a known single nucleotide polymorphism in TSPO, affecting the binding of most PET tracers for the protein, which leads to the stratification of subjects into high, mixed and low affinity binders (HABs/MABs/LABs).[53] *In vitro* data shows that ^{18}F-GE180 should be subject to the same polymorphism in the TPSO gene which affects other 'second generation' tracers, with greatest signal observed in HABs, then MABs, and with very low signal in LABs.[53-55]

III.3.5 ^{18}F-GE180 *in vivo* characteristics: necessity for an ^{18}F-GE180 'blocking study'

Prior to the work undertaken as part of this thesis, ^{18}F-GE180 had yet to be tested in humans, other than an unpublished Phase 1 study to assess safety.[56] Therefore, as an early part of the 'natalizumab study' described below, it was necessary to characterise the tracer kinetics of ^{18}F-GE180 in healthy controls (HCs). As reported under Results (Section III.5), these early pharmacokinetic results suggested that ^{18}F-GE180 has unexpectedly low brain penetration.

Given the disappointing characteristics of ^{18}F-GE180 suggested by these early results, it because important to consider whether the ligand was actually labelling its target receptor in the target organ. If ^{18}F-GE180 does not bind to TSPO in the MS, then of course one cannot use ^{18}F-GE180 to investigate the effect of DMTs on neuroinflammation in the MS brain. An additional study, referred to as the 'blocking study' in this chapter (see methods), was therefore added to the study protocol. Here, the non-displaceable (non-specific) component of the total volume of distribution is estimated for TSPO tracers, allowing the displaceable (specific) component to be derived.[57] In short, for the TSPO ligand of interest, the total volume of distribution is calculated both before and after blockade with the potent TSPO ligand XBD-173 (emapunil), to allow various approaches to derive the non-displaceable component of the volume of distribution. This is described further under the Methodology section.

III.3.6 Study overview

^{18}F-GE180 PET scans were completed in 16 patients with relapsing-remitting MS who were to receive natalizumab for clinical reasons, followed by two further PET scans after natalizumab initiation (week 10 and week 58). ^{18}F-GE180 PET scans were also performed in 11 HCs. In addition, 6 PwMS had a 'blocking study': baseline ^{18}F-GE180 PET, followed two weeks later by a repeat PET after administration of the potent TSPO ligand XBD-173. Other investigations including MRI were performed to further characterise the clinical significance of any change in PET signal.

The 'blocking study' aims to identify whether the ^{18}F-GE180 ligand is labelling TSPO.

The 'natalizumab cohort' aims to provide initial data on the response of ^{18}F-GE180 PET to natalizumab, and its predictive value for clinical response to treatment. The study could provide proof of concept for broader future studies required to confirm definitive clinical utility for TSPO PET in MS therapy response monitoring.

III.4 METHODOLOGY

III.4.1 Study administration

Funder: GE Healthcare collaboratively with Fast Forward LLC

Amount Awarded: £464,519.

Sponsor: Imperial College Healthcare NHS Trust London

Principle Investigator: Dr Richard Nicholas

Location of the research: All procedures involving study participants were undertaken within the sites of the hospitals that form part of Imperial Academic Health Sciences Centre (AHSC) i.e. the Hammersmith Hospital, St Mary's Hospital and Charing Cross Hospital. All MRI and PET scanning was performed at the Hammersmith Hospital site in the Imperial College Clinical Imaging Facility.

III.4.2 Objectives

Primary objectives

- To investigate tracer kinetics and identify whether the ^{18}F-GE180 ligand is labelling its target receptor in the target organ.

- To examine whether there are quantitative changes in TSPO, as measured by ^{18}F-GE180 PET imaging, induced by natalizumab at early (10 weeks) and late (58 weeks) time points in PwMS with active disease.

Secondary objectives

- To compare baseline ^{18}F-GE180 PET signal in MS patients with HCs.
- To correlate quantitative changes in ^{18}F-GE180 PET with markers of clinical response to natalizumab treatment.
- To determine the relationship between TSPO polymorphism and ^{18}F-GE180 signal.

III.4.3 Study hypotheses

- ^{18}F-GE180 will label TSPO in the central nervous system in HCs and PwMS.
- ^{18}F-GE180 TSPO PET signal will be higher in PwMS than aged-matched controls, in lesions, normal-appearing white matter, and normal-appearing grey matter.
- ^{18}F-GE180 TSPO PET signal will correlate with disability in PwMS
- ^{18}F-GE180 TSPO PET signal will decrease after treatment with natalizumab and will predict long-term progression of disability.

III.4.4 'Natalizumab cohort' overview

Subjects with MS underwent baseline MRI and 90-minute dynamic ^{18}F-GE180 PET, MRI, and clinical assessment prior to starting natalizumab. Study activities were repeated 10 weeks (between 3rd and 4th infusion) and 58 weeks (between 13th and 14th infusion) after commencing

natalizumab. HCs visited at baseline only (Figure 14). The study was observational, since participants were due to start natalizumab for clinical reasons, as part of their routine NHS care.

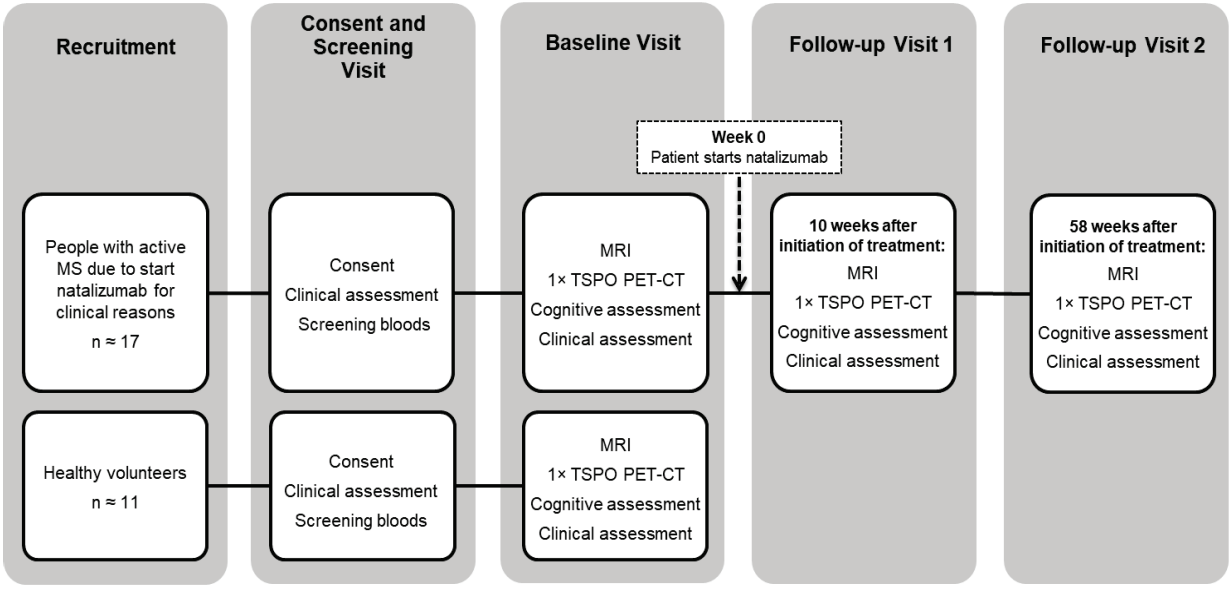


Figure 14: 'Natalizumab cohort' design. TSPO PET-CT = ^{18}F-GE180 PET and computerised tomography scan.

III.4.5 'Blocking study' overview

Subjects with MS underwent baseline MRI and 90-minute dynamic ^{18}F-GE180 PET. One week later, participants returned for a post-block ^{18}F-GE180 PET scan; they were administered a 90mg oral dose of XBD-173 two hours prior to a repeat PET scan (Figure 15).

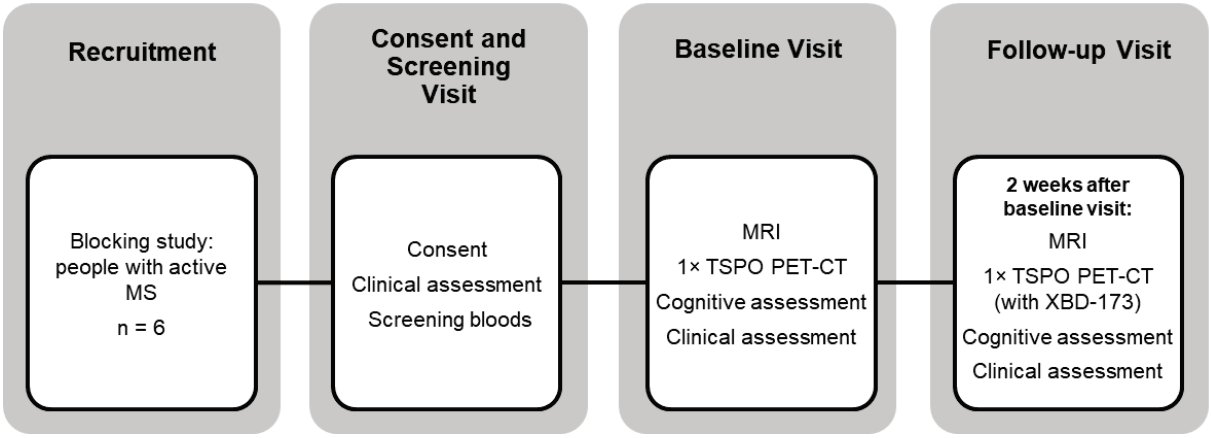


Figure 15: 'Blocking study' design. TSPO PET-CT = ^{18}F-GE180 PET and computerised tomography scan.

III.4.6 Subject recruitment

People with relapsing MS due to start natalizumab for clinical reasons were identified from NHS hospitals with outpatient neurology clinics within Imperial College Healthcare NHS Trust, including Charing Cross Hospital and St Mary's Hospital. Controls were recruited from friends and carers of patients, existing volunteer databases, and through advertisements on Imperial College London noticeboards. Potential study participants were given written and verbal information by an investigator about the study and invited to participate. Subjects were given at least one week to read the participant information sheets, before attending the consent and screening visit. Participants provided written informed consent, under ethics approved by the Westminster Research Ethics Committee, London (13/LO/1596), the Riverside Research Ethics Committee (13/LO/1916, 14/LO/0343), and the Administration of Radioactive Substances Advisory Committee (no. 631/336/30788).

At the screening visit, a blood test was taken for routine clinical laboratory blood tests including full blood count, renal function test, liver function test and clotting profile, and to assess the TSPO polymorphism.

III.4.7 Inclusion and exclusion criteria

Inclusion criteria

- Adequate visual, auditory and communication capabilities, and able to provide informed consent.
- Able to attend all study visits and have a high probability of completing the study in the opinion of the investigator.
- Clinically healthy, with no evidence of active neurological (other than MS), psychiatric, or systemic disease, for at least one month before inclusion in the study, as ascertained by detailed medical history, physical examination, and routine laboratory blood assessment. As a guide, those with chronic ischaemic heart disease, lung disease, liver disease, chronic kidney disease (stage IV or V), vascular disease, or diabetes would be excluded from the study, whereas those with well-controlled asthma, which is not currently active, could be included.
- Not currently on any medication that would interfere with the study or compromise participant safety.
- For women of childbearing potential, the results of a serum or urine human chorionic gonadotropin pregnancy test (performed at screening visit, and immediately prior to any TSPO PET scan) must be negative.

Additional inclusion criteria, healthy controls:

- aged 25-65 years old

Additional inclusion criteria, people with MS

- aged 25-65 years old
- Meet 2010 McDonald criteria for relapsing-remitting MS.[58]

Additional inclusion criteria, people with MS (natalizumab cohort only)

- The subject had decided, with their clinician, to commence natalizumab treatment for clinical reasons. For this, the subject needs to be eligible for NHS treatment with natalizumab under NICE guidelines (NICE Technology appraisal guidance 127)[59] under either of the two following categories:
    - 'Rapidly Evolving Severe MS': patients who have had two or more disabling relapses in one year and one or more gadolinium-enhancing lesions on brain MRI or a significant increase in T2 lesion load compared with a previous MRI

      Or
    - 'Suboptimal therapy group': patients who have failed to respond to a full and adequate course of a beta interferon. Patients should have had at least one relapse in the previous year while on therapy and have at least nine T2-hyperintensive lesions in cranial MRI or at least one gadolinium-enhancing lesion.

Exclusion criteria

- Low ^{18}F-GE180 binding polymorphism of TSPO on screening.
- Structural lesions on MRI.
- Previous participation in research involving nuclear medicine, PET, or other radiological investigations with significant ionizing radiation exposure (>2mSv) in the last 12 months.
- Previous participation in medicinal trial within 4 months of study entry.

- Pregnant or breast-feeding.
- History of alcohol and/or drug abuse within the last 2 years.
- Contraindication for MRI (such as pacemaker, presence of metallic fragments near the eyes or spinal cord, cochlear implant, claustrophobia).
- Contraindication to arterial line insertion (such as positive Allen's test indicating ulnar arterial insufficiency, prolonged prothrombin time).
- History of drug allergy or other allergy that, in the opinion of the investigators, contraindicates their participation in the study.

Withdrawal criteria

Potential participants and their relatives/carers were informed that their participation is entirely voluntary, and that they were free to change their mind or withdraw from the study at any time without needing to give a reason and without prejudicing their medical care in any way.

If a participant who has given informed consent loses capacity to give informed consent, the participant would be withdrawn from the study. A participant that suffers a serious adverse event would be withdrawn from the study.

III.4.8 Sample size considerations

For the 'natalizumab cohort', there were limited data with which to power the study. Previous TSPO PET studies of MS have used sample sizes of between 12 and 22 to show an overall effect of changes in TSPO binding in MS compared with control.[23, 35, 36, 39] The TSPO ligand used in this study, ^{18}F-GE180, was expected to provide increased sensitivity.[51] At study

conception, only one previous study had attempted to measure TSPO PET response to treatment; nine patients were enrolled to show a population-wide decrease in global [^{11}C]-PK11195 signal after glatiramer acetate.[44] However, this study was not powered to correlate individual change in [^{11}C]-PK11195 signal with individual clinical response to the medication. To do this – i.e. to gather enough pilot data to power future studies on the use of PET in predicting treatment response – expert opinion was that 25 patients should be investigated in this longitudinal observational study. After the initial disappointing results from this study relating to the unexpectedly low brain penetration of ^{18}F-GE180,[1] it was decided that the 17 patients that had already enrolled in the study should complete the study (after appropriate discussion with the participant), and that no further subjects should be recruited.

For the 'blocking study', six subjects were recruited, in keeping with previous TSPO blocking studies.[57]

III.4.9 Scanning protocol

^{18}F-GE180 was synthesised as previously described on a FastLab^{TM} platform.[51] Quality assurance checks were performed prior to injection to ensure the product meets specification as laid down by the local product manufacture specifications. A low dose computerised tomography scan was performed for attenuation correction immediately prior to a 90-minute dynamic PET scan on a Siemens Biograph 6 with a field of view of 168 × 168 × 148 mm^3.

The tracer was injected as an intravenous bolus over the course of 30 seconds with a target dose of 185 MBq. List-mode data were histogrammed into 24 frames (6 × 90s, 3 × 180s, 5 × 600s, 5 × 1500s and 5 × 3000s) and reconstructed using filtered back projection with a ramp filter.

Reconstructed voxel size and spatial resolution were 1.57 × 1.57 × 1.92 mm and ~5 mm respectively. Participants were asked to lie with their head still for the 90-minute duration of the scan.

All participants underwent MR scans at each study visit, including T1 magnetisation prepared rapid gradient echo before and after the injection of gadolinium, double-inversion recovery, and phase-sensitive inversion recovery sequences. All experiments were carried out using the same Siemens 3 Tesla Magnetom Verio MRI scanner with a 32-channel head coil. A magnetisation-prepared rapid gradient-echo sequence was used to obtain high-definition T1 weighted scans with the following parameters: repetition time (TR) = 2300ms; echo time (TE) = 3ms; inversion time (TI) = 900ms; 160 slices; voxel size 1x1x1mm, GRAPPA = 2. Double inversion recovery pulse (TR/TE/TI, 7500/325/3000ms, 128 slices, voxel size 1.3x1.3x1.3mm, GRAPPA = 2), and phase sensitive inversion recovery (TR/TE/TI, 10000/9.3/1500ms, 60 slices, voxel size 0.5x0.5x2mm, GRAPPA = 2) sequences were also acquired for the identification of white matter and grey matter lesions.

III.4.10 Arterial plasma measurement

Participants were cannulated in their radial artery and blood was withdrawn continuously at a target rate of 2.5 ml/min from the start of each scan for the first 15 minutes. In addition, six discrete blood samples were drawn at 0, 5, 10, 15, 30, 50, 70 and 90 minutes for metabolite analysis. Tracer concentrations in whole blood and plasma were measured in a well counter and radiometabolite analysis performed using two high performance liquid chromatography systems (Agilent 1260 Infinity and Agilent 110 Series) in isocratic mode. Briefly, samples were spun down to obtain plasma, which was then added to acetonitrile to precipitate proteins. After

centrifugation, the samples were rotary evaporated, analytes collected and reconstituted in 7% ethanol solution and filtered in 15mm syringe filters with a nylon membrane of pore-size 0.2μm. At the end of the PET scanning, the arterial lines were removed.

III.4.11 Image analysis

PET images were reconstructed with scatter correction and measured attenuation correction. PET images underwent frame-to-frame realignment and were co-registered with T1 MRI in PMOD (v3.6, PMOD Technologies Ltd., Switzerland). Co-registrations were quality checked manually. MRI was used to segment the brain into the 83 regions using the Hammers atlas.[60] These regions were inspected manually for overlap and edited where necessary to minimise spill-over from large-vessel vascular activity.

White and grey matter lesions were identified on T1 scans with co-registered double inversion recovery and phase sensitive inversion recovery sequences. Lesions were segmented in T1 space using a customised tool developed by the BioMedIA group at Department of Computing, Imperial College London (Figure 16). The tool makes use of a semi-automated segmentation method based on that of Criminisi *et al*.[61] Lesion masks were also used to derive total lesion volumes.

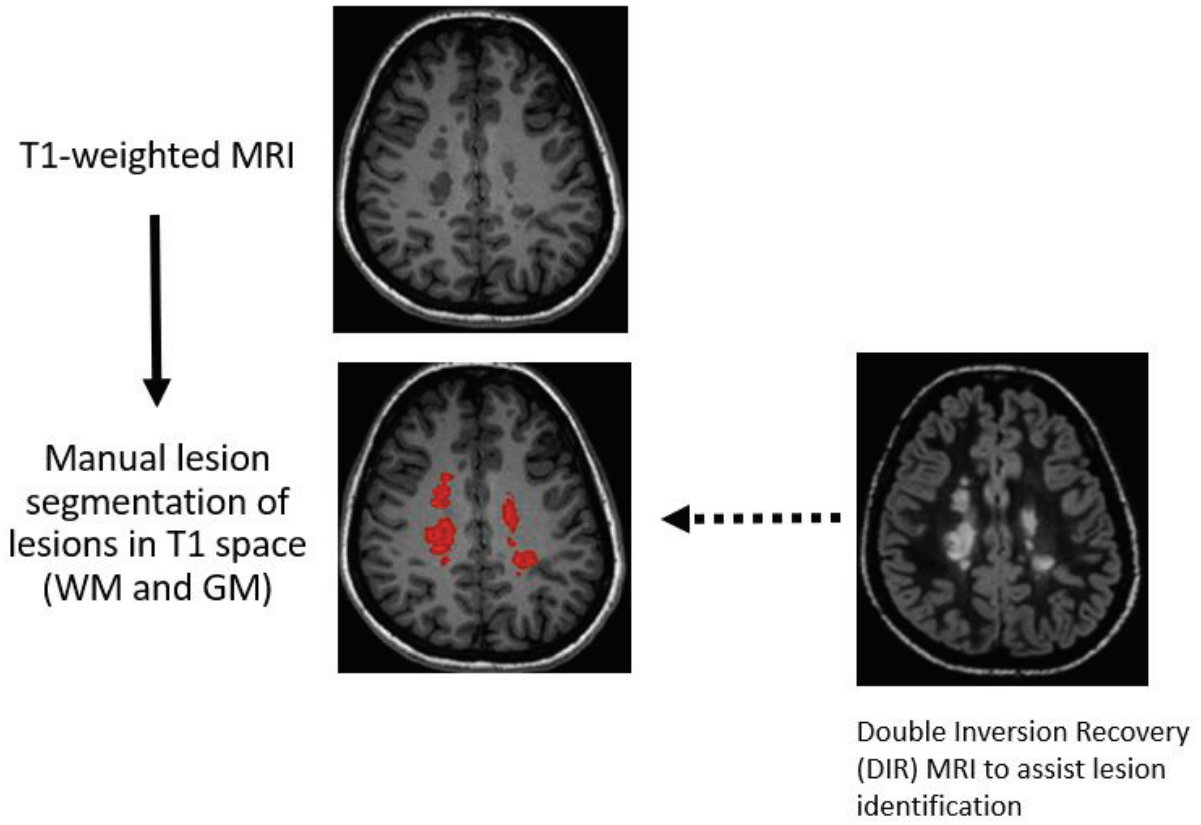


Figure 16: Method for lesion segmentation in T1 space. Co-registered double inversion recovery (as picture above) and phase-sensitive inversion recovery MRI were used to assist in the accurate segmentation of lesions in T1 space. WM = white matter; GM = grey matter.

III.4.12 Kinetic analysis

All kinetic analysis was performed in PMOD. Calibrated continuous and discrete blood data were corrected for decay and the parent fraction of tracer in plasma calculated for each discrete sample. Plasma-over-blood ratios were calculated and the parent fraction of tracer in plasma fitted to a Watabe parent fraction model of the form: $f_{parent}(t) = f_p \cdot \left\{ 1 - \left(\frac{1}{\frac{A^B_u}{u^B + C}} \right) \right\}$. [62] This was multiplied with the continuous whole blood data to produce a metabolite-corrected arterial plasma input function.

Selected regions of interest were chosen for further investigation. These included the thalami, cortical grey matter, cerebellum and normal appearing white matter. V_T was calculated from the unconstrained two-tissue compartment model as previously described.[1, 63]

III.4.13 Calculating the non-displaceable component of V_T [blocking study]

Three methods were used to determine the non-displaceable (V_{ND}), and displaceable (V_S) components of the total volume of distribution (V_T). Of these methods, two were independent: the occupancy plot (methods 1a and 1b) and the polymorphism plot (method 2).

Method 1a: Occupancy plot with individual V_{ND}

The occupancy plot is an adaptation of the Lassen plot described by Cunningham *et al.*[64] Given that $V_T^{baseline} = V_S + V_{ND}$ and $V_T^{block} = V_S(1 - Occ_{drug}) + V_{ND}$ (block condition), it follows that $V_T^{baseline} - V_T^{block} = Occ_{drug}.(V_T^{baseline} - V_{ND})$. Thus, plotting $V_T^{baseline}$ against $V_T^{baseline} - V_T^{block}$ in a variety of regions of interest allows derivation of V_{ND} (x-intercept) and the occupancy of XBD-173 (slope). This method assumes that V_{ND} is the same at pre and post-block time points and that the fractional occupancy of XBD-173 does not change across the brain. Method 1a plots these data for each individual participant.

Method 1b: Occupancy plot with constrained V_{ND}

In order to calculate a group V_{ND}, data from individual participants were plotted as described in Method 1a, and the x-intercept was forced to a best fit for all participants.

Method 2: Polymorphism plot

The polymorphism plot, described by Guo *et al.* does not require pharmacological blockade.[65] Instead, it relies upon the assumption that MABs express 50% HAB and 50% LAB binding sites.[54, 57] Thus, similarly to methods 1a and 1b, $V_T^{HAB} - V_T^{MAB} = \Delta(V_T^{HAB} - V_{ND})$, where Δ is a constant ($\frac{1}{2}(1 - \frac{B_{max}^{LAB}.K_D^{HAB}}{B_{max}^{HAB}.K_D^{LAB}})$ relating to the TSPO density (B_{max}) and dissociation constants (K_D) for HABs and LABs respectively. Again, a plot of V_T^{HAB} against $V_T^{HAB} - V_T^{MAB}$ gives V_{ND} as the x-intercept.

III.4.14 Clinical outcome measures

All assessments were conducted by a single physician throughout the study. Assessments were performed blinded to imaging results.

Clinical outcome measures were assessed at all study visits, including:

- Expanded Disability Status Scale (EDSS)
- 9-hole peg test
- Timed 25-foot walk
- the Symbol Digit Modalities Test (SDMT)
- the learning trials of the California Verbal Learning Test II (CVLT-II)
- the Brief Visuospatial Memory Test - Revised (BVMT-R)
- Global Multiple Sclerosis Severity Scores
- Multiple Sclerosis Quality of Life-54 patient reported outcome
- Work Productivity and Activity Impairment

Relapses were defined as '*a new symptom or worsening of an old symptom accompanied by a new neurologic abnormality, lasting at least 24 hours in the absence of fever and preceded by stability or improvement for at least 30 days*'.[66]

Disability progression was defined as an increase of 1 EDSS point in those with EDSS <5.5, or an increase of 0.5 EDSS points in those with EDSS ≥5.5. EDSS progression was confirmed over 6 months at subsequent clinic visits.

Natalizumab 'non-responders' were defined as those with on-going relapses while on natalizumab, and/or disability progression in EDSS score.

III.4.15 Statistical analysis

Participant demographic results are reported as mean (standard deviation (SD)). Parametric tests were used after testing for normal data distribution. Unpaired and paired *t* tests were used to compare the differences between means of two groups for unpaired and paired data, respectively. One-way analysis of variance (ANOVA) was used to compare the differences between means for three or more groups. Differences between HABs and MABs was investigated using both unpaired *t* tests, and with repeated measures ANOVA with 'region of interest' as the within-subjects factor, as appropriate. One-way repeated-measure ANOVA was used to investigate differences in V_T between different regions on interest. A mixed-effects model (restricted maximum likelihood) was used to investigate change in V_T over time in different regions of interest, to allow for missing data. Linear regressions were generated in MATLAB® (R2016b, The Mathworks, Inc., MA, USA). Statistical tests were performed in

GraphPad Prism (v7, GraphPad Software, Inc., San Diego, CA, USA) and IBM SPSS Statistics (version 20.0, IBM Corp 2011).

III.4.16 Contribution to work

Joel Raffel[1,2]	Led on overall scientific direction of project. Wrote the study protocol. Wrote application to obtain ethical consent for the study from National Research Ethics Service and Administration of Radioactive Substances Advisory Committee. Consented participants and organised study visits. Performed all clinical assessments and coordinated scanning procedures with assistance from radiographers. Performed image processing and segmented lesion maps. Analysis and interpretation of data once pharmacokinetic results obtained.
Sujata Sridharan[1]	PET methodologist, who led on PET pharmacokinetic analysis for 'blocking study' and 'natalizumab cohort' results.
Claire Feeney[1,2]	Consented and organised study visits for three HCs. Contributed towards PET pharmacokinetic analysis of HCs.
Greg Scott[1,2]	Contributed towards PET pharmacokinetic analysis of HCs.
Chris Record[2]	Contributed towards segmentation of lesion maps, as part of academic FY2 project based at Imperial.
Paolo Muraro[1,2]	Involved in initial conceptualisation of the study, and played important role in securing funding for the project.
David Sharp[1,2]	Provided advice on methodology and interpretation of results. Principle investigator of traumatic brain injury ^{18}F-GE180 project, which contributed data from three HCs for analysis.

David Brooks[1,3,4] Provided advice on methodology and interpretation of results.

David Owen[1] Provided advice on methodology and interpretation of results, particularly in relation to 'Blocking Study'.

Richard Nicholas[1,2] Principle investigator. Overall responsibility and supervision of the project.

1 Division of Brain Sciences, Faculty of Medicine, Imperial College London, London, United Kingdom.

2 Imperial College Healthcare NHS Trust, London, United Kingdom.

3 Institute of Neuroscience, Newcastle University, United Kingdom.

4 Department of Nuclear Medicine, Aarhus University, Denmark

III.5 RESULTS OF KINETIC ANALYSIS OF ^{18}F-GE180 FROM HEALTHY CONTROLS

Once 10 HCs had completed study procedures, the pharmacokinetics of ^{18}F-GE180 were characterised.

60 to 90-minute standardised uptake values images showed very low uptake of the tracer in brain tissue, with images dominated by blood vessel signal (Figure 17A). The concentration of ^{18}F-GE180 in the brain peaked at less than 1 minute.

The expectation was that *in vivo* binding of ^{18}F-GE180 in HABs should be approximately double that of binding in MABs.[1, 55, 67] However, group-averaged time-activity curves did not differ between HABs and MABs (Figure 17B). There was no difference in standardised update value curves between HABs and MABs ($F(1,48) = 1.396$, $p = 0.271$).

A reversible two-tissue compartment model best fitted the data. Again, ^{18}F-GE180 showed very low brain penetration. The mean regional delivery rate constant K_1 was very low (~0.01 mL/cm^3 min−1), suggesting poor extraction (~1%) across the blood-brain barrier. V_T values were correspondingly low, ranging from a mean of 0.16 mL/cm^3 in the striatum to 0.38 mL/cm^3 in the thalamus. There was no difference in V_T between HABs and MABs ($p > 0.186$ for all regions of interest); if anything, V_T was slightly greater in MABs (Figure 17C).

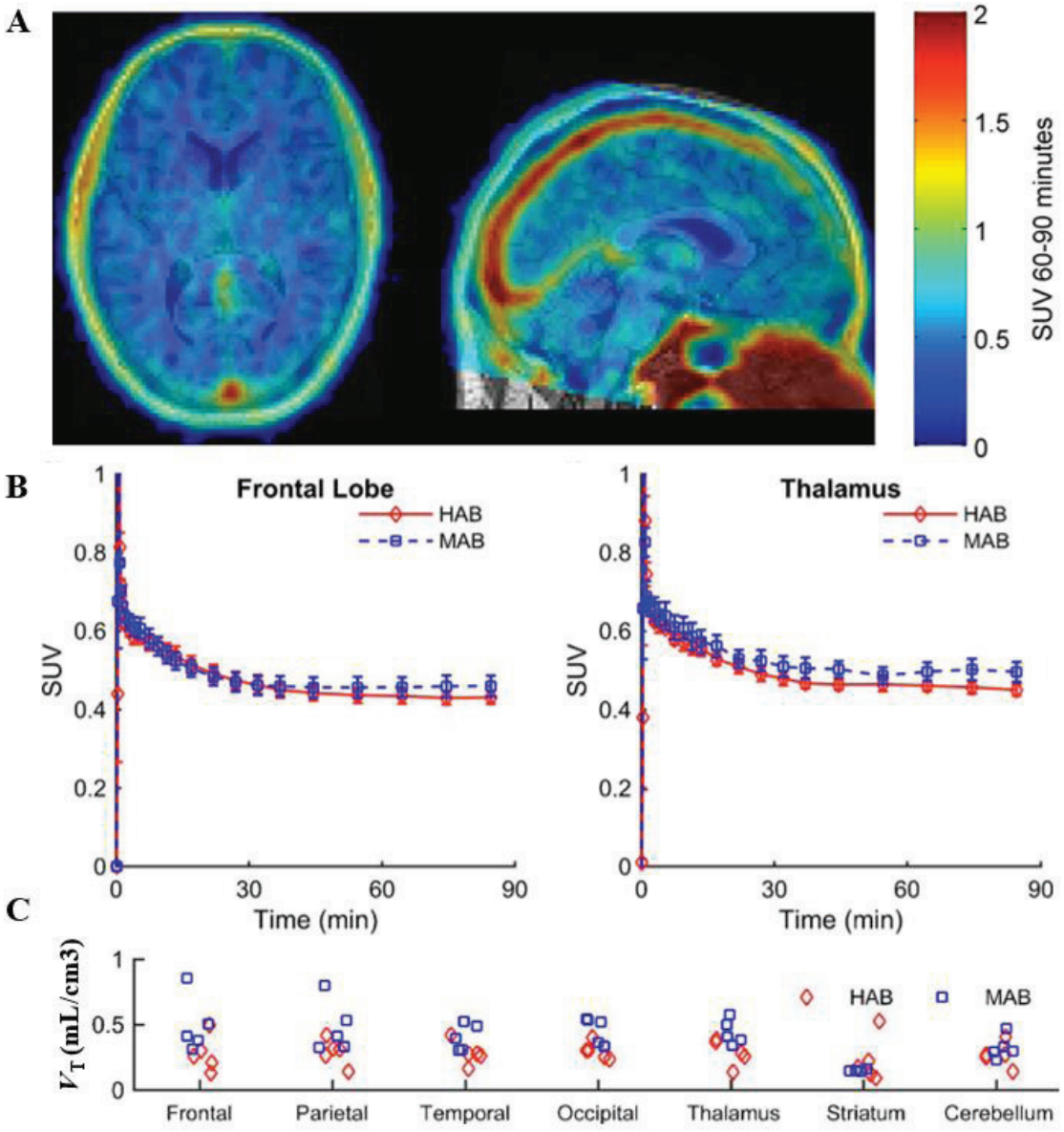


Figure 17: ^{18}F-GE180 Standardised uptake values and volume of distribution (V_T) in healthy controls. (A): 60 – 90-min Standardised uptake values superimposed on co-registered T1-weighted MR image in a representative MAB subject (B): Standardised uptake values in two representative regions of interest (frontal lobe and thalamus), plotted as mean ± SEM. (C): Two-tissue compartment model V_T for seven regions of interest, in HABS (red) and MABS (blue). Figure adapted from published.[1]

The full results of this kinetic analysis has been published, with the thesis author as co-author.[1] However, the content of this paper mainly relates to PET methodology and pharmacokinetics in HCs, which was not considered to be within the primary remit of this clinical thesis.

Therefore, the results relating to this analysis are not presented in full as part of this thesis chapter.

III.6 'BLOCKING STUDY' RESULTS

The results of this kinetic analysis called into question whether ^{18}F-GE180 could penetrate across the blood-brain barrier at all. If ^{18}F-GE180 shows no specific binding to TSPO, it would not be considered scientifically worthwhile to interpret the results of the natalizumab PET study. Because of this low brain penetration, an additional 'blocking study' was added to the study protocol, to further investigate whether ^{18}F-GE180 does bind to TSPO.

III.6.1 Subject characteristics

Six subjects with MS were recruited. The mean age of participants was 46.8 (9.1) years, mean age of onset was 36.2 (12.8) years and EDSS ranged between 3.5 and 7.5. All participants had been treated with a DMT. Participant demographics are summarised in Table 3.

Subject	HAB/ MAB	Sex	Age / Age at onset (yrs)	EDSS	Previous DMTs; current DMT
A	HAB	M	43/32	6.5	GA; GA
B	MAB	M	53/36	4.0	IVIG, natalizumab; IVIG
C	MAB	F	60/47	3.5	Alemtuzumab; alemtuzumab
D	HAB	F	33/20	5.5	IB-1a/1b, natalizumab, alemtuzumab, AHSCT; natalizumab
E	MAB	F	46/38	6.0	IB-1a, GA, fingolimod, natalizumab; alemtuzumab
F	HAB	M	46/32	7.5	Natalizumab; AHSCT

Table 3: Summary of participant demographics. HAB/MAB = high/mixed affinity binder, EDSS = Expanded Disability Status Scale, DMT = disease-modifying therapy, GA = glatiramer acetate, IVIG = intravenous immunoglobulin, IB = interferon-beta, AHSCT = autologous haematopoietic stem cell transplantation

III.6.2 ^{18}F-GE180 V_T does not differ between regions of interest or between TSPO HABs and MABs

Mean whole brain baseline V_T was 0.29 ± 0.17 ml/cm^3. Mean V_T for select regions of interest are presented in Table 4. There were no significant differences in V_T between any regions of interest, nor between HABs and MABs.

$V_T^{baseline}$ (mL/cm³)												
Subject	FL	TL	PL	OL	Str	Put	Thal	Cereb	CC	BS	WB	NAWM
A	0.29	0.28	0.31	0.31	0.32	0.16	0.32	0.25	0.43	0.39	0.27	0.40
B	0.33	0.18	0.49	0.18	0.17	0.21	0.35	0.13	0.15	0.17	0.26	0.17
C	0.26	0.29	0.26	0.35	0.20	0.26	0.37	0.24	0.18	0.36	0.25	0.28
D	0.59	0.59	0.48	0.68	0.65	0.61	0.63	0.63	0.64	0.60	0.61	0.61
E	0.10	0.12	0.10	0.11	0.07	0.07	0.05	0.11	0.06	0.18	0.09	0.11
F	0.23	0.25	0.23	0.24	0.16	0.29	0.36	0.26	0.18	0.30	0.24	0.22
Mean± SD	0.30 ±0.16	0.29 ±0.17	0.31 ±0.15	0.31 ±0.20	0.26 ±0.21	0.27 ±0.19	0.35 ±0.19	0.27 ±0.19	0.27 ±0.22	0.33 ±0.16	0.29 ±0.17	0.30 ±0.18

Table 4: Regional V_T estimates for regions of interest in individual participants. FL = frontal lobe, TL = temporal lobe, PL = parietal lobe, OL = occipital lobe, Str = striatum, Put = putamen, Thal = thalamus, Cereb = cerebellum, CC = corpus callosum, BS = brainstem, WB = whole brain, NAWM = normal appearing white matter. Participants in red are HABS.

III.6.3 Visual assessment of blockade of TSPO

60-90 minute sum PET images were generated for all participants. There was no obvious visual difference in sum PET images pre and post-block (e.g. as shown in Figure 18).

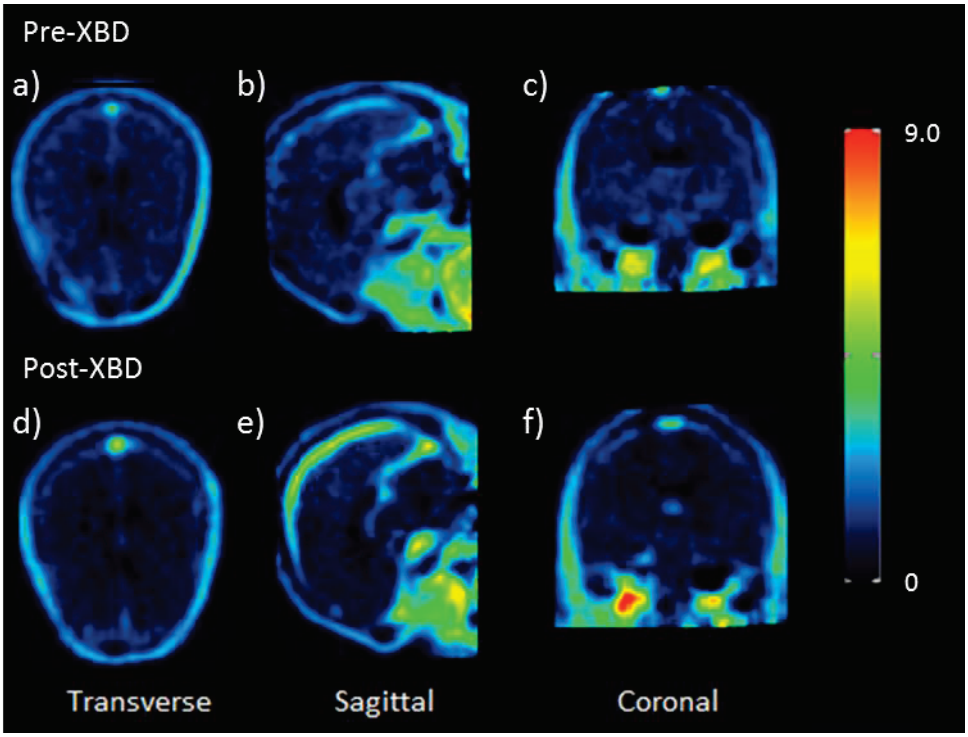


Figure 18: Sum 60-90 minute PET images (kBq.ml^{-3}) before and after XBD-173. Images shown in transverse, sagittal and coronal views pre (a, b, c) and post (d, e, f) XBD-173 administration for Participant F.

III.6.4 Calculation of V_{ND} suggests that ^{18}F-GE180 binds specifically to TSPO

Blockade with XBD-173 suggested that ^{18}F-GE180 exhibits some specific binding in the MS brain. Method 1a, the unconstrained occupancy plot, gave a mean V_{ND} of 0.18 ± 0.05 mL/cm^3 (Figure 19A). Method 1b, using an occupancy plot and constraining the *x*-intercept across participants, gave a mean V_{ND} estimate of 0.11 mL/cm^3, 95% CI 0.02-0.16 (Figure 19B). Method 2, using a polymorphism plot, produced a V_{ND} estimate of 0.20 mL/cm^3, 95% CI 0.16-0.34 (Figure 19C). Taking the mean V_{ND} estimate of 0.16 mL/cm^3 (mean of the three methods) and mean baseline whole brain V_T of 0.29 mL/cm^3, the specific binding ($V_S = V_T - V_{ND}$) accounted for 45 % of total V_T in the brain for ^{18}F-GE180 (57 % HABs; 20 % MABs). The reduction in uptake post-XBD-173 administration is further highlighted in Figure 20, where a

decrease in V_T in the majority of regions of interest is observed. Furthermore, BP_{ND} ((V_T / V_{ND}) −1) was used to calculate the mean HAB/MAB signal using these mean V_{ND} values, which was 5.45 ± 3.29 mL/cm^3 ($p < 0.01$). It should be noted that baseline V_Ts were greatest in Subject D (see Table 4), and these outlying values drove up mean V_Ts in the HAB group as well as overall.

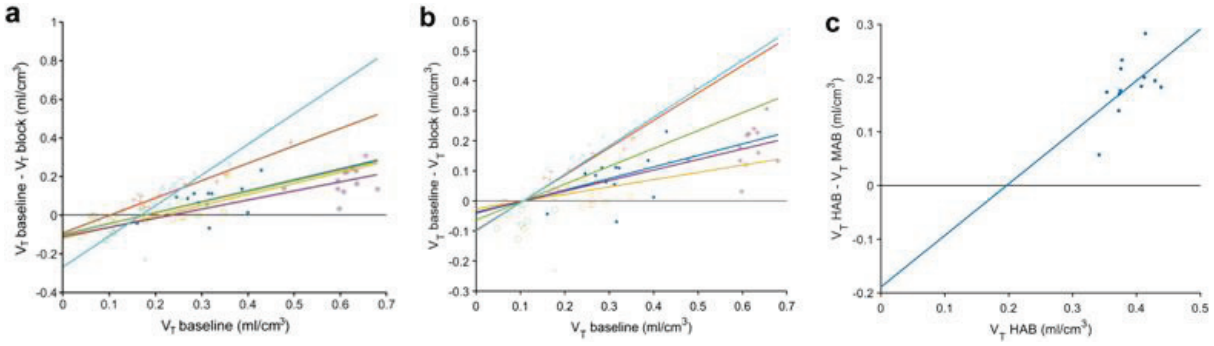


Figure 19: Occupancy and polymorphism plots. (a) Individual linear regression with occupancy plot, (b) constrained *x*-intercept occupancy plot and (c) polymorphism plot, bottom for ^{18}F-GE180. V_{ND} is derived from the *x*-intercept. Different symbols indicate individual patients for (a) and (b); each symbol represents a region of interest.

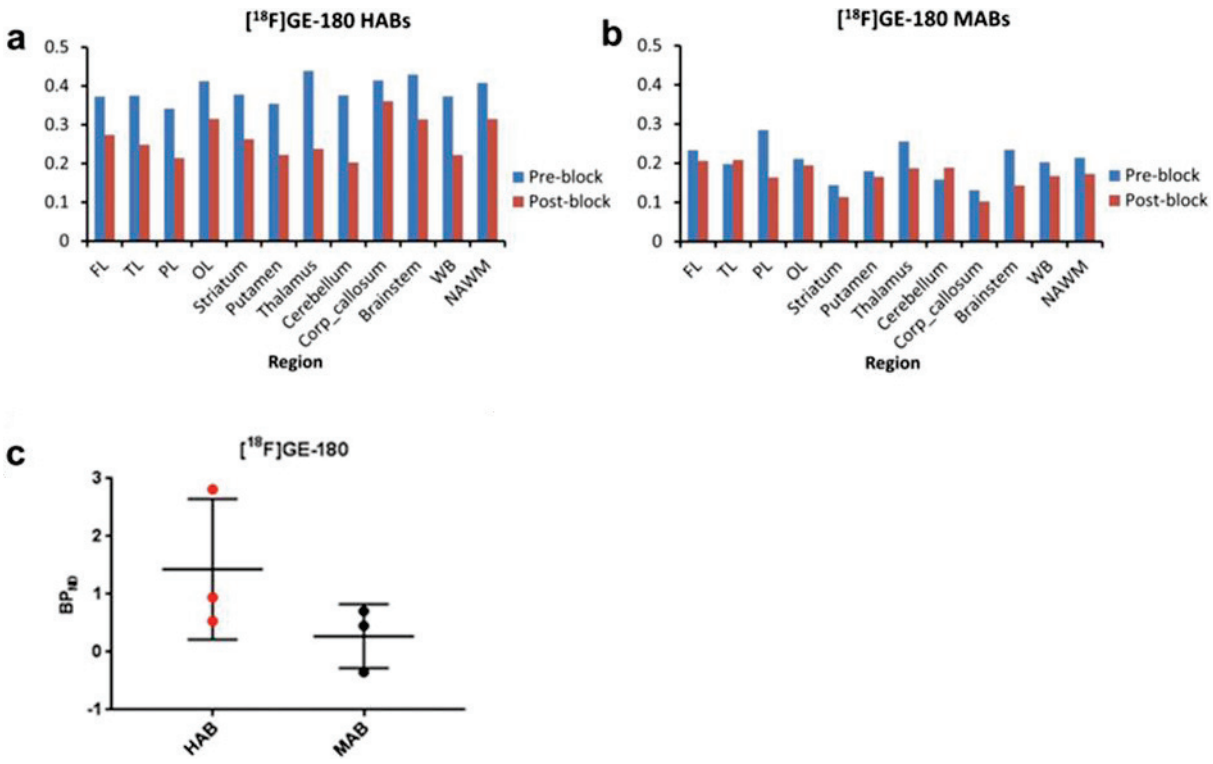


Figure 20: Reduction in uptake post-XBD-173 administration. Average regional V_T pre- and post-blockade for (a) HABs (b) MABs, and (c) HAB *vs.* MAB group V_T estimate ($n = 6$).

III.6.5 Specific binding to TSPO is ubiquitous in the MS brain

For ^{18}F-GE180, V_S accounted for between 39 % (striatum) and 54 % (thalamus) of total binding in the selected regions of interest (mean ± SD, 45 ± 5 %). All other regions of interest defined by the Hammers atlas, including the caudate and non-cortical grey matter (GM), exhibited mean V_T between 0.25 and 0.56 mL/cm^3. Thus, it follows that all regions of interest showed specific TSPO binding.

III.7 'NATALIZUMAB COHORT' RESULTS

Results of the 'blocking study' suggest that ^{18}F-GE180 does bind to TSPO in the MS brain and gives specific signal in all regions of interest, despite having unexpectedly low brain

penetration. This allows one to interrogate the results of the 'natalizumab cohort', albeit with the caveat that since ^{18}F-GE180 has very low brain extraction (~1%), results will be limited by poor signal-to-noise ratio.

III.7.1 Study procedures

17 subjects with relapsing MS due to start natalizumab for clinical reasons, along with 11 HCs, were recruited to the study. One subject with MS dropped out during the baseline visit since they experienced discomfort during the PET scan; baseline PET data were incomplete and the subject was therefore excluded from all analyses. The other 16 PwMS and 11 HCs completed all study activities, as specified in the protocol. Of the 59 completed scans (16 x 3 PwMS + 11 HC), 48 scans had data which could be used to construct Volume of Distribution results. Of the 11 scans without usable data, eight scans had unsuccessful arterial line insertion, two scans had recording errors for the arterial input function, and one scan had to be curtailed because of patient discomfort. The amount of injected radioactivity was similar between groups (PwMS: 183.2 (3.9) MBq; HC: 182.4 (3.0) MBq; p = ns).

III.7.2 Subject characteristics

Baseline characteristics are presented in Table 5. There were more males in the HC group. PwMS had increased disability at baseline compared to HCs, as expected (Table 6). Administration of ^{18}F-GE180 PET was safe, and well-tolerated by all participants.

	PwMS (n = 16)	HCs (n = 11)
Male/Female, n	6/10	8/3
Age, yrs	40.7 (11.1)	41.6 (8.6)
Weight, kg	72.8 (12.6)	82.9 (12.5)
Height, cm	169.1 (10.1)	175.8 (6.7)
Years of education	14.1 (2.4)	16.3 (3.2)
TSPO HABS / MABS / LABS, n	7/9/0	6/5/0
Age at MS onset, yrs	29.7 (10.4)	
Time since MS onset, yrs	11.6 (10.8)	
Number of previous DMTs, n	O DMTs: 8 1 DMT: 3 2 DMTs: 5	

Table 5: Baseline characteristics of PwMS and HCs. HAB/MAB/LAB = high/mixed/low affinity binder. DMT = disease-modifying therapy. Standard deviations shown in brackets.

	PwMS (n = 16)	HCs (n = 11)	*p*-value
T25FW, secs	6.6 (4.5)	3.5 (0.4)	*
9HPT, secs	30.9 (20.6)	17.9 (1.2)	*
MSQOL-54 Physical	42.3 (17.3)	88.0 (5.2)	***
MSQOL-54 Psych	56.9 (23.6)	81.4 (6.6)	**
WPAI:MS	58.7 (17.1)	3.6 (6.7)	***
SDMT	48.2 (12.7)	66.1 (9.9)	***
CVLT	54.0 (11.1)	66.1 (5.5)	**
BVMT-R	24.0 (6.8)	30.5 (4.9)	*
EDSS	4.2 (1.1)		
MSSS	5.8 (2.4)		
WM Lesion Volume, cm^3	10.5 (8.5)		
GM Lesion Volume, cm^3	0.3 (0.5)		

Table 6: Clinical and patient-reported outcomes in PwMS and HCs at baseline. T25FW = timed 25-foot walk; 9HPT = 9-hole peg test; MSQOL-54 = Multiple Sclerosis Quality of Life-54 patient reported outcome (physical and psychological subscores); WPAI:MS = Work Productivity and Activity Impairment, Multiple Sclerosis; SDMT = symbol digit modalities test; CVLT = California verbal learning test; BVMT-R = Brief Visuospatial Memory Test - Revised; EDSS = Expanded Disability Status Scale; MSSS = Global Multiple Sclerosis Severity Scores; GM = grey matter; WM = white matter. Standard deviations shown in brackets. *p*-values refer to unpaired *t* tests: * = $p < 0.05$; ** = $p < 0.01$; *** = $p < 0.001$. In all cases, the PwMS group had scores associated with greater disability, compared with the HC group.

III.7.3 Visual inspection of ^{18}F-GE180 signal

On visual inspection of 60-90 minute summed images, most subjects exhibited low uptake of the tracer in brain tissue with images dominated by blood vessel signal consistent with that reported in Results Sections III.5 and III.6 (Figure 17A, Figure 18A-C). Only one subject had a gadolinium-enhancing lesion on MRI at baseline. This subject had visually increased ^{18}F-GE180 signal in the gadolinium-enhancing lesion (Figure 21). No other subjects had obvious 'hot-spots' on visual examination of the PET scan.

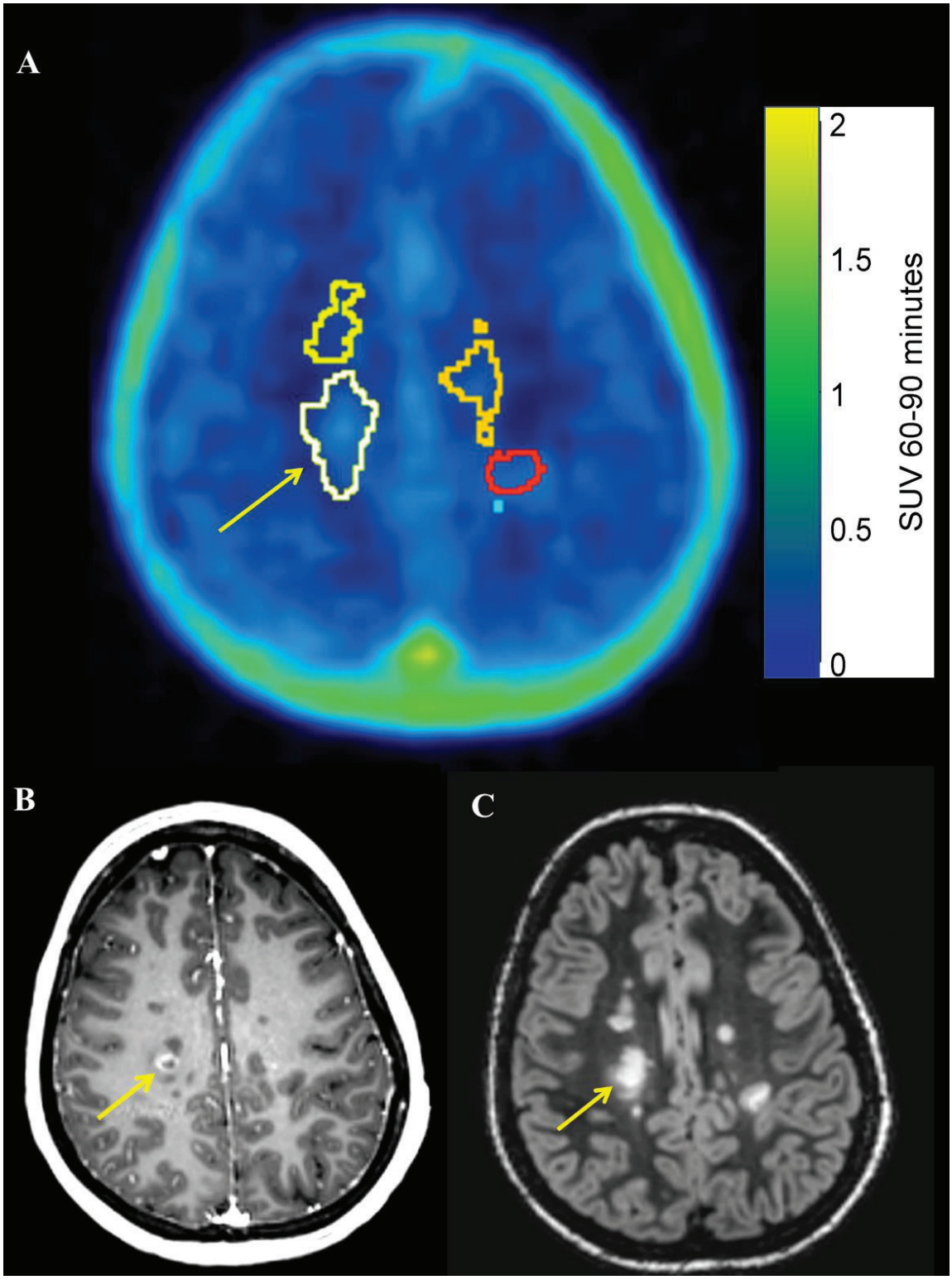


Figure 21: Increased 60–90 minute SUVs in a gadolinium-enhancing lesion. (A) Subject with multiple sclerosis, with increased ^{18}F-GE180 signal in a gadolinium-enhancing lesion (yellow arrow), but not in non-gadolinium-enhancing lesions (red, orange, yellow lesions). (B) T1-weighted MRI with gadolinium in same subject (gadolinium-enhancing lesion shown by yellow arrow). (C). Double Inversion Recovery MRI in same subject (gadolinium-enhancing lesion shown by yellow arrow). SUV = standardised uptake value.

III.7.4 ^{18}F-GE180 V_T does not differ between TSPO HABs and MABs

The expectation was that *in vivo* binding of ^{18}F-GE180 in HABs should be approximately double that of binding in MABs.[1, 55, 67]

However, in subjects with MS, there was no difference in V_T between HABS (n = 7) and MABS (n = 6) in any region of interest at baseline (**Grey matter** (**GM) –** HABs: mean 0.27 mL/cm^3, 95% CI 0.11 - 0.43; MABs: mean 0.23 mL/cm^3, 95% CI 0.16 – 0.30, p = 0.59. **Thalamus –** HABs: mean 0.32 mL/cm^3, 95% CI 0.14 - 0.50; MABs: mean 0.26 mL/cm^3, 95% CI 0.20 – 0.32, p = 0.49. **Normal appearing white matter (NAWM) –** HABs: mean 0.25 mL/cm^3, 95% CI 0.17 - 0.34; MABs: mean 0.26 mL/cm^3, 95% CI 0.22 – 0.31, p = 0.79. **Lesions –** HABs: mean 0.43 mL/cm^3, 95% CI 0.20 - 0.66; MABs: mean 0.52 mL/cm^3, 95% CI 0.30 – 0.74, p = 0.51; Figure 22A).

Consistent with the results reported in Section III.5, in the HC group there was no difference in V_T between HABS (n = 6) and MABS (n = 5) in any region of interest (**GM –** HABs: mean 0.24 mL/cm^3, 95% CI 0.17 - 0.31; MABs: mean 0.22 mL/cm^3, 95% CI 0.16 – 0.28, p = 0.56. **Thalamus –** HABs: mean 0.27 mL/cm^3, 95% CI 0.15 - 0.39; MABs: mean 0.23 mL/cm^3, 95% CI 0.19 – 0.27, p = 0.47. **White matter (WM) –** HABs: mean 0.24 mL/cm^3, 95% CI 0.14 - 0.34; MABs: mean 0.28 mL/cm^3, 95% CI 0.15 – 0.40, p = 0.53; Figure 22B).

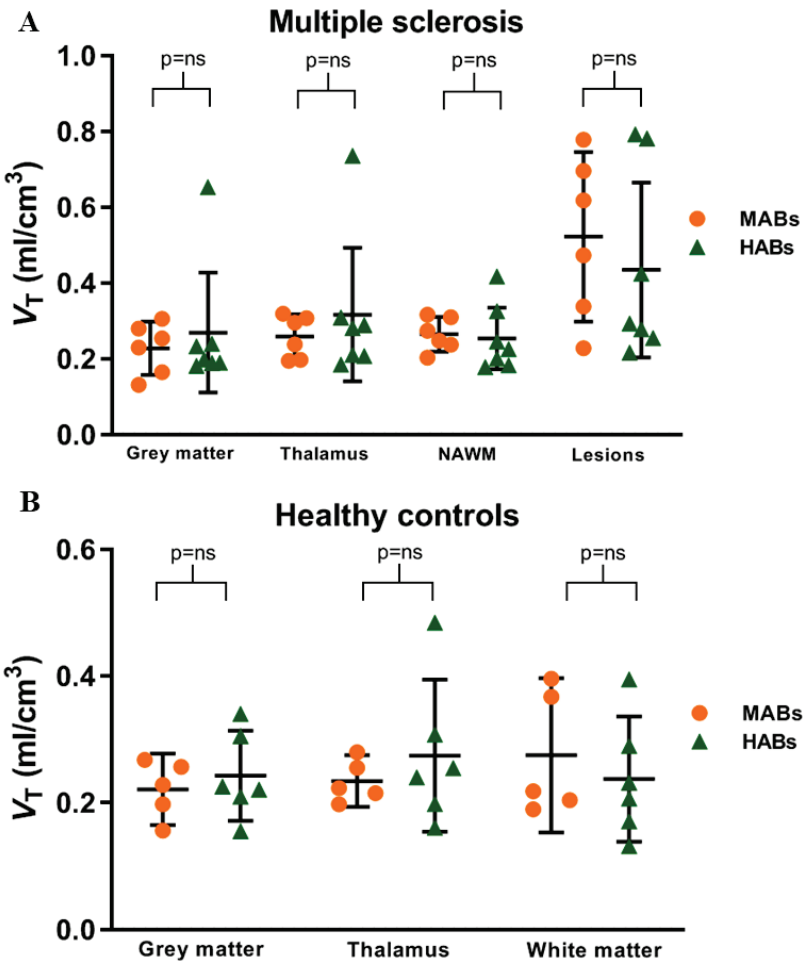


Figure 22: No effect of TSPO genetic polymorphism on ^{18}F-GE180 V_T. (A) MABs (orange circles) and HABs (green triangles) had no difference in ^{18}F-GE180 V_T in MS subjects at baseline. (B) MABs (orange circles) and HABs (green triangles) had no difference in ^{18}F-GE180 V_T in healthy controls. *p*-values generated using unpaired *t* test. Error bars represent mean +/- 95% confidence intervals. HAB/MAB = high/mixed affinity binder; NAWM = normal-appearing white matter; V_T = Volume of distribution. ns = not statistically significant.

At follow-up in subjects with MS, there was still no difference in V_T between HABS (n = 6) and MABS (n = 6) 10 weeks after initiation of natalizumab (**GM –** HABs: mean 0.26 mL/cm^3, 95% CI 0.15 - 0.37; MABs: mean 0.25 mL/cm^3, 95% CI 0.17 – 0.33, p = 0.90. **Thalamus –** HABs: mean 0.32 mL/cm^3, 95% CI 0.17 - 0.48; MABs: mean 0.23 mL/cm^3, 95% CI 0.19 – 0.27, p = 0.18. **NAWM –** HABs: mean 0.26 mL/cm^3, 95% CI 0.12 - 0.39; MABs: mean 0.30 mL/cm^3, 95% CI 0.19 – 0.40, p = 0.60. **Lesions –** HABs: mean 0.39 mL/cm^3, 95% CI 0.19 -

0.58; MABs: mean 0.41 mL/cm^3, 95% CI 0.18 – 0.65, p = 0.82). At final follow-up, there was still no difference in V_T between HABS (n = 7) and MABS (n = 5) 58 weeks after initiation of natalizumab (**GM –** HABs: mean 0.24 mL/cm^3, 95% CI 0.20 - 0.28; MABs: mean 0.24 mL/cm^3, 95% CI 0.11 – 0.37, p = 0.96. **Thalamus –** HABs: mean 0.31 mL/cm^3, 95% CI 0.20 - 0.43; MABs: mean 0.25 mL/cm^3, 95% CI 0.16 – 0.34, p = 0.32. **NAWM –** HABs: mean 0.24 mL/cm^3, 95% CI 0.20 - 0.28; MABs: mean 0.27 mL/cm^3, 95% CI 0.19 – 0.35, p = 0.36. **Lesions –** HABs: mean 0.34 mL/cm^3, 95% CI 0.24 - 0.43; MABs: mean 0.30 mL/cm^3, 95% CI 0.25 – 0.35, p = 0.48).

Subsequent results are therefore presented irrespective of genotype group.

III.7.5 ^{18}F-GE180 V_T is increased in MS lesions at baseline

At baseline, ^{18}F-GE180 V_T was no different between HCs (n = 11) and PwMS (n = 13) in the GM, thalamus, or in NAWM. However, V_T in lesions in PwMS was greater than V_T in white matter in HCs (**GM –** HC: mean 0.23 mL/cm^3, 95% CI 0.19 - 0.27; MS: mean 0.25 mL/cm^3, 95% CI 0.17 – 0.33, p = 0.70. **Thalamus –** HCs: mean 0.26 mL/cm^3, 95% CI 0.20 - 0.31; MS: mean 0.29 mL/cm^3, 95% CI 0.20 – 0.38, p = 0.50. **NAWM –** HCs: mean 0.25 mL/cm^3, 95% CI 0.19 - 0.32; MS: mean 0.26 mL/cm^3, 95% CI 0.22 – 0.30, p = 0.90. **Lesions –**MS: mean 0.47 mL/cm^3, 95% CI 0.34 – 0.61, p = 0.007 when compared against HC NAWM; Figure 23).

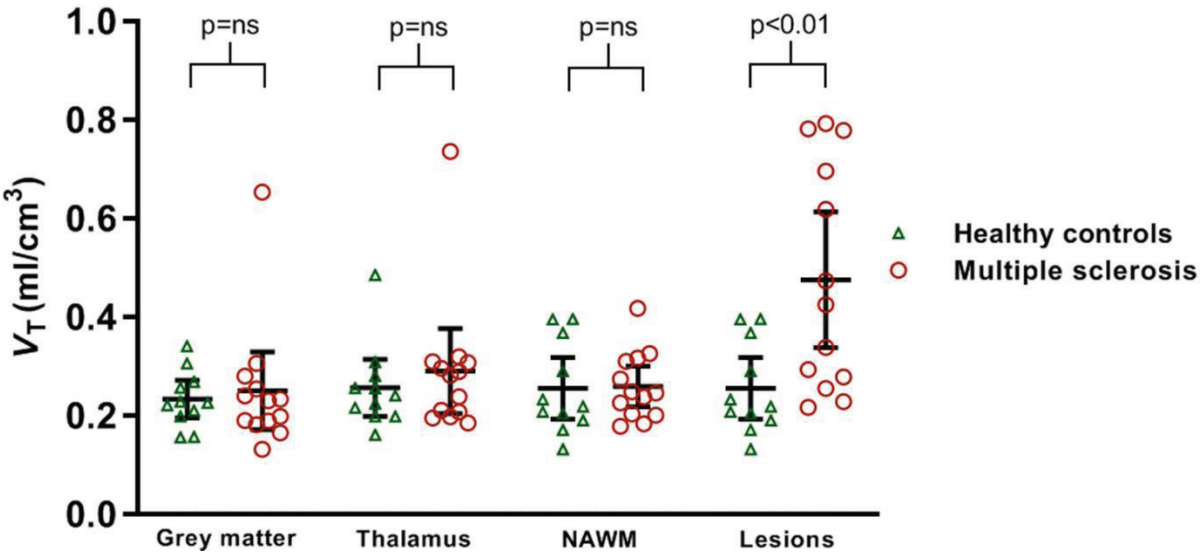


Figure 23: V_T in selected regions of interest in healthy controls and PwMS at baseline. There was no difference between HCs (green triangles) and PwMS (red circles) in the grey matter, thalamus, or NAWM. V_T in MS lesions was greater than V_T in HC white matter. In the above figure HC white matter is graphically represented as both 'HC NAWM' and 'HC lesions' for ease of comparison. *p*-values generated using unpaired *t* test. Error bars represent mean +/- 95% confidence intervals. NAWM = normal-appearing white matter; V_T = Volume of distribution. ns = not statistically significant.

III.7.6 ^{18}F-GE180 V_T decreases after natalizumab in white matter lesions, but not in other regions of interest

V_T in HCs did not differ between GM, thalamus, and WM ($F(3, 10) = 0.46$, $p = 0.54$, $\eta_p^2 = 0.04$; refer to Figure 23, green triangles).

In subjects with MS at baseline, V_T in lesions was greater than V_T in GM, thalamus, and NAWM in PwMS ($F(3, 12) = 12.60$, $p < 0.0001$, $\eta_p^2 = 0.51$; Figure 24).

After 10 weeks of natalizumab, V_T in lesions was still greater than V_T in GM, thalamus, and NAWM ($F(3, 11) = 6.9$, $p < 0.01$, $\eta_p^2 = 0.38$; Figure 24).

However, after 58 weeks of natalizumab treatment, V_T in lesions was not statistically different to that in GM, thalamus, and NAWM, although there was still a trend in that direction ($F(3, 11) = 3.2$, $p = 0.06$, $\eta_p^2 = 0.22$; Figure 24).

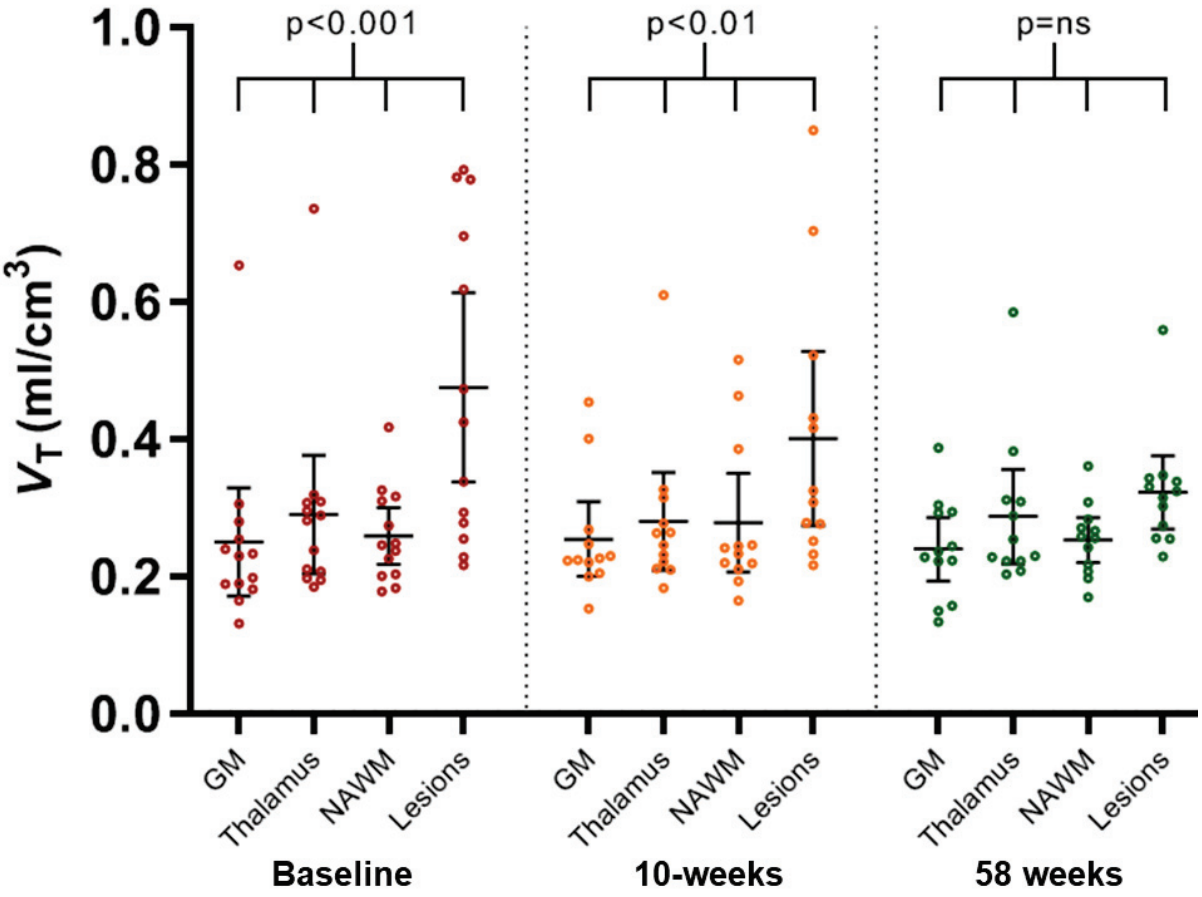


Figure 24: ^{18}F-GE180 V_T is increased in MS lesions compared to other regions of interest at baseline and 10 weeks after initiation of natalizumab, but not at 58 weeks after initiation of natalizumab. *p*-values generated using one-way repeated-measure ANOVA. Error bars represent mean +/- 95% confidence intervals. GM = grey matter; NAWM = normal-appearing white matter; V_T = Volume of distribution. ns = not statistically significant.

V_T decreased over time after natalizumab treatment in white matter lesions but not in grey matter lesions (**White matter lesions:** degrees of freedom = 3, 15; missing value = 8, $p < 0.05$; **Grey matter lesions**: degrees of freedom = 3, 15; missing value = 8, $p = 0.51$; Figure 25).

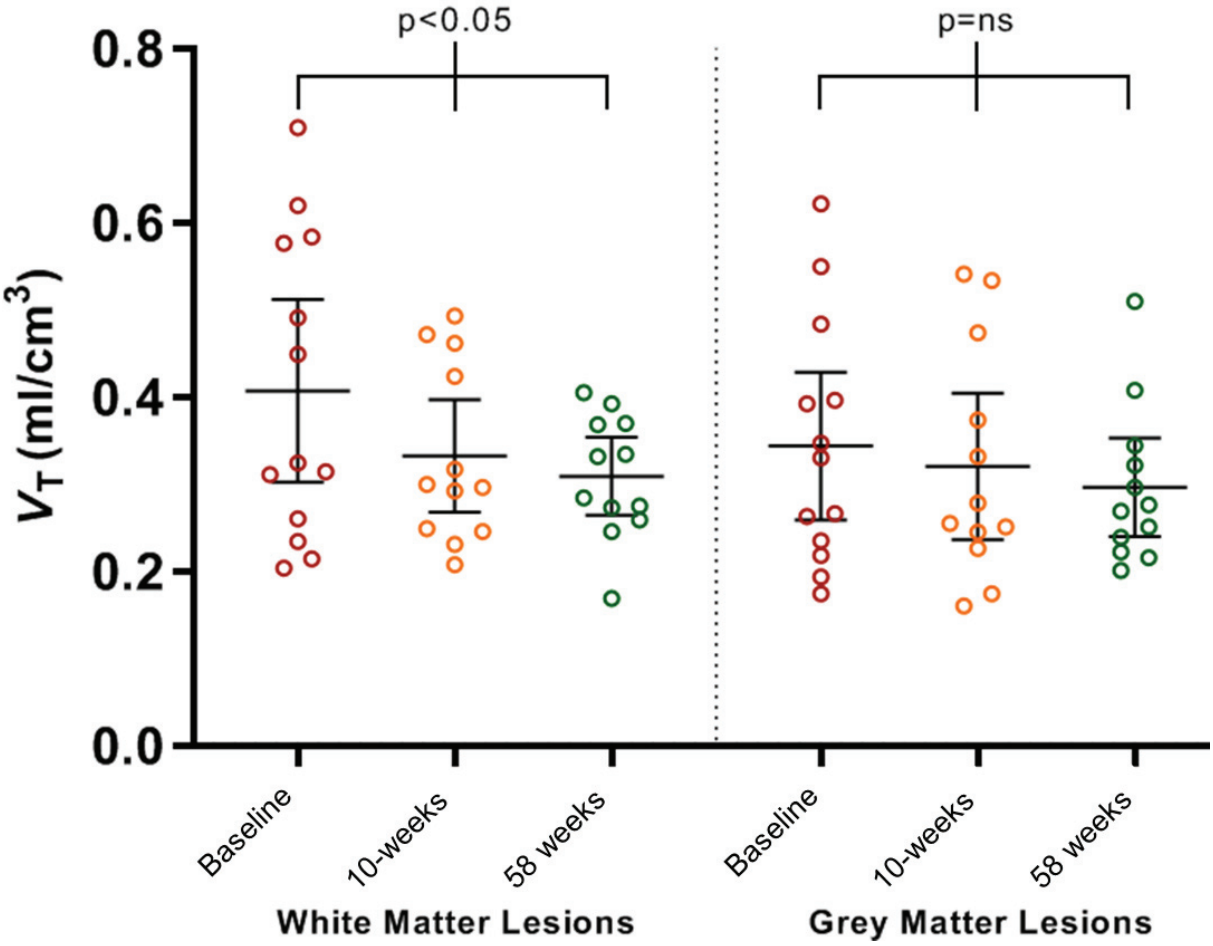


Figure 25: ^{18}F-GE180 V_T after 58 weeks of natalizumab reduces in white matter lesions but not grey matter lesions. *p*-values refer to mixed-effects model (restricted maximum likelihood; REML). Error bars represent mean +/- 95% confidence intervals. V_T = Volume of distribution. ns = not statistically significant.

III.7.7 ^{18}F-GE180 V_T increases prior to the development of new white matter lesions on MRI.

5 PwMS developed new lesions (n = 51) between the baseline scan and the 10 weeks after initiating natalizumab. V_T was increased in these new lesions, in comparison with NAWM at

10 weeks after initiation of natalizumab (**New lesions at 10 weeks V_T**: mean 0.55 mL/cm^3, 95% CI 0.48 - 0.63; **NAWM at 10 weeks V_T**: mean 0.34 mL/cm^3, 95% CI 0.29 – 0.39, $p < 0.0001$; Figure 26). After mapping these lesion areas back onto the same regions in the baseline scan, V_T was also slightly increased in these 'pre-lesion' areas in comparison to NAWM at baseline (**'Pre-lesions' at baseline V_T**: mean 0.36 mL/cm^3, 95% CI 0.31 - 0.42; **NAWM at baseline V_T**: mean 0.30 mL/cm^3, 95% CI 0.27 – 0.33, $p < 0.05$; Figure 26). By referring again to baseline MRI including double-inversion recovery, phase-sensitive inversion recovery, and magnetisation-prepared rapid gradient-echo sequences before and after gadolinium, it was confirmed that these areas had not yet developed a lesion on MRI at baseline scan.

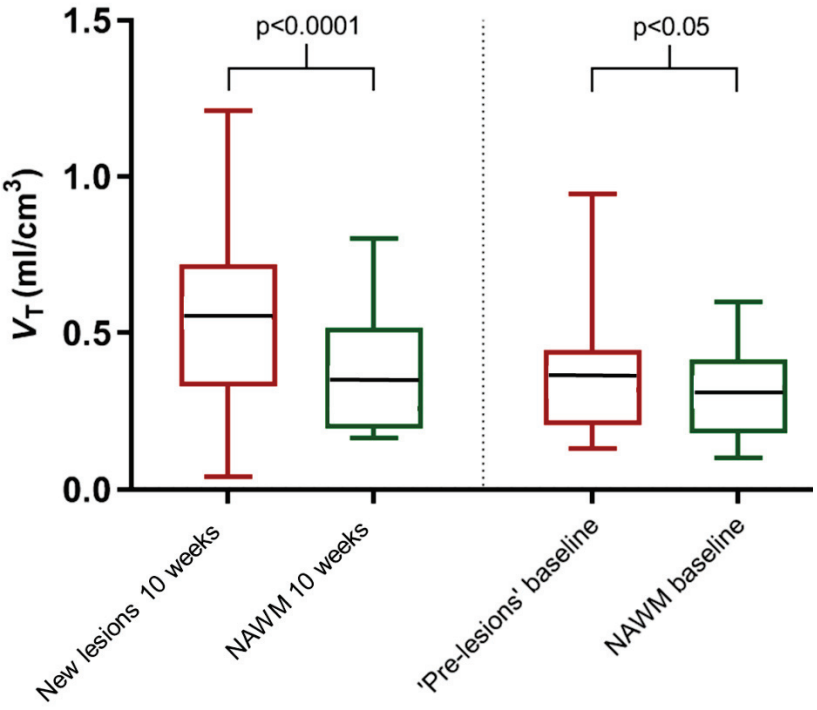


Figure 26: New lesions and 'pre-lesions' have increased V_T. In the 5 PwMS with new lesions (n = 51) on MRI 10 weeks after the initiation of natalizumab, V_T was increased in these lesions compared with NAWM. After mapping these lesion areas back onto the same regions in the baseline scan, V_T was also slightly increased in these 'pre-lesion' areas compared with NAWM at baseline. *p*-values generated with paired *t* tests. Boxes show 25th and 75th percentile, whiskers show minimum and maximum, black lines shows mean. V_T = Volume of distribution; NAWM = normal-appearing white matter.

III.7.8 ^{18}F-GE180 V_T does not predict response to natalizumab treatment

Clinical response to treatment was correlated with various PET outcomes in those with PET data with calculable V_T at baseline and 58 weeks after natalizumab initiation on an exploratory basis.

PET outcomes which were considered included:

- V_T at baseline
- V_T after treatment
- Change in V_T after treatment

- The above outcomes were tested in whole brain, GM, thalamus, NAWM, and in lesions.

Clinical outcomes which were considered included:

- 'Clinical response' (defined by lack of relapses or EDSS progression while on natalizumab)
- Change in timed 25-foot walk score
- Change in 9-hole peg test score
- Change in cognitive impairment assessment scores
- Change in patient-reported outcome scores

There were no associations between PET outcomes and clinical outcomes for any of the above variables. For example, change in whole brain V_T was no different in those that responded and those that did not response to natalizumab (Responders: -0.028 mL/cm^3, 95% CI -0.15 to 0.09; Non-responders: -0.086 mL/cm^3, 95% CI -0.33 to 0.16; $p = 0.57$).

III.8 DISCUSSION

This was the largest TSPO PET study performed in multiple sclerosis to date, and led to the first published study of ^{18}F-GE180 in humans.[1] Unfortunately, kinetic analyses suggested unexpectedly low brain penetration of ^{18}F-GE180, approximating 1% only. This was out of keeping with the preclinical studies on ^{18}F-GE180.[50-52] V_T values are correspondingly low, and about 20 times lower than those of TSPO tracer [^{11}C]PBR28, for example.[68] This makes kinetic modelling challenging since there is a poor signal-to-noise ratio, especially given the presence of persistent vascular signal. Regions of interest had to be manually edited where necessary to minimise spill-over from large-vessel vascular activity, which introduces operator variability and is not necessary with other TSPO tracers. There is a known difference of *in vitro* GE180 binding affinity between TSPO HABs and MABs, and the expectation was that *in vivo* binding

of ^{18}F-GE180 in HABs should be approximately double that of binding in MABs.[1, 55, 67] This expected genotype dependence of ^{18}F-GE180 V_T was not observed, presumably because of this low brain penetration and poor signal-to-noise ratio. This result was consistent in HCs and both MS cohorts. Poor extraction of ^{18}F-GE180 across the blood–brain barrier was a finding which was later replicated in other studies.[63, 68]

The reasons for the poor extraction of ^{18}F-GE180 across the blood–brain barrier are unclear, but could be due to, for example, the action of active efflux pumps such as P-glycoprotein, or unexpectedly high plasma protein binding.[69, 70]

The results of the kinetic analyses called into question whether ^{18}F-GE180 could penetrate across the blood-brain barrier at all. If ^{18}F-GE180 shows no specific binding to TSPO, it would not be considered scientifically worthwhile to interpret the results of the natalizumab PET study (initially planned to be the central focus of this thesis).

III.8.1 Blocking study

Because of this observed low brain penetration, ethical permission was sought to add an additional 'blocking study' to the study protocol, to further investigate whether ^{18}F-GE180 binds to TSPO at all. This study was designed to quantify the non-specific binding (V_{ND}) of the TSPO PET tracer ^{18}F-GE180 in a cohort of people with MS. The results of this study suggest that, despite low brain penetration *in vivo,* ^{18}F-GE180 does appear to exhibit some specific signal. V_{ND} accounts for, on average, 55% of the total volume of distribution (V_T) in the whole brain, meaning that, on average, approximately 45% of V_T is specific (V_S). Results were

published in *Molecular Imaging and Biology* journal, with the thesis author as 'joint first author'.[2]

These results have broad implications on how novel TSPO tracers should be validated and compared. TSPO PET tracers show great variation in the degree of their specific binding *in vitro*, but their specificity is not routinely quantified *in vivo.* Quantification of specific binding could theoretically be performed through comparison with a reference region devoid of target receptors. However, in this study of 6 subjects, it was demonstrated that V_T is greater than V_{ND} for ^{18}F-GE180 in all regions of interest; thus no 'reference regions' are devoid of specific TSPO binding. This argues against the scientific validity of a reference region approach as a method for quantifying the proportion of non-specific binding in TSPO tracers. Indeed, it argues more generally against the use of reference region approaches in TSPO PET studies, which remains commonplace.[40, 45, 71, 72] Instead, as with the reported study, quantification of the specific binding of TSPO tracers *in vivo* should be achieved using TSPO blockade. The results of this study support the argument that such an approach should be taken for all TSPO tracers undergoing clinical development.

The only other TSPO tracer to be validated with a blocking study to date is [^{11}C]PBR28, both in healthy controls,[57] and in disease cohorts.[2, 73] [^{11}C]PBR28 is generally accepted as an effective TSPO tracer *in vivo,*[40, 71, 74-76] although, counterintuitively, it exhibits decreased V_T in some subjects with neuroinflammation.[71] In this study of ^{18}F-GE180, the proportion of non-specific binding is similar to that of [^{11}C]PBR28,[2, 57] although absolute V_T values are far lower.[2, 57, 73] Unlike ^{18}F-GE180, [^{11}C]PBR28 is able to detect differences in TSPO binding affinity *in vivo,* presumably because of greater blood-brain barrier penetration and corresponding higher V_Ts and better signal-to-noise ratio.

Several caveats should be considered when interpreting the results of this study. Firstly, the cohort size was small. Secondly, although the mean V_{ND} was 0.16 mL/cm^3, there was substantial variability in V_{ND} between individuals, and the occupancy of XBD173 (slopes of the occupancy plots) varied between 24% and 95% in individuals. This has been observed previously,[57] and it is difficult to discriminate how much of this is due to biological variability, and how much is due to experimental variability. If there is indeed a biological spectrum of V_{ND} between individuals, this raises the possibility that blocking scans should be included for all participants in all TSPO PET studies to optimally quantity V_S. This would require two PET scans rather than one, which would increase cost, radiation exposure and participant discomfort. There was also variation in baseline V_T between individuals; baseline V_T was considerably greater in Subject D, and these outlying values drove up mean V_T in the HAB group as well as overall. If data from this subject were excluded, baseline whole brain V_T would be 0.22 mL/cm^3, and V_S therefore only 0.06 mL/cm^3 (28% of V_T). There was also considerably variability is V_{ND} results between the occupancy plot and the polymorphism plot method. Lastly, although this study was performed in a cohort of people with MS, it was not investigated how V_S differs in MS lesions since this cohort had low lesion load; lesions were instead studied in the 'natalizumab cohort'.

In summary, pharmacological blockade with XBD-173 suggests that at least a proportion of ^{18}F-GE180 tracer does end up bound specifically to TSPO. It is therefore possible that increased ^{18}F-GE180 signal observed in clinical studies reflects true increase in TSPO. However, because of the low brain penetration of ^{18}F-GE180, questions will remain whether large increases in ^{18}F-GE180 signal seen in disease states (for example as observed in a recent study of ^{18}F-GE180 in glioblastoma)[77] represent specific binding or are merely due to non-specific signal in areas of blood-brain barrier breakdown. Such 'false positives' could be distinguished from 'true

positives' using TSPO blockade with XBD-173 in all ^{18}F-GE180 PET studies, although double the number of PET scans would be required. There also remains a high risk of false-negatives (i.e. true differences in TSPO expression not observed because of low brain penetration and poor signal-to-noise ratio), for example as demonstrated by ^{18}F-GE180's inability to distinguish TSPO HABs and MABs. This has important implications for ongoing ^{18}F-GE180 studies worldwide.

III.8.2 Natalizumab cohort

The 'natalizumab cohort' did not use TSPO blockade with XBD-173, and so both false-negative and false-positive results are a possibility, as described above. The study results were interpreted with these limitations in mind, and only basic analyses are presented rather than the initial study objective to correlate ^{18}F-GE180 signal with a variety of clinical and radiological outcomes.

As with the reported data from healthy controls from this study,[1] across the full cohort there was no difference in V_T between HABS and MABS in any region of interest, in the HC group or the MS group, at any time point. There were also several other negative results, which conflict with positive results obtained using other TSPO tracers. For example, other TSPO PET studies in MS have found signal to be increased in peri-lesional white matter, normal-appearing white matter, and cortical grey matter, and have found the pattern of TSPO PET signal to correlate with other clinical outcomes.[35, 36, 38-40, 45] These results could not be replicated in this study, and may be 'false negatives' related to the low brain penetration of ^{18}F-GE180. The lack of increased ^{18}F-GE180 signal in the cortical grey matter may be a 'false negative', and meant that it could not be assessed whether grey matter TSPO expression is responsive to natalizumab

treatment, a topic which remains of interest since cortical neuroinflammation may be associated with neurodegeneration and the progression of disability in MS.[7, 11-15]

The study did find that ^{18}F-GE180 V_T was increased in lesions. However, even in lesions there was no difference in V_T between HABs and MABs. This is in keeping with a recent cross-sectional study by Unterrainer *et al*, which found increased ^{18}F-GE180 signal in lesions of nineteen subjects with relapsing-remitting MS.[78] Unterrainer *et al*. reported no associations between underlying binding affinity status (HAB=11, MAB=5 and LAB=3) and the signal intensity in any region of interest, including lesions. This led some to argue that the increased ^{18}F-GE180 uptake seen in lesions of PwMS is merely an 'aspecific accumulation through a broken blood−brain barrier', especially since LABs had equivalent signal (who would be expected to show very low binding).[79] Unterrainer *et al*. retorted that the lack of association between TSPO binding affinity and ^{18}F-GE180 signal may instead reflect the small sample size of their study and heterogeneity of TSPO expression in MS lesions.[80] It has been suggested that studies with larger sample sizes are necessary to conclude whether ^{18}F-GE180 can detect genotype differences.[81] The 'natalizumab cohort' reported here does have a substantially greater sample size of scans and lesions than that of Unterrainer *et al*., and also has the advantage of employing arterial blood sampling, thereby allowing analyses based upon V_T rather than only standardised uptake value ratios. These results therefore lend support to the conclusion that increased ^{18}F-GE180 uptake seen in lesions of PwMS is mainly due to aspecific accumulation through a disrupted blood−brain barrier, rather than a true representation of TSPO expression.

This is not out-of-keeping with the results of the 'blocking study', since it is not incongruous to state both that a proportion of ^{18}F-GE180 tracer ends up bound specifically to TSPO, but also that signal intensity is affected to a far greater degree by differences in blood-brain barrier

permeability. Visually, ^{18}F-GE180 can display high lesion-to-background ratio in gadolinium-enhancing lesions,[78] or in other disease such as glioblastoma,[77] although again this is explained by the passing of ^{18}F-GE180 through a disrupted blood-brain barrier, displayed starkly alongside the low ^{18}F-GE180 signal in brain areas with healthy blood−brain barrier.

The usefulness of ^{18}F-GE180 for research or in the clinic is significantly limited by these conclusions. That said, there are still some additional observations that can be drawn from the results of the 'natalizumab cohort'. Firstly, ^{18}F-GE180 was most prominent in gadolinium-enhancing lesions but was also increased in lesions which were not gadolinium-enhancing (which made up a large majority of lesions studied). This is supported by results reported by Unterrainer *et al*.[78] These data can be interpreted as suggesting that ^{18}F-GE180 PET is a more sensitive (albeit less specific) way of identifying blood-brain barrier disruption than the standard protocols for MRI with gadolinium administration. It is known that standard protocols for MRI with gadolinium are only sensitive enough to detect the most overt breakdowns in the blood-brain barrier,[82, 83] and histopathological studies have reported blood−brain barrier abnormalities in inactive MS lesions as well as normal-appearing white matter.[84-87] PET can detect signal at picomolar concentrations, whereas gadolinium-MRI has a sensitivity at micromolar concentrations.[88] However, it seems unlikely that ^{18}F-GE180 could be used clinically as a more sensitive marker of blood-brain barrier breakdown, given its low specificity, as well as the cost, patient discomfort, and radiation exposure of a PET scan. Alternative MRI methods such as using longitudinal relaxation time (T1) maps or dynamic contrast-enhanced MRI (DCE-MRI) may offer a way to improve sensitivity when investigating blood-brain barrier permeability in MS,[82, 83, 89-91] or PET tracers specific to blood−brain barrier integrity such as ^{11}C-Verapamil or ^{11}C-N-desmethyl-loperamide.[92, 93]

Similarly, mean ^{18}F-GE180 V_T was also slightly increased at baseline in 'pre-lesions' (MRI NAWM areas which would later develop lesions on subsequent MRI). Again, this probably relates to ^{18}F-GE180 PET being a more sensitive way of identifying blood-brain barrier disruption than standard protocols for MRI with gadolinium administration. These data support evidence that blood-brain barrier breakdown is an early event in the pathophysiology of lesion genesis and may precede myelin damage and leucocyte infiltration.[94-98] Although ^{18}F-GE180 V_T was slightly increased in 'pre-lesions' at the group level, this technique could not reliably identify individual pre-lesions at the baseline scan, since V_T was not sensitive or specific at discriminating 'pre-lesions' from other NAWM.

Lastly, this study found that ^{18}F-GE180 V_T decreases in lesions after the initiation of natalizumab. The likely interpretation of this is that natalizumab is an effective DMT, and its efficacy as an immunomodulator results in improved integrity of the blood-brain barrier. This is supported by *in vitro* and *in vivo* studies which have shown that DMTs including natalizumab can improve the integrity of the blood-brain barrier.[91, 99, 100]

Other than these results related to ^{18}F-GE180 PET, the 'natalizumab study' also collected a variety of MRI, clinical, and patient-reported outcome data before and after natalizumab treatment. These data were investigated independently from the PET data, and have led to several other areas of work, for example:

- The MRI technique 'arterial spin labelling' suggested improved cerebral blood flow after natalizumab treatment. This has been presented as an abstract with the thesis author as 'senior author', and is being worked into a paper for submission.[101]
- The MRI technique 'magnetic resonance spectroscopy' suggested decrease glutamate in the thalamus of people with MS, which correlated with lesion load and normalised after

treatment with natalizumab. This has been presented as an abstract with the thesis author as 'senior author', and is being worked into a paper for submission.[102]

- The model 'Brain-Predicted Age' which uses machine learning analysis of T1-weighted MRI was tested in the 'natalizumab cohort', and then further developed in larger multiple sclerosis cohorts. Results have been published as pre-prints with the thesis author as 'joint first author',[103] and are reported in Chapter 4.
- The patient-reported outcome 'Multiple Sclerosis Impact Scale (MSIS-29)' was investigated in the 'natalizumab cohort', and then tested for prognostic value in a larger multiple sclerosis cohort. Results have been published in *PLOS Medicine* with the thesis author as first author,[104] and are reported in Chapter 5.

III.8.3 Conclusion

These studies showed that ^{18}F-GE180 has considerably lower extraction across the blood-brain barrier than expected from animal studies and compared to other TSPO tracers. The 'blocking study' suggested that ^{18}F-GE180 does exhibit some specific signal. However, the tracer is still substantially limited by poor signal-to-noise ratio. ^{18}F-GE180 V_T was not able to detect increased TSPO in MS in the GM or NAWM as reported with other tracers, or differences in TSPO binding affinity as expected. The 'natalizumab cohort' showed increased ^{18}F-GE180 V_T in white matter lesions, which is responsive to natalizumab treatment, although these results are likely to reflect differences in blood-brain barrier permeability rather than TSPO expression. Overall, these results lend support to the conclusion that ^{18}F-GE180 is not a useful marker of TSPO expression in HCs or PwMS. Other TSPO tracers with improved performance over ^{18}F-GE180 may be useful in evaluating response to DMTs at an early time point.

III.9 ACKNOWLEDGEMENTS

Thank you to the staff at the Clinical Imaging Facility, Imperial College London, especially Albert Busza, Hope McDevitt, Andy Blyth, Vijay Vaja, and Gokul Kolipaka. Thank you most of all to the 33 subjects that volunteered to take part in this study and underwent study activities including arterial line insertion and lengthy clinical and radiological testing; without their generous contribution this work would not have been possible.

III.10 CONFLICTS OF INTEREST

The thesis author Dr Raffel received funding for his salary from GE Healthcare Ltd with support from Fast Forward LLC (National Multiple Sclerosis Society). GE Healthcare provided ^{18}F-GE180 free of charge for this study.

Dr Sridharan received funding for her salary from GE Healthcare

Dr Nicholas received funding from GE Healthcare. Dr Nicholas has received outside the submitted work: grants, personal fees and non-financial support from Novartis; grants, personal fees and non-financial support from Biogen Idec; personal fees from Genzyme; and personal fees from Roche.

Dr Muraro declares honoraria for speaking and travel support from Bayer, Biogen, Merck Serono and Novartis.

Dr Brooks holds consultancies with GE Healthcare and Biogen.

Other authors declare no conflicts of interest related to this chapter.

III.11 REFERENCES

1. Feeney C, Scott G, Raffel J, Roberts S, Coello C, Jolly A, Searle G, Goldstone AP, Brooks DJ, Nicholas RS, Trigg W, Gunn RN, Sharp DJ. Kinetic analysis of the translocator protein positron emission tomography ligand [(18)F]GE-180 in the human brain. Eur J Nucl Med Mol Imaging. 2016;43(12):2201-10. Epub 2016/06/29. doi: 10.1007/s00259-016-3444-z. PubMed PMID: 27349244; PubMed Central PMCID: PMCPMC5047949.
2. Sridharan S, Raffel J, Nandoskar A, Record C, Brooks DJ, Owen D, Sharp D, Muraro PA, Gunn R, Nicholas R. Confirmation of Specific Binding of the 18-kDa Translocator Protein (TSPO) Radioligand [(18)F]GE-180: a Blocking Study Using XBD173 in Multiple Sclerosis Normal Appearing White and Grey Matter. Mol Imaging Biol. 2019;21(5):935-44. Epub 2019/02/24. doi: 10.1007/s11307-019-01323-8. PubMed PMID: 30796709.
3. Nijeholt GJ, van Walderveen MA, Castelijns JA, van Waesberghe JH, Polman C, Scheltens P, Rosier PF, Jongen PJ, Barkhof F. Brain and spinal cord abnormalities in multiple sclerosis. Correlation between MRI parameters, clinical subtypes and symptoms. Brain : a journal of neurology. 1998;121 (Pt 4):687-97. Epub 1998/05/13. doi: 10.1093/brain/121.4.687. PubMed PMID: 9577394.
4. Davis FA. The clinico-radiological paradox in multiple sclerosis: novel implications of lesion size. Multiple sclerosis. 2014;20(4):515-6. Epub 2013/07/28. doi: 10.1177/1352458513498949. PubMed PMID: 23886827.
5. Gilbert JJ, Sadler M. Unsuspected multiple sclerosis. Archives of neurology. 1983;40(9):533-6. Epub 1983/09/01. doi: 10.1001/archneur.1983.04050080033003. PubMed PMID: 6615282.
6. Engell T. A clinical patho-anatomical study of clinically silent multiple sclerosis. Acta Neurol Scand. 1989;79(5):428-30. Epub 1989/05/01. doi: 10.1111/j.1600-0404.1989.tb03811.x. PubMed PMID: 2741673.
7. Kidd D, Barkhof F, McConnell R, Algra PR, Allen IV, Revesz T. Cortical lesions in multiple sclerosis. Brain : a journal of neurology. 1999;122 (Pt 1):17-26. Epub 1999/03/02. doi: 10.1093/brain/122.1.17. PubMed PMID: 10050891.
8. Duddy M, Lee M, Pearson O, Nikfekr E, Chaudhuri A, Percival F, Roberts M, Whitlock C. The UK patient experience of relapse in Multiple Sclerosis treated with first disease modifying therapies. Mult Scler Relat Disord. 2014;3(4):450-6. Epub 2015/04/17. doi: 10.1016/j.msard.2014.02.006. PubMed PMID: 25877056.
9. Avasarala J. Redefining Acute Relapses in Multiple Sclerosis: Implications for Phase 3 Clinical Trials and Treatment Algorithms. Innov Clin Neurosci. 2017;14(3-4):38-40. Epub 2017/06/07. PubMed PMID: 28584696; PubMed Central PMCID: PMCPMC5451037.
10. Dobson R, Rudick RA, Turner B, Schmierer K, Giovannoni G. Assessing treatment response to interferon-beta: is there a role for MRI? Neurology. 2014;82(3):248-54. doi: 10.1212/WNL.0000000000000036. PubMed PMID: 24336144; PubMed Central PMCID: PMCPMC3902760.

11. Lassmann H. Multiple sclerosis: Is there neurodegeneration independent from inflammation? J Neurol Sci. 2007;259(1-2):3-6. doi: DOI 10.1016/j.jns.2006.08.016. PubMed PMID: WOS:000248617400002.

12. Bevan RJ, Evans R, Griffiths L, Watkins LM, Rees MI, Magliozzi R, Allen I, McDonnell G, Kee R, Naughton M, Fitzgerald DC, Reynolds R, Neal JW, Howell OW. Meningeal inflammation and cortical demyelination in acute multiple sclerosis. Annals of neurology. 2018;84(6):829-42. Epub 2018/10/27. doi: 10.1002/ana.25365. PubMed PMID: 30362156.

13. Herranz E, Gianni C, Louapre C, Treaba CA, Govindarajan ST, Ouellette R, Loggia ML, Sloane JA, Madigan N, Izquierdo-Garcia D, Ward N, Mangeat G, Granberg T, Klawiter EC, Catana C, Hooker JM, Taylor N, Ionete C, Kinkel RP, Mainero C. Neuroinflammatory component of gray matter pathology in multiple sclerosis. Annals of neurology. 2016;80(5):776-90. Epub 2016/10/26. doi: 10.1002/ana.24791. PubMed PMID: 27686563; PubMed Central PMCID: PMCPMC5115951.

14. Howell OW, Reeves CA, Nicholas R, Carassiti D, Radotra B, Gentleman SM, Serafini B, Aloisi F, Roncaroli F, Magliozzi R, Reynolds R. Meningeal inflammation is widespread and linked to cortical pathology in multiple sclerosis. Brain : a journal of neurology. 2011;134(Pt 9):2755-71. Epub 2011/08/16. doi: 10.1093/brain/awr182. PubMed PMID: 21840891.

15. Reynolds R, Roncaroli F, Nicholas R, Radotra B, Gveric D, Howell O. The neuropathological basis of clinical progression in multiple sclerosis. Acta Neuropathol. 2011;122(2):155-70. Epub 2011/06/01. doi: 10.1007/s00401-011-0840-0. PubMed PMID: 21626034.

16. Sanders P, De Keyser J. Janus faces of microglia in multiple sclerosis. Brain Res Rev. 2007;54(2):274-85. doi: DOI 10.1016/j.brainresrev.2007.03.001. PubMed PMID: WOS:000247918500003.

17. Muzio L, Martino G, Furlan R. Multifaceted aspects of inflammation in multiple sclerosis: The role of microglia. Journal of neuroimmunology. 2007;191(1-2):39-44. doi: DOI 10.1016/j.jneuroim.2007.09.016. PubMed PMID: WOS:000251521900006.

18. Howell OW, Palser A, Polito A, Melrose S, Zonta B, Scheiermann C, Vora AJ, Brophy PJ, Reynolds R. Disruption of neurofascin localization reveals early changes preceding demyelination and remyelination in multiple sclerosis. Brain : a journal of neurology. 2006;129(Pt 12):3173-85. Epub 2006/10/17. doi: 10.1093/brain/awl290. PubMed PMID: 17041241.

19. Sriram S, Rodriguez M. Indictment of the microglia as the villain in multiple sclerosis. Neurology. 1997;48(2):464-70. PubMed PMID: WOS:A1997WH53500031.

20. Lassmann H, van Horssen J. The molecular basis of neurodegeneration in multiple sclerosis. Febs Lett. 2011;585(23):3715-23. doi: DOI 10.1016/j.febslet.2011.08.004. PubMed PMID: WOS:000297318000016.

21. Bogan RL, Davis TL, Niswender GD. Peripheral-type benzodiazepine receptor (PBR) aggregation and absence of steroidogenic acute regulatory protein (StAR)/PBR association in the mitochondrial membrane as determined by bioluminescence resonance energy transfer (BRET). J Steroid Biochem Mol Biol. 2007;104(1-2):61-7. Epub 2007/01/02. doi: 10.1016/j.jsbmb.2006.10.007. PubMed PMID: 17197174.

22. Cosenza-Nashat M, Zhao ML, Suh HS, Morgan J, Natividad R, Morgello S, Lee SC. Expression of the translocator protein of 18 kDa by microglia, macrophages and astrocytes based on immunohistochemical localization in abnormal human brain. Neuropath Appl Neuro. 2009;35(3):306-28. doi: DOI 10.1111/j.1365-2990.2008.01006.x. PubMed PMID: WOS:000265556600007.

23. Banati RB, Newcombe J, Gunn RN, Cagnin A, Turkheimer F, Heppner F, Price G, Wegner F, Giovannoni G, Miller DH, Perkin GD, Smith T, Hewson AK, Bydder G, Kreutzberg GW, Jones T, Cuzner ML, Myers R. The peripheral benzodiazepine binding site in the brain in multiple sclerosis - Quantitative in vivo imaging of microglia as a measure of disease activity. Brain : a journal of neurology. 2000;123:2321-37. doi: DOI 10.1093/brain/123.11.2321. PubMed PMID: WOS:000165413200014.

24. Venneti S, Lopresti BJ, Wiley CA. The peripheral benzodiazepine receptor (Translocator protein 18kDa) in microglia: from pathology to imaging. Prog Neurobiol. 2006;80(6):308-22. Epub 2006/12/13. doi: 10.1016/j.pneurobio.2006.10.002. PubMed PMID: 17156911; PubMed Central PMCID: PMCPMC1849976.

25. Yasuno F, Ota M, Kosaka J, Ito H, Higuchi M, Doronbekov TK, Nozaki S, Fujimura Y, Koeda M, Asada T, Suhara T. Increased binding of peripheral benzodiazepine receptor in Alzheimer's disease measured by positron emission tomography with [11C]DAA1106. Biol Psychiatry. 2008;64(10):835-41. Epub 2008/06/03. doi: 10.1016/j.biopsych.2008.04.021. PubMed PMID: 18514164.

26. Edison P, Archer HA, Gerhard A, Hinz R, Pavese N, Turkheimer FE, Hammers A, Tai YF, Fox N, Kennedy A, Rossor M, Brooks DJ. Microglia, amyloid, and cognition in Alzheimer's disease: An [11C](R)PK11195-PET and [11C]PIB-PET study. Neurobiol Dis. 2008;32(3):412-9. Epub 2008/09/13. doi: 10.1016/j.nbd.2008.08.001. PubMed PMID: 18786637.

27. Cagnin A, Rossor M, Sampson EL, Mackinnon T, Banati RB. In vivo detection of microglial activation in frontotemporal dementia. Annals of neurology. 2004;56(6):894-7. Epub 2004/11/25. doi: 10.1002/ana.20332. PubMed PMID: 15562429.

28. Ouchi Y, Yoshikawa E, Sekine Y, Futatsubashi M, Kanno T, Ogusu T, Torizuka T. Microglial activation and dopamine terminal loss in early Parkinson's disease. Annals of neurology. 2005;57(2):168-75. Epub 2005/01/26. doi: 10.1002/ana.20338. PubMed PMID: 15668962.

29. Turner MR, Cagnin A, Turkheimer FE, Miller CC, Shaw CE, Brooks DJ, Leigh PN, Banati RB. Evidence of widespread cerebral microglial activation in amyotrophic lateral sclerosis: an [11C](R)-PK11195 positron emission tomography study. Neurobiol Dis. 2004;15(3):601-9. Epub 2004/04/02. doi: 10.1016/j.nbd.2003.12.012. PubMed PMID: 15056468.

30. Messmer K, Reynolds GP. Increased peripheral benzodiazepine binding sites in the brain of patients with Huntington's disease. Neurosci Lett. 1998;241(1):53-6. Epub 1998/03/21. doi: 10.1016/s0304-3940(97)00967-1. PubMed PMID: 9502214.

31. Banati RB, Goerres GW, Myers R, Gunn RN, Turkheimer FE, Kreutzberg GW, Brooks DJ, Jones T, Duncan JS. [11C](R)-PK11195 positron emission tomography imaging of activated microglia in vivo in Rasmussen's encephalitis. Neurology. 1999;53(9):2199-203. Epub 1999/12/22. doi: 10.1212/wnl.53.9.2199. PubMed PMID: 10599809.

32. Cagnin A, Myers R, Gunn RN, Lawrence AD, Stevens T, Kreutzberg GW, Jones T, Banati RB. In vivo visualization of activated glia by [11C] (R)-PK11195-PET following herpes encephalitis reveals projected neuronal damage beyond the primary focal lesion. Brain : a journal of neurology. 2001;124(Pt 10):2014-27. Epub 2001/09/26. doi: 10.1093/brain/124.10.2014. PubMed PMID: 11571219.

33. Kaunzner UW, Kang Y, Zhang S, Morris E, Yao Y, Pandya S, Hurtado Rua SM, Park C, Gillen KM, Nguyen TD, Wang Y, Pitt D, Gauthier SA. Quantitative susceptibility mapping identifies inflammation in a subset

of chronic multiple sclerosis lesions. Brain : a journal of neurology. 2019;142(1):133-45. Epub 2018/12/19. doi: 10.1093/brain/awy296. PubMed PMID: 30561514; PubMed Central PMCID: PMCPMC6308309.

34. Nutma E, Stephenson JA, Gorter RP, de Bruin J, Boucherie DM, Donat CK, Breur M, van der Valk P, Matthews PM, Owen DR, Amor S. A quantitative neuropathological assessment of translocator protein expression in multiple sclerosis. Brain : a journal of neurology. 2019. Epub 2019/10/04. doi: 10.1093/brain/awz287. PubMed PMID: 31578541.

35. Debruyne JC, Versijpt J, Van Laere KJ, De Vos F, Keppens J, Strijckmans K, Achten E, Slegers G, Dierckx RA, Korf J, De Reuck JL. PET visualization of microglia in multiple sclerosis patients using [C-11]PK11195. European Journal of Neurology. 2003;10(3):257-64. doi: DOI 10.1046/j.1468-1331.2003.00571.x. PubMed PMID: WOS:000182651000009.

36. Versijpt J, Debruyne JC, Van Laere KJ, De Vos F, Keppens J, Strijckmans K, Achten E, Slegers G, Dierckx RA, Korf J, De Reuck JL. Microglial imaging with positron emission tomography and atrophy measurements with magnetic resonance imaging in multiple sclerosis: a correlative study. Mult Scler J. 2005;11(2):127-34. doi: Doi 10.1191/1352458505ms1140oa. PubMed PMID: WOS:000227717400001.

37. Vas A, Shchukin Y, Karrenbauer VD, Cselenyi Z, Kostulas K, Hillert J, Savic I, Takano A, Halldin C, Gulyas B. Functional neuroimaging in multiple sclerosis with radiolabelled glia markers: Preliminary comparative PET studies with [C-11]vinpocetine and [C-11]PK11195 in patients. J Neurol Sci. 2008;264(1-2):9-17. doi: DOI 10.1016/j.jns.2007.07.018. PubMed PMID: WOS:000252686200002.

38. Colasanti A, Guo Q, Muhlert N, Giannetti P, Onega M, Newbould RD, Ciccarelli O, Rison S, Thomas C, Nicholas R, Muraro PA, Malik O, Owen DR, Piccini P, Gunn RN, Rabiner EA, Matthews PM. In Vivo Assessment of Brain White Matter Inflammation in Multiple Sclerosis with (18)F-PBR111 PET. Journal of nuclear medicine : official publication, Society of Nuclear Medicine. 2014;55(7):1112-8. Epub 2014/06/07. doi: 10.2967/jnumed.113.135129. PubMed PMID: 24904112.

39. Politis M, Giannetti P, Su P, Turkheimer F, Keihaninejad S, Wu K, Waldman A, Malik O, Matthews PM, Reynolds R, Nicholas R, Piccini P. Increased PK11195 PET binding in the cortex of patients with MS correlates with disability. Neurology. 2012;79(6):523-30. PubMed PMID: WOS:000307458800011.

40. Datta G, Colasanti A, Kalk N, Owen D, Scott G, Rabiner EA, Gunn RN, Lingford-Hughes A, Malik O, Ciccarelli O, Nicholas R, Nei L, Battaglini M, Stefano ND, Matthews PM. (11)C-PBR28 and (18)F-PBR111 Detect White Matter Inflammatory Heterogeneity in Multiple Sclerosis. Journal of nuclear medicine : official publication, Society of Nuclear Medicine. 2017;58(9):1477-82. Epub 2017/03/18. doi: 10.2967/jnumed.116.187161. PubMed PMID: 28302760.

41. Chen MK, Guilarte TR. Translocator protein 18 kDa (TSPO): Molecular sensor of brain injury and repair. Pharmacol Therapeut. 2008;118(1):1-17. doi: DOI 10.1016/j.pharmthera.2007.12.004. PubMed PMID: WOS:000256240900001.

42. Olsson B, Malmestrom C, Basun H, Annas P, Hoglund K, Lannfelt L, Andreasen N, Zetterberg H, Blennow K. Extreme Stability of Chitotriosidase in Cerebrospinal Fluid makes it a Suitable Marker for Microglial Activation in Clinical Trials. J Alzheimers Dis. 2012;32(2):273-6. doi: Doi 10.3233/Jad-2012-120931. PubMed PMID: WOS:000309977800003.

43. Airas L, Dickens AM, Elo P, Marjamaki P, Johansson J, Eskola O, Jones PA, Trigg W, Solin O, Haaparanta-Solin M, Anthony DC, Rinne J. In Vivo PET Imaging Demonstrates Diminished Microglial

Activation After Fingolimod Treatment in an Animal Model of Multiple Sclerosis. Journal of nuclear medicine : official publication, Society of Nuclear Medicine. 2015;56(2):305-10. doi: 10.2967/jnumed.114.149955. PubMed PMID: 25572093.

44. Ratchford JN, Endres CJ, Hammoud DA, Pomper MG, Shiee N, McGready J, Pham DL, Calabresi PA. Decreased microglial activation in MS patients treated with glatiramer acetate. J Neurol. 2012;259(6):1199-205. doi: DOI 10.1007/s00415-011-6337-x. PubMed PMID: WOS:000304859300026.

45. Sucksdorff M, Rissanen E, Tuisku J, Nuutinen S, Paavilainen T, Rokka J, Rinne J, Airas L. Evaluation of the Effect of Fingolimod Treatment on Microglial Activation Using Serial PET Imaging in Multiple Sclerosis. Journal of nuclear medicine : official publication, Society of Nuclear Medicine. 2017;58(10):1646-51. Epub 2017/03/25. doi: 10.2967/jnumed.116.183020. PubMed PMID: 28336784.

46. Kropholler MA, Boellaard R, van Berckel BN, Schuitemaker A, Kloet RW, Lubberink MJ, Jonker C, Scheltens P, Lammertsma AA. Evaluation of reference regions for (R)-[(11)C]PK11195 studies in Alzheimer's disease and mild cognitive impairment. J Cereb Blood Flow Metab. 2007;27(12):1965-74. Epub 2007/04/05. doi: 10.1038/sj.jcbfm.9600488. PubMed PMID: 17406654.

47. Schuitemaker A, van Berckel BN, Kropholler MA, Veltman DJ, Scheltens P, Jonker C, Lammertsma AA, Boellaard R. SPM analysis of parametric (R)-[11C]PK11195 binding images: plasma input versus reference tissue parametric methods. Neuroimage. 2007;35(4):1473-9. Epub 2007/03/17. doi: 10.1016/j.neuroimage.2007.02.013. PubMed PMID: 17363280.

48. Kropholler MA, Boellaard R, Schuitemaker A, Folkersma H, van Berckel BN, Lammertsma AA. Evaluation of reference tissue models for the analysis of [11C](R)-PK11195 studies. J Cereb Blood Flow Metab. 2006;26(11):1431-41. Epub 2006/03/03. doi: 10.1038/sj.jcbfm.9600289. PubMed PMID: 16511500.

49. Tu Z, Mach RH. C-11 radiochemistry in cancer imaging applications. Curr Top Med Chem. 2010;10(11):1060-95. Epub 2010/04/15. doi: 10.2174/156802610791384261. PubMed PMID: 20388115.

50. Dickens AM, Vainio S, Marjamaki P, Johansson J, Lehtiniemi P, Rokka J, Rinne J, Solin O, Haaparanta-Solin M, Jones PA, Trigg W, Anthony DC, Airas L. Detection of microglial activation in an acute model of neuroinflammation using PET and radiotracers 11C-(R)-PK11195 and 18F-GE-180. Journal of nuclear medicine : official publication, Society of Nuclear Medicine. 2014;55(3):466-72. doi: 10.2967/jnumed.113.125625. PubMed PMID: 24516258.

51. Wadsworth H, Jones PA, Chau WF, Durrant C, Fouladi N, Passmore J, O'Shea D, Wynn D, Morisson-Iveson V, Ewan A, Thaning M, Mantzilas D, Gausemel I, Khan I, Black A, Avory M, Trigg W. [F-18]GE-180: A novel fluorine-18 labelled PET tracer for imaging Translocator protein 18 kDa (TSPO). Bioorg Med Chem Lett. 2012;22(3):1308-13. doi: DOI 10.1016/j.bmcl.2011.12.084. PubMed PMID: WOS:000300404200002.

52. Boutin H, Murray K, Pradillo J, Maroy R, Smigova A, Gerhard A, Jones PA, Trigg W. 18F-GE-180: a novel TSPO radiotracer compared to 11C-R-PK11195 in a preclinical model of stroke. Eur J Nucl Med Mol Imaging. 2015;42(3):503-11. Epub 2014/10/30. doi: 10.1007/s00259-014-2939-8. PubMed PMID: 25351507.

53. Owen DR, Yeo AJ, Gunn RN, Song K, Wadsworth G, Lewis A, Rhodes C, Pulford DJ, Bennacef I, Parker CA, StJean PL, Cardon LR, Mooser VE, Matthews PM, Rabiner EA, Rubio JP. An 18-kDa translocator protein (TSPO) polymorphism explains differences in binding affinity of the PET radioligand PBR28. J Cereb Blood Flow Metab. 2012;32(1):1-5. doi: 10.1038/jcbfm.2011.147. PubMed PMID: 22008728; PubMed Central PMCID: PMC3323305.

54. Owen DR, Howell OW, Tang SP, Wells LA, Bennacef I, Bergstrom M, Gunn RN, Rabiner EA, Wilkins MR, Reynolds R, Matthews PM, Parker CA. Two binding sites for [3H]PBR28 in human brain: implications for TSPO PET imaging of neuroinflammation. J Cereb Blood Flow Metab. 2010;30(9):1608-18. Epub 2010/04/29. doi: 10.1038/jcbfm.2010.63. PubMed PMID: 20424634; PubMed Central PMCID: PMC2949260.

55. Owen DRJ, Gunn RN, Rabiner EA, Bennacef I, Fujita M, Kreisl WC, Innis RB, Pike VW, Reynolds R, Matthews PM, Parker CA. Mixed-Affinity Binding in Humans with 18-kDa Translocator Protein Ligands. Journal of Nuclear Medicine. 2011;52(1):24-32. doi: DOI 10.2967/jnumed.110.079459. PubMed PMID: WOS:000285686400010.

56. GE-180 Phase 1 Study Canada 2014 [February 2015]. Available from: https://www.clinicaltrials.gov/ct2/show/NCT01738347?term=GE180&rank=1.

57. Owen DR, Guo Q, Kalk NJ, Colasanti A, Kalogiannopoulou D, Dimber R, Lewis YL, Libri V, Barletta J, Ramada-Magalhaes J, Kamalakaran A, Nutt DJ, Passchier J, Matthews PM, Gunn RN, Rabiner EA. Determination of [(11)C]PBR28 binding potential in vivo: a first human TSPO blocking study. J Cereb Blood Flow Metab. 2014;34(6):989-94. Epub 2014/03/20. doi: 10.1038/jcbfm.2014.46. PubMed PMID: 24643083; PubMed Central PMCID: PMCPMC4050243.

58. Polman CH, Reingold SC, Banwell B, Clanet M, Cohen JA, Filippi M, Fujihara K, Havrdova E, Hutchinson M, Kappos L, Lublin FD, Montalban X, O'Connor P, Sandberg-Wollheim M, Thompson AJ, Waubant E, Weinshenker B, Wolinsky JS. Diagnostic criteria for multiple sclerosis: 2010 revisions to the McDonald criteria. Annals of neurology. 2011;69(2):292-302. Epub 2011/03/10. doi: 10.1002/ana.22366. PubMed PMID: 21387374; PubMed Central PMCID: PMCPMC3084507.

59. NICE technological appraisal - TA127 - Natalizumab for the treatment of adults with highly active relapsing–remitting multiple sclerosis. Published 22 August 2017. URL: https://www.nice.org.uk/guidance/ta127. Last accessed October 2019.

60. Hammers A, Allom R, Free SL, Myers R, Lemieux L, Mitchell TN, Brooks DJ, Koepp MJ, Duncan JS. Three-dimensional probabilistic atlas of the human brain. Neuroimage. 2002;16(3):S86-S. PubMed PMID: WOS:000176861900086.

61. Criminisi A, Sharp T, Blake A. Geos: Geodesic image segmentation. Computer Vision–ECCV 2008 2008:99-112.

62. Watabe H, Channing MA, Der MG, Adams HR, Jagoda E, Herscovitch P, Eckelman WC, Carson RE. Kinetic analysis of the 5-HT2A ligand [11C]MDL 100,907. J Cereb Blood Flow Metab. 2000;20(6):899-909. doi: 10.1097/00004647-200006000-00002. PubMed PMID: 10894173.

63. Fan Z, Calsolaro V, Atkinson RA, Femminella GD, Waldman A, Buckley C, Trigg W, Brooks DJ, Hinz R, Edison P. Flutriciclamide (18F-GE180) PET: First-in-Human PET Study of Novel Third-Generation In Vivo Marker of Human Translocator Protein. Journal of nuclear medicine : official publication, Society of Nuclear Medicine. 2016;57(11):1753-9. Epub 2016/11/03. doi: 10.2967/jnumed.115.169078. PubMed PMID: 27261523.

64. Cunningham VJ, Rabiner EA, Slifstein M, Laruelle M, Gunn RN. Measuring drug occupancy in the absence of a reference region: the Lassen plot re-visited. J Cereb Blood Flow Metab. 2010;30(1):46-50. Epub 2009/09/10. doi: 10.1038/jcbfm.2009.190. PubMed PMID: 19738632; PubMed Central PMCID: PMCPMC2949110.

65. Guo Q, Colasanti A, Owen DR, Onega M, Kamalakaran A, Bennacef I, Matthews PM, Rabiner EA, Turkheimer FE, Gunn RN. Quantification of the specific translocator protein signal of 18F-PBR111 in healthy humans: a genetic polymorphism effect on in vivo binding. J Nucl Med. 2013;54(11):1915-23. doi: 10.2967/jnumed.113.121020. PubMed PMID: 24071511.

66. Schumacher GA. Problems of experimental trials of therapy in MS: report of the panel on evaluation of experimental trials in MS. Annals of the New York Academy of Sciences, vol. 122, p. 552–68., 1968.

67. Qiao L, Fisher E, McMurray L, Milicevic Sephton S, Hird M, Kuzhuppilly-Ramakrishnan N, Williamson DJ, Zhou X, Werry E, Kassiou M, Luthra S, Trigg W, Aigbirhio FI. Radiosynthesis of (R,S)-[(18) F]GE387: A Potential PET Radiotracer for Imaging Translocator Protein 18 kDa (TSPO) with Low Binding Sensitivity to the Human Gene Polymorphism rs6971. ChemMedChem. 2019;14(9):982-93. Epub 2019/03/23. doi: 10.1002/cmdc.201900023. PubMed PMID: 30900397; PubMed Central PMCID: PMCPMC6563049.

68. Zanotti-Fregonara P, Pascual B, Rizzo G, Yu M, Pal N, Beers D, Carter R, Appel SH, Atassi N, Masdeu JC. Head-to-Head Comparison of (11)C-PBR28 and (18)F-GE180 for Quantification of the Translocator Protein in the Human Brain. Journal of nuclear medicine : official publication, Society of Nuclear Medicine. 2018;59(8):1260-6. Epub 2018/01/20. doi: 10.2967/jnumed.117.203109. PubMed PMID: 29348317.

69. Lockhart A, Davis B, Matthews JC, Rahmoune H, Hong G, Gee A, Earnshaw D, Brown J. The peripheral benzodiazepine receptor ligand PK11195 binds with high affinity to the acute phase reactant alpha1-acid glycoprotein: implications for the use of the ligand as a CNS inflammatory marker. Nucl Med Biol. 2003;30(2):199-206. Epub 2003/03/08. doi: 10.1016/s0969-8051(02)00410-9. PubMed PMID: 12623120.

70. Toth M, Haggkvist J, Varrone A, Finnema SJ, Doorduin J, Tokunaga M, Higuchi M, Gulyas B, Halldin C. ABC transporter-dependent brain uptake of the 5-HT1B receptor radioligand [(11)C]AZ10419369: a comparative PET study in mouse, rat, and guinea pig. EJNMMI Res. 2014;4(1):64. Epub 2015/06/28. doi: 10.1186/s13550-014-0064-0. PubMed PMID: 26116125; PubMed Central PMCID: PMCPMC4452686.

71. Bloomfield PS, Selvaraj S, Veronese M, Rizzo G, Bertoldo A, Owen DR, Bloomfield MA, Bonoldi I, Kalk N, Turkheimer F, McGuire P, de Paola V, Howes OD. Microglial activity in people at ultra high risk of psychosis and in schizophrenia: an [(11)C]PBR28 PET brain imaging study. Am J Psychiatry. 2016;173(1):44-52. doi: 10.1176/appi.ajp.2015.14101358. PubMed PMID: 26472628; PubMed Central PMCID: PMCPMC4821370.

72. Turkheimer FE, Rizzo G, Bloomfield PS, Howes O, Zanotti-Fregonara P, Bertoldo A, Veronese M. The methodology of TSPO imaging with positron emission tomography. Biochem Soc Trans. 2015;43(4):586-92. doi: 10.1042/BST20150058. PubMed PMID: 26551697; PubMed Central PMCID: PMCPMC4613512.

73. Veronese M, Reis Marques T, Bloomfield PS, Rizzo G, Singh N, Jones D, Agushi E, Mosses D, Bertoldo A, Howes O, Roncaroli F, Turkheimer FE. Kinetic modelling of [11C]PBR28 for 18 kDa translocator protein PET data: A validation study of vascular modelling in the brain using XBD173 and tissue analysis. J Cereb Blood Flow Metab. 2017:271678X17712388. Epub 2017/06/06. doi: 10.1177/0271678X17712388. PubMed PMID: 28580888.

74. Albrecht D, Shcherbinin S, Wooten D, Schwarz A, Zurcher N, Barth V, Atassi N, Normandin M, Hooker J, Loggia M. Occipital lobe as a pseudo-reference region for [11C]PBR28 PET imaging: validation in chronic pain and amyotrophic lateral sclerosis cohorts. Journal of Nuclear Medicine. 2016;57(supplement 2):1814.

75. Kreisl WC, Fujita M, Fujimura Y, Kimura N, Jenko KJ, Kannan P, Hong J, Morse CL, Zoghbi SS, Gladding RL, Jacobson S, Oh U, Pike VW, Innis RB. Comparison of [(11)C]-(R)-PK 11195 and [(11)C]PBR28, two radioligands for translocator protein (18 kDa) in human and monkey: Implications for positron emission tomographic imaging of this inflammation biomarker. Neuroimage. 2010;49(4):2924-32. Epub 2009/12/02. doi: 10.1016/j.neuroimage.2009.11.056. PubMed PMID: 19948230; PubMed Central PMCID: PMC2832854.

76. Park E, Gallezot JD, Delgadillo A, Liu S, Planeta B, Lin SF, O'Connor KC, Lim K, Lee JY, Chastre A, Chen MK, Seneca N, Leppert D, Huang Y, Carson RE, Pelletier D. (11)C-PBR28 imaging in multiple sclerosis patients and healthy controls: test-retest reproducibility and focal visualization of active white matter areas. Eur J Nucl Med Mol Imaging. 2015;42(7):1081-92. doi: 10.1007/s00259-015-3043-4. PubMed PMID: 25833352.

77. Albert NL, Unterrainer M, Fleischmann DF, Lindner S, Vettermann F, Brunegraf A, Vomacka L, Brendel M, Wenter V, Wetzel C, Rupprecht R, Tonn JC, Belka C, Bartenstein P, Niyazi M. TSPO PET for glioma imaging using the novel ligand (18)F-GE-180: first results in patients with glioblastoma. Eur J Nucl Med Mol Imaging. 2017;44(13):2230-8. Epub 2017/08/20. doi: 10.1007/s00259-017-3799-9. PubMed PMID: 28821920.

78. Unterrainer M, Mahler C, Vomacka L, Lindner S, Havla J, Brendel M, Boning G, Ertl-Wagner B, Kumpfel T, Milenkovic VM, Rupprecht R, Kerschensteiner M, Bartenstein P, Albert NL. TSPO PET with [(18)F]GE-180 sensitively detects focal neuroinflammation in patients with relapsing-remitting multiple sclerosis. Eur J Nucl Med Mol Imaging. 2018;45(8):1423-31. Epub 2018/03/11. doi: 10.1007/s00259-018-3974-7. PubMed PMID: 29523925.

79. Zanotti-Fregonara P, Veronese M, Pascual B, Rostomily RC, Turkheimer F, Masdeu JC. The validity of (18)F-GE180 as a TSPO imaging agent. Eur J Nucl Med Mol Imaging. 2019;46(6):1205-7. Epub 2019/01/19. doi: 10.1007/s00259-019-4268-4. PubMed PMID: 30656358.

80. Albert NL, Unterrainer M, Brendel M, Kaiser L, Zweckstetter M, Cumming P, Bartenstein P. In response to: The validity of 18F-GE180 as a TSPO imaging agent. Eur J Nucl Med Mol Imaging. 2019 ;46(6):1208-1211.

81. Werry EL, Bright FM, Piguet O, Ittner LM, Halliday GM, Hodges JR, Kiernan MC, Loy CT, Kril JJ, Kassiou M. Recent Developments in TSPO PET Imaging as A Biomarker of Neuroinflammation in Neurodegenerative Disorders. Int J Mol Sci. 2019;20(13). Epub 2019/07/03. doi: 10.3390/ijms20133161. PubMed PMID: 31261683; PubMed Central PMCID: PMCPMC6650818.

82. Heye AK, Culling RD, Valdes Hernandez Mdel C, Thrippleton MJ, Wardlaw JM. Assessment of blood-brain barrier disruption using dynamic contrast-enhanced MRI. A systematic review. Neuroimage Clin. 2014;6:262-74. Epub 2014/11/08. doi: 10.1016/j.nicl.2014.09.002. PubMed PMID: 25379439; PubMed Central PMCID: PMCPMC4215461.

83. Soon D, Tozer D, Altmann D, Tofts P, Miller D. Quantification of subtle blood-brain barrier disruption in non-enhancing lesions in multiple sclerosis: a study of disease and lesion subtypes. Multiple sclerosis. 2007;13(7):884-94. Epub 2007/05/01. doi: 10.1177/1352458507076970. PubMed PMID: 17468443.

84. Vos CM, Geurts JJ, Montagne L, van Haastert ES, Bo L, van der Valk P, Barkhof F, de Vries HE. Blood-brain barrier alterations in both focal and diffuse abnormalities on postmortem MRI in multiple sclerosis. Neurobiol Dis. 2005;20(3):953-60. Epub 2005/07/26. doi: 10.1016/j.nbd.2005.06.012. PubMed PMID: 16039866.

85. Plumb J, McQuaid S, Mirakhur M, Kirk J. Abnormal endothelial tight junctions in active lesions and normal-appearing white matter in multiple sclerosis. Brain Pathol. 2002;12(2):154-69. Epub 2002/04/18. PubMed PMID: 11958369.

86. McQuaid S, Cunnea P, McMahon J, Fitzgerald U. The effects of blood-brain barrier disruption on glial cell function in multiple sclerosis. Biochem Soc Trans. 2009;37(Pt 1):329-31. Epub 2009/01/16. doi: 10.1042/BST0370329. PubMed PMID: 19143657.

87. Kirk J, Plumb J, Mirakhur M, McQuaid S. Tight junctional abnormality in multiple sclerosis white matter affects all calibres of vessel and is associated with blood-brain barrier leakage and active demyelination. J Pathol. 2003;201(2):319-27. Epub 2003/10/01. doi: 10.1002/path.1434. PubMed PMID: 14517850.

88. Gauberti M, Montagne A, Quenault A, Vivien D. Molecular magnetic resonance imaging of brain-immune interactions. Front Cell Neurosci. 2014;8:389. Epub 2014/12/17. doi: 10.3389/fncel.2014.00389. PubMed PMID: 25505871; PubMed Central PMCID: PMCPMC4245913.

89. Montagne A, Barnes SR, Sweeney MD, Halliday MR, Sagare AP, Zhao Z, Toga AW, Jacobs RE, Liu CY, Amezcua L, Harrington MG, Chui HC, Law M, Zlokovic BV. Blood-brain barrier breakdown in the aging human hippocampus. Neuron. 2015;85(2):296-302. Epub 2015/01/23. doi: 10.1016/j.neuron.2014.12.032. PubMed PMID: 25611508; PubMed Central PMCID: PMCPMC4350773.

90. Bester M, Forkert ND, Stellmann JP, Sturner K, Aly L, Drabik A, Young KL, Heesen C, Fiehler J, Siemonsen S. Increased perfusion in normal appearing white matter in high inflammatory multiple sclerosis patients. PLoS One. 2015;10(3):e0119356. Epub 2015/03/17. doi: 10.1371/journal.pone.0119356. PubMed PMID: 25774497; PubMed Central PMCID: PMCPMC4361628.

91. Cramer SP, Simonsen H, Frederiksen JL, Rostrup E, Larsson HB. Abnormal blood-brain barrier permeability in normal appearing white matter in multiple sclerosis investigated by MRI. Neuroimage Clin. 2014;4:182-9. Epub 2013/12/29. doi: 10.1016/j.nicl.2013.12.001. PubMed PMID: 24371801; PubMed Central PMCID: PMCPMC3872721.

92. Luurtsema G, Molthoff CF, Schuit RC, Windhorst AD, Lammertsma AA, Franssen EJ. Evaluation of (R)-[11C]verapamil as PET tracer of P-glycoprotein function in the blood-brain barrier: kinetics and metabolism in the rat. Nucl Med Biol. 2005;32(1):87-93. Epub 2005/02/05. doi: 10.1016/j.nucmedbio.2004.06.007. PubMed PMID: 15691665.

93. Zoghbi SS, Liow JS, Yasuno F, Hong J, Tuan E, Lazarova N, Gladding RL, Pike VW, Innis RB. 11C-loperamide and its N-desmethyl radiometabolite are avid substrates for brain permeability-glycoprotein efflux. Journal of nuclear medicine : official publication, Society of Nuclear Medicine. 2008;49(4):649-56. Epub 2008/03/18. doi: 10.2967/jnumed.107.047308. PubMed PMID: 18344435.

94. Werring DJ, Brassat D, Droogan AG, Clark CA, Symms MR, Barker GJ, MacManus DG, Thompson AJ, Miller DH. The pathogenesis of lesions and normal-appearing white matter changes in multiple sclerosis: a serial diffusion MRI study. Brain : a journal of neurology. 2000;123 (Pt 8):1667-76. Epub 2000/07/25. doi: 10.1093/brain/123.8.1667. PubMed PMID: 10908196.

95. Filippi M, Rocca MA, Martino G, Horsfield MA, Comi G. Magnetization transfer changes in the normal appearing white matter precede the appearance of enhancing lesions in patients with multiple sclerosis. Annals of neurology. 1998;43(6):809-14. Epub 1998/06/18. doi: 10.1002/ana.410430616. PubMed PMID: 9629851.

96. Goodkin DE, Rooney WD, Sloan R, Bacchetti P, Gee L, Vermathen M, Waubant E, Abundo M, Majumdar S, Nelson S, Weiner MW. A serial study of new MS lesions and the white matter from which they arise. Neurology. 1998;51(6):1689-97. Epub 1998/12/17. doi: 10.1212/wnl.51.6.1689. PubMed PMID: 9855524.

97. Larochelle C, Alvarez JI, Prat A. How do immune cells overcome the blood-brain barrier in multiple sclerosis? Febs Lett. 2011;585(23):3770-80. Epub 2011/05/10. doi: 10.1016/j.febslet.2011.04.066. PubMed PMID: 21550344.

98. Kermode AG, Thompson AJ, Tofts P, MacManus DG, Kendall BE, Kingsley DP, Moseley IF, Rudge P, McDonald WI. Breakdown of the blood-brain barrier precedes symptoms and other MRI signs of new lesions in multiple sclerosis. Pathogenetic and clinical implications. Brain : a journal of neurology. 1990;113 (Pt 5):1477-89. Epub 1990/10/01. doi: 10.1093/brain/113.5.1477. PubMed PMID: 2245307.

99. Cramer SP, Simonsen HJ, Varatharaj A, Galea I, Frederiksen JL, Larsson HBW. Permeability of the blood-brain barrier predicts no evidence of disease activity at 2 years after natalizumab or fingolimod treatment in relapsing-remitting multiple sclerosis. Annals of neurology. 2018;83(5):902-14. Epub 2018/04/01. doi: 10.1002/ana.25219. PubMed PMID: 29604233; PubMed Central PMCID: PMCPMC6032831.

100. Kraus J, Voigt K, Schuller AM, Scholz M, Kim KS, Schilling M, Schabitz WR, Oschmann P, Engelhardt B. Interferon-beta stabilizes barrier characteristics of the blood-brain barrier in four different species in vitro. Multiple sclerosis. 2008;14(6):843-52. Epub 2008/05/29. doi: 10.1177/1352458508088940. PubMed PMID: 18505778.

101. Record C, De Simoni S, Feeney C, Sharp D, Nicholas R, Raffel J. Improved cerebral blood flow after natalizumab treatment in multiple sclerosis. ECTRIMS annual conference. London, UK. October, 2016.

102. Peress L, Ribeiro Violante I, Scott G, Zimmerman K, Sharp D, Nicholas R, Raffel J. Thalamic magnetic resonance spectroscopy in highly active multiple sclerosis. ECTRIMS annual conference. London, UK. October, 2016.

103. Cole JH, Raffel J, Friede T, Eshaghi A, Brownlee W, Chard D, De Stefano N, Enzinger C, Pirpamer L, Filippi M, Gasperini C, Rocca MA, Rovira A, Ruggieri S, Sastre-Garriga J, Stromillo ML, Uitdehaag BMJ, Vrenken H, Barkhof F, Nicholas R, Ciccarelli O, on behalf of the MAGNIMS study group. Accelerated brain ageing and disability in multiple sclerosis. bioRxiv 584888; doi: https://doi.org/10.1101/584888.

104. Raffel J, Wallace A, Gveric D, Reynolds R, Friede T, Nicholas R. Patient-reported outcomes and survival in multiple sclerosis: A 10-year retrospective cohort study using the Multiple Sclerosis Impact Scale-29. PLoS Med. 2017;14(7):e1002346. doi: 10.1371/journal.pmed.1002346. PubMed PMID: 28692670; PubMed Central PMCID: PMCPMC5503162.

Chapter 4

Brain Predicted Age in Multiple Sclerosis:

A Model using Machine Learning Analysis of MRI

IV.1 ABSTRACT

Background: As the human brain ages, there is non-linear and spatially variable change in brain volume. Previous work based at Imperial College London has developed a neuroimaging biomarker 'Brain Predicted Age', using machine learning to predict chronological age based solely upon a T1-weighted MRI of the brain. It is possible that the Brain Predicted Age model could be used to quantify damage and accelerated ageing-like changes, including brain atrophy, in the multiple sclerosis (MS) brain.

Objective: To apply the Brain Predicted Age model to a cohort of people with clinically isolated syndrome (CIS), MS, and healthy controls (HCs), to provide initial data regarding whether Brain Predicted Age is increased in CIS/MS, and whether it is associated with clinical outcomes.

Methods: 'Brain Predicted Age' scores were investigated using the small 'natalizumab cohort' described in Chapter 3. After this, 'Brain Predicted Age' scores were measured in a larger longitudinal cohort. Brain Predicted Age Difference (Brain-PAD) was defined as the Brain Predicted Age minus the true chronological age. The association between Brain-PAD and both cross-sectional and longitudinal clinical outcomes was explored.

Results: In the small 'natalizumab cohort', Brain-PAD was increased in MS, correlated with clinical outcomes, and appeared to be associated with clinical response to natalizumab treatment.

In the larger cohort, 1652 T1-weighted MRI scans in people with CIS or MS (n = 391) and HCs (n = 150) were analysed. HCs had mean Brain-PAD close to zero, as expected. All disease subgroups had substantially older-appearing brains than their chronological age (CIS: mean Brain-PAD +4.0 years; relapsing-remitting MS: mean Brain-PAD +10.3 years, secondary progressive MS: mean Brain-PAD +17.4 years; primary progressive MS: mean Brain-PAD +11.5 years). At baseline, higher Brain Predicted Age and Brain-PAD was associated with longer time since diagnosis, younger age at diagnosis, and higher EDSS. Brain Predicted Age and Brain-PAD at baseline predicted survival from EDSS milestones and EDSS progression. The model compared favourably with conventional univariate measures of brain atrophy. Longitudinal change in Brain Predicted Age increased at a rate ~46% faster in subjects with MS than in HCs.

Conclusions: MS and CIS brains appeared 'older' than HCs across all subtypes, with the brains of people with secondary progressive MS appearing 17.4 years older than chronological age. An older-appearing brain at baseline was associated with increased disability, and increased risk of future disability progression. The Brain Predicted Age model could provide conceptually simple and clinically meaningful quantitative data from a standard T1-weighted MRI scan, and will be further evaluated using the MAGNIMS multi-centre cohort.

Publication outcome: Study results used to setup collaboration using multi-centre international MAGNIMS cohort. After analysis of MAGNIMS cohort (not described in this thesis), findings published as pre-prints with the thesis author as 'joint first author'.[1] Paper under review, *Annals of Neurology*.

IV.2 ABBREVIATIONS

Brain-PAD	Brain Predicted Age Difference
CI	Confidence intervals
CIS	Clinically isolated syndrome
EDSS	Expanded disability status scale
GM	Grey matter
HC	Healthy control
MS	Multiple sclerosis
PET	Positron emission tomography
PwMS	People with multiple sclerosis
PPMS	Primary progressive multiple sclerosis
RRMS	Relapsing-remitting multiple sclerosis
SPMS	Secondary progressive multiple sclerosis
UCL	University College London
WM	White matter

IV.3 INTRODUCTION

In the previous chapter, data were presented to conclude that ^{18}F-GE180 positron emission tomography (PET) was limited in its ability to assess neuroinflammation in a cohort of subjects with multiple sclerosis (MS) initiating natalizumab treatment. Cortical neuroinflammation is known to be associated with neurodegeneration and the progression of disability in MS.[2-7] Unfortunately, ^{18}F-GE180 PET was not able to detect this cortical neuroinflammation, or to measure whether it responds to natalizumab treatment.

A more conventional surrogate marker of neurodegeneration in MS is to measure brain atrophy on MRI.[8, 9] Whereas PET can measure specific biologically active functional processes, brain atrophy is a pathologically non-specific measure of irreversible tissue loss. Since these structural changes develop slowly over time, brain atrophy is unlikely to be able to predict response in the early months after initiation of treatment.

Nevertheless, brain atrophy is an important outcome measure in MS. Brain volume correlates with lesion load on T2-weighted MRI,[10-14] although most strongly with cortical lesions.[15] Brain atrophy is associated with measures of disability.[16-18] Disability has a stronger association with brain atrophy than with white matter lesion volume.[10] Brain atrophy, especially grey matter atrophy, is also associated with cognitive impairment in MS.[19-22] Brain atrophy can be slowed by disease-modifying therapies, and the slowing of brain atrophy correlates with treatment effect on disability at a group level.[23, 24]

However, brain atrophy has limitations as an outcome measure. It cannot integrate complex patterns of structural damage to the MS brain, it mostly relies upon longitudinal data, and the output is not intuitive.[25-27] It is not widely utilised in clinical practice.[28] In this chapter a neuroimaging biomarker 'Brain Predicted Age', which may offer some advantages over conventional 'brain atrophy' measures, is evaluated for its applicability to MS. This biomarker uses machine learning to predict chronological age based solely upon a subject's T1-weighted MRI, and has been previously developed at Imperial College London.[29-31] The Brain Predicted Age model is applied to the 'natalizumab cohort' described in chapter 3, before being applied to a much larger longitudinal cohort of MRI scans.

IV.3.1 Brain ageing

Normal ageing is a time-dependent modification of biological processes, characterised by a complex set of biological hallmarks, a loss of complexity and loss of physiological reserve.[32-34] This results in reduced resilience, impairing an individual's ability to respond to stressors that may disrupt normal physiological homeostasis.[35] The situation is further complicated by inter-individual variability in the aging process. While 25% of the variation in human longevity is attributed to genetic factors, there is a clear impact from multiple environmental factors, including disease-related factors. In the context of normal ageing, a disease may trigger a sequence of events which result in an acceleration of the biological processes seen in normal ageing, both systemically,[36-38] and in the brain.[30, 39] The consequences of ageing for the brain include motor dysfunction, cognitive decline and brain volume loss.[40]

IV.3.2 Quantifying brain ageing

The acceleration of the brain ageing process, and the theoretical goal to quantify accelerated brain ageing, is illustrated in Figure 27 (adapted from Cole *et al*., 2015).[31] It may be useful if a tool could quantify the 'difference between a normally ageing and abnormally ageing brain' (Figure 27).

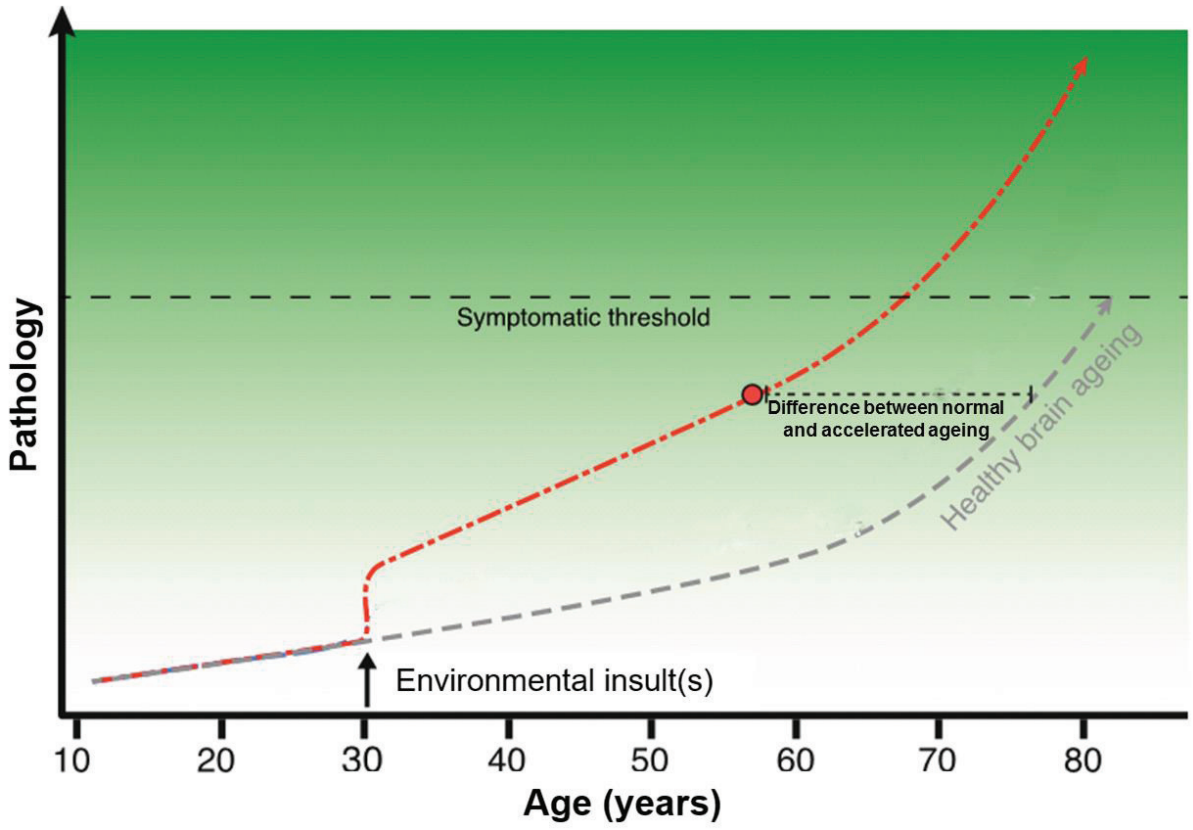


Figure 27: Model of premature brain ageing after environmental insult. The grey dashed line represents the normal trajectory of healthy brain ageing. An environmental insult (black arrow) could cause an immediate increase in brain pathology, and could also cause an accelerated trajectory of brain ageing (red dash-dotted line). Further environmental insults could occur in some diseases, although are not shown in the Figure. As shown in the black dotted line, for a given level of brain pathology, one could aim to quantify the difference between the subject's expected age for that level of brain pathology, with the subject's true chronological age. Figure adapted from Cole *et al*., 2015.[31]

The physical hallmarks of brain ageing involve non-linear and spatially variable change in brain volume and structure, which cannot be fully captured using conventional univariate measures.[29, 30] Instead, the evolution of machine-learning techniques has enabled 'Brain Age' to be quantified. Here, machine-learning can be used to estimate the chronological age of a subject based solely on the appearance of their neuroimaging data. Most commonly, these techniques use conventional three-dimensional T1-weighted MRI.[41, 42] These machine-learning models can estimate chronological age with greater accuracy than conventional measures.[30, 41, 43]

Using machine-learning analysis of brain MRIs from healthy subjects of varying chronological age, the so-called Brain Predicted Age model has previously been developed at Imperial College London which can accurately predict chronological age in healthy subjects based solely upon T1-weighted MRI data (r * 0.96, R2 * 0.91, mean absolute error * 4.4 years).[31] The 'Brain Predicted Age Difference' (Brain-PAD) is then defined as 'Brain Predicted Age minus chronological age'. This model can identify individuals whose 'Brain Age' appears younger (negative Brain-PAD) or older (positive Brain-PAD) than their chronological age, as illustrated in Figure 28. In the general population, Brain-PAD correlates with clinical outcome measures such as mortality.[31, 44] Moreover, disease such as traumatic brain disease, Down's syndrome, epilepsy, and HIV have been shown to be associated with a positive Brain-PAD.[29-31, 42, 45-47] This approach has not yet been applied to MS.

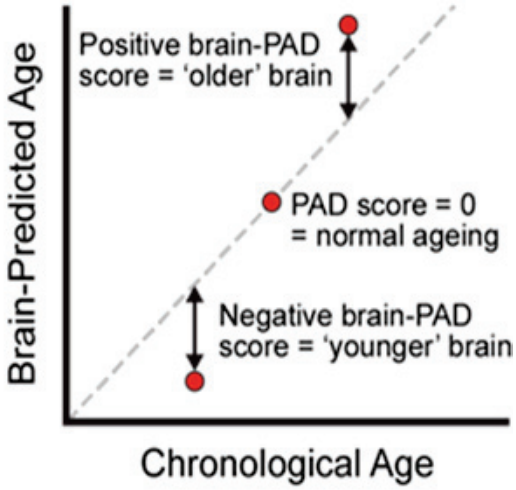


Figure 28: 'Brain Predicted Age Difference' (Brain-PAD) = Brain Predicted Age minus chronological age. For example, if Brain Predicted Age is identical to chronological age, Brain-PAD is 0. If Brain Predicted Age is 5 years older than true chronological age, Brain-PAD is +5. In populations of healthy subjects, the mean Brain-PAD is expected to be ~0. Figure adapted from Cole *et al.*, 2017.[44]

IV.3.3 Applicability to multiple sclerosis

The 'Brain Predicted Age' model has potential applicability to MS research, to quantify damage and accelerated ageing-like changes in the MS brain. Age has been implicated as a dominant driver of disability progression in MS.[48] Age is known to influence the onset of progression and other clinical milestones.[49-54] Brain atrophy is intimately linked with ageing and occurs at a faster rate in MS.[9, 55, 56] It has been hypothesised that disease processes in MS interact with neurobiological drivers of brain ageing, leading to accelerated ageing, increased brain atrophy, and poor prognosis.[57]

Quantifying 'Brain Predicted Age' in MS has theoretical advantages over the univariate approaches often used to quantify 'brain atrophy rates'. The Brain Predicted Age model:

- Is compatible with cross-sectional data, and places a patient's disease and disability in context of their age.

- Can capture complex and non-linear variables, including spatially variable cortical thinning, sulcal widening and ventricular enlargement, alongside more macroscopic loss of tissue volume.

- Produces a conceptually simple and intuitive output – a single number (Brain-PAD), which represents the difference between Brain Predicted Age and true chronological age.

In this study, Brain Predicted Age was measured using T1-weighted MRIs in healthy controls (HCs) and subjects with MS or clinically isolated syndrome (CIS). The study objectives were as follows:

- Characterise the 'Brain Predicted Age' of HCs and subjects with MS or CIS at study entry, and characterise how Brain-PAD is associated with MS subtype.

- Investigate the association between Brain-PAD and both cross-sectional and longitudinal clinical outcomes, and compare the performance of Brain Predicted Age against conventional univariate measures of brain atrophy.

- Explore how Brain-PAD changes longitudinally in HCs and subjects with MS or CIS.

The 'natalizumab cohort' and 'University College London (UCL) cohort' described under Methodology, below, were intended as 'proof of concept' and 'pilot' studies, respectively.

These data were then used to initiate an ongoing collaboration with seven European MS centres (MAGNIMS: www.magnims.eu), which aims to further evaluate the use of Brain Predicted Age in MS, using a larger multi-centre cohort (n = 3565 T1-weighted MRI scans). The results presented in this thesis chapter relate to the proof-of-concept and pilot study only, since this represents the main work of the thesis author. Results from the extended MAGNIMS dataset have been published as a pre-print with the thesis author as 'joint first author',[1] but are not included in this chapter.

IV.4 METHODOLOGY

IV.4.1 Study population

This study used data collected from UCL and Imperial College London (Table 7). The Imperial College London data were from the 'natalizumab cohort' described in Chapter 3 of this thesis, including subjects at baseline and after the initiation of natalizumab. Methodology for this natalizumab cohort is not repeated here, and readers are requested to refer to Chapter 3 for further information. The UCL data were taken from a variety of different cohorts, and overlap with data described in previous work.[58]

Patients had been diagnosed with CIS,[59] or MS according to 2010 McDonald Criteria.[60] HCs had no known history of neurological or psychiatric disorders. The HCs used to generate the training model for Brain Predicted Age are described elsewhere.[29, 31]

Clinical and imaging data were anonymised and were subject to the appropriate ethics approval (Imperial College London data: London Riverside Research Ethics Committee 14/LO/0343; UCL data: European MAGNIMS collaboration).

IV.4.2 MRI acquisition

T1-weighted MRI scans were performed according to local MRI protocols and acquisition parameters. These parameters were similar between cohorts. Details of the different scanners and acquisition parameters are presented in Table 7.

Centre	**University College London**				**Imperial College London (natalizumab cohort)**
Magnetic field	1.5 Tesla			3 Tesla	3 Tesla
Vendor	GE	GE	GE	Philips	Siemens
Model	Signa	Signa	Signa	Achieva	Verio
Years of recruitment	1999-2006	1998-2005	1998-2010	2011-2016	2014-2016
Included studies	1	1	2	2	1
Acquisition dimensions	3D	3D	3D	3D	3D
Voxel dimensions (mm)	1.2x1.2x1.5	1.2x1.2x1.2	1.2x1.2x1.5	1x1x1	1x1x1
TR (ms)	13.3	14.3	29	6.8	2300
TE (ms)	4.2	5.1	15	3.1	2.98
Matrix size	256x256	256x256	256x256	256x256	256x256

Number of slices	124	156	124	256	160
Numbers of participants prior to exclusions					
Controls	44	10	0	98	8
CIS	24	4	70	1	0
RRMS	33	7	67	52	17
SPMS	0	0	0	32	0
PPMS	42	0	0	42	0

Table 7: MRI acquisition protocols. TE = echo time; TR = repetition time; ms = milliseconds; mm = millimetre; HC = healthy controls; CIS = clinically isolated syndrome; RRMS = relapsing-remitting multiple sclerosis; SPMS = secondary progressive multiple sclerosis; PPMS = primary progressive multiple sclerosis.

IV.4.3 Clinical outcomes

MS/CIS patients were assessed using the Expanded Disability Status Scale (EDSS).[61] Disability progression was defined as an increase of 1 EDSS point in those with EDSS <5.5, or an increase of 0.5 EDSS points in those with EDSS ≥5.5. Data were also collected on sex, age, date of disease diagnosis, and date of study visits.

In the 'natalizumab cohort', 'non-responders' were defined as those with on-going relapses while on natalizumab, and/or disability progression in EDSS score.

IV.4.4 Brain Predicted Age analysis

Brain Predicted Age analysis was in line with a previously reported protocol developed at Imperial College London.[29, 31] In brief, structural images were pre-processed using SPM12

(https://www.fil.ion.ucl.ac.uk/spm/software/spm12/) to segment white matter (WM), grey matter (GM) and cerebrospinal fluid. Quality control was conducted by visual inspection of all images after segmentation; and images which failed segmentation were excluded. Segmented WM and GM images were registered non-linearly to a template which had been customised based on the training dataset using SPM *DARTEL.*[62] Images were then affine registered to MNI152 space (voxel size 1.5mm^3) and resampled using modulation and 4mm smoothing. Summary volumetric measures of WM, GM, cerebrospinal fluid and intracranial volume (ICV) were generated.

Brain Predicted Ages were generated using the Pattern Recognition for Neuroimaging Toolbox (PRoNTo v2.0, www.mlnl.cs.ucl.ac.uk/pronto) software package.[63] Healthy brain ageing had been previously defined using brain volumetric maps from an independent training dataset of controls with no known psychiatric or neurological disease (n = 2001). The model achieved a mean absolute error of 4.41 years, explaining 91% of the variance in chronological age from T1-weighted MRI data. The coefficients from the training model were then applied to the MS/CIS patients and HCs in the 'natalizumab cohort' and 'UCL cohort', to generate Brain Predicted Ages. These values were adjusted to remove age-related variance, as previously described.[31] Brain-PAD scores were defined as Brain Predicted Age minus chronological age. The pipeline used to generate Brain-PAD scores is illustrated in Figure 29 (adapted from Cole *et al*., 2015 and Cole *et al*., 2017).[31,44]

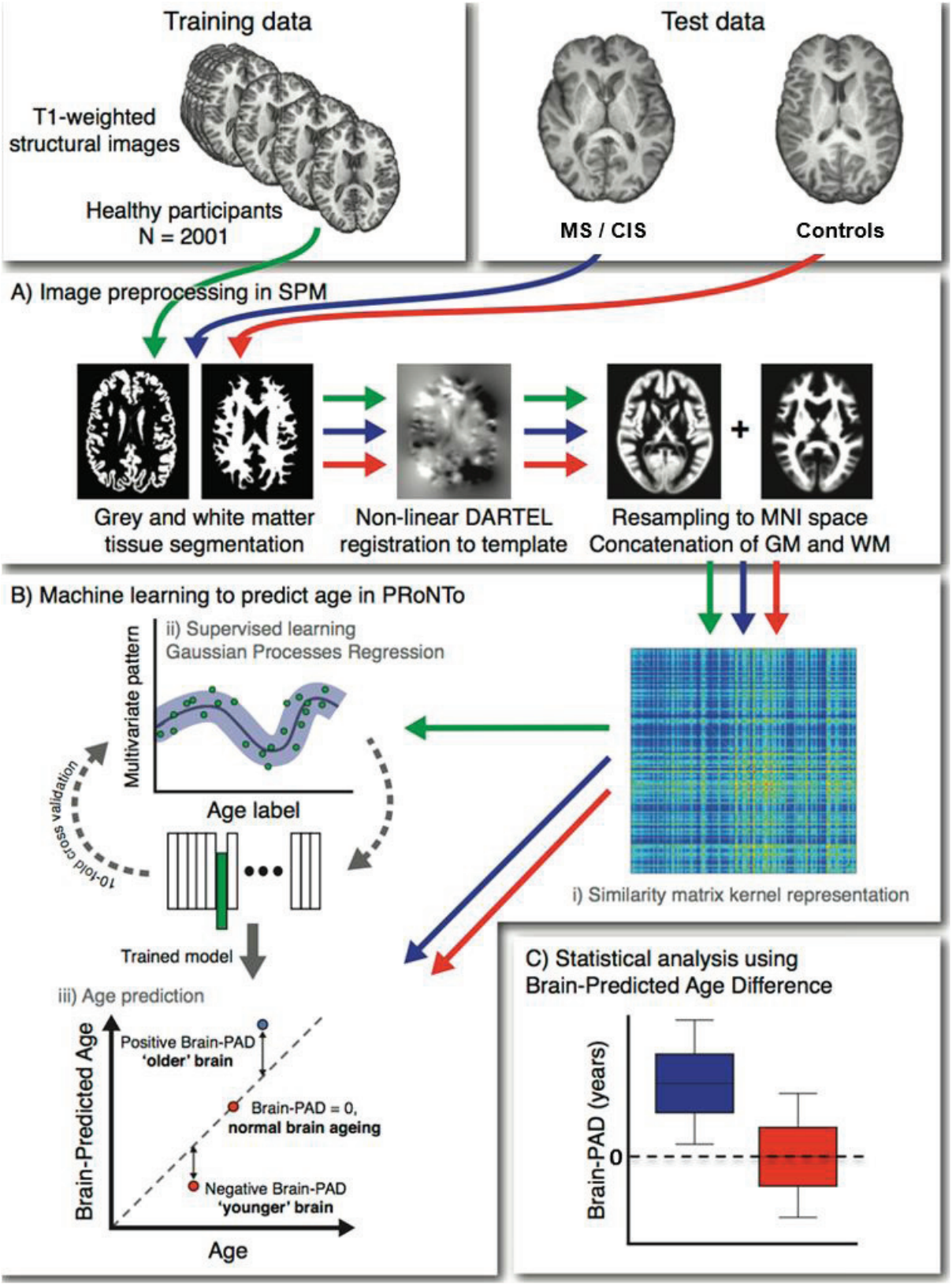


Figure 29: Overview of Brain Predicted Age model methodology. The training set used MRI data from 2,001 healthy controls from multiple cohorts, and is described in Cole *et al.*, (2015).[31] Test data were from the 'natalizumab cohort' and 'UCL cohort'. (A) Statistical Parametric Mapping (SPM) structural pre-

processing pipeline generated white matter (WM) and grey matter (GM) maps, normalised to Montreal Neurological Institute (MNI) space and modulated to retain data relating to brain size. (B) For WM and GM separately, training data were converted to a voxelwise similarity kernel matrix using Pronto. Training data only were run through a Gaussian Processes Regression (GPR) machine which was trained to recognise patterns of imaging data that matched a given chronological. Model validity was tested, as previously described.[31] The trained model was applied to the test data sets, to assess accuracy of the model on healthy controls and assess Brain Predicted Age in subjects with MS and CIS, and Brain-PAD calculated (C).

IV.4.5 Lesion filling

On cross-sectional data from a subset of MS/CIS scans, for which annotated lesion maps were available or were created, the relationship between MS lesions and measurements of Brain-PAD was explored by using the FSL lesion filling algorithm to artificially remove lesions from T1-weighted MRI scans (Figure 30).[64] Lesions segmented for the purpose of this project were segmented in T1 space using a customised tool developed by the BioMedIA group at Department of Computing, Imperial College London. The tool makes use of a semi-automated segmentation method based on that of Criminisi *et al*.[65] Dummy lesion masks were also used for a small cohort of HCs, to investigate for a systematic effect of the FSL Lesion Filling process on Brain Predicted Age. Lesion masks were also used to derive total lesion volumes. Both lesion-filled and unfilled scans were run through the Brain Age model, and comparison in Brain-PAD between the two datasets was carried out. Lesion-filled images were used for this analysis only, while unfilled images were used in all other analyses.

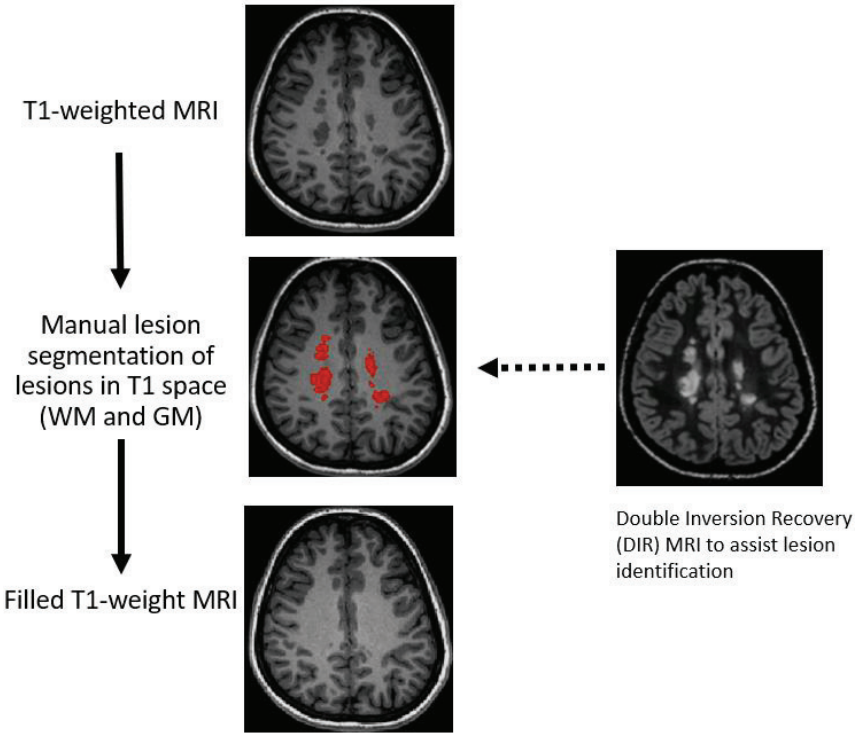


Figure 30: Lesion segmentation methodology. Lesion segmentation was manually created or was already available in T1 space on n = 575 T1-weighted scans. Co-registered scans (for example double inversion recovery, as picture above) were used to assist in the accurate segmentation of lesions. FSL lesion filling algorithm was used to artificially remove lesions from T1-weighted MRI scans

IV.4.6 Statistical analysis

Participant demographic results are reported as mean (standard deviation). Brain Predicted Age and Brain-PAD data are presented as mean (+/- 95% confidence intervals, CIs) unless otherwise specified. Parametric tests were used after testing for normal data distribution. Unpaired *t* test or paired *t* tests were used to compare the differences between means of two unpaired or paired groups, respectively. One-way analysis of variance was used to compare the differences between means for three or more groups. Pearson's correlation was used to investigate the relationship between quantitative continuous variables. Survival curves of time-to-EDSS progression were generated, dividing subjects into groups defined by baseline

Brain-PAD cut-offs. Survival curves were compared using a log rank (Mantel-Cox) test. Longitudinal imaging analysis was exploratory and used a linear mixed effects model. To establish to what extent brain volume measurements were driving variability in Brain-PAD, ordinary least squares linear regression with hierarchical partitioning was performed, with Brain-PAD as the outcome variable and GM volume (relative to ICV), WM volume (relative to ICV), age and sex as predictors. To establish to what extent Brain Predicted Age and other univariate outcomes could predict EDSS, ordinary least squares linear regression with hierarchical partitioning was performed, with EDSS as the outcome variable and Brain Predicted Age, GM volume (relative to ICV), WM volume (relative to ICV), age and sex as predictors. *p*-values < 0.05 were considered statistically significant. Multiple testing correction was not used for these proof-of-concept and pilot data. Statistical analysis was carried out using R v3.4.3 (R Core Team, 2015) and GraphPad Prism (v7, GraphPad Software, Inc., San Diego, CA, USA).

IV.4.7 Contribution to work

Joel Raffel[1,2]	Led on overall scientific direction of project. For 'natalizumab cohort', obtained ethical approval, consented all subjects, organised study visits, performed all clinical assessments and coordinated scanning procedures with assistance from radiographers. For both 'natalizumab cohort' and 'UCL cohort', performed image processing through pipeline, and quality check. Led on analysis and interpretation of data. Presented data to potential collaborators (UCL and then MAGNIMS consortium), to help setup access to additional cohorts.

James Cole[1]	Developed the Brain Predicted Age model as part of previous project. Helped to process scans through the Brain Predicted Age pipeline. Contributed towards analysis and overall direction of project (in particular with the MAGNIMS cohort, not presented in this thesis chapter).
Tim Friede[3]	Medical statistician. Assisted with statistical methodology, in particular longitudinal imaging analysis, and ordinary least squares linear regression with hierarchical partitioning.
Arman Eshaghi[4,5]	Helped to organise and process imaging data from the UCL cohort
Olga Ciccarelli[4,6]	Assisted in providing access to UCL cohort. Contributed ideas towards direction of project.
Richard Nicholas[1,2]	Overall responsibility and supervision of the project throughout.

1 Division of Brain Sciences, Faculty of Medicine, Imperial College London, London, United Kingdom,

2 Imperial College Healthcare NHS Trust, London, United Kingdom,

3 Department of Medical Statistics, University Medical Center Göttingen, Göttingen, Germany

4 Queen Square Multiple Sclerosis Centre, Department of Neuroinflammation, UCL Institute of Neurology, London, UK.

5 Centre for Medical Image Computing, Department of Computer Science, University College London, UK.

6 National Institute for Health Research (NIHR), University College London Hospitals (UCLH) Biomedical Research Centre (BRC), London, UK.

IV.5 NATALIZUMAB COHORT RESULTS

Brain Predicted Age was first examined in the small natalizumab cohort described in Chapter 3, before being applied to the larger cohort of subjects recruited by UCL.

IV.5.1 Study procedures

17 PwMS and 8 HCs had baseline T1-weighted MRI scans. One subject with MS did not have follow-up scans, as they left the study for personal reasons. The other 16 PwMS had follow-up MRI scans 10 weeks and 58 weeks after the initiation of natalizumab, as described in Chapter 3.

IV.5.2 Subject characteristics

The study cohort overlapped with that described in Chapter 3, although one additional subject with MS was available for analysis (due to failed PET but successful MRI), and three fewer HCs were available (due to this analysis being performed prior to study completion).

Baseline characteristics are presented in Table 8. PwMS had increased disability at baseline compared to HCs, as expected (Table 9).

	PwMS (n = 17)	HCs (n = 8)
Male/Female, n	6/11	5/3
Age, yrs	41.6 (10.8)	42.0 (7.4)
Years of education	14.4 (2.6)	16.4 (3.9)
Age at MS onset, yrs	29.5 (10.0)	N/A
Time since MS onset, yrs	12.1 (10.6)	N/A
Number of previous DMTs, n	O DMTs: 9 1 DMT: 3 2 DMTs: 5	N/A

Table 8: Baseline characteristics of PwMS and HCs. DMT = disease-modifying therapy. Standard deviations shown in brackets.

	PwMS (n = 17)	HCs (n = 8)	*p*-value
T25FW, secs	6.6 (4.4)	3.5 (0.4)	NS ($p = 0.06$)
9HPT, secs	30.9 (19.9)	17.8 (1.3)	NS ($p = 0.07$)
MSQOL-54 Physical	42.8 (16.8)	87.8 (5.9)	***
MSQOL-54 Psych	58.7 (24.0)	80.8 (7.3)	*
WPAI:MS	59.4 (16.8)	3.7 (7.4)	***
SDMT	49.7 (13.7)	67.7 (10.2)	**
CVLT	54.2 (10.8)	66.0 (6.4)	**
BVMT	24.1 (6.6)	30.1 (5.6)	*
EDSS	4.2 (1.1)	N/A	
MSSS	5.6 (2.4)	N/A	
WM Lesion Volume, cm^3	10.3 (8.5)	N/A	
GM Lesion Volume, cm^3	0.3 (0.5)	N/A	

Table 9: Clinical and patient-reported outcomes in PwMS and HCs at baseline. T25FW = timed 25-foot walk; 9HPT = 9-hole peg test; MSQOL-54 = Multiple Sclerosis Quality of Life-54 patient reported outcome (physical and psychological subscores); WPAI:MS = Work Productivity and Activity Impairment, Multiple Sclerosis; SDMT = symbol digit modalities test; CVLT = California verbal learning test; BVMT = Brief Visuospatial Memory Test; EDSS = Expanded Disability Status Scale; MSSS = Global Multiple Sclerosis Severity Scores. Standard deviations shown in brackets. *p*-values refer to unpaired *t* tests: * = $p < 0.05$; ** = $p < 0.01$; *** = $p < 0.001$. The PwMS group had scores associated with greater disability, compared with the HC group.

IV.5.3 Brain-PAD is increased in subjects with MS, and correlates with radiological markers of disease severity

On visual inspection of T1-weight MRI scans, the severity of disease on MRI scan appeared to correlate with the Brain-PAD score (e.g. Figure 31A).

In HCs, mean Brain-PAD (defined as Brain Predicted Age minus chronological age) was not statistically different from 0, as expected. In PwMS in the baseline scan, mean Brain-PAD was +10.0. Even in this limited cohort, Brain-PAD was significantly greater in PwMS at baseline scan than in HCs (MS: mean +10.0 years, 95% CI +5.8 to +14.2; HC -1.4 years, 95% CI -7.8 to +5.1; $p < 0.01$; Figure 31B).

In PwMS, lesion volume was calculated after segmentation of all WM and GM lesions. Brain-PAD correlated strongly with lesion volume in the baseline scans (r=0.78, n = 17, $p < 0.001$; Figure 31C).

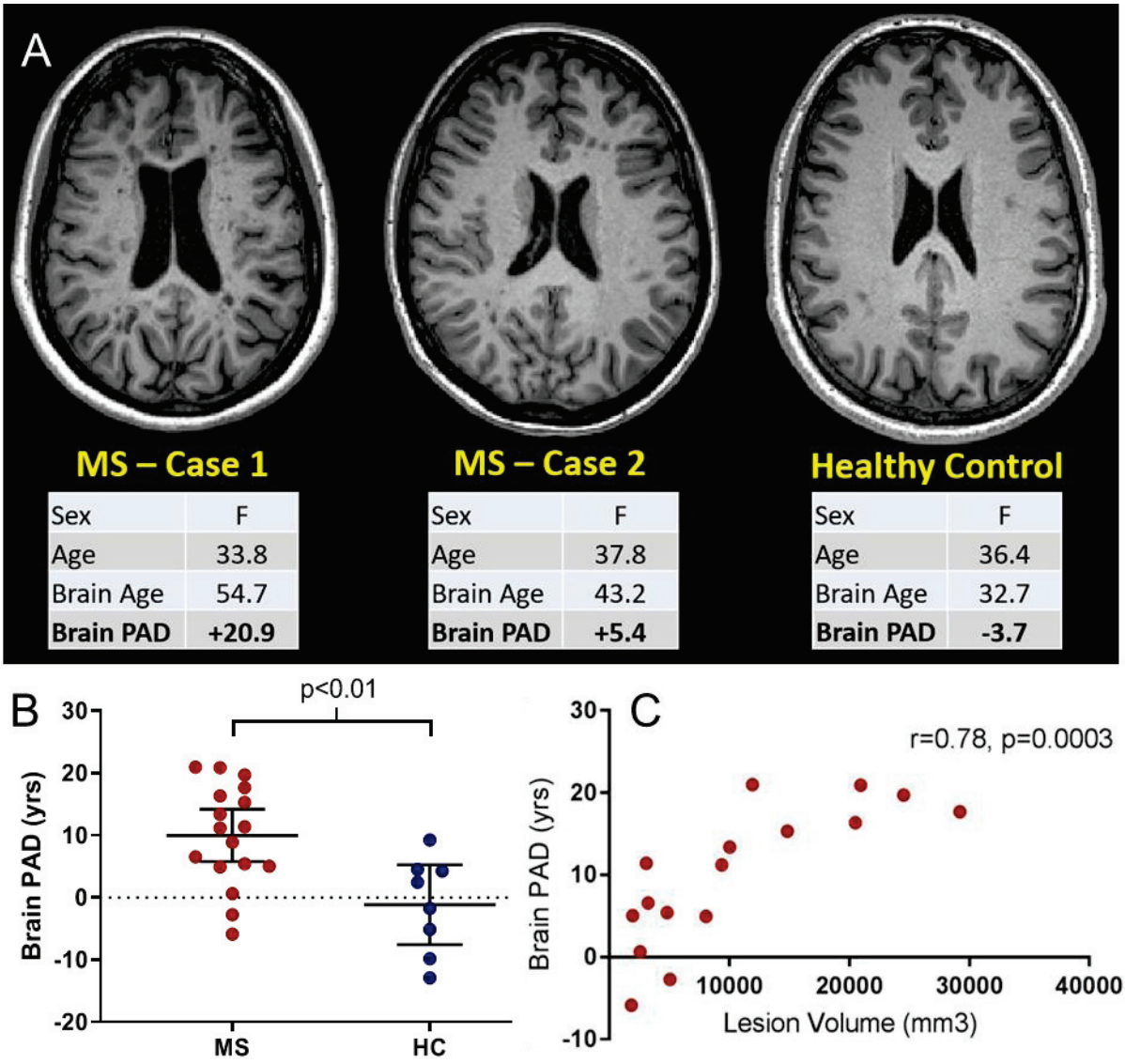


Figure 31: Brain Predicted Age and Brain-PAD in multiple sclerosis and healthy controls. (A): In three females in their mid-30s. MS Case 1, with the most severe disease, had Brain Predicted Age 20.9 years greater than chronological age. MS Case 2, with less severe disease, had Brain Predicted Age 5.4 years greater than chronological age. The Healthy Control had Brain Predicted Age 3.7 years less than chronological age. (B): On average, Brain-PAD in subjects with MS was greater than Brain-PAD in HCs. (C): Brain-PAD correlated with Lesion Volume. *p*-value generated using unpaired *t* test (B) and Pearson correlation coefficient (C). Error bars represent mean +/- 95% confidence intervals. 'Brain Age' = 'Brain Predicted Age'. Brain PAD = Brain Predicted Age Difference. MS = multiple sclerosis. HC = healthy controls.

IV.5.4 Results consistent after lesion filling

The results reported in the above section remained consistent after lesion filling of T1-weighted MRI. HC MRI data were also lesion filled, by using 'dummy' lesion masks generated in PwMS and then transformed into matched HC space.

On visual inspection of filled T1-weight MRI scans, the severity of disease on MRI scan still appeared to correlate with the Brain-PAD score (e.g. Figure 32A).

In PwMS in the baseline filled scans, mean Brain-PAD was +8.2. Brain-PAD remained significantly greater in PwMS at baseline scan than in HCs (MS: +8.2 years, 95% CI +4.6 to +11.8; HC -0.7 years, 95% CI -7.1 to +5.7; $p < 0.01$; Figure 32B). Brain-PAD remained correlated strongly with (pre-filling) lesion volume in the filled baseline scans ($r=0.72$, $n = 17$, $p < 0.001$; Figure 32C).

The effect of lesion filling on Brain-PAD is further investigated in the UCL cohort results.

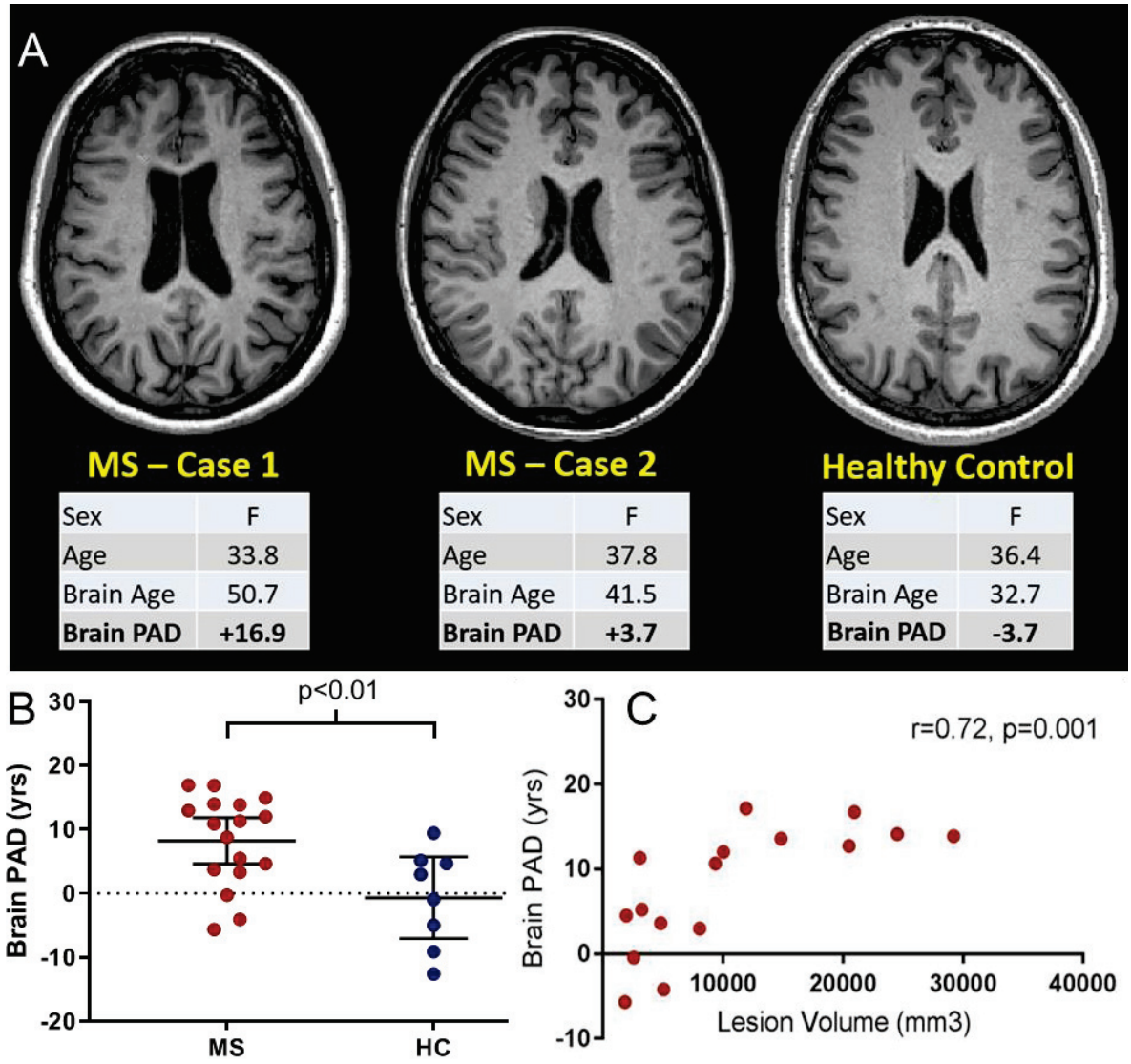


Figure 32. Lesion-Filled scans. These are the same data as shown in Figure 31, but with lesion-filled T1-weighted MRI data. (A): Brain Predicted Age and Brain-PAD in three females in their mid-30s. MS Case 1, with the most severe disease, had Brain Predicted Age 16.9 years greater than chronological age. MS Case 2, with less severe disease, had Brain Predicted Age 3.7 years greater than chronological age. The Healthy Control had Brain Predicted Age 3.7 years less than chronological age. (B): On average, Brain-PAD in subjects with MS was greater than Brain-PAD in HCs. Error bars represent mean +/- 95% confidence intervals. (C): Brain-PAD correlated with Lesion Volume. *p*-values generated using unpaired *t* test (B) and Pearson correlation coefficient (C). 'Brain Age' = 'Brain Predicted Age'. Brain PAD = Brain Predicted Age Difference. MS = multiple sclerosis. HC = healthy controls.

IV.5.5 Brain-PAD decreases after natalizumab in those responding to treatment

Although this cohort was limited by sample size, it was investigated whether Brain-PAD was modified by natalizumab treatment in the 16 PwMS with MRI scans at baseline and 58 weeks after initiating natalizumab.

After 58 weeks of treatment, mean Brain-PAD was +9.9 years, which was not significantly different from the mean Brain-PAD at baseline of +10.1 years (baseline: 10.1 (2.1); 58 weeks: 9.9 (2.1); n = 16; p = ns; Figure 33A). Without a control group of untreated PwMS, it was not possible to conclude whether Brain-PAD at 58 weeks would have been greater were it not for natalizumab treatment.

The mean Brain-PAD increased after 58 weeks in the patients classified as natalizumab non-responders, whereas the mean Brain-PAD decreased after 58 weeks in the patients classified as natalizumab responders (non-responders: n = 5, Change in Brain-PAD +1.1 years, 95% CI --0.5 to +2.7; responders: n = 11, Change in Brain-PAD -0.7 years, 95% CI -1.6 to +0.3; $p < 0.05$; Figure 33B).

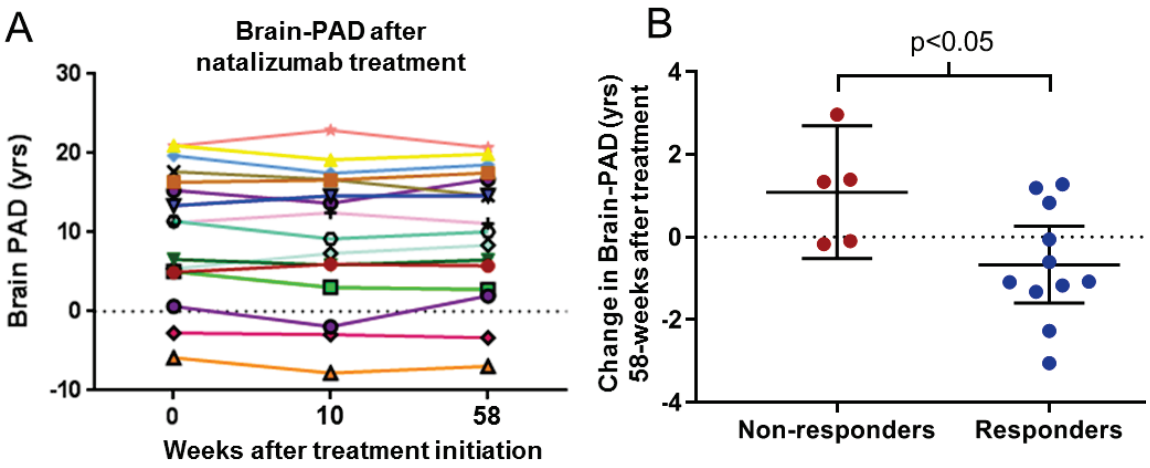


Figure 33: Longitudinal Brain-PAD after natalizumab treatment. (A): Each individual PwMS represented by a colour/symbol. Across the group, mean Brain-PAD decreased non-significantly from +10.1 to +9.9 from baseline to 58 weeks after treatment initiation. (B): Mean Brain-PAD decreased in those that responded to treatment and increased in those that did not respond to treatment. *p*-value generated using unpaired *t* test. Error bars represent mean +/- 95% confidence intervals. Brain-PAD = Brain Predicted Age Difference.

IV.6 UCL COHORT RESULTS

After results had been generated in the small natalizumab cohort, the Brain Age model was applied to a larger cohort of subjects with MS, CIS, and HCs.

IV.6.1 Study procedures

1658 T1-weighted MRI scans were available. 33 scans were excluded since the chronological age of the subject was unknown, while 26 scans were excluded for failing quality check, leaving 1599 for analysis from 541 different subjects (Figure 34).

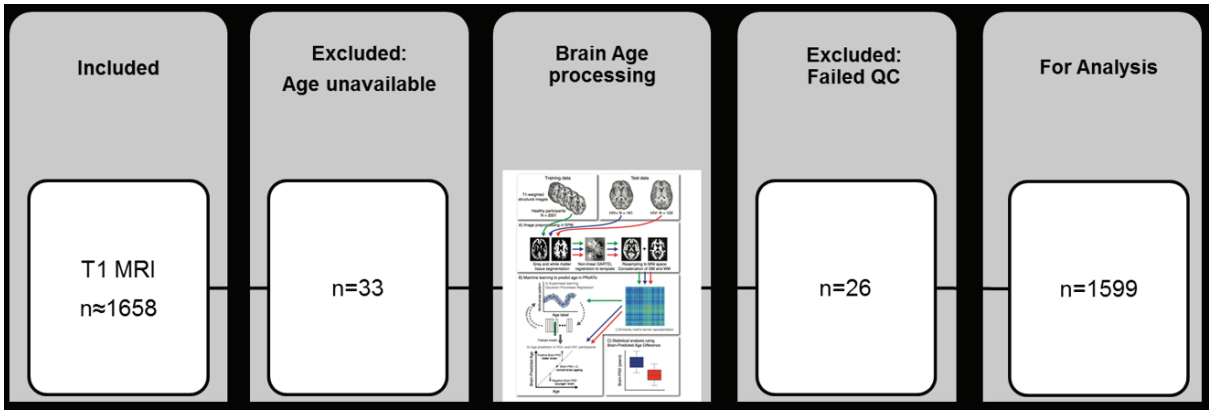


Figure 34: Flowchart of exclusions for UCL cohort. QC = quality check.

IV.6.2 Subject characteristics

Baseline characteristics are presented in Table 10. Chronological age at baseline scan between those with MS/CIS and HCs was similar. 45.3% of HCs were male, versus only 37.6% of those with MS or CIS. Only 40 subjects were known to be on disease-modifying therapy. In the MS/CIS group, 131 subjects had >5 years of follow-up, and 77 subjects had >10 years of follow-up.

	PwMS (n = 391)	HCs (n = 150)
Male/Female, n	147 / 244	68 / 82
Age at baseline scan, yrs	39.8 (11.0)	37.3 (10.0)
Subtype at baseline scan, n	CIS: 99 RRMS: 175 SPMS: 33 PPMS: 84	HC: 150
Total number of MRI scans, n	1: 33 2: 156 3: 73 4: 59 5: 56	1: 39 2: 47 3: 21 4: 21 5: 7

	6: 8 7: 6 8: 0 9: 0 10: 0	6: 7 7: 2 8: 3 9: 2 10: 1
Follow-up duration in those with >1 scan (time from first until last scan), n	O - 1 years: 7 1 - 2 years: 86 2 - 3 years: 100 3 - 5 years: 34 5 - 10 years: 54 10 - 15 years: 77	O - 1 years: 17 1 - 2 years: 45 2 - 3 years: 30 3 - 5 years: 10 5 - 10 years: 9 10 - 15 years: 0
Age at MS onset, yrs	34.8 (9.9)	N/A
On DMT at baseline scan, n	Yes: 40 No/unknown: 351	N/A
EDSS at baseline scan	0: 38 1 - 1.5: 124 2 - 2.5: 42 3 - 3.5: 34 4 - 4.5: 37 5 - 5.5: 15 6 - 6.5: 64 7 - 7.5: 3 8 - 8.5: 4 Unknown: 30	

Table 10: Baseline characteristics of PwMS and HCs. CIS = clinically isolated syndrome; RRMS = relapsing-remitting multiple sclerosis; SPMS = secondary progressive multiple sclerosis; PPMS = primary progressive multiple sclerosis; HC = healthy control; DMT = disease-modifying therapy. EDSS = Expanded Disability Status Scale. Standard deviations shown in brackets.

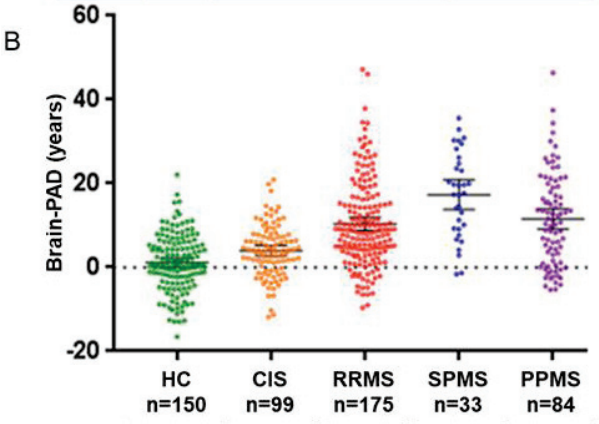
IV.6.3 Brain-PAD is increased in people with MS and CIS

Brain-PAD was calculated for all subjects in their baseline (first available) T1-weighted MRI scan.

Those with relapsing-remitting MS (RRMS) had a mean Brain-PAD of +10.3 years, consistent with the results from the natalizumab cohort. Those with CIS had a mean Brain-PAD of +4.0 years. Those with primary progressive MS (PPMS) had a mean Brain-PAD of +11.5 years. Those with secondary progressive MS (SPMS) had a mean Brain-PAD of +17.4 years. People with CIS, RRMS, SPMS, and PPMS all had Brain-PAD significantly greater than the HC group (Figure 35A-B). Data are also represented on a graph of Chronological Age vs Brain Predicted Age, where Brain-PAD could be derived as the 'vertical distance from each data point to the y=x line' (Figure 35C).

A

Grou	n	Mean Brain-PAD (95% CI)	P-value vs HC
HC	150	+1.1 (0.0 to +2.2)	NA
CIS	99	+4.0 (+2.7 to +5.2)	0.015
RRMS	175	+10.3 (+8.8 to +11.9)	<0.0001
SPMS	33	+17.4 (+13.8 to +20.1)	<0.0001
PPMS	85	+11.5 (+9.1 to 13.9)	<0.0001



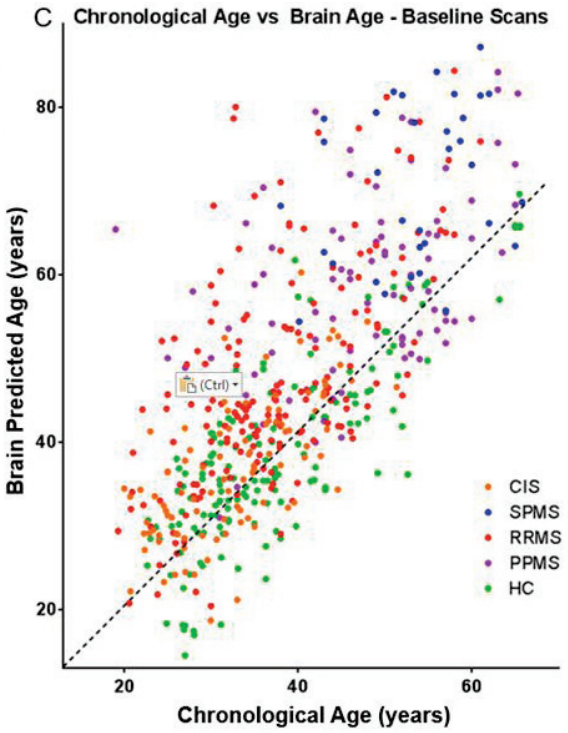


Figure 35: Baseline scans by disease subtype. (A): Brain-PAD (years) in baseline scans by disease subtype. *p*-values versus healthy control generated using unpaired *t* tests. (B): Same dataset in graphical format. Error bars represent mean +/- 95% confidence intervals. (C): Same data are also represented on a graph of Chronological Age vs Brain Predicted Age, where Brain-PAD could be derived as the distance along the y-axis from each data point to the y=x line. Brain-PAD = Brain Predicted Age Difference; CIS = clinically isolated syndrome; RRMS = relapsing-remitting multiple sclerosis; SPMS = secondary progressive multiple sclerosis; PPMS = primary progressive multiple sclerosis; HC = healthy control.

IV.6.4 Brain Predicted Age and Brain-PAD at baseline scan correlate with disease characteristics

In CIS, RRMS, and SPMS, Brain-PAD in the baseline scan correlated with time since MS diagnosis (r = 0.37, n = 246, $p < 0.0001$; Figure 36A). In this analysis, those with CIS were included only if they ultimately were diagnosed with RRMS. In these subjects, the 'time from MS diagnosis' is given a negative value, since they had yet to be diagnosed with MS at the time of the baseline scan. Subjects with PPMS were not included in this analysis since the

diagnostic process may be different. Brain-PAD also correlated negatively with age of diagnosis (r = -0.26, n = 387, $p < 0.0001$; Figure 36B).

Brain-PAD correlated with EDSS at baseline scan in subjects with CIS, RRMS, SPMS, and PPMS (r = 0.34, n = 361, $p < 0.0001$; Figure 36C). Brain Predicted Age correlated more strongly with EDSS (r = 0.65, n = 361, $p < 0.0001$; Figure 36D), as may be expected since Brain Predicted Age relates also to chronological age, which is known to be an important driver for disability progression.

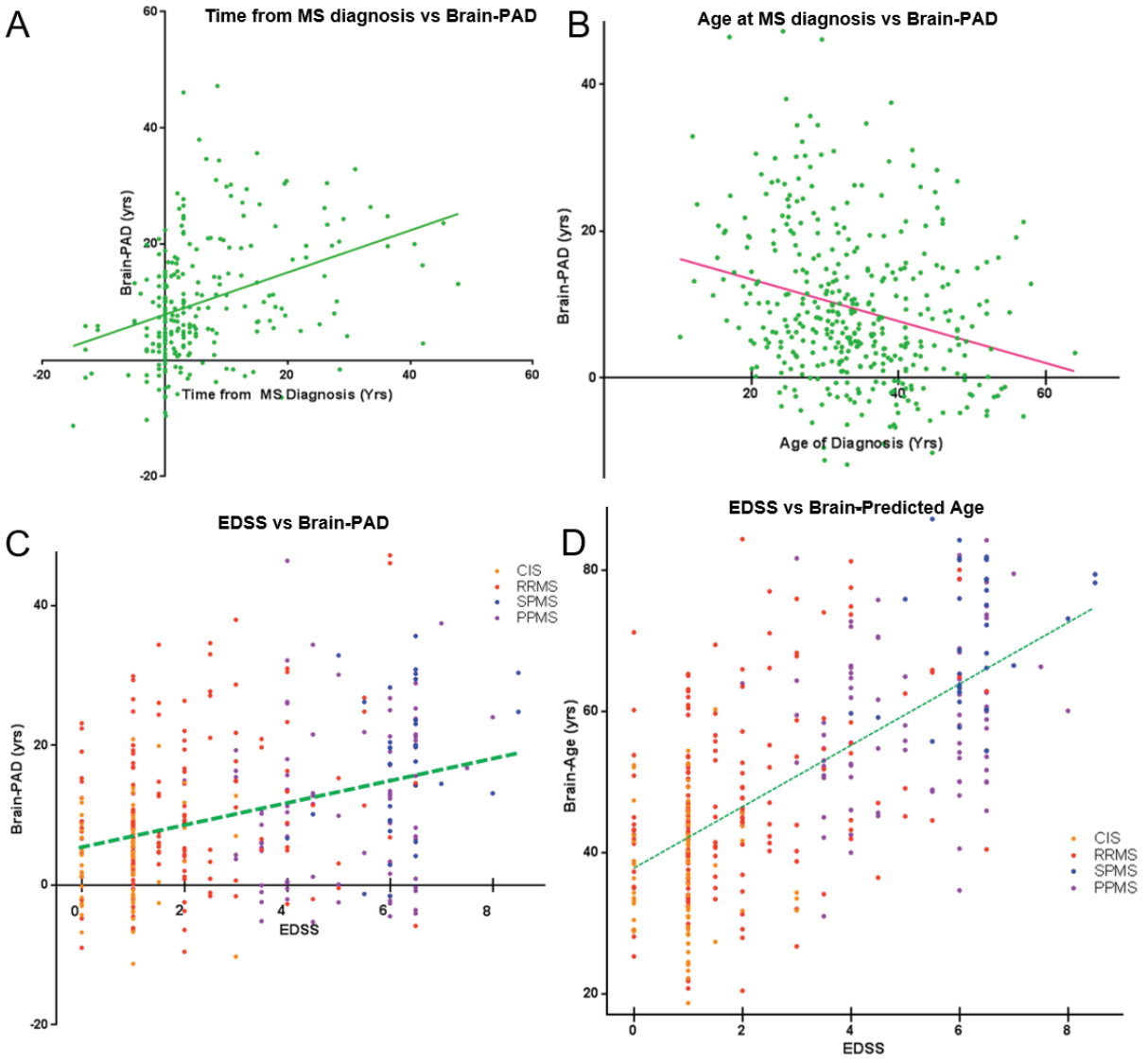


Figure 36: Brain Predicted Age and Brain-PAD correlate with disease characteristics. (A): Brain-PAD (yrs) at baseline scans correlates with time from MS diagnosis (yrs) in those with relapsing MS. Those with CIS were included only if they ultimately were diagnosed with RRMS. Subjects with PPMS were not included in this analysis since the diagnostic process may be different. Line of best fit shown in green. r = 0.37, n = 246, $p < 0.0001$. (B): Brain-PAD (yrs) correlates with age at MS diagnosis (yrs). Line of best fit shown in pink. r = -0.26, n = 387, $p < 0.0001$. (C): Brain-PAD (yrs) correlates with EDSS. r = 0.34, n = 361, $p < 0.0001$ (D): Brain Predicted Age (yrs) correlates with EDSS. r = 0.65, n = 361, $p < 0.0001$. Pearson's correlation coefficient used for all statistical analyses. Brain-PAD = Brain Predicted Age difference. CIS = clinically isolated syndrome; RRMS = relapsing-remitting multiple sclerosis; SPMS = secondary progressive multiple sclerosis; PPMS = primary progressive multiple sclerosis; HC = healthy control; EDSS = Expanded Disability Status Scale.

IV.6.5 Baseline Brain Predicted Age and Brain-PAD are associated with risk of future disability progression

Brain Predicted Age at the baseline scan was correlated with risk of reaching future disability milestones. Of those with EDSS <6 at baseline, the risk of reaching EDSS 6 at follow-up was increased in those with baseline Brain Predicted Age greater than 45 years (**Brain Predicted Age <45 yrs**: events in 6/133, median survival undefined; **Brain Predicted Age >45 yrs**: events in 28/133, median survival 14 years; $p < 0.0001$; Figure 37A). Of those with EDSS <4 at baseline, the risk of reaching EDSS 4 at follow-up was increased in those with baseline Brain Predicted Age greater than 45 years (**Brain Predicted Age <45 years**: events in 10/126, median survival undefined; **Brain Predicted Age >45 years**: events in 17/90, median survival 14 years; $p < 0.001$; Figure 37B).

While Brain Predicted Age predicted the risk of reaching disability milestones, Brain-PAD predicted the risk of any EDSS disability progression (**Brain-PAD <10 years**: events in 72/188, median survival 13 years; **Brain-PAD >10 years**: events in 57/141, median survival 5 years; $p < 0.0001$; Figure 37C).

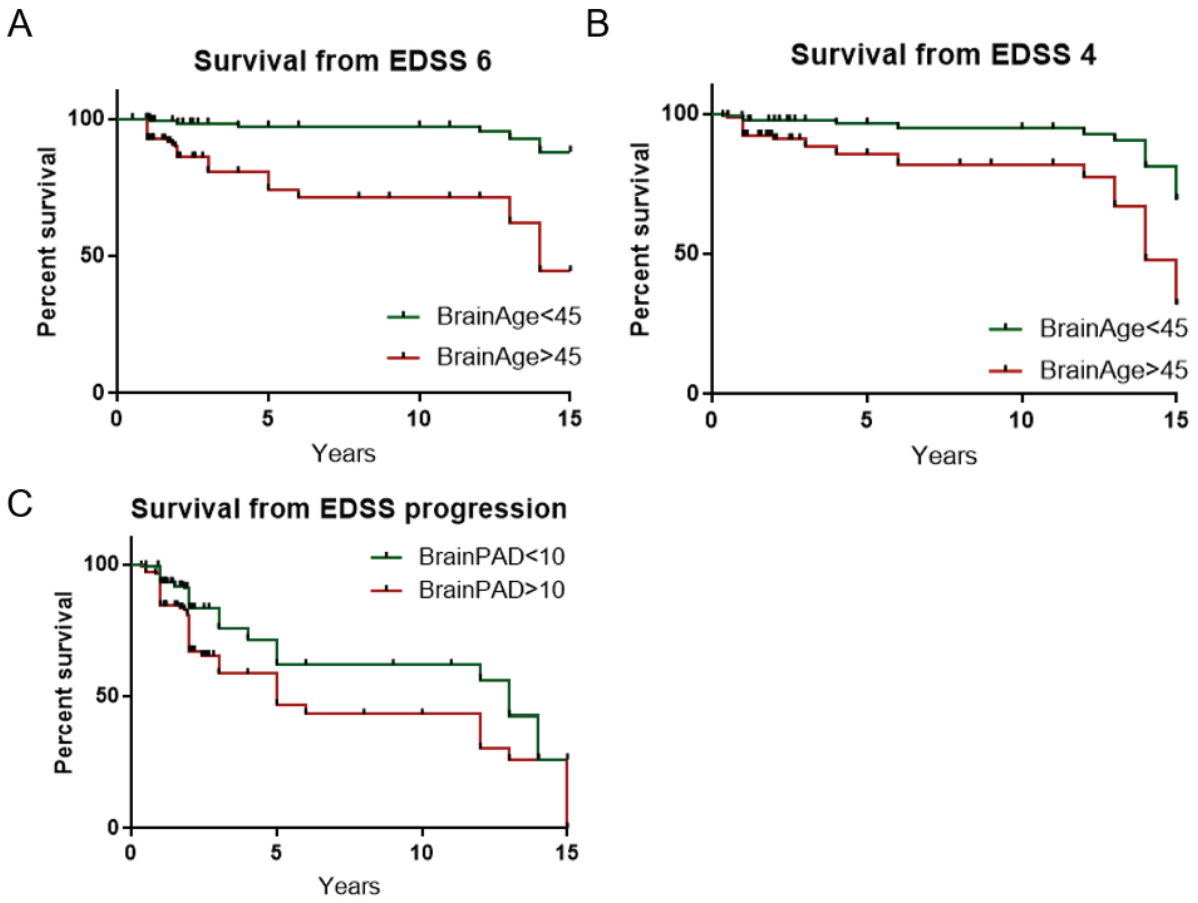


Figure 37: Survival from disability milestones and EDSS progression as a function of Brain Predicted Age and Brain-PAD. (A): Those with Brain Predicted Age less than 45 years had decreased risk of reaching EDSS 6. $p < 0.0001$. (B): Those with Brain Predicted Age less than 45 years had decreased risk of reaching EDSS 4. $p < 0.001$. (C): Those with Brain-PAD less than +10 years had decreased risk of EDSS progression. $p < 0.0001$. Log-rank (Mantel-Cox) survival analyses used for all statistics. Brain-PAD = Brain Predicted Age difference. EDSS = Expanded Disability Status Scale.

IV.6.6 Longitudinal Brain Predicted Age analysis shows 'faster ageing' in people with MS

All analyses presented thus far have considered Brain Predicted Age or Brain-PAD from only the baseline T1-weighted MRI scan. Longitudinal MRI data were available in 469 out of 541 subjects.

The ‘longitudinal change in Brain Predicted Age’ was investigated. A linear mixed effects model was used comparing HCs with people with CIS/MS. HCs had a slope of 0.87 with intercept of 6.0, while people with CIS/MS had a slope of 1.27 with intercept of 1.0. Therefore, longitudinal change in Brain Predicted Age increased at a rate ~46% faster in subjects with MS than in HCs (1.27/0.87). The two lines crossed at x= 12.2 years (Figure 38). Important limitations of these analyses are considered in the discussion.

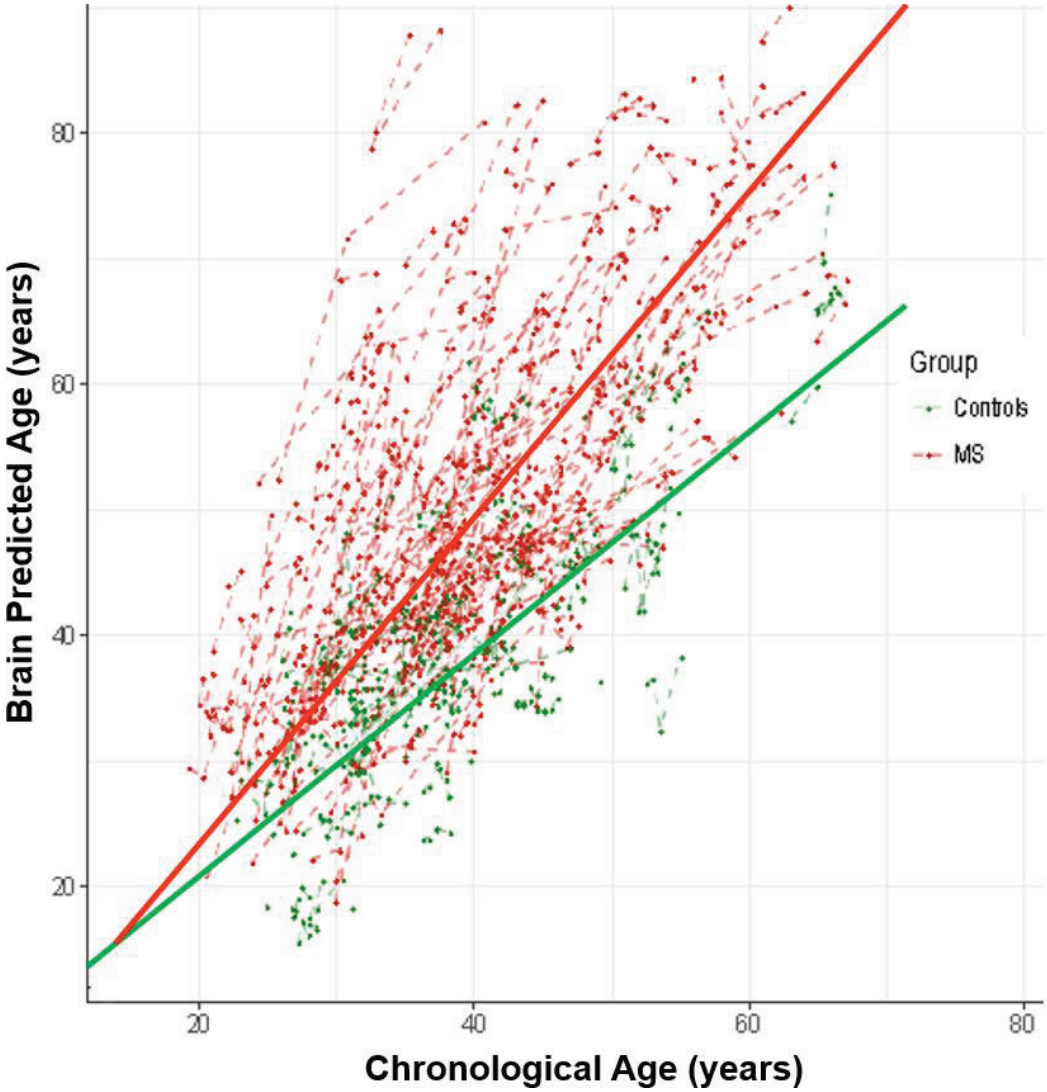


Figure 38: Longitudinal change in Brain Predicted Age in people with multiple sclerosis and healthy controls. Dots = scans. Dotted lines = change in Brain Predicted Age in individual subjects. Solid line = average slope. Red = multiple sclerosis; Green = Healthy control.

IV.6.7 Brain-PAD is increased in CIS, but may normalise in those who do not develop MS

In this cohort, there were 99 subjects with CIS at the baseline scan.

Of these 99 subjects, 42 were later diagnosed with RRMS during follow-up, while 43 retained the diagnosis of CIS (14 of these with >10 years follow-up: 'long-term CIS'). The remainder had no recorded follow-up.

At baseline scan, there was no significant difference in Brain-PAD between the 14 subjects with 'long-term CIS' and the 42 subjects that converted to RRMS (CIS: Baseline Brain-PAD+ 2.6 years, 95% CI -0.3 to +5.5; CIS to RRMS: Brain-PAD +4.5 years, 95% CI + 2.3 to + 6.8; p = ns; Figure 39A). Those with 'CIS to RRMS' with >10 years follow-up had a non-significant longitudinal increase in Brain-PAD (Baseline Brain-PAD: +3.2 years, 95% CI -0.3 to +6.7, >10 year Brain-PAD: +6.5 years, 95% CI +1.8 to +11.1, n = 21, p = ns; Figure 39B). However, Brain-PAD decreased longitudinally in those with 'Long-term CIS' (Baseline Brain-PAD: +2.6 years, 95% CI -0.3 to + 5.5; >10 year Brain-PAD: -2.5 years, 95% CI -4.7 to -0.4, n = 14, $p < 0.0001$; Figure 39C). The longitudinal change in Brain-PAD over 10 years between these two groups was significantly different (Long-term CIS group: -5.1 years, 95% CI -7.4 to -2.9, n = 14; CIS to RRMS group: = +3.3 years, 95% CI -0.8 to + 7.4, n = 21; $p < 0.01$).

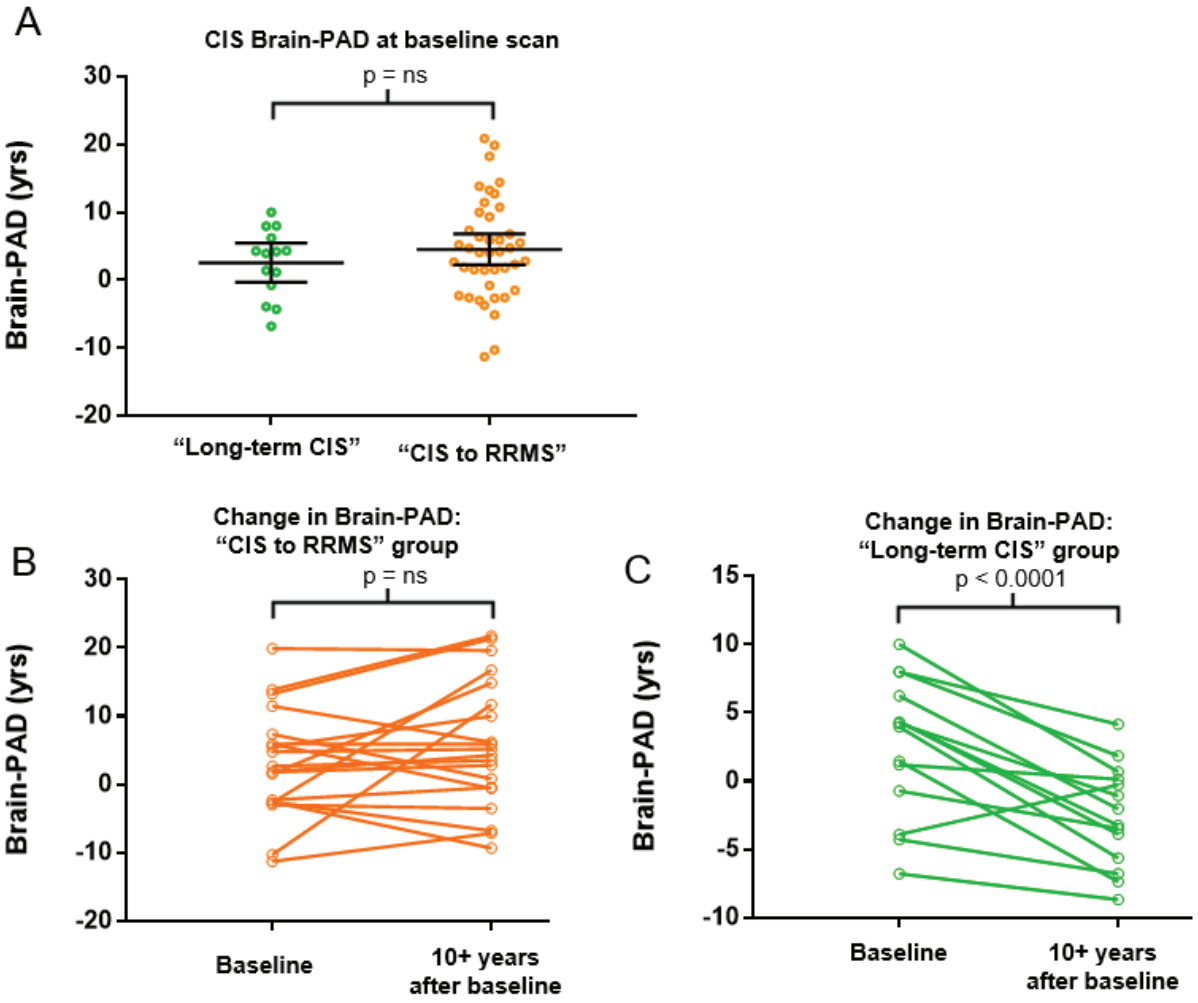


Figure 39: Brain-PAD in those with 'long-term CIS' (no RRMS diagnosed and > 10 years follow-up), and those who converted from 'CIS to RRMS'. (A): Baseline Brain-PAD does not differ between these groups. Error bars represent mean +/- 95% confidence intervals. (B): In those that converted to RRMS, there was a non-significant increase in Brain-PAD longitudinally. (C): In those that had 'long-term CIS', there was a substantial decrease in Brain-PAD longitudinally. *p*-value generated by unpaired *t* test (A) and paired *t* test (B) and (C). Brain-PAD = Brain Predicted Age difference. CIS = clinically isolated syndrome; RRMS = relapsing-remitting multiple sclerosis.

IV.7 FACTORS WHICH CONTRIBUTE TO BRAIN PREDICTED AGE

The analyses presented above find that Brain Predicted Age and Brain-PAD correlate with a variety of clinical outcomes. Other measures that can be derived from T1-weighted MRI are

also known to correlate with clinical outcomes, such as GM volume and WM volume. The following results sections consider what factors contribute to Brain Predicted Age, and whether it may offer any advantages over these conventional brain atrophy measures. These results also consider whether Brain Predicted Age could be influenced by the magnetic field of the MRI and by MS lesions.

IV.7.1 MRI magnetic field has no effect on Brain-PAD

It is plausible that features of the MRI acquisition such as magnetic field strength could influence Brain Predicted Age.

HC Brain-PAD results (both baseline and follow-up) were compared between scans acquired using a 1.5 Tesla MRI scan and scans acquired using a 3.0 Tesla MRI scan. There was no difference in Brain-PAD between these groups (1.5 Tesla Brain-PAD: +1.1 years, 95% CI -0.2 to +2.4, n = 168; 3-Tesla Brain-PAD: +0.9 years, 95% CI +0.3 to +1.6, n = 255; $p = 0.8$; Figure 40).

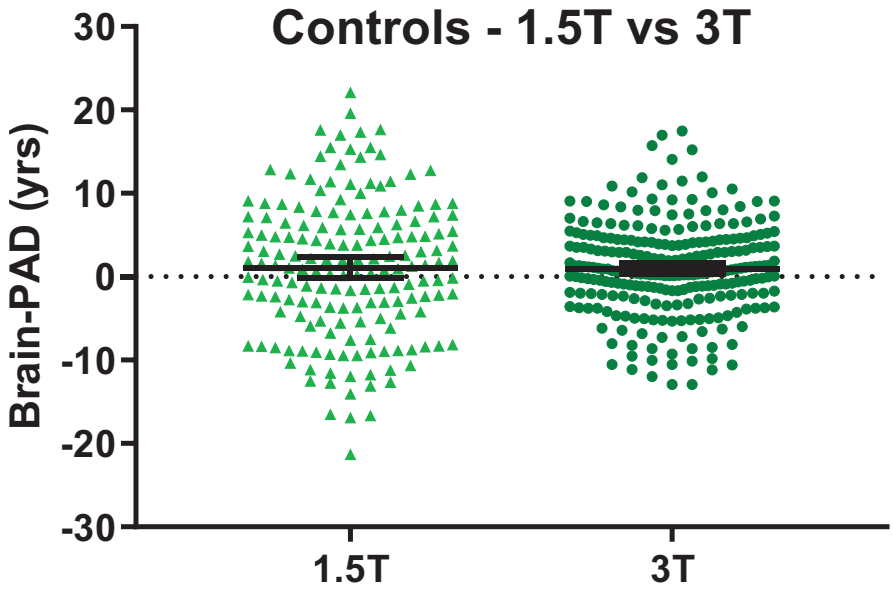


Figure 40: There was no difference in healthy control Brain-PAD between scans acquired using a 1.5 Tesla MRI scan and scans acquired using a 3.0 Tesla MRI scan. Error bars represent mean +/- 95% confidence intervals.

IV.7.2 'Filling MS lesions' has minimal effect on Brain-PAD

As presented under the 'natalizumab cohort' results Section IV.5.4, the association between Brain-PAD and clinical outcomes remained consistent after lesion filling MRI scans.

This was further investigated using the larger UCL cohort. 306 baseline scans had a filled version in addition to the unfilled version analysed in the above results. Brain-PAD was generated for both versions of these 306 scans, to investigate the effect of lesions on Brain-PAD. There was a very strong correlation between the Brain-PAD in the filled and unfilled version of scans (n = 306, $R^2 = 0.98$; $p < 0.0001$; Figure 41). 'Filling' the MRI did result in a systematic decrease in Brain-PAD, as perhaps should be expected, but this decrease was only by 0.4 years on average (Mean unfilled Brain-PAD: 12.1 (0.6); mean filled Brain-PAD: 11.7 (0.6); $p < 0.0001$).

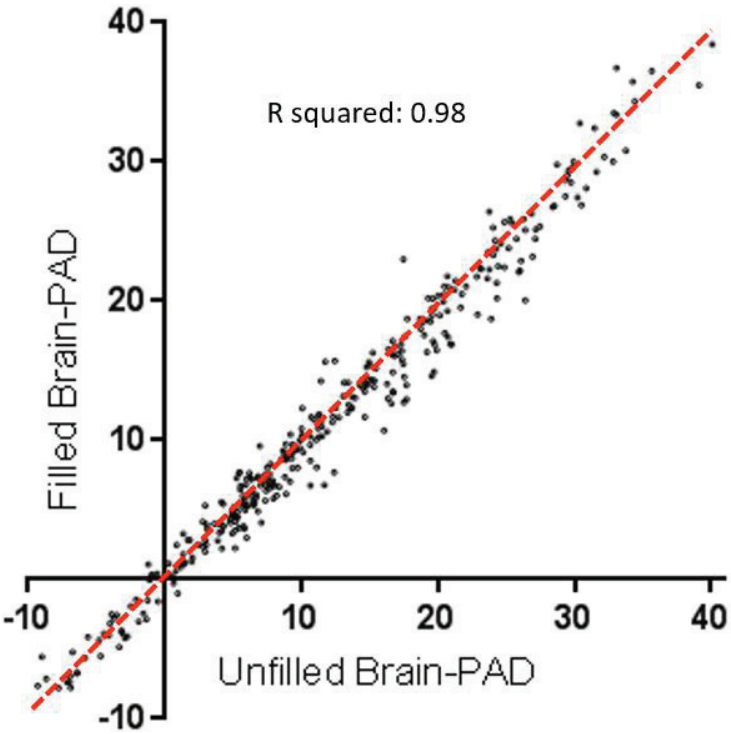


Figure 41: Unfilled Brain-PAD at baseline correlates strongly with lesion-filled Brain-PAD at baseline in those with CIS or MS. Red line represents y = x. Pearson's correlation coefficient: n = 306, $R^2 = 0.98$; $p < 0.0001$. Brain-PAD = Brain Predicted Age Difference.

IV.7.3 Brain Predicted Age is driven by a variety of known and unknown variables

Since Brain Predicted Age is based on a machine-learning model of normal ageing, one would anticipate that the Brain Predicted Age output for each subject is determined by the complex interplay of a variety of non-linear and spatially variable change in brain volume and structure. Nevertheless, it of interest to examine how much of the Brain Predicted Age output can be predicted by combining standard univariate measures.

Using all 391 baseline scans from people with CIS/MS from the UCL cohort, ordinary least squares linear regression with hierarchical partitioning was used to investigate what drives

Brain Predicted-Age. As shown in Table 11, the variables GM volume (as a ratio to intracranial volume; GMV/ICV), WM volume (as a ratio to intracranial volume; WMV/ICV), chronological age, and sex explain 81% of the Brain Age result. GMV/ICV and chronological age are the most important contributors, as one may expect. 19% of the Brain Age result is explained by other unknown variables not included in this model.

	R^2	*p*-value
GMV/ICV	0.416	<1e-15
WMV/ICV	0.082	<1e-15
Chronological age	0.293	<1e-15
Male sex	0.017	0.26
TOTAL	**0.808**	<1e-15

Table 11: Ordinary least squares linear regression with hierarchical partitioning, to predict Brain Age.

IV.7.4 Brain Predicted Age is more closely associated with disability outcomes than existing univariate measures of brain atrophy

As reported in the UCL cohort results section, above, Brain Predicted Age is associated with the disability outcome EDSS. It should be investigated whether Brain-Predicted Age is associated with EDSS more closely than standard univariate measures: GMV/ICV, WMV/ICV, chronological age, and sex.

When comparing the Pearson's Correlation Coefficient, Brain Predicted Age correlates most strongly with EDSS (r = 0.65, n = 361, $p < 0.0001$), followed by GMV/ICV (r = -0.58, n =

361, $p < 0.0001$), chronological age (r = 0.56, n = 361, $p < 0.0001$), WMV/ICV (r = 0.30, n = 361, $p < 0.0001$), and sex (r = 0.18, n = 361, $p < 0.001$).

Moreover, a multivariate model including Brain Predicted Age, GMV/ICV, WMV/ICV, chronological age, and sex correlates only slightly more strongly with EDSS (r = 0.67, n = 361, $p < 0.0001$) than the univariate model including Brain-Predicted Age alone (r = 0.65, n = 361, $p < 0.0001$). Ordinary least squares linear regression with hierarchical partitioning was used to investigate the above multivariate model. As shown in Table 12, Brain-Predicted Age was the strongest predictor of EDSS in the multivariate model, followed by chronological age.

	R^2	p value
Brain Age	0.16	0.0015
GMV/ICV	0.12	0.0831
WMV/ICV	0.04	0.0014
Chronological age	0.13	<0.0001
Male sex	0.01	0.2137
TOTAL	**0.46**	<1e-10

Table 12: Ordinary least squares linear regression with hierarchical partitioning, to predict cross-sectional EDSS score. Brain Age = Brain Predicted Age; GMV = grey matter volume; WMV = white matter volume; ICV = intracranial volume.

IV.8 DISCUSSION

This chapter reports results from two studies in which the Brain Predicted Age model was used to predict chronological age in people with CIS or MS and HCs, based solely upon T1-weighted MRI data. People with CIS, RRMS, SPMS, and PPMS had an older-appearing brain (positive Brain-PAD) compared with HCs. Brain Predicted Age and Brain-PAD correlated with time since MS diagnosis, age at diagnosis and the disability outcome EDSS. Baseline Brain-Predicted Age and Brain-PAD were able to predict the risk of future disability progression. Longitudinal T1-weighted MRI data showed that MS brains 'age faster' than the HC brain. There was also preliminary evidence from the 'natalizumab cohort' that Brain-PAD decreases after natalizumab treatment, especially in those who respond to treatment. A collaboration has been setup with the multi-centre international MAGNIMS cohort, after presentation of the above results by the thesis author. Data from the MAGNIMS cohort have been analysed, but are not presented in this thesis chapter, and have been published as pre-prints with the thesis author as 'joint first author'.[1]

The Brain Predicted Age model offers several possible advantages over brain atrophy measures. Firstly, the output places a patient's disease and disability in the context of their age, since Brain-PAD measures change relative to a model of healthy ageing. This allows the model to provide informative output without the need for longitudinal scans. Secondly, the Brain Predicted Age and Brain-PAD outputs are single numbers, which should be conceptually simple and intuitive to interpret for both healthcare professionals and patients. Thirdly, the model incorporates voxelwise MRI data, capturing more information that simple summary statistics. Therefore, non-linear and spatially variables patterns (i.e. voxelwise GM and WM volumes) can be captured, so that, for example, patterns of cortical thinning, sulcal

widening and ventricular enlargement can contribute to the model. Indeed, in this study, the association between Brain Predicted Age and EDSS was relatively strong, and performed better than GM volume, WM volume, or chronological age when these variables were considered in isolation. The Brain Predicted Age model can run through a pipeline and is mostly automated; the results for the 1658 scans in the UCL cohort were generated overnight. Therefore, the Brain Predicted Age model could be applied with relative ease to large cohorts in future research projects.

Other results reported in this chapter can be interpreted in the context of previous research. Brain-PAD has been shown to correlate with clinical outcomes in the general population, and is increased in diseases such as Alzheimer's disease (+9 years),[66] traumatic brain injury (+4.7 years),[31] Down's syndrome (+2.15 years),[46] and HIV (+2.15 years),[47] By comparison, the average increase in Brain-PAD in this study was +4.0 years for CIS, +10.3 years for RRMS, +17.4 years for SPMS, and +11.5 years for PPMS. These substantial increases in 'brain age' in the MS cohorts seem in keeping with the severity of disease.[67-69]

The UCL cohort results found increased Brain-PAD even in those recently diagnosed with CIS. This is supportive of previous research which shows that brain atrophy and cognitive impairment has started to occur even prior to the diagnosis of CIS.[70-73] Although limited by a small sample size, the UCL cohort results also suggest that those who are diagnosed with CIS but ultimately do not develop MS seem to have an improvement in Brain-PAD longitudinally, in contrast with those that do develop MS. A larger cohort is required to test the replicability of this finding, and to investigate whether there are any other features that discriminate those with CIS that ultimately do not develop MS.

It was also investigated how Brain-PAD changes longitudinally across the whole cohort. On average, longitudinal change in Brain Predicted Age increased at a rate ~46% faster in subjects with MS than in HCs. This figure could overestimate 'brain ageing rate', for example if subjects recruited to studies had more aggressive disease activity compared with the MS population on average. The figure could also underestimate 'brain ageing rate', for example since survivor bias may mean that those with the most severe disease were less likely to return for follow-up. It should be emphasised that this longitudinal analysis is considered exploratory, and will need to be further investigated with larger cohorts using multivariate statistical methods which do not assume a linear trajectory of brain ageing in MS. In the simple model used in this study, the MS and HC 'lines of best fit' crossed at 12.2 years; it will be of interest to see whether a similar number is derived in the multicentre studies with multivariate analyses, since such a figure could be taken to relate to the average age at which preclinical disease processes begin in MS.

It would also be of interest to test whether the longitudinal trajectory of Brain-PAD in MS could be modified by disease-modifying therapy. Although the 'natalizumab cohort' is limited by the small number of participants, it provides preliminary evidence that suggests Brain-PAD might improve after natalizumab treatment, especially in those who respond to treatment. The results from the UCL cohort support the concept that Brain-Predicted Age and Brain-PAD have prognostic significance for hard clinical endpoints. However, it does not necessarily follow that a change in these measures after treatment will help predict long-term outcomes after treatment, and the validity of surrogate outcomes should be tested against the Prentice criteria.[74] The effect of disease-modifying therapy on Brain-PAD was not tested in the 'UCL cohort', since only 40 subjects were known to be on disease-modifying therapies in this cohort, and since the dataset could include missing or incorrect data relating to disease-

modifying therapy initiation and discontinuation dates. The effect of disease-modifying therapies on Brain-PAD should be investigated in other cohorts. If disease-modifying therapies can improve Brain-PAD, and if this is shown to predict clinical outcomes according to the Prentice criteria, this could offer a conceptually simple and intuitive method to compare the efficacy of different disease-modifying therapies across large imaging cohorts.

The question then arises as to whether the Brain Predicted Age model could eventually be used in clinical practice, for example to contribute towards a clinician's assessment of prognosis or response to treatment. However, much like brain atrophy measures, the Brain Predicted Age model is likely to be susceptible to artefact.[75] Indeed, in the longitudinal data presented in this study, there are instances where Brain-PAD changes longitudinally by amounts which seem biologically implausible, including in apparently HCs. Therefore, at this stage, the Brain Predicted Age model appears most appropriate as a research tool to investigate questions at a group-level, where the occasional influence of artefact is controlled between groups. The factors which contribute to artefact should be investigated, in case these relate to features of the MRI image which can be quality checked. Adding longitudinal HC imaging cohorts into the training set could also reduce intra-subject variation in Brain-PAD caused by artefact.

There are additional limitations of the results reported in this chapter. Univariate statistical analyses are used to investigate relationship which are likely to be complex, multivariate, and non-linear. The use of these statistics is considered acceptable since these were conceived as proof-of-concept ('natalizumab cohort') and pilot ('UCL cohort') studies, to generate initial evidence regarding how Brain Predicted Age may relate to clinical outcomes and other MRI outcomes. A medical statistician will assist in future work, including analysis from the multi-

centre MAGNIMS cohort.[1] A further limitation is that data were not available relating to the presence of comorbidities in the UCL cohort. Comorbidities may increase Brain Predicted Age in the general population. If comorbidities were less prevalent in HCs in the UCL cohort, this could contribute to the difference in Brain-PAD between HC and MS groups, although any effect would be expected to be small.[44] More fundamentally, the Brain Predicted Age model could be criticised for a lack of applicability to MS, since it was developed as a non-specific ageing biomarker which is not trained to capture pathological features specific to MS. That said, by lesion filling brain lesions on the T1-weighted MRI images the 'natalizumab cohort' and 'UCL cohort', it appears that the effect of MRI lesions on Brain-Predicted Age is minimal. Other features of ageing, such as brain atrophy, are shared between MS and normal ageing, although the pattern of changes could be different.[76] A parallel workstream for this project would be to develop a new training set, using MRI scans from PwMS with clinical outcomes, to build a new machine learning model specific to MS. Of course, if the Brain Predicted Age model proves useful as a tool for quantifying MS-related damage to the brain, the lack of specificity of the model to MS becomes a moot point.

Overall, this work supports the continued investigation of the Brain Predicted Age model in MS. The strengths of the model include the following:

1. A patient's disease and disability can be placed in the context of their age.
2. Data from a wide range of different centres with different scanners can be integrated.
3. Longitudinal scans are not necessary to provide informative outcome.
4. The output is a single number, which should be conceptually simple and intuitive to interpret for both healthcare professionals and patients.
5. The model incorporates voxelwise MRI data, allowing non-linear and spatially variable patterns to be captured.

This model has been further investigated using the MAGNIMS multi-centre cohort,[1] and will be further developed as a tool for use in MS research.

IV.9 CONFLICTS OF INTEREST

The thesis author has no conflicts of interest relevant to this chapter.

Dr Nicholas received funding from GE Healthcare. Dr Nicholas has received outside the submitted work: grants, personal fees and non-financial support from Novartis; grants, personal fees and non-financial support from Biogen Idec; personal fees from Genzyme; and personal fees from Roche.

Other authors declare no conflicts of interest related to this chapter.

IV.10 REFERENCES

1. Cole JH, Raffel J, Friede T, Eshaghi A, Brownlee W, Chard D, De Stefano N, Enzinger C, Pirpamer L, Filippi M, Gasperini C, Rocca MA, Rovira A, Ruggieri S, Sastre-Garriga J, Stromillo ML, Uitdehaag BMJ, Vrenken H, Barkhof F, Nicholas R, Ciccarelli O, on behalf of the MAGNIMS study group. Accelerated brain ageing and disability in multiple sclerosis. bioRxiv 584888; doi: https://doi.org/10.1101/584888.
2. Lassmann H. Multiple sclerosis: Is there neurodegeneration independent from inflammation? J Neurol Sci. 2007;259(1-2):3-6. doi: DOI 10.1016/j.jns.2006.08.016. PubMed PMID: WOS:000248617400002.
3. Kidd D, Barkhof F, McConnell R, Algra PR, Allen IV, Revesz T. Cortical lesions in multiple sclerosis. Brain : a journal of neurology. 1999;122 (Pt 1):17-26. Epub 1999/03/02. doi: 10.1093/brain/122.1.17. PubMed PMID: 10050891.
4. Bevan RJ, Evans R, Griffiths L, Watkins LM, Rees MI, Magliozzi R, Allen I, McDonnell G, Kee R, Naughton M, Fitzgerald DC, Reynolds R, Neal JW, Howell OW. Meningeal inflammation and cortical demyelination in acute multiple sclerosis. Annals of neurology. 2018;84(6):829-42. Epub 2018/10/27. doi: 10.1002/ana.25365. PubMed PMID: 30362156.

5. Herranz E, Gianni C, Louapre C, Treaba CA, Govindarajan ST, Ouellette R, Loggia ML, Sloane JA, Madigan N, Izquierdo-Garcia D, Ward N, Mangeat G, Granberg T, Klawiter EC, Catana C, Hooker JM, Taylor N, Ionete C, Kinkel RP, Mainero C. Neuroinflammatory component of gray matter pathology in multiple sclerosis. Annals of neurology. 2016;80(5):776-90. Epub 2016/10/26. doi: 10.1002/ana.24791. PubMed PMID: 27686563; PubMed Central PMCID: PMCPMC5115951.

6. Howell OW, Reeves CA, Nicholas R, Carassiti D, Radotra B, Gentleman SM, Serafini B, Aloisi F, Roncaroli F, Magliozzi R, Reynolds R. Meningeal inflammation is widespread and linked to cortical pathology in multiple sclerosis. Brain : a journal of neurology. 2011;134(Pt 9):2755-71. Epub 2011/08/16. doi: 10.1093/brain/awr182. PubMed PMID: 21840891.

7. Reynolds R, Roncaroli F, Nicholas R, Radotra B, Gveric D, Howell O. The neuropathological basis of clinical progression in multiple sclerosis. Acta Neuropathol. 2011;122(2):155-70. Epub 2011/06/01. doi: 10.1007/s00401-011-0840-0. PubMed PMID: 21626034.

8. Grassiot B, Desgranges B, Eustache F, Defer G. Quantification and clinical relevance of brain atrophy in multiple sclerosis: a review. J Neurol. 2009;256(9):1397-412. Epub 2009/04/09. doi: 10.1007/s00415-009-5108-4. PubMed PMID: 19353226.

9. Bermel RA, Bakshi R. The measurement and clinical relevance of brain atrophy in multiple sclerosis. Lancet Neurol. 2006;5(2):158-70. Epub 2006/01/24. doi: 10.1016/S1474-4422(06)70349-0. PubMed PMID: 16426992.

10. Sanfilipo MP, Benedict RH, Sharma J, Weinstock-Guttman B, Bakshi R. The relationship between whole brain volume and disability in multiple sclerosis: a comparison of normalized gray vs. white matter with misclassification correction. Neuroimage. 2005;26(4):1068-77. Epub 2005/06/18. doi: 10.1016/j.neuroimage.2005.03.008. PubMed PMID: 15961046.

11. Rudick RA, Fisher E, Lee JC, Simon J, Jacobs L. Use of the brain parenchymal fraction to measure whole brain atrophy in relapsing-remitting MS. Multiple Sclerosis Collaborative Research Group. Neurology. 1999;53(8):1698-704. Epub 1999/11/24. doi: 10.1212/wnl.53.8.1698. PubMed PMID: 10563615.

12. Hardmeier M, Wagenpfeil S, Freitag P, Fisher E, Rudick RA, Kooijmans-Coutinho M, Clanet M, Radue EW, Kappos L, European r IFNb-aiRMSDCTSG. Atrophy is detectable within a 3-month period in untreated patients with active relapsing remitting multiple sclerosis. Archives of neurology. 2003;60(12):1736-9. Epub 2003/12/17. doi: 10.1001/archneur.60.12.1736. PubMed PMID: 14676048.

13. Fisher E, Rudick RA, Simon JH, Cutter G, Baier M, Lee JC, Miller D, Weinstock-Guttman B, Mass MK, Dougherty DS, Simonian NA. Eight-year follow-up study of brain atrophy in patients with MS. Neurology. 2002;59(9):1412-20. Epub 2002/11/13. doi: 10.1212/01.wnl.0000036271.49066.06. PubMed PMID: 12427893.

14. Chard DT, Griffin CM, Parker GJ, Kapoor R, Thompson AJ, Miller DH. Brain atrophy in clinically early relapsing-remitting multiple sclerosis. Brain : a journal of neurology. 2002;125(Pt 2):327-37. Epub 2002/02/15. doi: 10.1093/brain/awf025. PubMed PMID: 11844733.

15. Bakshi R, Ariyaratana S, Benedict RH, Jacobs L. Fluid-attenuated inversion recovery magnetic resonance imaging detects cortical and juxtacortical multiple sclerosis lesions. Archives of neurology. 2001;58(5):742-8. Epub 2001/05/18. doi: 10.1001/archneur.58.5.742. PubMed PMID: 11346369.

16. Sharma J, Sanfilipo MP, Benedict RH, Weinstock-Guttman B, Munschauer FE, 3rd, Bakshi R. Whole-brain atrophy in multiple sclerosis measured by automated versus semiautomated MR imaging segmentation. AJNR Am J Neuroradiol. 2004;25(6):985-96. Epub 2004/06/19. PubMed PMID: 15205136.

17. Kassubek J, Tumani H, Ecker D, Kurt A, Ludolph AC, Juengling FD. Age-related brain parenchymal fraction is significantly decreased in young multiple sclerosis patients: a quantitative MRI study. Neuroreport. 2003;14(3):427-30. Epub 2003/03/14. doi: 10.1097/00001756-200303030-00026. PubMed PMID: 12634497.

18. De Stefano N, Matthews PM, Filippi M, Agosta F, De Luca M, Bartolozzi ML, Guidi L, Ghezzi A, Montanari E, Cifelli A, Federico A, Smith SM. Evidence of early cortical atrophy in MS: relevance to white matter changes and disability. Neurology. 2003;60(7):1157-62. Epub 2003/04/12. doi: 10.1212/01.wnl.0000055926.69643.03. PubMed PMID: 12682324.

19. Gioia MC, Cerasa A, Liguori M, Passamonti L, Condino F, Vercillo L, Valentino P, Clodomiro A, Quattrone A, Fera F. Impact of individual cognitive profile on visuo-motor reorganization in relapsing-remitting multiple sclerosis. Brain Res. 2007;1167:71-9. Epub 2007/08/11. doi: 10.1016/j.brainres.2007.06.023. PubMed PMID: 17689504.

20. Benedict RH, Bruce JM, Dwyer MG, Abdelrahman N, Hussein S, Weinstock-Guttman B, Garg N, Munschauer F, Zivadinov R. Neocortical atrophy, third ventricular width, and cognitive dysfunction in multiple sclerosis. Archives of neurology. 2006;63(9):1301-6. Epub 2006/09/13. doi: 10.1001/archneur.63.9.1301. PubMed PMID: 16966509.

21. Amato MP, Portaccio E, Goretti B, Zipoli V, Battaglini M, Bartolozzi ML, Stromillo ML, Guidi L, Siracusa G, Sorbi S, Federico A, De Stefano N. Association of neocortical volume changes with cognitive deterioration in relapsing-remitting multiple sclerosis. Archives of neurology. 2007;64(8):1157-61. Epub 2007/08/19. doi: 10.1001/archneur.64.8.1157. PubMed PMID: 17698706.

22. Amato MP, Bartolozzi ML, Zipoli V, Portaccio E, Mortilla M, Guidi L, Siracusa G, Sorbi S, Federico A, De Stefano N. Neocortical volume decrease in relapsing-remitting MS patients with mild cognitive impairment. Neurology. 2004;63(1):89-93. Epub 2004/07/14. doi: 10.1212/01.wnl.0000129544.79539.d5. PubMed PMID: 15249616.

23. Zivadinov R, Reder AT, Filippi M, Minagar A, Stuve O, Lassmann H, Racke MK, Dwyer MG, Frohman EM, Khan O. Mechanisms of action of disease-modifying agents and brain volume changes in multiple sclerosis. Neurology. 2008;71(2):136-44. Epub 2008/07/09. doi: 10.1212/01.wnl.0000316810.01120.05. PubMed PMID: 18606968.

24. Sormani MP, Arnold DL, De Stefano N. Treatment effect on brain atrophy correlates with treatment effect on disability in multiple sclerosis. Annals of neurology. 2014;75(1):43-9. Epub 2013/09/06. doi: 10.1002/ana.24018. PubMed PMID: 24006277.

25. De Stefano N, Stromillo ML, Giorgio A, Bartolozzi ML, Battaglini M, Baldini M, Portaccio E, Amato MP, Sormani MP. Establishing pathological cut-offs of brain atrophy rates in multiple sclerosis. J Neurol Neurosurg Psychiatry. 2016;87(1):93-9. Epub 2015/04/24. doi: 10.1136/jnnp-2014-309903. PubMed PMID: 25904813; PubMed Central PMCID: PMCPMC4717444.

26. Uher T, Vaneckova M, Krasensky J, Sobisek L, Tyblova M, Volna J, Seidl Z, Bergsland N, Dwyer MG, Zivadinov R, De Stefano N, Sormani MP, Havrdova EK, Horakova D. Pathological cut-offs of global and regional

brain volume loss in multiple sclerosis. Multiple sclerosis. 2019;25(4):541-53. Epub 2017/11/17. doi: 10.1177/1352458517742739. PubMed PMID: 29143562.

27. Giorgio A, Battaglini M, Smith SM, De Stefano N. Brain atrophy assessment in multiple sclerosis: importance and limitations. Neuroimaging Clin N Am. 2008;18(4):675-86, xi. Epub 2008/12/11. doi: 10.1016/j.nic.2008.06.007. PubMed PMID: 19068408.

28. Rocca MA, Battaglini M, Benedict RH, De Stefano N, Geurts JJ, Henry RG, Horsfield MA, Jenkinson M, Pagani E, Filippi M. Brain MRI atrophy quantification in MS: From methods to clinical application. Neurology. 2017;88(4):403-13. Epub 2016/12/18. doi: 10.1212/wnl.0000000000003542. PubMed PMID: 27986875; PubMed Central PMCID: PMCPMC5272969.

29. Cole JH, Poudel RPK, Tsagkrasoulis D, Caan MWA, Steves C, Spector TD, Montana G. Predicting brain age with deep learning from raw imaging data results in a reliable and heritable biomarker. Neuroimage. 2017;163:115-24. Epub 2017/08/03. doi: 10.1016/j.neuroimage.2017.07.059. PubMed PMID: 28765056.

30. Cole JH. Neuroimaging Studies Illustrate the Commonalities Between Ageing and Brain Diseases. Bioessays. 2018;40(7):e1700221. Epub 2018/06/09. doi: 10.1002/bies.201700221. PubMed PMID: 29882974.

31. Cole JH, Leech R, Sharp DJ, Alzheimer's Disease Neuroimaging I. Prediction of brain age suggests accelerated atrophy after traumatic brain injury. Annals of neurology. 2015;77(4):571-81. Epub 2015/01/28. doi: 10.1002/ana.24367. PubMed PMID: 25623048; PubMed Central PMCID: PMCPMC4403966.

32. Lopez-Otin C, Blasco MA, Partridge L, Serrano M, Kroemer G. The hallmarks of aging. Cell. 2013;153(6):1194-217. Epub 2013/06/12. doi: 10.1016/j.cell.2013.05.039. PubMed PMID: 23746838; PubMed Central PMCID: PMCPMC3836174.

33. Dong J, Jing B, Ma X, Liu H, Mo X, Li H. Hurst Exponent Analysis of Resting-State fMRI Signal Complexity across the Adult Lifespan. Front Neurosci. 2018;12:34. Epub 2018/02/20. doi: 10.3389/fnins.2018.00034. PubMed PMID: 29456489; PubMed Central PMCID: PMCPMC5801317.

34. Cohen AA. Complex systems dynamics in aging: new evidence, continuing questions. Biogerontology. 2016;17(1):205-20. Epub 2015/05/21. doi: 10.1007/s10522-015-9584-x. PubMed PMID: 25991473; PubMed Central PMCID: PMCPMC4723638.

35. Schorr A, Carter C, Ladiges W. The potential use of physical resilience to predict healthy aging. Pathobiol Aging Age Relat Dis. 2017 21;8(1):1403844. .

36. Franceschi C, Garagnani P, Morsiani C, Conte M, Santoro A, Grignolio A, Monti D, Capri M, Salvioli S. The Continuum of Aging and Age-Related Diseases: Common Mechanisms but Different Rates. Front Med (Lausanne). 2018;5:61. Epub 2018/04/18. doi: 10.3389/fmed.2018.00061. PubMed PMID: 29662881; PubMed Central PMCID: PMCPMC5890129.

37. Franceschi C, Bonafe M, Valensin S, Olivieri F, De Luca M, Ottaviani E, De Benedictis G. Inflamm-aging. An evolutionary perspective on immunosenescence. Ann N Y Acad Sci. 2000;908:244-54. Epub 2000/07/27. doi: 10.1111/j.1749-6632.2000.tb06651.x. PubMed PMID: 10911963.

38. Simon NM, Smoller JW, McNamara KL, Maser RS, Zalta AK, Pollack MH, Nierenberg AA, Fava M, Wong KK. Telomere shortening and mood disorders: preliminary support for a chronic stress model of accelerated aging. Biol Psychiatry. 2006;60(5):432-5. Epub 2006/04/04. doi: 10.1016/j.biopsych.2006.02.004. PubMed PMID: 16581033.

39. Mattson MP, Arumugam TV. Hallmarks of Brain Aging: Adaptive and Pathological Modification by Metabolic States. Cell Metab. 2018;27(6):1176-99. Epub 2018/06/07. doi: 10.1016/j.cmet.2018.05.011. PubMed PMID: 29874566; PubMed Central PMCID: PMCPMC6039826.

40. Raz N. Decline and compensation in aging brain and cognition: promises and constraints. Preface. Neuropsychol Rev. 2009;19(4):411-4. Epub 2009/11/26. doi: 10.1007/s11065-009-9122-1. PubMed PMID: 19936932; PubMed Central PMCID: PMCPMC2809780.

41. Franke K, Ziegler G, Kloppel S, Gaser C, Alzheimer's Disease Neuroimaging I. Estimating the age of healthy subjects from T1-weighted MRI scans using kernel methods: exploring the influence of various parameters. Neuroimage. 2010;50(3):883-92. Epub 2010/01/15. doi: 10.1016/j.neuroimage.2010.01.005. PubMed PMID: 20070949.

42. Cole JH, Franke K. Predicting Age Using Neuroimaging: Innovative Brain Ageing Biomarkers. Trends Neurosci 2017; 40(12): 681-690. .

43. Dosenbach NU, Nardos B, Cohen AL, Fair DA, Power JD, Church JA, Nelson SM, Wig GS, Vogel AC, Lessov-Schlaggar CN, Barnes KA, Dubis JW, Feczko E, Coalson RS, Pruett JR, Jr., Barch DM, Petersen SE, Schlaggar BL. Prediction of individual brain maturity using fMRI. Science. 2010;329(5997):1358-61. Epub 2010/09/11. doi: 10.1126/science.1194144. PubMed PMID: 20829489; PubMed Central PMCID: PMCPMC3135376.

44. Cole JH, Ritchie SJ, Bastin ME, Valdes Hernandez MC, Munoz Maniega S, Royle N, Corley J, Pattie A, Harris SE, Zhang Q, Wray NR, Redmond P, Marioni RE, Starr JM, Cox SR, Wardlaw JM, Sharp DJ, Deary IJ. Brain age predicts mortality. Mol Psychiatry. 2017. doi: 10.1038/mp.2017.62. PubMed PMID: 28439103.

45. Pardoe HR, Cole JH, Blackmon K, Thesen T, Kuzniecky R, Human Epilepsy Project I. Structural brain changes in medically refractory focal epilepsy resemble premature brain aging. Epilepsy Res. 2017;133:28-32. Epub 2017/04/15. doi: 10.1016/j.eplepsyres.2017.03.007. PubMed PMID: 28410487.

46. Cole JH, Annus T, Wilson LR, Remtulla R, Hong YT, Fryer TD, et al. Brain-predicted age in Down Syndrome is associated with β-amyloid deposition and cognitive decline. Neurobiology of aging. 2017;56:41-9.

47. Cole JH, Underwood J, Caan MW, De Francesco D, van Zoest RA, Leech R, Wit FW, Portegies P, Geurtsen GJ, Schmand BA, Schim van der Loeff MF, Franceschi C, Sabin CA, Majoie CB, Winston A, Reiss P, Sharp DJ, collaboration C. Increased brain-predicted aging in treated HIV disease. Neurology. 2017;88(14):1349-57. Epub 2017/03/05. doi: 10.1212/WNL.0000000000003790. PubMed PMID: 28258081; PubMed Central PMCID: PMCPMC5379929.

48. Leray E, Yaouanq J, Le Page E, Coustans M, Laplaud D, Oger J, Edan G. Evidence for a two-stage disability progression in multiple sclerosis. Brain : a journal of neurology. 2010;133(Pt 7):1900-13. Epub 2010/04/27. doi: 10.1093/brain/awq076. PubMed PMID: 20423930.

49. Tutuncu M, Tang J, Zeid NA, et al. Onset of progressive phase is an age-dependent clinical milestone in multiple sclerosis. Mult Scler 2013;19(2):188-98.

50. Koch M, Mostert J, Heersema D, De Keyser J. Progression in multiple sclerosis: further evidence of an age dependent process. J Neurol Sci. 2007;255(1-2):35-41. Epub 2007/03/03. doi: 10.1016/j.jns.2007.01.067. PubMed PMID: 17331540.

51. Kremenchutzky M, Rice GP, Baskerville J, Wingerchuk DM, Ebers GC. The natural history of multiple sclerosis: a geographically based study 9: observations on the progressive phase of the disease. Brain : a journal of neurology. 2006;129(Pt 3):584-94. Epub 2006/01/13. doi: 10.1093/brain/awh721. PubMed PMID: 16401620.

52. Confavreux C, Vukusic S. Natural history of multiple sclerosis: a unifying concept. Brain : a journal of neurology. 2006;129(Pt 3):606-16. Epub 2006/01/18. doi: 10.1093/brain/awl007. PubMed PMID: 16415308.

53. Scalfari A, Neuhaus A, Daumer M, Ebers GC, Muraro PA. Age and disability accumulation in multiple sclerosis. Neurology. 2011;77(13):1246-52. Epub 2011/09/16. doi: 10.1212/WNL.0b013e318230a17d. PubMed PMID: 21917763; PubMed Central PMCID: PMCPMC3179646.

54. Scalfari A, Lederer C, Daumer M, Nicholas R, Ebers GC, Muraro PA. The relationship of age with the clinical phenotype in multiple sclerosis. Multiple sclerosis. 2016;22(13):1750-8. Epub 2016/02/13. doi: 10.1177/1352458516630396. PubMed PMID: 26869531.

55. Simon JH, Jacobs LD, Campion MK, Rudick RA, Cookfair DL, Herndon RM, Richert JR, Salazar AM, Fischer JS, Goodkin DE, Simonian N, Lajaunie M, Miller DE, Wende K, Martens-Davidson A, Kinkel RP, Munschauer FE, 3rd, Brownscheidle CM. A longitudinal study of brain atrophy in relapsing multiple sclerosis. The Multiple Sclerosis Collaborative Research Group (MSCRG). Neurology. 1999;53(1):139-48. Epub 1999/07/17. doi: 10.1212/wnl.53.1.139. PubMed PMID: 10408550.

56. De Stefano N, Giorgio A, Battaglini M, Rovaris M, Sormani MP, Barkhof F, Korteweg T, Enzinger C, Fazekas F, Calabrese M, Dinacci D, Tedeschi G, Gass A, Montalban X, Rovira A, Thompson A, Comi G, Miller DH, Filippi M. Assessing brain atrophy rates in a large population of untreated multiple sclerosis subtypes. Neurology. 2010;74(23):1868-76. Epub 2010/06/10. doi: 10.1212/WNL.0b013e3181e24136. PubMed PMID: 20530323.

57. Oost W, Talma N, Meilof JF, Laman JD. Targeting senescence to delay progression of multiple sclerosis. J Mol Med (Berl). 2018;96(11):1153-66. Epub 2018/09/20. doi: 10.1007/s00109-018-1686-x. PubMed PMID: 30229272; PubMed Central PMCID: PMCPMC6208951.

58. Eshaghi A, Prados F, Brownlee WJ, Altmann DR, Tur C, Cardoso MJ, De Angelis F, van de Pavert SH, Cawley N, De Stefano N, Stromillo ML, Battaglini M, Ruggieri S, Gasperini C, Filippi M, Rocca MA, Rovira A, Sastre-Garriga J, Vrenken H, Leurs CE, Killestein J, Pirpamer L, Enzinger C, Ourselin S, Wheeler-Kingshott C, Chard D, Thompson AJ, Alexander DC, Barkhof F, Ciccarelli O, group Ms. Deep gray matter volume loss drives disability worsening in multiple sclerosis. Annals of neurology. 2018;83(2):210-22. Epub 2018/01/14. doi: 10.1002/ana.25145. PubMed PMID: 29331092; PubMed Central PMCID: PMCPMC5838522.

59. Lublin FD, Reingold SC, Cohen JA, Cutter GR, Sorensen PS, Thompson AJ, Wolinsky JS, Balcer LJ, Banwell B, Barkhof F, Bebo B, Jr., Calabresi PA, Clanet M, Comi G, Fox RJ, Freedman MS, Goodman AD, Inglese M, Kappos L, Kieseier BC, Lincoln JA, Lubetzki C, Miller AE, Montalban X, O'Connor PW, Petkau J, Pozzilli C, Rudick RA, Sormani MP, Stuve O, Waubant E, Polman CH. Defining the clinical course of multiple sclerosis: the 2013 revisions. Neurology. 2014;83(3):278-86. Epub 2014/05/30. doi: 10.1212/WNL.0000000000000560. PubMed PMID: 24871874; PubMed Central PMCID: PMCPMC4117366.

60. Polman CH, Reingold SC, Banwell B, Clanet M, Cohen JA, Filippi M, Fujihara K, Havrdova E, Hutchinson M, Kappos L, Lublin FD, Montalban X, O'Connor P, Sandberg-Wollheim M, Thompson AJ, Waubant E, Weinshenker B, Wolinsky JS. Diagnostic criteria for multiple sclerosis: 2010 revisions to the McDonald

criteria. Annals of neurology. 2011;69(2):292-302. Epub 2011/03/10. doi: 10.1002/ana.22366. PubMed PMID: 21387374; PubMed Central PMCID: PMCPMC3084507.

61. Kurtzke JF. Rating Neurologic Impairment in Multiple-Sclerosis - an Expanded Disability Status Scale (Edss). Neurology. 1983;33(11):1444-52. PubMed PMID: WOS:A1983RP86600009.

62. Ashburner J. A fast diffeomorphic image registration algorithm. Neuroimage. 2007;38(1):95-113. Epub 2007/09/01. doi: 10.1016/j.neuroimage.2007.07.007. PubMed PMID: 17761438.

63. Schrouff J, Rosa MJ, Rondina JM, Marquand AF, Chu C, Ashburner J, Phillips C, Richiardi J, Mourao-Miranda J. PRoNTo: pattern recognition for neuroimaging toolbox. Neuroinformatics. 2013;11(3):319-37. Epub 2013/02/19. doi: 10.1007/s12021-013-9178-1. PubMed PMID: 23417655; PubMed Central PMCID: PMCPMC3722452.

64. Battaglini M, Jenkinson M, De Stefano N. Evaluating and reducing the impact of white matter lesions on brain volume measurements. Hum Brain Mapp. 2012;33(9):2062-71. Epub 2011/09/02. doi: 10.1002/hbm.21344. PubMed PMID: 21882300.

65. Criminisi A, Sharp T, Blake A. Geos: Geodesic image segmentation. Computer Vision–ECCV 2008 2008:99-112.

66. Franke K, Gaser C. Longitudinal changes in individual BrainAGE in healthy aging,mild cognitive impairment, and Alzheimer's Disease. GeroPsych 2012; 25: 235–245.

67. Sadovnick AD, Ebers GC, Wilson RW, Paty DW. Life expectancy in patients attending multiple sclerosis clinics. Neurology. 1992;42(5):991-4. Epub 1992/05/01. doi: 10.1212/wnl.42.5.991. PubMed PMID: 1579256.

68. Weinshenker BG. The natural history of multiple sclerosis: update 1998. Semin Neurol. 1998;18(3):301-7. Epub 1998/11/17. doi: 10.1055/s-2008-1040881. PubMed PMID: 9817534.

69. Weinshenker BG. Natural history of multiple sclerosis. Annals of neurology. 1994;36 Suppl:S6-11. Epub 1994/01/01. PubMed PMID: 8017890.

70. Feuillet L, Reuter F, Audoin B, Malikova I, Barrau K, Cherif AA, Pelletier J. Early cognitive impairment in patients with clinically isolated syndrome suggestive of multiple sclerosis. Multiple sclerosis. 2007;13(1):124-7. Epub 2007/02/14. doi: 10.1177/1352458506071196. PubMed PMID: 17294621.

71. Perez-Miralles F, Sastre-Garriga J, Tintore M, Arrambide G, Nos C, Perkal H, Rio J, Edo MC, Horga A, Castillo J, Auger C, Huerga E, Rovira A, Montalban X. Clinical impact of early brain atrophy in clinically isolated syndromes. Multiple sclerosis. 2013;19(14):1878-86. Epub 2013/05/09. doi: 10.1177/1352458513488231. PubMed PMID: 23652215.

72. Henry RG, Shieh M, Okuda DT, Evangelista A, Gorno-Tempini ML, Pelletier D. Regional grey matter atrophy in clinically isolated syndromes at presentation. J Neurol Neurosurg Psychiatry. 2008;79(11):1236-44. Epub 2008/05/13. doi: 10.1136/jnnp.2007.134825. PubMed PMID: 18469033; PubMed Central PMCID: PMCPMC4827711.

73. Dalton CM, Chard DT, Davies GR, Miszkiel KA, Altmann DR, Fernando K, Plant GT, Thompson AJ, Miller DH. Early development of multiple sclerosis is associated with progressive grey matter atrophy in patients presenting with clinically isolated syndromes. Brain : a journal of neurology. 2004;127(Pt 5):1101-7. Epub 2004/03/05. doi: 10.1093/brain/awh126. PubMed PMID: 14998914.

74. Prentice RL. Surrogate endpoints in clinical trials: definition and operational criteria. Stat Med. 1989;8(4):431-40. Epub 1989/04/01. doi: 10.1002/sim.4780080407. PubMed PMID: 2727467.

75. Sharma S, Noblet V, Rousseau F, Heitz F, Rumbach L, Armspach JP. Evaluation of brain atrophy estimation algorithms using simulated ground-truth data. Med Image Anal. 2010;14(3):373-89. Epub 2010/03/12. doi: 10.1016/j.media.2010.02.002. PubMed PMID: 20219411.

76. Ghione E, Bergsland N, Dwyer MG, Hagemeier J, Jakimovski D, Paunkoski I, Ramasamy DP, Carl E, Hojnacki D, Kolb C, Weinstock-Guttman B, Zivadinov R. Aging and Brain Atrophy in Multiple Sclerosis. J Neuroimaging. 2019;29(4):527-35. Epub 2019/05/11. doi: 10.1111/jon.12625. PubMed PMID: 31074192.

Chapter 5

Patient-Reported Outcomes can Predict Survival Time in Multiple Sclerosis: A Cohort Study using the Multiple Sclerosis Impact Scale–29

V.1 ABSTRACT

Background: There is increasing emphasis on using patient-reported outcomes (PROs) to complement traditional clinical outcomes in medical research, including in multiple sclerosis (MS). Research, particularly in oncology and heart failure, has shown that PROs can be prognostic of hard clinical endpoints such as survival time (time from study entry until death). However, unlike in oncology or cardiology, it is unknown whether PROs can be associated with survival time in neurological diseases.

The Multiple Sclerosis Impact Scale–29 (MSIS-29) is a PRO sensitive to short-term change in MS, with questions covering both physical and psychological quality of life.

Objective: To assess the prognostic value of MSIS-29 scores on hard clinical endpoints including 'survival time' in people with MS.

Methods: MSIS-29 scores were investigated using the 'natalizumab cohort' described in Chapter 3.

After this, MSIS-29 scores were investigated using a large available dataset. From 15th July 2004 onwards, the MSIS-29 was completed by people with MS registered with the MS Society Tissue Bank. MSIS-29 scores were correlated with survival outcomes over a 10-year follow-up period.

Results: In the small 'natalizumab cohort', MSIS-29 scores improved after natalizumab, and were associated with clinical response to treatment.

In the MS Society Tissue Bank cohort, 2,126 participants completed the MSIS-29, with 872 participants completing an additional MSIS-29 one year later. The mean population age at MSIS-29 assessment was 54 years, with a mean disease length of 18.5 years. 10-years after study initiation, 264 participants (12.4%) had died. Higher baseline MSIS-29 physical (MSIS-29-PHYS) score was associated with reduced survival time (subgroup with highest scores versus subgroup with lowest scores: hazard ratio [HR] 5.7, 95% confidence interval [CI] 3.1–10.5, $p < 0.001$). Higher baseline MSIS-29 psychological score was also associated with reduced survival time (subgroup with highest scores versus subgroup with lowest scores: HR 2.8, 95% CI 1.8–4.4, $p < 0.001$). In those with high baseline MSIS-29 scores, mortality risk was even greater if the MSIS-29 score increased over one year (HR 2.3, 95% CI 1.2–4.4, $p = 0.02$). MSIS-29-PHYS scores were associated with survival time independent of age, sex, and patient-reported Expanded Disability Status Scale score in a Cox regression analysis (per 1-standard deviation increase in MSIS-29-PHYS score: HR 1.8, 95% CI 1.1–2.9, $p = 0.03$).

Conclusions: MSIS-29 scores can be prognostic for hard clinical endpoints in MS. This is the first study to associate PROs with survival in any neurological disease. Future studies should evaluate whether MSIS-29 scores can be used as a surrogate for response to treatment. PROs are cheap and easy to administer, and could allow MS studies with large cohorts which would otherwise be financially unfeasible.

Publication outcome: Study published in *PLOS Medicine* with the thesis author as first author.[1]

V.2 ABBREVIATIONS

CI	Confidence interval
Df	Degrees of freedom
EDSS	Expanded Disability Status Scale
HC	Healthy control
HR	Hazard ratio
MS	Multiple sclerosis
MSIS-29	Multiple Sclerosis Impact Scale–29
MSIS-29-PHYS	MSIS-29 physical
MSIS-29-PSYCH	MSIS-29 psychological
MSSTB	MS Society Tissue Bank
prEDSS	Patient-reported Expanded Disability Status Scale
PRO	Patient-reported outcome
SD	Standard deviation

V.3 INTRODUCTION

V.3.1 Surrogates for prognosis: capturing the patient experience

The previous thesis chapters have considered how relapses or new MRI lesions (Chapter 2), TSPO-PET (Chapter 3), or the Brain-Predicted Age model (Chapter 4), could be useful outcomes in MS for assessing disease severity and predicting response to disease-modifying therapy. Further work is required to develop and better understand these outcomes. However, a more straightforward and more immediately available approach is to simply ask patients how they feel. Might it be that a patient's self-report can predict prognosis, perhaps as well as any radiological or physician-assessed outcome? Might a patient's self-report after the initiation of a new disease modifying therapy predict long-term response to treatment?

Of course, understanding a patient's experience is already a vital part of the decision-making process in the MS clinic. A patient's report of their past and present symptoms will influence a clinician's assessment of prognosis, and advice whether to initiate treatment. Similarly, a patient's report of their experience on a disease-modifying therapy will influence a clinician in advising whether to continue, discontinue, or switch therapies.

Such doctor-patient interactions do not follow a set format, and will naturally vary depending on the patient's personality and experience, the doctor's personality and experience, the setting, and other factors. This promotes a fluid and natural consultation, and the flexibility to address the issues most important to the patient at that time. However, if one wants to systematically assess whether patient reports can predict disease outcomes, then a more formal approach using patient-reported outcomes (PROs) is required.

V.3.2 Patient reported outcomes in other disease areas

PROs are defined as '*any report of the status of a patient's health condition that comes directly from the patient, without interpretation of the patient's response by a clinician or anyone else*'.[2] PROs are increasingly being used to complement traditional outcome measures in disciplines such as oncology, cardiology, and neurology. PROs can enhance clinical care in areas such as symptom screening, monitoring treatment response, care coordination, care systems assessment, and improving communication in the doctor–patient clinical encounter.[3-6] In interventional trials, the increasing use of PROs is partly driven by the need for pharmaceutical companies to justify labelling and promotional claims in post-licensing marketing.[2, 7] However, research and clinical practice in oncology has led the way in showing that PROs are also useful prognostic measures. In oncology, it is well established that PROs are associated with hard clinical endpoints such as survival time (time from study entry until death) and can add prognostic value to more traditional physician-reported outcome measures.[8-10] PROs are also well established as prognostic for survival time in heart failure.[11-13] This validates PROs as clinically meaningful outcome measures, and supports their increasing use to enhance decision making in research and in clinical practice. However, such associations are more difficult to study in neurological research, in part because it is rarer for the clinical endpoint of trials in neurological disease to be survival.

PROs could be useful in MS research, to complement established radiological and physician-reported outcome measures.[14, 15] Compared to physician-reported outcome measures, PROs may be better able to capture the impact of disease on the person, may be easier and cheaper to administer, and may be completed from the home environment. Therefore, further

validation of PROs could allow for long-term, geographically diverse, and large-scale observational and interventional studies which would not be possible with physician-reported or radiological outcome measures.[16]

V.3.3 The Multiple Sclerosis Impact Scale–29

The Multiple Sclerosis Impact Scale–29 (MSIS-29) is a PRO that attempts to assess both physical and psychological quality of life in MS.[17] In a systematic comparison of eight PROs used most commonly in MS clinical trials, the MSIS-29 had the best overall mean score using the '*Evaluating the Measurement of Patient-Reported Outcomes'* tool.[14] The MSIS-29 is self-reported and can be distributed by post. It could potentially be utilised in MS trials, as it appears sensitive to clinically relevant change over short time frames.[18] It could complement the physician-assessed Expanded Disability Status Scale (EDSS), which is the primary outcome favoured in most MS trials despite several well-documented limitations, including poor inter-rater and intra-rater reliability and a limited sensitivity to change over the time frame of 2–3 years, especially in progressive MS.[19-26] Though small studies have correlated MSIS-29 score with cross-sectional EDSS score, it is unknown whether the MSIS-29 can predict hard clinical endpoints such as survival time.[27, 28] Indeed, to our knowledge, no PROs have been associated with survival time in MS or any other neurological disease.

In this study, MSIS-29 scores were investigated using the 'natalizumab cohort' described in Chapter 3. Following this, a large observational cohort of people with MS from the MS Society Tissue Bank (MSSTB) was used to investigate whether MSIS-29 scores can be prognostic for survival time (time from MSIS-29 completion to death). The primary study hypothesis was that MSIS-29 scores are associated with survival time in MS.

V.4 METHODOLOGY

V.4.1 Study population

Data were collated from the 'natalizumab cohort' reported in Chapter 3 of this thesis, including subjects at baseline and after the initiation of natalizumab. Methodology for this natalizumab cohort is not repeated here, and readers are requested to refer to Chapter 3 for further information. In this cohort, the MSIS-29 was also completed by healthy controls (HCs). Questions 1-3 of the MSIS-29 mention MS specifically, and so were adapted for this HC population by changing '*In the past two weeks, how much has your MS limited your ability to...'* to *'In the past two weeks, how much have you been limited in your ability to'*.

For the MSSTB study, data were collated from a large observational cohort of people with MS. Since 1998, the MSSTB has operated a nationwide community-based scheme for people with MS and non-MS controls in the UK to donate their brain and spinal cord after death, by providing written consent while alive (ethics approval in 1998: London Multicentre Research Ethics Committee—MREC/02/2/39; then in 2008: Wales Research Ethics Committee 3—08/MRE09/31; then in 2013: Wales Research Ethics Committee 3—08/MRE09/31+5).[29] This cohort is a unique population in that the participants are followed from registration to death, with eventual pathological confirmation.[29] On 15th July 2004, the MSIS-29 was sent out to all registered donors. For those who completed a MSIS-29 at this time, a second MSIS-29 was sent out one year later, to measure change in MSIS-29 score. In addition, since 15th July 2004, all new registered donors have been sent a single MSIS-29 at the time of registration, as well

as a 'patient-reported EDSS' (prEDSS).[30, 31] This study included people with MS registered in the MSSTB up until 1st January 2014 who had completed at least one MSIS-29.

V.4.2 Outcome measures

The MSIS-29 consists of 29 questions answered on a 5-point Likert scale, giving 2 scores: the MSIS-29 physical (MSIS-29-PHYS) score (questions 1–20; score range 20–100 for these 20 questions) and the MSIS-29 psychological (MSIS-29-PSYCH) score (questions 21–29; score range 9–45 for these 9 questions).[17, 32] Imputation was used to address questionnaires returned with missing data using the following rule: if more than 66% of questions had been answered within MSIS-29-PHYS or within MSIS-29-PSYCH, missing answers were imputed using the mean of the answered questions from the MSIS-29-PHYS or MSIS-29-PSYCH of that individual participant.[33] If ≤66% of questions had been answered, then all data from that MSIS-29-PHYS or MSIS-29-PSYCH were excluded. The prEDSS uses the same scale as the physician-reported EDSS and can be completed without physician input, with good correlation.[30]

The MSIS-29 is copyright by the Neurological Outcome Measures Unit. A copy of the MSIS-29 is included in the Appendix, Section V.11. Permission to use the scale can be obtained by contacting Dr Jeremy Hobart at J.Hobart@ion.ucl.ac.uk. Here, MSIS-29-PHYS questions are questions 1-20, and MSIS-29-PSYCH questions are questions 21-29.

The prEDSS is copyright by L. Kappos, Department of Neurology, University Hospitals Basel. Permission to use the scale can be obtained by contacting Dr. Ludwig Kappos at lkappos@uhbs.ch

Ten-year data on mortality were collected up until 1st June 2014. Survival time was defined using date of the first MSIS-29 as the entry point, date of death as the endpoint, and date of study completion (1st June 2014) as the censorship date for those still alive.

Baseline MSIS-29 scores were categorised into 5 equally spaced subgroups as follows:

- MSIS-29-PHYS scores: 20–35, 36–51, 52–68, 69–84, 85–100
- MSIS-29-PSYCH scores: 9–16, 17–23, 24–30, 31–37, 38–45.

In addition, for those that completed a repeat MSIS-29 one year after baseline, the following subgroups were used:

- Subgroup 1: initial MSIS-29-PHYS score 20–84, no increase after one year
- Subgroup 2: initial MSIS-29-PHYS score 20–84, increase after one year (≥1 point)
- Subgroup 3: initial MSIS-29-PHYS score 85–100, no increase after one year
- Subgroup 4: initial MSIS-29-PHYS score 85–100, increase after one year (≥1 point).

V.4.3 Statistical analysis

Population demographics are presented as mean (standard deviation [SD]) and frequency (percentage) for continuous and categorical variables, respectively, unless otherwise stated. Differences between continuous variables were tested with the unpaired or paired *t* test, or one-way analysis of variance (ANOVA) when more than 2 groups, with repeated-measures as appropriate. Differences between categorical data were tested with the chi-square test. To assess whether MSIS-29-PHYS score, MSIS-29-PSYCH score, prEDSS score, and change in MSIS-29-PHYS score are associated with mortality, survival times were modelled using Cox proportional hazard models where the hazard ratios (HRs) for the respective instruments were

adjusted for age and sex. The HRs are presented with 95% confidence intervals (CIs) and *p*-values testing the null hypothesis of the HRs being equal to 1. Survival curves within the subgroups were estimated using Kaplan–Meier estimators. Correlations between the 3 PRO scales (MSIS-29-PHYS, MSIS-29-PSYCH, and prEDSS) were estimated using rank-based Spearman correlations, which are reported with *p*-values testing the null hypothesis of no correlation. To investigate whether MSIS-29-PHYS and MSIS-29-PSYCH scores are associated with survival independent of prEDSS score, survival times were modelled using a Cox regression with prEDSS score, MSIS-29-PHYS score, MSIS-29-PSYCH score, age, and sex as independent variables. Statistical analysis was carried out using SAS 9.4 platform and GraphPad Prism (v7, GraphPad Software, Inc., San Diego, CA, USA).

V.4.4 Analysis history

Some analysis methods changed over the course of the study, and after peer-review by *PLOS Medicine* journal, in which these results are already published.[1] The changes in the methods employed are summarised below.

1. The study was motivated by the primary research question 'Can MSIS-29, or change in MSIS-29, be prognostic for mortality data in MS?' This study question was defined prior to the analysis of any data.

2. Data collation took place after 2014, after the cut-off date for study data. Imputation rules were decided upon at this point and have not changed. A preliminary univariate multivariable regression analysis concluded that MSIS-29 scores was associated with survival.

3. Methods for statistical analysis were refined in 2016 after consultation with a statistician (Dr Tim Friede) to develop the Cox proportional hazard models presented in this chapter. This was done to improve analysis methods to those suited to the dataset from a statistical perspective, and had no impact on the relationships and overall message reported in the results. Subgroup analyses were also decided upon at this point, including the categorisation of participants into five subgroups based upon baseline MSIS-29 scores. The subgroup range values were originally chosen after interrogation of the data to achieve a compromise between 'number of participants' and 'number of deaths' in each subgroup, to allow for sufficient power in statistical analyses.

4. After peer-review from *PLOS Medicine*, the subgroup range values for MSIS-29 groups were modified so that the five subgroups were equally spaced in terms of MSIS-29 scores. This change was undertaken to make the subgroup ranges for MSIS-29 subgroups more intuitive to the reader. This had no impact on the relationships and overall message reported in the results. Other new analyses performed after *PLOS Medicine* peer review were the comparison of subgroups shown in Table 15, and the comparison of subgroups by MSIS-29 score shown in Table 16.

V.4.5 Contribution to work

Joel Raffel[1,2]	Led on overall scientific direction of project. Collated data and performed data analysis and interpretation. Supervised Alison Wallace during data collection. Wrote the manuscript published in *PLOS Medicine*, adapted for thesis chapter.[1]

Alison Wallace[1]	Medical student. Helped with data collection as part of BSc project: converted MSIS-29 questionnaires from paper format into computerised format. Reviewed text prior to submission of *PLOS Medicine* paper.
Richard Reynolds[1]	Helped arrange for people registered on the MSSTB to complete the MSIS-29 from 2004 onwards. Reviewed text prior to submission of *PLOS Medicine* paper.
Tim Friede[3]	Medical statistician. Assisted with statistical methodology including the Cox proportional hazards models. Reviewed text prior to submission of *PLOS Medicine* paper.
Richard Nicholas[1,2]	Helped arrange for people registered on the MSSTB to complete the MSIS-29 from 2004 onwards. Initial conceptualisation of the project. Overall responsibility and supervision of the project throughout.

1 Division of Brain Sciences, Faculty of Medicine, Imperial College London, London, United Kingdom,

2 Imperial College Healthcare NHS Trust, London, United Kingdom,

3 Department of Medical Statistics, University Medical Center, Göttingen, Germany

V.5 NATALIZUMAB COHORT RESULTS

MSIS-29 results were first examined in the natalizumab cohort described in Chapter 3, before being applied to the larger MSSTB cohort.

V.5.1 Study procedures

17 PwMS and 8 HCs completed the MSIS-29 questionnaire at baseline. 16 PwMS had follow-up MSIS-29 questionnaires 10 weeks and 58 weeks after the initiation of natalizumab, as

described in Chapter 3. One subject with MS did not have follow-up, having dropped out of the study after the baseline visit.

V.5.2 Subject characteristics

The study cohort overlapped with that described in Chapter 3, although one additional subject with MS was available for analysis (due to failed PET but available MSIS-29 questionnaire).

Baseline characteristics are presented in Table 13. PwMS had increased disability at baseline compared to HCs, as expected (Table 14).

	PwMS (n = 17)	HCs (n = 11)
Male/Female, n	6/11	8/3
Age, yrs	41.6 (10.8)	41.6 (8.6)
Years of education	14.4 (2.6)	16.3 (3.2)
Age at MS onset, yrs	29.5 (10.0)	N/A
Time since MS onset, yrs	12.1 (10.6)	N/A
Number of previous DMTs, n	O DMTs: 9 1 DMT: 3 2 DMTs: 5	N/A

Table 13: Baseline characteristics of PwMS and HCs. DMT = disease-modifying therapy. Standard deviations shown in brackets.

	PwMS (n = 17)	HCs (n = 11)	*p*-value
T25FW, secs	6.6 (4.4)	3.5 (0.4)	<0.05
9HPT, secs	30.9 (19.9)	17.9 (1.2)	<0.05
MSQOL-54 Physical	42.8 (16.8)	88.0 (5.2)	<0.0001
MSQOL-54 Psych	58.7 (24.0)	81.4 (6.6)	<0.01
WPAI:MS	59.4 (16.8)	3.6 (6.7)	<0.0001
SDMT	49.7 (13.7)	66.1 (9.9)	<0.01
CVLT	54.2 (10.8)	66.1 (5.5)	<0.01
BVMT	24.1 (6.6)	30.5 (4.9)	<0.05
EDSS	4.2 (1.1)	N/A	
MSSS	5.6 (2.4)	N/A	

Table 14: Clinical and patient-reported outcomes in PwMS and HCs at baseline. T25FW = timed 25-foot walk; 9HPT = 9-hole peg test; MSQOL-54 = Multiple Sclerosis Quality of Life-54 patient reported outcome (physical and psychological subscores); WPAI:MS = Work Productivity and Activity Impairment, Multiple Sclerosis; SDMT = symbol digit modalities test; CVLT = California verbal learning test; BVMT = Brief Visuospatial Memory Test; EDSS = Expanded Disability Status Scale; MSSS = Global Multiple Sclerosis Severity Scores. Standard deviations shown in brackets. *p*-values refer to unpaired *t* tests: * = $p < 0.05$; ** = $p < 0.01$; *** = $p < 0.001$. The PwMS group had scores associated with greater disability, compared with the HC group.

V.5.3 MSIS-29 score is increased in subjects with MS

MSIS-29-PHYS score and MSIS-29-PSYCH score were significantly greater in PwMS at baseline than HCs, as expected (**MSIS-29-PHYS**: MS mean 50.1, 95% CI 40.1 to 59.3; HC mean 21.1, 95% CI 20.1 to 22.1, $p < 0.001$; Figure 42A. **MSIS-29-PSYCH**: MS – mean 27.1, 95% CI 21.8 to 32.4; HC - mean 9.9, 95% CI 8.7 to 11.1, $p < 0.001$; Figure 42B).

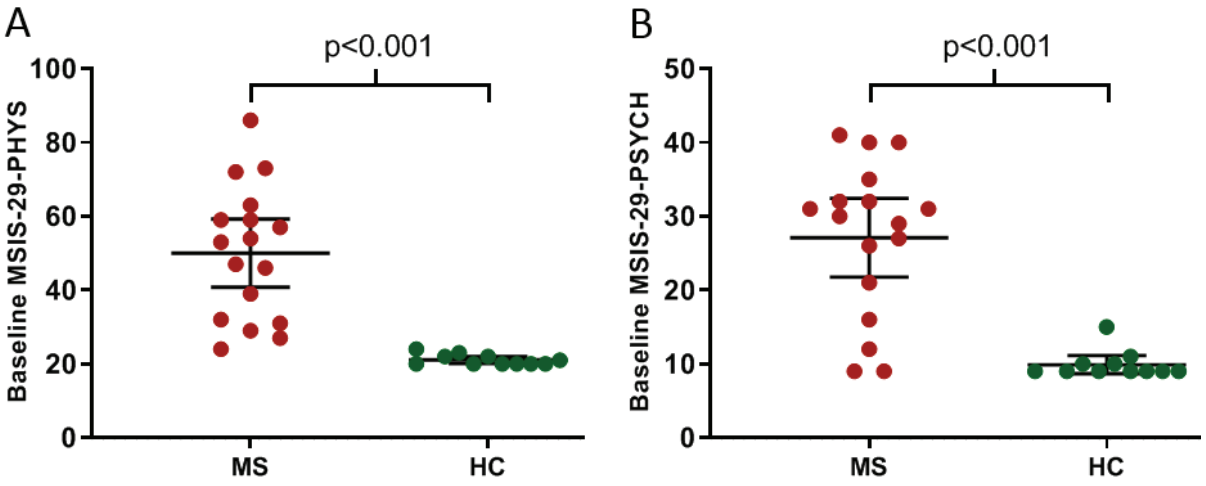


Figure 42: MSIS-29 scores are higher in subjects with MS than HCs. (A): MSIS-29-PHYS scores are higher in subjects with MS than HCs. (B): MSIS-29-PSYCH scores are higher in subjects with MS than HCs. *p*-value generated using unpaired *t* test. Error bar represent mean +/- 95% confidence intervals. MSIS-29 = Multiple Sclerosis Impact Scale–29; PHYS = physical subscale. PSYCH – psychological subscale.

V.5.4 MSIS-29 scores improve after natalizumab in those responding to treatment

Although this cohort was limited by sample size, it was investigated whether MSIS-29 scores were modified by natalizumab treatment in the 16 PwMS with available data.

After 10 weeks and 58 weeks of treatment, mean MSIS-29-PHYS score was significantly improved than at baseline ($F(2, 15) = 5.4$, $p < 0.05$, $\eta_p^2 = 0.26$; Figure 43A). MSIS-29-PHYS score at 10 weeks had improved in those who were later classified as natalizumab responders at 58 weeks, but had not improved in those who were later classified as natalizumab non-responders at 58 weeks (**58 week responders,** mean change at 10 weeks: -10.6, 95% CI -16.1 to -5.0; **58 week non-responders**, mean change at 10 weeks: +3.4, 95% CI -0.2 to +7.0, $p < 0.01$; Figure 43B).

Similarly, after 10 weeks and 58 weeks of treatment, mean MSIS-29-PSYCH score was significantly improved than at baseline ($F(2, 15) = 8.4$, $p < 0.01$, $\eta_p^2 = 0.36$; Figure 43C). MSIS-29-PSYCH score at 10 weeks had improved in those who were later classified as natalizumab responders at 58 weeks, but had not improved in those who were later classified as natalizumab non-responders at 58 weeks (**58 week responders,** mean change at 10 weeks: -7.3, 95% CI -11.0 to -3.6; **58 week non-responders**, mean change at 10 weeks: +1.0, 95% CI -2.5 to +4.5, $p < 0.01$; Figure 43D).

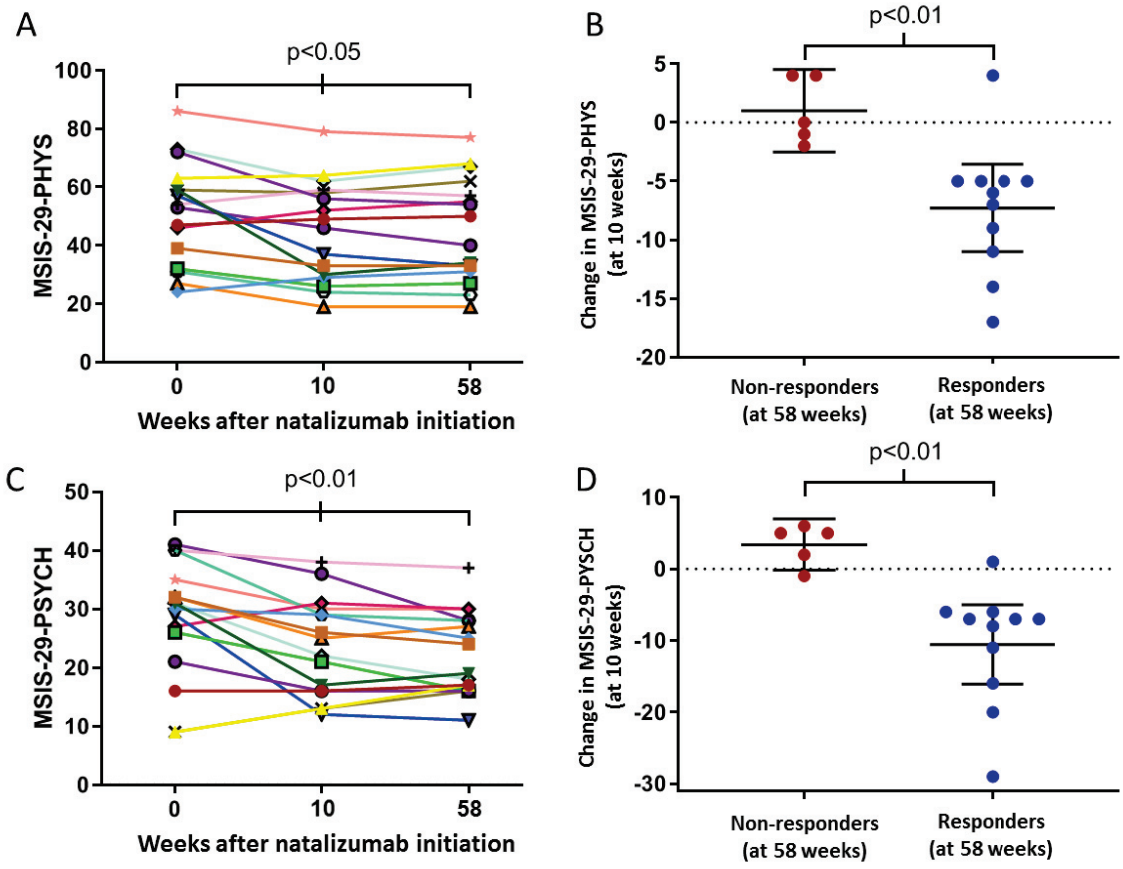


Figure 43: Change in MSIS-29 scores are associated with response to treatment. (A): Each individual PwMS represented by a colour/symbol. Across the group, mean MSIS-29-PHYS score decreased significantly. (B): Mean MSIS-29-PHYS score improved by 10 weeks in those that responded to treatment (assessed at 58 weeks), but not in those that did not respond to treatment. (C): Each individual PwMS represented by a colour/symbol. Across the group, mean MSIS-29-PSYCH score decreased significantly. (D): Mean MSIS-29-PSYCH score improved by 10 weeks in those that responded to treatment (assessed at 58 weeks), but not in those that did not respond to treatment. For (A) and (C), *p*-values generated using repeated-measure one way ANOVA. For (B) and (D), *p*-value generated using unpaired *t* test. Error bars represent mean +/- 95% confidence intervals. MSIS-29 = Multiple Sclerosis Impact Scale–29; PHYS = physical subscale. PSYCH – psychological subscale.

V.6 MSSTB STUDY RESULTS

Given the results of interest in the above small natalizumab cohort, MSIS-29 scores were analysed in the larger MSSTB cohort. This cohort did not have treatment outcomes, but had long-term data on survival.

V.6.1 Study participants

In all, 2,914 people with MS were enrolled in the MSSTB over the study period. 2,126 participants completed the MSIS-29 for inclusion in this study (participation rate 73.0%). Of these, 2,119 participants completed both the MSIS-29-PHYS and MSIS-29-PSYCH questionnaire, and 7 participants completed only the MSIS-29-PHYS questionnaire. Data were imputed for 273 participants, as described under Section V.4.2. A prEDSS assessment was available at the same time as the MSIS-29 assessment in 630 participants. A repeat MSIS-29 was completed one year after baseline by 872 participants. Differences in baseline characteristics between those included and those not included in the study, those with and without imputed data, those with and without prEDSS data, and those with and without longitudinal MSIS-29 data are presented in Table 15.

Characteristic	*n*	Male sex	Age	Disease duration	Baseline MSIS-29-PHYS	Baseline MSIS-29-PSYCH
Included in the study?						
Yes	2,126	496 (23.3%)	54.0 (11.9)	18.5 (15.0)	62.0 (20.5)	23.6 (8.7)
No	788	182 (23.1%)	55.8 (13.3)	18.4 (11.3)	N/A	N/A
p-value		0.894	**<0.001**	0.827	N/A	N/A
Imputed data?						
No	1,853	439 (23.7%)	53.5 (11.7)	17.9 (14.5)	61.4 (20.5)	23.6 (8.8)
Yes	273	57 (20.9%)	57.4 (12.9)	23.3 (16.8)	65.8 (20.4)	23.3 (8.6)
p-value		0.305	**<0.001**	**<0.001**	**0.001**	0.484
prEDSS completed?						
Yes	630	152 (24.1%)	50.9 (12.3)	16.9 (17.0)	62.1 (20.4)	23.8 (8.7)
No	1,496	344 (23.0%)	55.2 (11.5)	19.2 (13.9)	61.9 (20.6)	23.5 (8.7)
p-value		0.573	**<0.001**	**<0.001**	0.909	0.457
1-year repeat MSIS-29 completed?						
Yes	872	188 (21.6%)	55.1 (11.1)	18.2 (13.4)	60.6 (19.5)	23.0 (8.3)
No	1,254	308 (24.6%)	53.1 (12.4)	18.8 (15.9)	63.0 (21.1)	24.0 (9.0)
p-value		0.107	**<0.001**	0.407	**0.008**	**0.007**

Table 15: **Differences in baseline characteristics between those included and those not included in the study, those with and without imputed data, those with and without prEDSS data, and those with and without**

longitudinal MSIS-29 data. Data are presented as *n* (percent) or mean (SD). Differences between categorical data (sex) were tested with the chi-square test. Differences between continuous data (age, disease duration, MSIS-29-PHYS, MSIS-29-PSYCH) were tested with the unpaired *t* test. Significant *p*-values are highlighted in bold. MSIS-29, Multiple Sclerosis Impact Scale–29; MSIS-29-PHYS, MSIS-29 physical; MSIS-29-PSYCH, MSIS-29 psychological; n/a, not applicable; prEDSS, patient-reported Expanded Disability Status Scale.

The mean population age at MSIS-29 assessment was 54 (SD 11.9) years, with a disease length of 18.5 (SD 15.0) years, and 1,630 (76.7%) were female. At baseline, mean MSIS-29-PHYS score was 62 (SD 20.5), mean MSIS-29-PSYCH score was 23.6 (SD 8.7), and mean prEDSS score was 5.7 (SD 2.2).

Median follow-up time was 9 years. 865 participants had the maximum 10 years of follow-up. By the data cut-off date, 264 (12.4%) of the total group had died.

V.6.2 A higher MSIS-29-PHYS score is associated with reduced survival time

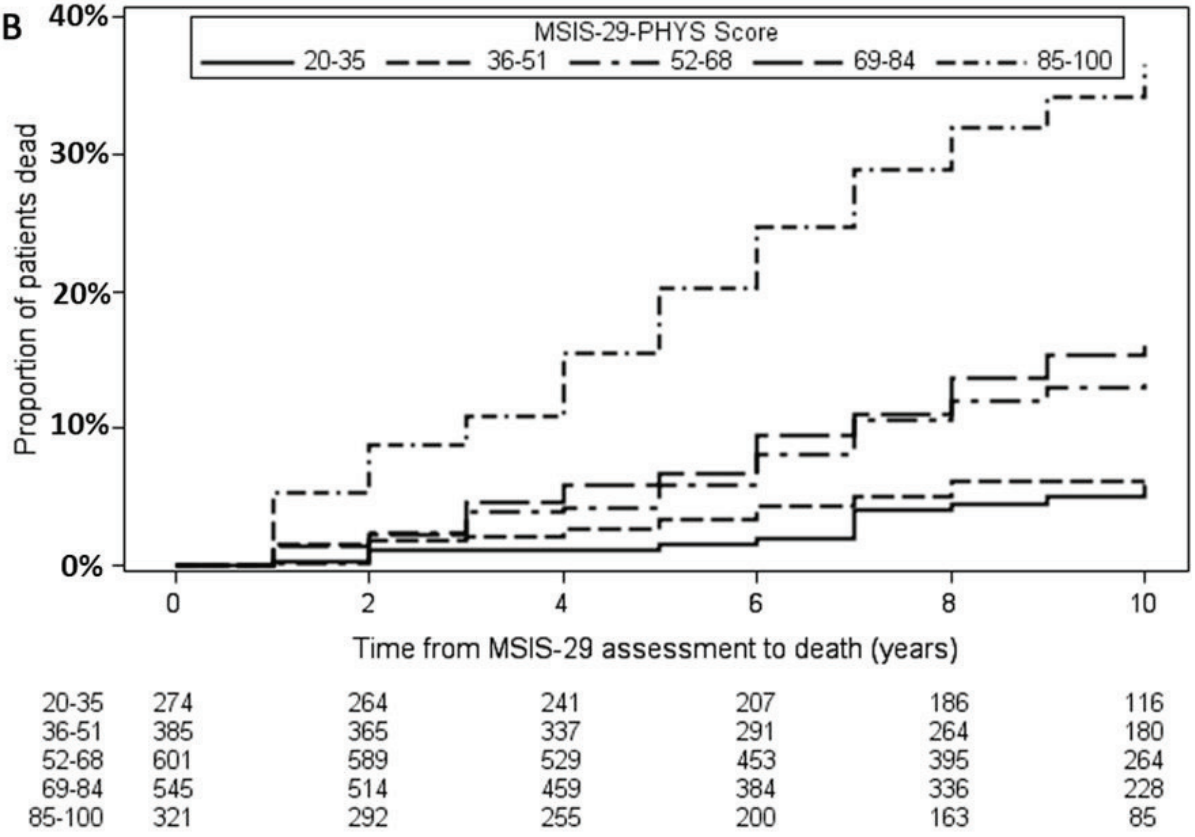
Cox regression models demonstrated that higher MSIS-29-PHYS score was associated with reduced survival time independently of age and sex (Wald chi-square, [degrees of freedom (df) = 4, n = 2,126] = 98.5, $p < 0.001$; Figure 44A). Older age at first MSIS-29 completion (Wald chi-square [df = 1, n = 2,126] = 88.6, $p < 0.001$) and male sex (Wald chi-square [df = 1, n = 2,126] = 24.8, $p < 0.001$) were also associated with reduced survival time in the model. HRs for death were greater, and reduced survival times were observed, with higher MSIS-29-PHYS score, using the ranges 20–35, 36–51, 52–68, 69–84, and 85–100 (Figure 44B). The HR for death was 5.7 in the subgroup with the highest MSIS-29-PHYS scores compared to the subgroup with the lowest MSIS-29-PHYS score (MSIS-29-PHYS score 85-100 group vs

MSIS-29-PHYS score 20-35 group: HR 5.7, 95% CI 3.1–10.5, $p < 0.001$). Those with higher MSIS-29-PHYS scores were more likely to be male (chi-square [df = 4, n = 2,126] = 25.2, $p < 0.001$) and had older age (F[df = 4, n = 2,121] = 16.1, $p < 0.001$) and longer disease duration (F[df = 4, n = 2,121] = 4.1, $p < 0.01$; Table 16).

A

Parameter		Hazard Ratio	95% Hazard Ratio Confidence Limits		p-value	p-value factor
MSIS-29-PHYS score (compared to 20-35)	36-51	0.995	0.486	2.038	0.989	<0.001
	52-68	1.853	0.998	3.438	0.051	
	69-84	2.140	1.155	3.966	0.016	
	85-100	5.728	3.131	10.479	<0.001	
Age	per year	1.051	1.041	1.063		<0.001
Sex	male vs. female	1.906	1.479	2.457		<0.001

B



20-35	274	264	241	207	186	116
36-51	385	365	337	291	264	180
52-68	601	589	529	453	395	264
69-84	545	514	459	384	336	228
85-100	321	292	255	200	163	85

Figure 44: Higher MSIS-29-PHYS scores are associated with reduced survival time. (A) Table: Higher MSIS-29-PHYS score was associated with reduced survival time (greater hazard ratio for death), as were older age at first MSIS-29 completion and male sex. (B) Kaplan–Meier failure curves (*n* = 2,126). Note that Kaplan–Meier curves do not account for the effect of age and sex on survival time. Data at bottom of figure show number of data points at each time point for each MSIS-29-PHYS subgroup. MSIS-29 = Multiple Sclerosis Impact Scale–29; MSIS-29-PHYS = MSIS-29 physical.

Characteristic	*n*	Male sex	Age	Disease duration	Baseline MSIS-29-PHYS	Baseline MSIS-29-PSYCH
MSIS-29-PHYS score						
20–35	274	44 (16.1%)	49.1 (11.1)	15.8 (14.0)	27.5 (4.7)	14.6 (5.0)
36–51	385	70 (18.2%)	53.0 (11.8)	17.4 (15.5)	44.0 (4.5)	19.8 (6.6)
52–68	601	146 (24.3%)	54.9 (12.0)	19.0 (15.1)	60.6 (4.8)	23.6 (7.2)
69–84	545	137 (25.1%)	55.4 (12.1)	19.5 (15.5)	76.0 (4.6)	26.7 (7.9)
85–100	321	99 (30.8%)	55.1 (11.2)	19.7 (13.2)	92.0 (4.9)	30.5 (9.0)
p-value		**<0.001**	**<0.001**	**0.003**	**<0.001**	**<0.001**
MSIS-29-PSYCH score						
9–16	525	115 (21.9%)	55.3 (12.0)	19.8 (15.6)	46.8 (20.0)	12.9 (2.2)
17–23	598	143 (23.9%)	54.6 (12.1)	18.9 (15.0)	59.2 (17.6)	20.1 (2.0)
24–30	512	124 (24.2%)	53.6 (11.7)	17.9 (14.8)	67.2 (16.4)	26.7 (2.0)
31–37	326	83 (25.5%)	52.4 (11.8)	18.0 (14.9)	74.0 (14.7)	33.7 (2.0)
38–45	158	30 (19.0%)	51.4 (11.2)	16.2 (12.4)	82.1 (14.7)	40.8 (2.3)
p-value		0.834	**<0.001**	0.053	**<0.001**	**<0.001**

Table 16: Variation in characteristics between those with different baseline MSIS-29 scores. Data are presented as *n* (percent) or mean (SD). Differences between categorical data (sex) were tested with the chi-square test. Differences between continuous data (age, disease duration, MSIS-29-PHYS, MSIS-29-PSYCH) were tested with one-way analysis of variance (ANOVA). Significant *p*-values are highlighted in bold. MSIS-29, Multiple Sclerosis Impact Scale–29; MSIS-29-PHYS, MSIS-29 physical; MSIS-29-PSYCH, MSIS-29 psychological.

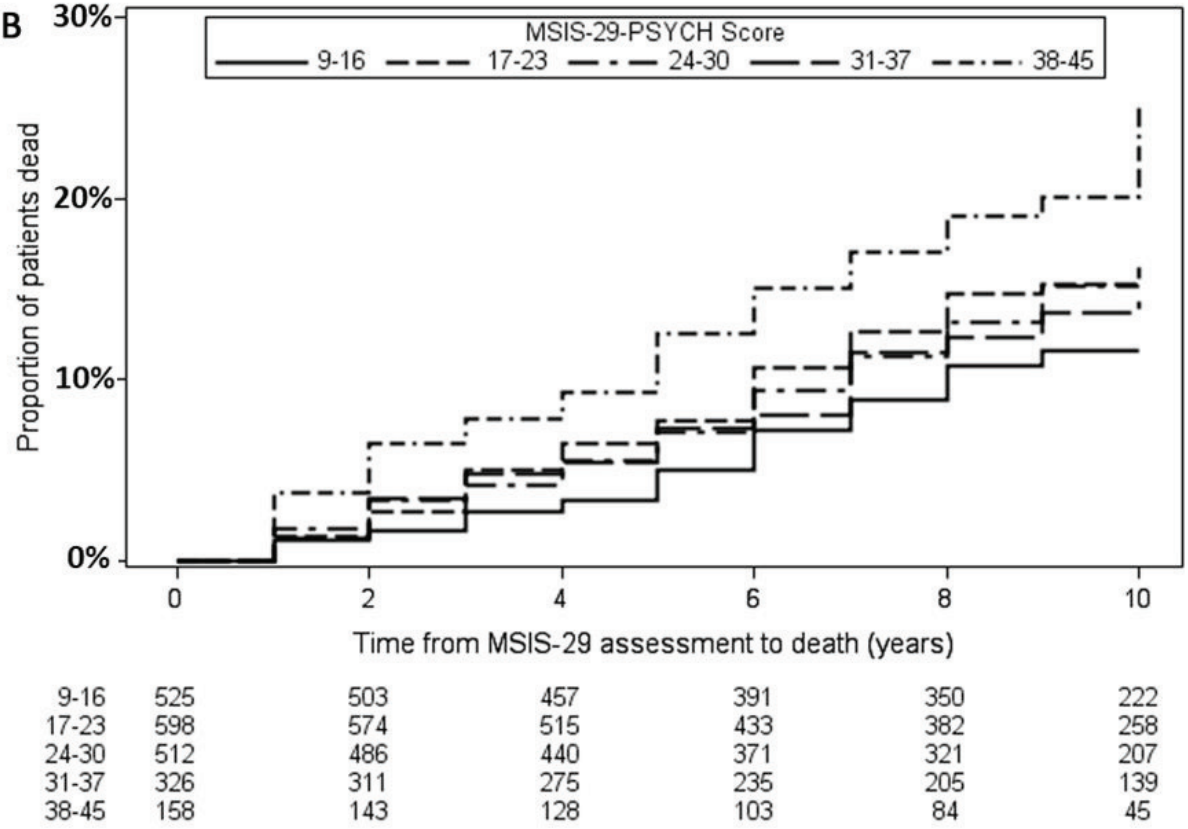
V.6.3 A higher MSIS-29-PSYCH score is associated with reduced survival time

Similarly, Cox regression models demonstrated that higher MSIS-29-PSYCH score was associated with reduced survival time independently of age and sex (Wald chi-square [df = 4, n = 2,119] = 19.2, $p < 0.001$; Figure 45A), although the effect was less pronounced than with MSIS-29-PHYS. HRs for death were greater, and reduced survival times were observed, with higher MSIS-29-PSYCH score, using the ranges 9–16, 17–23, 24–30, 31–37, and 38–45 (Figure 45B). The HR for death was 2.8 in the subgroup with highest MSIS-29-PSYCH scores compared to the subgroup with lowest MSIS-29-PHYS scores (MSIS-29-PSYCH score 38-45 group vs MSIS-29-PSYCH score 9-16 group: HR 2.8, 95% CI 1.8–4.4, $p < 0.001$). In contrast to MSIS-29-PHYS score, higher MSIS-29-PSYCH score was associated with younger age (F[df = 4, n = 2,114] = 5.5, $p < 0.001$; Table 16), and was not associated with male sex or longer disease duration.

A

Parameter		Hazard Ratio	95% Hazard Ratio Confidence Limits		p-value	p-value factor
MSIS-29-PSYCH score (compared to 9-16)	17-23	1.475	1.036	2.101	0.031	<0.001
	24-30	1.441	0.995	2.087	0.053	
	31-37	1.474	0.965	2.250	0.073	
	38-45	2.789	1.762	4.414	<0.001	
Age	per year	1.057	1.046	1.068		<0.001
Sex	male vs. female	2.110	1.638	2.716		<0.001

B



9-16	525	503	457	391	350	222
17-23	598	574	515	433	382	258
24-30	512	486	440	371	321	207
31-37	326	311	275	235	205	139
38-45	158	143	128	103	84	45

Figure 45: Higher MSIS-29-PSYCH scores are associated with reduced survival time. (A) Table: Higher MSIS-29-PSYCH score was associated with reduced survival time (greater hazard ratio for death), as were older age at first MSIS-29 completion and male sex. (B) Kaplan–Meier failure curves (*n* = 2,119). Note that Kaplan–Meier curves do not account for the effect of age and sex on survival time. Data at bottom of figure show number of data points at each time point for each MSIS-29-PSYCH subgroup. MSIS-29 = Multiple Sclerosis Impact Scale–29; MSIS-29-PSYCH = MSIS-29 psychological.

V.6.4 MSIS-29-PHYS score is correlated with prEDSS score but is independently associated with survival time

There was a strong correlation between the MSIS-29-PHYS and MSIS-29-PSYCH scores (r[df = 2,117] = 0.54, $p < 0.001$, Figure 46A). There was a strong correlation between the MSIS-29-PHYS score and the prEDSS score (r[df = 628] = 0.52, $p < 0.001$, Figure 46B) and a weak correlation between the MSIS-29-PSYCH score and the prEDSS score (r[df = 623] = 0.19, $p < 0.001$, Figure 46C). To determine whether the MSIS-29-PHYS and MSIS-29-PSYCH scores were associated with survival time independently of prEDSS score, all measures were included in a Cox regression model, along with age and sex, in the limited number of participants who completed MSIS-29-PHYS, MSIS-29-PSYCH, and prEDSS (n = 625; Table 17). Reduced survival time was associated with older age at baseline (per year: HR 1.07, 95% CI 1.04–1.10, $p < 0.001$), a higher prEDSS score (per 1 SD [2.2]: HR 2.0, 95% CI 1.0–3.7, $p < 0.05$), and a higher MSIS-29-PHYS score (per 1 SD [20.3]: HR 1.8, 95% CI 1.1–2.9, $p < 0.05$).

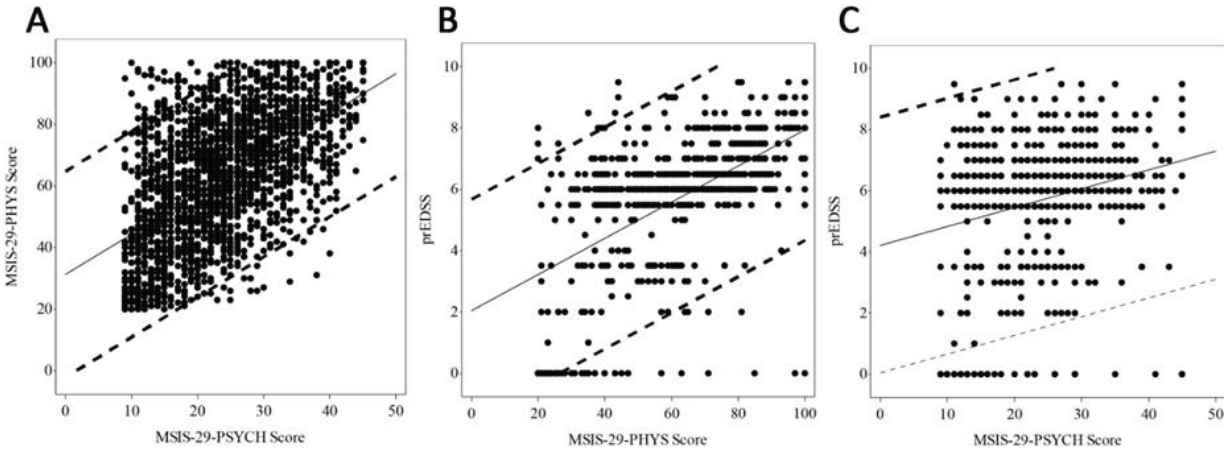


Figure 46: Correlation between different outcome measures. (A) MSIS-29-PHYS and MSIS-29-PSYCH (n = 2119). (B) MSIS-29-PHYS and prEDSS (n = 630). (C) MSIS-29-PSYCH and prEDSS (n = 625). Regression line (solid) with 95% confidence limits for individual predicted values (dashed). MSIS-29-PHYS = MSIS-29 physical; MSIS-29-PSYCH = MSIS-29 psychological; prEDSS = patient-reported Expanded Disability Status Scale.

Parameter	Hazard ratio	95% hazard ratio confidence limits		*p*-value
		Lower	Upper	
prEDSS, per 1 SD (2.2)	1.952	1.025	3.718	0.042
MSIS-29-PHYS, per 1 SD (20.3)	1.762	1.057	2.938	0.030
MSIS-29-PSYCH, per 1 SD (8.7)	0.905	0.631	1.297	0.587
Age, per year	1.070	1.042	1.099	<0.001
Sex, male versus female	1.237	0.622	2.459	0.544

Table 17: Reduced survival time (greater hazard ratio for death) was associated with older age, higher prEDSS score, and higher MSIS-29-PHYS score in the limited cohort with prEDSS score available (*n* = 625). MSIS-29 = Multiple Sclerosis Impact Scale–29; MSIS-29-PHYS = MSIS-29 physical; MSIS-29-PSYCH = MSIS-29 psychological; prEDSS = patient-reported Expanded Disability Status Scale.

V.6.5 Increase in the MSIS-29-PHYS score over one year is associated with reduced survival time

The MSIS-29 questionnaire was repeated after one year in a subgroup (n = 872) of those who had originally completed the MSIS-29 in 2004. Comparing participants with stable/improving MSIS-29-PHYS score, against participants with increasing MSIS-29-PHYS score (change in MSIS-29-PHYS ≤ 0 versus > 0), there was no statistically significant difference in mortality (Cox regression adjusted for age and sex: n = 872, HR = 1.2, 95% CI 0.9–1.2, p = 0.28).

Figure 47 shows the survival curves for the following four subgroups:

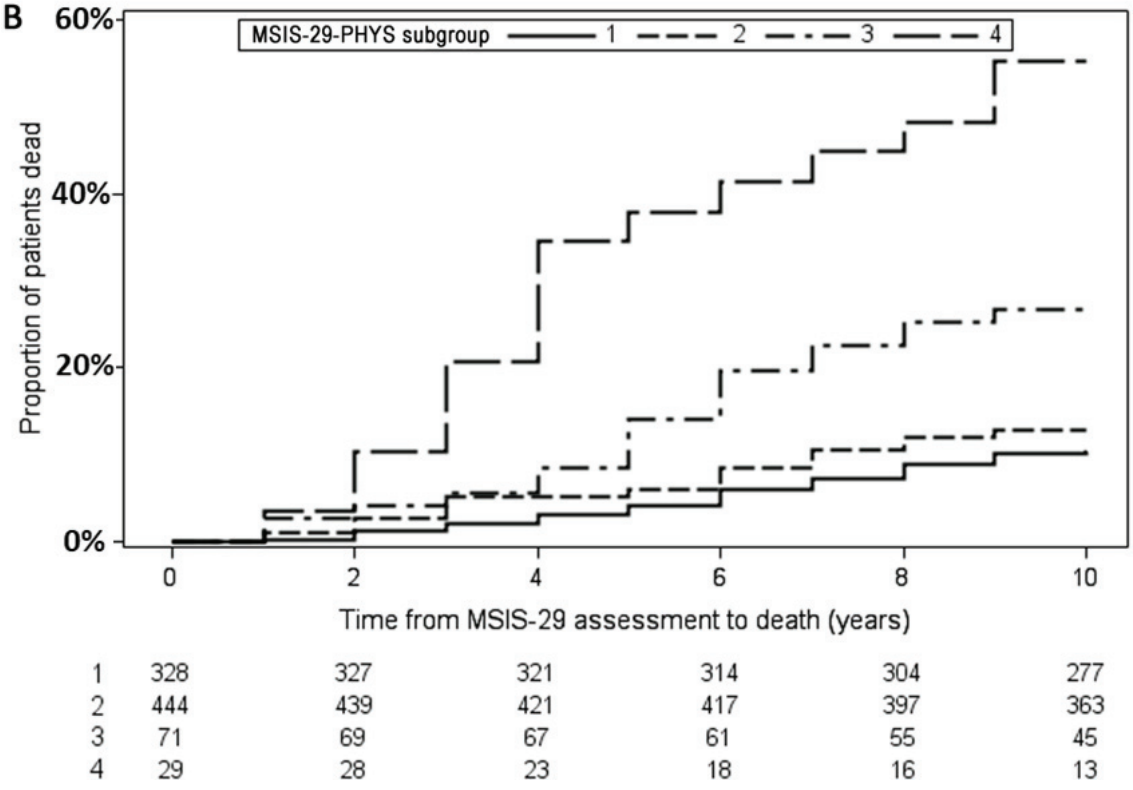
- Subgroup 1: initial MSIS-29-PHYS score 20–84, no increase after one year
- Subgroup 2: initial MSIS-29-PHYS score 20–84, increase after one year (≥1 point)
- Subgroup 3: initial MSIS-29-PHYS score 85–100, no increase after one year
- Subgroup 4: initial MSIS-29-PHYS score 85–100, increase after one year (≥1 point).

In the subgroup of participants with the highest initial MSIS-29-PHYS scores (subgroups 3 and 4), a longitudinal increase in MSIS-29-PHYS score was associated with reduced survival time (Subgroup 4 vs Subgroup 3: HR = 2.3, 95% CI 1.2–4.4, p = 0.016; Figure 47).

A

Parameter		Hazard Ratio	95% Hazard Ratio Confidence Limits		p-value	p-value factor
MSIS-29-PHYS subgroup (compared to subgroup 1)	subgroup 2	1.289	0.843	1.972	0.241	<0.001
	subgroup 3	2.577	1.469	4.519	0.001	
	subgroup 4	5.839	3.213	10.611	<0.001	
Age	per year	1.055	1.038	1.071		<0.001
Sex	male vs. female	2.238	1.557	3.218		<0.001

B



1	328	327	321	314	304	277
2	444	439	421	417	397	363
3	71	69	67	61	55	45
4	29	28	23	18	16	13

Figure 47: Longitudinally increase in MSIS-29-PHYS score is associated with reduced survival time. Four subgroups are presented in this figure: Subgroup 1 - initial MSIS-29-PHYS score 20–84, no increase after one year (solid line); Subgroup 2 - initial MSIS-29-PHYS score 20–84, increase after one year (short-dashed line); Subgroup 3 - initial MSIS-29-PHYS score 85–100, no increase after one year (dot-dashed line); Subgroup 4 - initial MSIS-29-PHYS score 85–100, increase after one year (long-dashed line). (A) Table: Subgroups 1 and 2 had no statistically significant difference in survival time. Subgroup 3 had reduced survival time compared with subgroup 1 and 2. Subgroup 4 had reduced survival time compared with subgroup 1, 2, and 3. $p < 0.001$ for differences between the 4 subgroups. (B) Kaplan–Meier failure curves ($n = 872$). Data at bottom of figure show number of data points at each time point for each subgroup. Note that Kaplan–Meier curves do not account for the effect of age and sex on survival time. HR = hazard ratio; MSIS-29 = Multiple Sclerosis Impact Scale–29; MSIS-29-PHYS = MSIS-29 physical.

V.7 DISCUSSION

Results from the 'natalizumab cohort' suggested that the change in MSIS-29-PHYS and MSIS-29-PSYCH score at 10 weeks was associated with the clinician's assessment of 'response to treatment' at 58 weeks. This supports the concept that PROs can capture meaningful data relating to health and wellbeing, and correlate with conventional clinician-reported outcome measures. These data also support the evidence that natalizumab is effective in the early months after initiation of therapy.[34] Although results seem promising in that MSIS-29 scores appeared able to predict response to treatment, results should be interpreted with caution given the small cohort size of the 'natalizumab cohort'. The ability of the MSIS-29 to predict hard clinical outcome was further investigated using the MSSTB cohort.

The MSSTB study is the largest known cohort with reported MSIS-29 results to date, other than one web-based cohort,[35, 36] and the MSSTB has by far the longest follow-up after MSIS-29 completion (up to 10 years, median 9 years). The MSSTB cohort had 264 deaths within the study period. This number of deaths allowed the prognostic value of MSIS-29 scores for survival time to be studied. The study found that higher MSIS-29-PHYS and MSIS-29-PSYCH scores were both associated with reduced survival time. MSIS-29-PHYS score has stronger prognostic value, and associates with survival time independently of age, sex, and prEDSS score. Higher MSIS-29-PSYCH scores were associated with reduced survival time, even though higher MSIS-29-PSYCH scores were also associated with younger age. In the subgroup with initial MSIS-29-PHYS score 85–100, a 1-year longitudinal increase in the MSIS-29-PHYS score is associated with an even poorer prognosis. To our knowledge, this is

the first study to associate PROs with survival outcomes in any neurological disease. The study was published in *PLOS Medicine* with the thesis author as first author.[1]

The previous thesis chapters have considered how relapses or new MRI lesions (Chapter 2), TSPO-PET (Chapter 3), or the Brain-Predicted Age model (Chapter 4) could be useful outcomes in MS for assessing disease severity and predicting response to disease-modifying therapy. The results presented in this chapter suggest that PROs such as the MSIS-29 should also be considered as outcome measures with the potential to contribute to models of disease severity. This could complement conventional physician-assessed measures such as EDSS, which is the primary outcome measure in most clinical trials but is limited by poor inter-rater and intra-rater reliability and a limited sensitivity to change over the time frame of 2–3 years, especially in progressive MS.[19-26] The MSIS-29 can be responsive to clinically relevant change over short time frames.[18, 37] The MSIS-29 can also be sent to large cohorts of people with MS, and completed by post or online.[36] PROs such as the MSIS-29 could therefore enable large cohort studies, which would otherwise be financially unfeasible, such as comparative clinical effectiveness research.

The data presented in this study could also be used to inform recruitment to clinical research. Interventional and observational studies in progressive MS may choose 'death' as the primary outcome measure, and may therefore aim to recruit a cohort of participants with increased likelihood of dying within the study timeframe. To achieve this, the MSIS-29 could be remotely completed by patients on a MS registry. If patients with MSIS-29-PHYS score ≥85 were recruited, this study suggests that approximately 20% would die within 5 years, and 37% within 10 years. These patients have a hazard ratio for mortality of 5.7, compared with those with MSIS-29-PHYS scores ≤35. Moreover, if patients with MSIS-29-PHYS score ≥85 and

whose MSIS-29-PHYS score deteriorate after one year were recruited, approximately 38% would die within 5 years, and 55% within 10 years. Such 'clinical registry trials' have been adopted successfully in disciplines such as cardiology, and could be necessary in future MS research especially given the increasingly crowded pharmaceutical market and increasing difficulty satisfying entry criteria for clinical trials.[38, 39]

Outside of the research setting, PROs such as the MSIS-29 may be able to benefit individual patients if they are utilised in routine clinical practice. Oncology has again led the way, where PROs are routinely used to enhance patient care.[5] PROs can help screen for changes in physical or psychological symptoms, and identify unmet health, care and support needs. They can be used as a decision aid when devising or evaluating treatment plans.[40] Patients and doctors can have differing views on which outcomes matter most, and the effective use of PROs can help refocus care goals to the views of the individual patient.[41, 42] This might also empower patients towards improved self-management of their condition.[43] When assessed in a randomised controlled trial, PROs enhanced doctor–patient communication and improved patient health-related quality of life and emotional well-being.[4] Further work is required to incorporate PROs such as the MSIS-29 into routine MS clinical care.

Limitations to the MSSTB study should be considered. Only a subset completed the prEDSS questionnaire (n = 630), and only a subset completed a longitudinal MSIS-29 (n = 872), mostly because of changes to the study protocol over time. Also, this study used a prEDSS rather than the traditional physician-reported EDSS, although these have previously been shown to correlate well.[30] Data on disease subtype, relapses, and disease-modifying therapy were not available for this study, and could influence the relationship between MSIS-29 score and survival time. Like most clinical outcome measures, PROs are susceptible to random

measurement error, and hence regression dilution bias likely causes a decrease in the prognostic value of the MSIS-29 for mortality.[44] However, previous studies have reported the test–retest reliability of MSIS-29-PHYS and MSIS-29-PSYCH to be high (intraclass correlation coefficients of 0.94 and 0.87, respectively), and so this effect is likely minimal.[17]

One should also consider the external validity of this cohort's results to the general MS population. The MSSTB recruitment strategy is based entirely in the community, relying upon community-based presentations and a quarterly magazine, *MS Matters,* distributed to approximately 30,000 members of the Multiple Sclerosis Society of Great Britain and Northern Ireland.[45] Factors that are known to associate with reduced survival, such as male sex, older age at baseline, and higher prEDSS score, were also found to associate with reduced survival time in this cohort.[46-48] The MSSTB population has previously been shown to be representative of the UK MS population in terms of disease characteristics and clinical milestones, when considered over the course of their disease.[29] However, at the time of enrolment into the MSSTB, participants are often late in their disease course, as evidenced by this study's mean disease duration of 18.5 years and mean prEDSS score of 5.7 at baseline MSIS-29 questionnaire. Therefore, this study underrepresents those with earlier disease and less disability, and it is uncertain how MSIS-29 scores and their prognostic value for mortality will vary in this group. One might hypothesize that those with earlier disease would have lower MSIS-29 scores and increased survival times, on average.[36]

Further research questions emerge from this study. Since this study has demonstrated that MSIS-29 score is associated with death, similar methods could be used to investigate whether MSIS-29 score is associated with disability outcomes, such as time until wheelchair use.

Multiple variables, including other PROs collected at multiple time points, could be incorporated into more complex models to better predict outcomes in large cohorts.

In addition, the effect of disease-modifying therapy on the MSIS-29 and long-term clinical endpoints needs further attention to assess whether MSIS-29 scores could be used as a surrogate for response to treatment. The results of the MSSTB study support the concept that MSIS-29 scores, and longitudinal change in MSIS-29 score, have prognostic significance for hard clinical endpoints. However, it does not necessarily follow that a change in MSIS-29 score after treatment will help predict long-term outcomes after treatment, and the validity of surrogate outcomes should be tested against the Prentice criteria.[49] In the 'natalizumab cohort' it was reported that change in MSIS-29 scores was associated with clinical response to therapy. Further studies are required with larger cohorts of people with MS on a range of disease-modifying therapies, with long-term clinical follow-up.

PROs in MS could previously be criticised for their unknown association with hard clinical endpoints like survival. By reporting the association between MSIS-29 score and long-term survival time, this study opens the possibility to validate other PROs against hard clinical outcomes in MS and other neurological diseases. In oncology, PROs are now established as influential and clinically relevant measures, and it is accepted that the classic clinical endpoints do not fully capture the benefits, risks, and costs of treatment.[8-10] MS and neurology research will continue to rely upon clinical trials, as well as 'big data' gathered from clinical registries. The careful incorporation of PROs can enrich such datasets and allow the investigation of research questions beyond what traditional physician-based assessments can offer.

V.8 ACKNOWLEDGEMENTS

Clinical data were supplied by the MSSTB, funded by the Multiple Sclerosis Society of Great Britain and Northern Ireland, registered charity 207495. Thank you to Djordje Gveric for his assistance in collating these data. Thank you to the donors registered with the MSSTB for their consent and participation.

V.9 CONFLICTS OF INTEREST

The thesis author has no conflicts of interest relevant to this chapter.

Dr Nicholas has received a grant from the UK MS/PD society for the MS Society Tissue Bank. The funders had no role in study design, data collection and analysis, decision to publish, or preparation of the manuscript. Dr Nicholas received funding from GE Healthcare. Dr Nicholas has received outside the submitted work: grants, personal fees and non-financial support from Novartis; grants, personal fees and non-financial support from Biogen Idec; personal fees from Genzyme; and personal fees from Roche.

Other authors declare no conflicts of interest related to this chapter.

V.10 REFERENCES

1. Raffel J, Wallace A, Gveric D, Reynolds R, Friede T, Nicholas R. Patient-reported outcomes and survival in multiple sclerosis: A 10-year retrospective cohort study using the Multiple Sclerosis Impact Scale-29. PLoS Med. 2017;14(7):e1002346. doi: 10.1371/journal.pmed.1002346. PubMed PMID: 28692670; PubMed Central PMCID: PMCPMC5503162.

2. U.S. Department of Health and Human Services, Food and Drug Administration. Patient-Reported Outcome Measures: Use in Medical Product Development to Support Labeling Claims. Available from www.fda.gov/downloads/Drugs/.../Guidances/UCM193282.pdf. 2009.

3. Hilarius DL, Kloeg PH, Gundy CM, Aaronson NK. Use of health-related quality-of-life assessments in daily clinical oncology nursing practice - A community hospital-based intervention study. Cancer. 2008;113(3):628-37. doi: 10.1002/cncr.23623. PubMed PMID: WOS:000257825700023.

4. Velikova G, Booth L, Smith AB, Brown PM, Lynch P, Brown JM, Selby PJ. Measuring quality of life in routine oncology practice improves communication and patient well-being: a randomized controlled trial. J Clin Oncol. 2004;22(4):714-24. doi: 10.1200/JCO.2004.06.078. PubMed PMID: 14966096.

5. Howell D, Molloy S, Wilkinson K, Green E, Orchard K, Wang K, Liberty J. Patient-reported outcomes in routine cancer clinical practice: a scoping review of use, impact on health outcomes, and implementation factors. Annals of Oncology. 2015;26(9):1846-58. doi: 10.1093/annonc/mdv181. PubMed PMID: WOS:000361392700007.

6. Snyder CF, Aaronson NK, Choucair AK, Elliott TE, Greenhalgh J, Halyard MY, Hess R, Miller DM, Reeve BB, Santana M. Implementing patient-reported outcomes assessment in clinical practice: a review of the options and considerations. Quality of Life Research. 2012;21(8):1305-14. doi: 10.1007/s11136-011-0054-x. PubMed PMID: WOS:000314912500001.

7. McLeod LD, Coon CD, Martin SA, Fehnel SE, Hays RD. Interpreting patient-reported outcome results: US FDA guidance and emerging methods. Expert Rev Pharmacoecon Outcomes Res. 2011;11(2):163-9. doi: 10.1586/erp.11.12. PubMed PMID: 21476818; PubMed Central PMCID: PMCPMC3125671.

8. Secord AA, Coleman RL, Havrilesky LJ, Abernethy AP, Samsa GP, Cella D. Patient-reported outcomes as end points and outcome indicators in solid tumours. Nat Rev Clin Oncol. 2015;12(6):358-70. doi: 10.1038/nrclinonc.2015.29. PubMed PMID: WOS:000355253200008.

9. Lipscomb J, Gotay CC, Snyder CF. Patient-reported outcomes in cancer: a review of recent research and policy initiatives. CA Cancer J Clin. 2007;57(5):278-300. doi: 10.3322/CA.57.5.278. PubMed PMID: 17855485.

10. Gotay CC, Kawamoto CT, Bottomley A, Efficace F. The prognostic significance of patient-reported outcomes in cancer clinical trials. J Clin Oncol. 2008;26(8):1355-63. doi: 10.1200/JCO.2007.13.3439. PubMed PMID: 18227528.

11. Kosiborod M, Soto GE, Jones PG, Krumholz HM, Weintraub WS, Deedwania P, Spertus JA. Identifying heart failure patients at high risk for near-term cardiovascular events with serial health status assessments. Circulation. 2007;115(15):1975-81. doi: 10.1161/Circulationaha.106.670901. PubMed PMID: WOS:000245741500003.

12. Tate CW, Robertson AD, Zolty R, Shakar SF, Lindenfeld J, Wolfel EE, Bristow MR, Lowes BD. Quality of life and prognosis in heart failure: Results of the Beta-Blocker Evaluation of Survival Trial (BEST). J Card Fail. 2007;13(9):732-7. doi: 10.1016/j.cardfail.2007.07.001. PubMed PMID: WOS:000251593200007.

13. Heidenreich PA, Spertus JA, Jones PG, Weintraub WS, Rumsfeld JS, Rathore SS, Peterson ED, Masoudi FA, Krumholz HM, Havranek EP, Conard MW, Williams RE, Cons COR. Health status identifies heart failure outpatients at risk for hospitalization or death. J Am Coll Cardiol. 2006;47(4):752-6. doi: 10.1016/j.jacc.2005.11.021. PubMed PMID: WOS:000235422900011.

14. Khurana V, Sharma H, Afroz N, Callan A, Medin J. Patient-reported outcomes in multiple sclerosis: a systematic comparison of available measures. European journal of neurology : the official journal of the European Federation of Neurological Societies. 2017;24(9):1099-107. Epub 2017/07/12. doi: 10.1111/ene.13339. PubMed PMID: 28695634.

15. D'Amico E, Haase R, Ziemssen T. Review: Patient-reported outcomes in multiple sclerosis care. Mult Scler Relat Disord. 2019;33:61-6. Epub 2019/06/04. doi: 10.1016/j.msard.2019.05.019. PubMed PMID: 31154262.

16. Fayers P, Machin D. Quality of life: the assessment, analysis and interpretation of patient-reported outcomes.: John Wiley & Sons.; 2013.

17. Hobart J, Lamping D, Fitzpatrick R, Riazi A, Thompson A. The Multiple Sclerosis Impact Scale (MSIS-29) - A new patient-based outcome measure. Brain : a journal of neurology. 2001;124:962-73. doi: DOI 10.1093/brain/124.5.962. PubMed PMID: WOS:000168927400010.

18. Bosma LVAE, Sonder JM, Kragt JJ, Polman CH, Uitdehaag BMJ. Detecting clinically-relevant changes in progressive multiple sclerosis. Mult Scler J. 2015;21(2):171-9. doi: 10.1177/1352458514540969. PubMed PMID: WOS:000349764700010.

19. Kurtzke JF. Rating neurologic impairment in multiple sclerosis: an expanded disability status scale (EDSS). Neurology. 1983;33(11):1444-52. PubMed PMID: 6685237.

20. Noseworthy JH, Vandervoort MK, Wong CJ, Ebers GC. Interrater Variability with the Expanded Disability Status Scale (Edss) and Functional-Systems (Fs) in a Multiple-Sclerosis Clinical-Trial. Neurology. 1990;40(6):971-5. PubMed PMID: WOS:A1990DG80000021.

21. Hobart J, Freeman J, Thompson A. Kurtzke scales revisited: the application of psychometric methods to clinical intuition. Brain : a journal of neurology. 2000;123:1027-40. doi: DOI 10.1093/brain/123.5.1027. PubMed PMID: WOS:000087580900016.

22. Cohen JA, Reingold SC, Polman CH, Wolinsky JS, Trial IACC. Disability outcome measures in multiple sclerosis clinical trials: current status and future prospects. Lancet Neurol. 2012;11(5):467-76. PubMed PMID: WOS:000303138300017.

23. European Medicines Agency. Guideline on clinical investigation of medicinal products for the treatment of Multiple Sclerosis. Available from www.ema.europa.eu/docs/en_GB/document_library/Scientific_guideline/2015/03/WC500185161.pdf. 2015.

24. Verdiertaillefer MH, Zuber M, Lyoncaen O, Clanet M, Gout O, Louis C, Alperovitch A. Observer Disagreement in Rating Neurologic Impairment in Multiple-Sclerosis - Facts and Consequences. Eur Neurol. 1991;31(2):117-9. doi: Doi 10.1159/000116658. PubMed PMID: WOS:A1991FE07300011.

25. van Winsen LML, Kragt JJ, Hoogervorst ELJ, Polman CH, Uitdehaag BMJ. Outcome measurement in multiple sclerosis: detection of clinically relevant improvement. Mult Scler J. 2010;16(5):604-10. doi: 10.1177/1352458509359922. PubMed PMID: WOS:000277837200014.

26. Kragt JJ, Thompson AJ, Montalban X, Tintore M, Rio J, Polman CH, Uitdehaag BMJ. Responsiveness and predictive value of EDSS and MSFC in primary progressive MS. Neurology. 2008;70(13):1084-91. PubMed PMID: WOS:000254297700012.

27. Hoogervorst ELJ, Zwemmer JNP, Jelles B, Polman CH, Uitdehaag BMJ. Multiple Sclerosis Impact Scale (MSIS-29): relation to established measures of impairment and disability. Multiple sclerosis. 2004;10(5):569-74. doi: 10.1191/1352458504ms1078oa. PubMed PMID: WOS:000223639400016.

28. McGuigan C, Hutchinson M. The multiple sclerosis impact scale (MSIS-29) is a reliable and sensitive measure. J Neurol Neurosur Ps. 2004;75(2):266-9. PubMed PMID: WOS:000188393600020.

29. Reynolds R, Roncaroli F, Nicholas R, Radotra B, Gveric D, Howell O. The neuropathological basis of clinical progression in multiple sclerosis. Acta Neuropathol. 2011;122(2):155-70. doi: 10.1007/s00401-011-0840-0. PubMed PMID: WOS:000292780500004.

30. Collins CD, Ivry B, Bowen JD, Cheng EM, Dobson R, Goodin DS, Lechner-Scott J, Kappos L, Galea I. A comparative analysis of Patient-Reported Expanded Disability Status Scale tools. Multiple sclerosis. 2016;22(10):1349-58. doi: 10.1177/1352458515616205. PubMed PMID: 26564998; PubMed Central PMCID: PMCPMC5015760.

31. Lechner-Scott J, Kappos L, Hofman M, Polman CH, Ronner H, Montalban X, Tintore M, Frontoni M, Buttinelli C, Amato MP, Bartolozzi ML, Versavel M, Dahlke F, Kapp JF, Gibberd R. Can the expanded disability status scale be assessed by telephone? Multiple sclerosis. 2003;9(2):154-9. doi: 10.1191/1352458503ms884oa. PubMed PMID: WOS:000182187100007.

32. Ramp M, Khan F, Misajon RA, Pallant JF. Rasch analysis of the Multiple Sclerosis Impact Scale (MSIS-29). Health Qual Life Out. 2009;7. doi: Artn 58 10.1186/1477-7525-7-58. PubMed PMID: WOS:000268169400001.

33. Sterne JAC, White IR, Carlin JB, Spratt M, Royston P, Kenward MG, Wood AM, Carpenter JR. Multiple imputation for missing data in epidemiological and clinical research: potential and pitfalls. Brit Med J. 2009;339. doi: ARTN b2393 10.1136/bmj.b2393. PubMed PMID: WOS:000267678300003.

34. Kappos L, O'Connor PW, Polman CH, Vermersch P, Wiendl H, Pace A, Zhang A, Hotermans C. Clinical effects of natalizumab on multiple sclerosis appear early in treatment course. J Neurol. 2013;260(5):1388-95. Epub 2013/01/08. doi: 10.1007/s00415-012-6809-7. PubMed PMID: 23292204; PubMed Central PMCID: PMCPMC3642366.

35. Jones KH, Jones PA, Middleton RM, Ford DV, Lockhart-Jones H, Tuite-Dalton K, Peng J, Noble G, John A, Lyons RA. Physical disability, anxiety and depression in people with MS: an internet-based survey via the UK MS Register. Mult Scler J. 2014;20:419-20. PubMed PMID: WOS:000354441300963.

36. Jones KH, Ford DV, Jones PA, John A, Middleton RM, Lockhart-Jones H, Peng J, Osborne LA, Noble JG. The Physical and Psychological Impact of Multiple Sclerosis Using the MSIS-29 via the Web Portal of the UK MS Register. Plos One. 2013;8(1). doi: ARTN e55422 10.1371/journal.pone.0055422. PubMed PMID: WOS:000314610600101.

37. Hobart JC, Riazi A, Lamping DL, Fitzpatrick R, Thompson AJ. How responsive is the Multiple Sclerosis Impact Scale (MSIS-29)? A comparison with some other self report scales. J Neurol Neurosur Ps. 2005;76(11):1539-43. doi: 10.1136/jnnp.2005.064584. PubMed PMID: WOS:000232581400018.

38. Frobert O, Lagerqvist B, Gudnason T, Thuesen L, Svensson R, Olivecrona GK, James SK. Thrombus Aspiration in ST-Elevation myocardial infarction in Scandinavia (TASTE trial). A multicenter, prospective, randomized, controlled clinical registry trial based on the Swedish angiography and angioplasty registry (SCAAR)

platform. Study design and rationale. Am Heart J. 2010;160(6):1042-8. doi: 10.1016/j.ahj.2010.08.040. PubMed PMID: WOS:000285187600013.

39. Lauer MS, D'Agostino RB. The Randomized Registry Trial - The Next Disruptive Technology in Clinical Research? New Engl J Med. 2013;369(17):1579-81. doi: 10.1056/NEJMp1310102. PubMed PMID: WOS:000326031100004.

40. Greenhalgh J. The applications of PROs in clinical practice: what are they, do they work, and why? Quality of Life Research. 2009;18(1):115-23. doi: 10.1007/s11136-008-9430-6. PubMed PMID: WOS:000263025600013.

41. Marshall S, Haywood K, Fitzpatrick R. Impact of patient-reported outcome measures on routine practice: a structured review. J Eval Clin Pract. 2006;12(5):559-68. doi: DOI 10.1111/j.1365-2753.2006.00650.x. PubMed PMID: WOS:000240605700010.

42. Rothwell PM, McDowell Z, Wong CK, Dorman PJ. Doctors and patients don't agree: Cross sectional study of patient's and doctors' perceptions and assessments of disability in multiple sclerosis. Brit Med J. 1997;314(7094):1580-3. PubMed PMID: WOS:A1997XC50000019.

43. Stimson GV. Obeying doctor's orders: a view from the other side. Soc Sci Med. 1974;8(2):97-104. PubMed PMID: 4821252.

44. Hutcheon JA, Chiolero A, Hanley JA. Random measurement error and regression dilution bias. Bmj. 2010;340:c2289. doi: 10.1136/bmj.c2289. PubMed PMID: 20573762.

45. MS Society Website. MS Matters Magazine. Accessed April 2017. Available from https://www.mssociety.org.uk/get-involved/membership/ms-matters-magazine.

46. Weinshenker BG. Natural-History of Multiple-Sclerosis. Annals of neurology. 1994;36:S6-S11. doi: DOI 10.1002/ana.410360704. PubMed PMID: WOS:A1994NW70200003.

47. Kingwell E, van der Kop M, Zhao Y, Shirani A, Zhu F, Oger J, Tremlett H. Relative mortality and survival in multiple sclerosis: findings from British Columbia, Canada. J Neurol Neurosur Ps. 2012;83(1):61-6. doi: 10.1136/jnnp-2011-300616. PubMed PMID: WOS:000298399600013.

48. Levic ZM, Dujmovic I, Pekmezovic T, Jarebinski M, Marinkovic J, Stojsavljevic N, Drulovic J. Prognostic factors for survival in multiple sclerosis. Multiple sclerosis. 1999;5(3):171-8. doi: Doi 10.1191/135245899678846005. PubMed PMID: WOS:000080688000006.

49. Prentice RL. Surrogate endpoints in clinical trials: definition and operational criteria. Stat Med. 1989;8(4):431-40. Epub 1989/04/01. doi: 10.1002/sim.4780080407. PubMed PMID: 2727467.

V.11 APPENDIX - MULTIPLE SCLEROSIS IMPACT SCALE (MSIS-29)

- The following questions ask for your views about the impact of MS on your day-to-day life **during the past two weeks**
- For each statement, please **circle** the **one** number that **best** describes your situation
- Please answer **all** questions

In the <u>past two weeks</u>, how much has your MS limited your ability to...		Not at all	A little	Moderately	Quite a bit	Extremely
1.	**Do physically demanding tasks?**	1	2	3	4	5
2.	**Grip things tightly (e.g. turning on taps)?**	1	2	3	4	5
3.	**Carry things?**	1	2	3	4	5

In the <u>past two weeks</u>, how much have you been bothered by...		Not at all	A little	Moderately	Quite a bit	Extremely
4.	**Problems with your balance?**	1	2	3	4	5
5.	**Difficulties moving about indoors?**	1	2	3	4	5
6.	**Being clumsy?**	1	2	3	4	5

7.	**Stiffness?**	1	2	3	4	5
8.	**Heavy arms and/or legs?**	1	2	3	4	5
9.	**Tremor of your arms or legs?**	1	2	3	4	5
10.	**Spasms in your limbs?**	1	2	3	4	5
11.	**Your body not doing what you want it to do?**	1	2	3	4	5
12.	**Having to depend on others to do things for you?**	1	2	3	4	5

Please check that you have answered all the questions before going on to the next page

®2000 Neurological Outcome Measures Unit, 4th Floor Queen Mary Wing, NHNN, Queen Square, London WC1N 3BG, UK

In the past two weeks, how much have you been bothered by...		Not at all	A little	Moderately	Quite a bit	Extremely
13.	**Limitations in your social and leisure activities at home?**	1	2	3	4	5
14.	**Being stuck at home more than you would like to be?**	1	2	3	4	5
15.	**Difficulties using your hands in everyday tasks?**	1	2	3	4	5
16.	**Having to cut down the amount of time you spent on work or other daily activities?**	1	2	3	4	5
17.	**Problems using transport (e.g. car, bus, train, taxi, etc.)?**	1	2	3	4	5
18.	**Taking longer to do things?**	1	2	3	4	5
19.	**Difficulty doing things spontaneously (e.g. going out on the spur of the moment)?**	1	2	3	4	5

20.	**Needing to go to the toilet urgently?**	1	2	3	4	5
21.	**Feeling unwell?**	1	2	3	4	5
22.	**Problems sleeping?**	1	2	3	4	5
23.	**Feeling mentally fatigued?**	1	2	3	4	5
24.	**Worries related to your MS?**	1	2	3	4	5
25.	**Feeling anxious or tense?**	1	2	3	4	5
26.	**Feeling irritable, impatient, or short tempered?**	1	2	3	4	5
27.	**Problems concentrating?**	1	2	3	4	5
28	**Lack of confidence?**	1	2	3	4	5
29.	**Feeling depressed?**	1	2	3	4	5

Please check that you have circled ONE number for EACH question

□ 2000 Neurological Outcome Measures Unit, 4th Floor Queen Mary Wing, NHNN, Queen Square, London WC1N 3BG, UK

Chapter 6

Conclusions

VI.1 ABBREVIATIONS

DMT	Disease-modifying therapy
MS	Multiple sclerosis
MSIS-29	Multiple Sclerosis Impact Scale-29
PET	Positron emission tomography
TSPO	18kDa translocator protein

VI.2 CONCLUSIONS

The past 30 years have brought tremendous progress in our understanding of multiple sclerosis (MS) and our approach to treatment.[1,2] We now have a range of licensed disease-modifying therapies (DMTs) including β-interferons, glatiramer acetate, dimethyl fumarate, teriflunomide, fingolimod, cladribine, alemtuzumab, natalizumab and ocrelizumab, with more potential therapies in the therapeutic pipeline.[3] For subjects with relapsing MS, these DMTs are effective in reducing relapse rate and new MRI lesions.[4, 5] However, DMTs are only somewhat effective at slowing the gradual progression of disability in people with relapsing MS, and appear ineffective in those with non-relapsing progressive MS.[3-8] What's more, there is marked heterogeneity between individuals in response to treatment, and the factors that determine this heterogeneity remain largely undefined.[2, 9-11]

To improve future care in MS, we need:

- Novel DMTs which are more effective at slowing neurodegeneration and the gradual progression of disability.
- To make best use of the available DMTs, by working towards the personalised medicine ideals of '*the right treatment for the right patient at the right time*'.[12]

Improved outcome measures are required to help address the above needs.

A biomarker which can quantify the *rate* of neurodegeneration, rather than merely the *extent* of neurodegeneration, may be able to assess treatment efficacy at an early time point, as depicted in Figure 48. Such a biomarker could be used in the therapeutic pipeline as an early surrogate for a medication's efficacy, and in clinical practice for the early empirical assessment of therapy response in individuals.

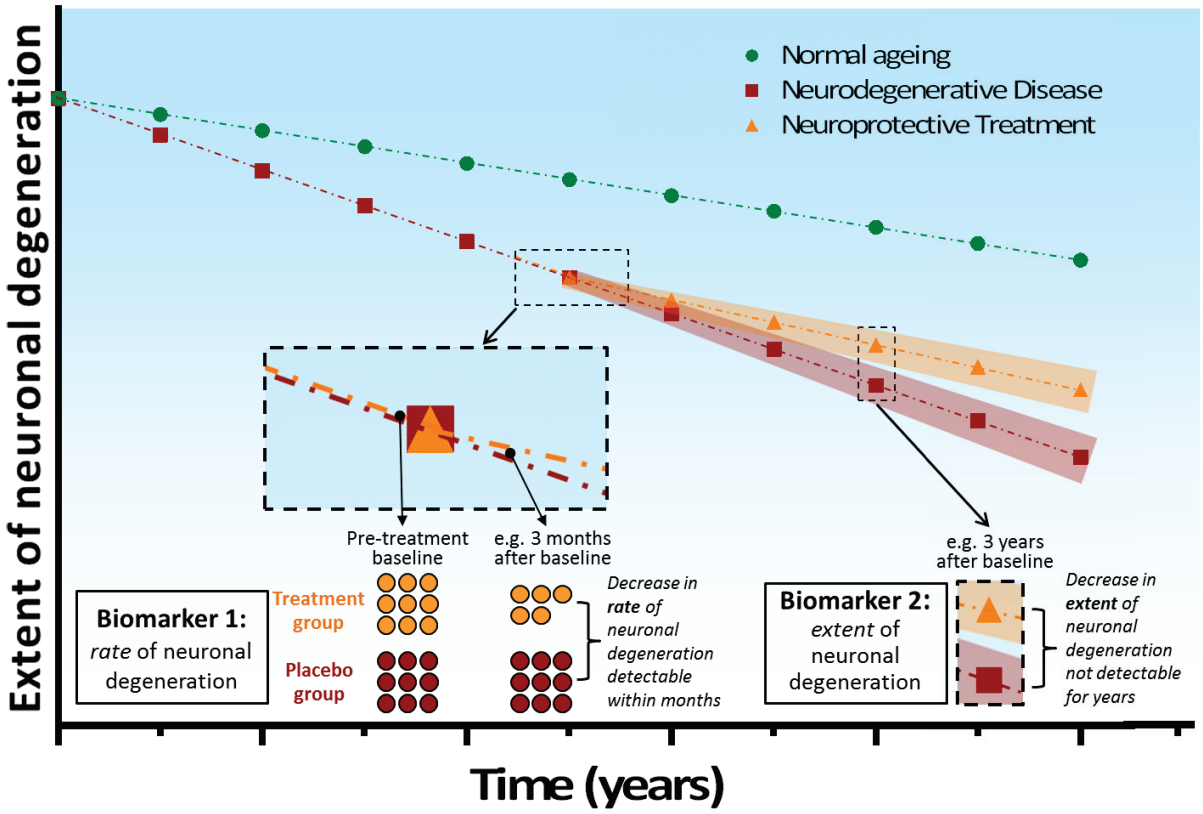


Figure 48: Biomarkers of *in vivo* rate of neurodegeneration ('Biomarker 1') should be able to detect treatment effect at earlier time point than those of *in vivo* extent of neurodegeneration ('Biomarker 2').

Chapter 2 of this thesis suggested that available outcome measures - relapses and MRI activity – are not sufficient for these needs, as they predicted short-term but not long-term disability outcomes after the initiation of natalizumab. Future work could test the replicability of these findings in cohorts with, for example, a greater number of participants, prospective data collation, lower baseline disability level, and including DMTs other than natalizumab. While clinicians will continue to use on-treatment breakthrough inflammatory activity as a marker of treatment response, there is a need for new biomarkers which are objective, quantitative, respond earlier to treatment, and which relate more closely to neurodegenerative activity.

18kDa translocator protein (TSPO) positron emission tomography (PET) may have the potential to meet these requirements, and assess the rate of neurodegenerative activity as

depicted in Figure 48.[13] In Chapter 3, the novel PET molecular imaging radiotracer [18F]GE180 was evaluated as a biomarker for focal inflammatory and neurodegenerative disease activity in MS, and as a surrogate for response to natalizumab treatment. Unfortunately, ^{18}F-GE180 had considerably lower extraction across the blood-brain barrier than expected, and poor signal-to-noise ratio especially given the presence of persistent vascular signal. A 'blocking study' confirmed ^{18}F-GE180 does exhibit some specific binding, but ^{18}F-GE180 was not able to detect increased TSPO in MS in the grey matter or normal-appearing white matter as previously reported with other tracers, or differences in TSPO binding affinity as expected.[14-20] ^{18}F-GE180 volume of distribution was increased in MS lesions, and decreased after natalizumab treatment, although these results may reflect changes in blood-brain barrier permeability rather than changes in TSPO expression. Future work should investigate whether other TSPO tracers with improved pharmacokinetic performance may be useful biomarkers in evaluating early response to DMTs in MS. Other biomarkers for rate of neurodegeneration are also being developed, such as neurofilament light chain measured in the cerebrospinal fluid.[21, 22] The thesis author and primary supervisor also have an interest in developing Detection of Apoptosing Retinal Cells, a technique developed for glaucoma which allows the visualisation and quantification of single retinal neuronal cell apoptosis *in vivo* in real time,[23, 24] as a potential biomarker for neurodegeneration in MS; a grant has been awarded to test this in a pilot study.

In addition to outcome measures which can guide clinical decision-making in individuals, personalised medicine will require the collection and analysis of 'big data': large datasets from clinical registry tools, which collect and codify patient characteristics, disease events, therapies, and outcome measures.[25-28] One of many challenges is to develop outcome measures which are compatible with large multicentre cohorts, and which can be tracked over time to capture meaningful data related to the impact of disease on people with MS. In Chapter

4, the Brain Predicted Age model, which uses machine learning to predict chronological age based solely upon T1 MRI data, was investigated as a marker of MS disease severity in an observational cohort of 541 subjects with 1,652 scans and up to 15 years of follow-up. All disease subgroups had substantially older-appearing brains than their chronological age. Brain Predicted Age correlated with disability outcomes, predicted future disability progression, and increased longitudinally in MS at a rate ~46% faster than in HCs. The model compared favourably with conventional univariate measures of brain atrophy, and is being further evaluated using the MAGNIMS multi-centre cohort. The model could provide conceptually simple and clinically meaningful quantitative data, and should be compatible across large imaging cohorts.

Like the Brain Predicted Age model, patient reported outcomes could also allow for long-term, geographically diverse, and large-scale observational and interventional studies.[29] However, it was not known whether patient reported outcomes could be prognostic of hard clinical endpoints in MS. Chapter 5 presented a large observational cohort study of the Multiple Sclerosis Impact Scale-29 (MSIS-29), and found it to predict reduced survival time independently of age and sex. This was the first study to associate patient reported outcomes with survival outcomes in any neurological disease.

Both the Brain Predicted Age model and the MSIS-29 require further development, in particular to test whether changes in the outcome measures after disease-modifying therapy predict long-term disability in accordance with the Prentice criteria.[30] With further development and validation, these outcome measures could be incorporated into MS clinical registry databases, as clinically meaningful outcome measures which can track the impact of MS on individuals.

Substantial progress has been made over recent decades in our approach to treating MS. However, clinicians and researchers do not yet have the tools to assess response to treatment, or to tailor their clinical decision-making to individuals to ensure '*the right treatment is given to the right patient at the right time*'. Researchers must continue to develop and validate new and existing outcome measures. Only then will we get the effective treatments, and the optimised use of available treatments, that people with MS deserve.

VI.3 REFERENCES

1. Perumal J, Khan O. Emerging disease-modifying therapies in multiple sclerosis. Curr Treat Options Neurol. 2012;14(3):256-63. Epub 2012/03/20. doi: 10.1007/s11940-012-0173-x. PubMed PMID: 22426573.

2. Ransohoff RM, Hafler DA, Lucchinetti CF. Multiple sclerosis-a quiet revolution. Nat Rev Neurol. 2015;11(3):134-42. Epub 2015/02/18. doi: 10.1038/nrneurol.2015.14. PubMed PMID: 25686758; PubMed Central PMCID: PMCPMC4556342.

3. Rae-Grant A, Day GS, Marrie RA, Rabinstein A, Cree BAC, Gronseth GS, Haboubi M, Halper J, Hosey JP, Jones DE, Lisak R, Pelletier D, Potrebic S, Sitcov C, Sommers R, Stachowiak J, Getchius TSD, Merillat SA, Pringsheim T. Comprehensive systematic review summary: Disease-modifying therapies for adults with multiple sclerosis: Report of the Guideline Development, Dissemination, and Implementation Subcommittee of the American Academy of Neurology. Neurology. 2018;90(17):789-800. Epub 2018/04/25. doi: 10.1212/WNL.0000000000005345. PubMed PMID: 29686117.

4. Fogarty E, Schmitz S, Tubridy N, Walsh C, Barry M. Comparative efficacy of disease-modifying therapies for patients with relapsing remitting multiple sclerosis: Systematic review and network meta-analysis. Mult Scler Relat Disord. 2016;9:23-30. Epub 2016/09/21. doi: 10.1016/j.msard.2016.06.001. PubMed PMID: 27645339.

5. Rubin SM. Management of multiple sclerosis: an overview. Dis Mon. 2013;59(7):253-60. Epub 2013/06/22. doi: 10.1016/j.disamonth.2013.03.012. PubMed PMID: 23786659.

6. D'Amico E, Ziemssen T, Cottone S. To stop or not to stop disease modifying therapies in secondary progressive multiple sclerosis, that is the question. Expert Rev Neurother. 2017;17(9):847-9. Epub 2017/06/09. doi: 10.1080/14737175.2017.1340831. PubMed PMID: 28594298.

7. Wolinsky JS, Arnold DL, Bar-Or A, de Seze J, Giovannoni G, Hemmer B, Rammohan K, Chin P, Fontoura P, Garren H, Masterman D, Sauter A, Montalban X, Porter A. Efficacy of ocrelizumab in patients with PPMS with and without T1 gadolinium-enhancing lesions at baseline in a phase III placebo-controlled trial (LB148). Mult Scler J, 22 (2016), pp. 67-68.

8. Montalban X, Hauser SL, Kappos L, Arnold DL, Bar-Or A, Comi G, de Seze J, Giovannoni G, Hartung HP, Hemmer B, Lublin F, Rammohan KW, Selmaj K, Traboulsee A, Sauter A, Masterman D, Fontoura P,

Belachew S, Garren H, Mairon N, Chin P, Wolinsky JS, Investigators OC. Ocrelizumab versus Placebo in Primary Progressive Multiple Sclerosis. The New England journal of medicine. 2017;376(3):209-20. Epub 2016/12/22. doi: 10.1056/NEJMoa1606468. PubMed PMID: 28002688.

9. Lassmann H, Bruck W, Lucchinetti C. Heterogeneity of multiple sclerosis pathogenesis: implications for diagnosis and therapy. Trends Mol Med. 2001;7(3):115-21. Epub 2001/04/05. PubMed PMID: 11286782.

10. Disanto G, Berlanga AJ, Handel AE, Para AE, Burrell AM, Fries A, Handunnetthi L, De Luca GC, Morahan JM. Heterogeneity in multiple sclerosis: scratching the surface of a complex disease. Autoimmune Dis. 2010;2011:932351. Epub 2011/01/05. doi: 10.4061/2011/932351. PubMed PMID: 21197462; PubMed Central PMCID: PMCPMC3005811.

11. Derfuss T. Personalized medicine in multiple sclerosis: hope or reality? Bmc Med. 2012;10:116. Epub 2012/10/06. doi: 10.1186/1741-7015-10-116. PubMed PMID: 23035757; PubMed Central PMCID: PMCPMC3523020.

12. Abrahams E. Right drug-right patient-right time: personalized medicine coalition. Clin Transl Sci. 2008;1(1):11-2. Epub 2008/05/01. doi: 10.1111/j.1752-8062.2008.00003.x. PubMed PMID: 20443813; PubMed Central PMCID: PMCPMC5439586.

13. Chen MK, Guilarte TR. Translocator protein 18 kDa (TSPO): Molecular sensor of brain injury and repair. Pharmacol Therapeut. 2008;118(1):1-17. doi: DOI 10.1016/j.pharmthera.2007.12.004. PubMed PMID: WOS:000256240900001.

14. Colasanti A, Guo Q, Muhlert N, Giannetti P, Onega M, Newbould RD, Ciccarelli O, Rison S, Thomas C, Nicholas R, Muraro PA, Malik O, Owen DR, Piccini P, Gunn RN, Rabiner EA, Matthews PM. In Vivo Assessment of Brain White Matter Inflammation in Multiple Sclerosis with (18)F-PBR111 PET. Journal of nuclear medicine : official publication, Society of Nuclear Medicine. 2014;55(7):1112-8. Epub 2014/06/07. doi: 10.2967/jnumed.113.135129. PubMed PMID: 24904112.

15. Datta G, Colasanti A, Kalk N, Owen D, Scott G, Rabiner EA, Gunn RN, Lingford-Hughes A, Malik O, Ciccarelli O, Nicholas R, Nei L, Battaglini M, Stefano ND, Matthews PM. (11)C-PBR28 and (18)F-PBR111 Detect White Matter Inflammatory Heterogeneity in Multiple Sclerosis. Journal of nuclear medicine : official publication, Society of Nuclear Medicine. 2017;58(9):1477-82. Epub 2017/03/18. doi: 10.2967/jnumed.116.187161. PubMed PMID: 28302760.

16. Sucksdorff M, Rissanen E, Tuisku J, Nuutinen S, Paavilainen T, Rokka J, Rinne J, Airas L. Evaluation of the Effect of Fingolimod Treatment on Microglial Activation Using Serial PET Imaging in Multiple Sclerosis. Journal of nuclear medicine : official publication, Society of Nuclear Medicine. 2017;58(10):1646-51. Epub 2017/03/25. doi: 10.2967/jnumed.116.183020. PubMed PMID: 28336784.

17. Versijpt J, Debruyne JC, Van Laere KJ, De Vos F, Keppens J, Strijckmans K, Achten E, Slegers G, Dierckx RA, Korf J, De Reuck JL. Microglial imaging with positron emission tomography and atrophy measurements with magnetic resonance imaging in multiple sclerosis: a correlative study. Mult Scler J. 2005;11(2):127-34. doi: Doi 10.1191/1352458505ms1140oa. PubMed PMID: WOS:000227717400001.

18. Debruyne JC, Versijpt J, Van Laere KJ, De Vos F, Keppens J, Strijckmans K, Achten E, Slegers G, Dierckx RA, Korf J, De Reuck JL. PET visualization of microglia in multiple sclerosis patients using [C-11]PK11195. European Journal of Neurology. 2003;10(3):257-64. doi: DOI 10.1046/j.1468-1331.2003.00571.x. PubMed PMID: WOS:000182651000009.

19. Politis M, Giannetti P, Su P, Turkheimer F, Keihaninejad S, Wu K, Waldman A, Malik O, Matthews PM, Reynolds R, Nicholas R, Piccini P. Increased PK11195 PET binding in the cortex of patients with MS correlates with disability. Neurology. 2012;79(6):523-30. PubMed PMID: WOS:000307458800011.

20. Feeney C, Scott G, Raffel J, Roberts S, Coello C, Jolly A, Searle G, Goldstone AP, Brooks DJ, Nicholas RS, Trigg W, Gunn RN, Sharp DJ. Kinetic analysis of the translocator protein positron emission tomography ligand [(18)F]GE-180 in the human brain. Eur J Nucl Med Mol Imaging. 2016;43(12):2201-10. Epub 2016/06/29. doi: 10.1007/s00259-016-3444-z. PubMed PMID: 27349244; PubMed Central PMCID: PMCPMC5047949.

21. Ziemann U, Wahl M, Hattingen E, Tumani H. Development of biomarkers for multiple sclerosis as a neurodegenerative disorder. Prog Neurobiol. 2011;95(4):670-85. Epub 2011/04/29. doi: 10.1016/j.pneurobio.2011.04.007. PubMed PMID: 21524682.

22. Gunnarsson M, Malmestrom C, Axelsson M, Sundstrom P, Dahle C, Vrethem M, Olsson T, Piehl F, Norgren N, Rosengren L, Svenningsson A, Lycke J. Axonal damage in relapsing multiple sclerosis is markedly reduced by natalizumab. Annals of neurology. 2011;69(1):83-9. Epub 2011/02/01. doi: 10.1002/ana.22247. PubMed PMID: 21280078.

23. Cordeiro MF, Normando EM, Cardoso MJ, Miodragovic S, Jeylani S, Davis BM, Guo L, Ourselin S, A'Hern R, Bloom PA. Real-time imaging of single neuronal cell apoptosis in patients with glaucoma. Brain : a journal of neurology. 2017;140(6):1757-67. doi: 10.1093/brain/awx088. PubMed PMID: 28449038; PubMed Central PMCID: PMCPMC5445254.

24. Guo L, Cordeiro MF. Assessment of neuroprotection in the retina with DARC. Prog Brain Res. 2008;173:437-50. doi: 10.1016/S0079-6123(08)01130-8. PubMed PMID: 18929126; PubMed Central PMCID: PMCPMC2603274.

25. Kalincik T, Butzkueven H. The MSBase registry: Informing clinical practice. Multiple sclerosis. 2019:1352458519848965. Epub 2019/05/24. doi: 10.1177/1352458519848965. PubMed PMID: 31120376.

26. Butzkueven H, Chapman J, Cristiano E, Grand'Maison F, Hoffmann M, Izquierdo G, Jolley D, Kappos L, Leist T, Pohlau D, Rivera V, Trojano M, Verheul F, Malkowski JP. MSBase: an international, online registry and platform for collaborative outcomes research in multiple sclerosis. Multiple sclerosis. 2006;12(6):769-74. Epub 2007/02/01. doi: 10.1177/1352458506070775. PubMed PMID: 17263005.

27. Bebo BF, Jr., Fox RJ, Lee K, Utz U, Thompson AJ. Landscape of MS patient cohorts and registries: Recommendations for maximizing impact. Multiple sclerosis. 2018;24(5):579-86. Epub 2017/03/11. doi: 10.1177/1352458517698250. PubMed PMID: 28279128; PubMed Central PMCID: PMCPMC5987851.

28. Nickerson M, Marrie RA. The multiple sclerosis relapse experience: patient-reported outcomes from the North American Research Committee on Multiple Sclerosis (NARCOMS) Registry. BMC Neurol. 2013;13:119. Epub 2013/09/11. doi: 10.1186/1471-2377-13-119. PubMed PMID: 24016260; PubMed Central PMCID: PMCPMC3848753.

29. Derfuss T. Personalized medicine in multiple sclerosis: hope or reality? Bmc Med. 2012;10. doi: Artn 116, 10.1186/1741-7015-10-116. PubMed PMID: WOS:000312393100001.

30. Prentice RL. Surrogate endpoints in clinical trials: definition and operational criteria. Stat Med. 1989;8(4):431-40. Epub 1989/04/01. doi: 10.1002/sim.4780080407. PubMed PMID: 2727467.

Appendix A

Publications by the thesis author directly related to the work presented in the thesis

Publications by the thesis author directly related to the work presented in the thesis:

1) **Raffel J**, Gafson AR, Dahdaleh S, Malik O, Jones B, Nicholas R. Inflammatory activity on natalizumab predicts short-term but not long-term disability in multiple sclerosis. *PLOS One*. 2017;12(1):e0169546.

2) Feeney C, Scott G, **Raffel J**, Roberts S, Coello C, Jolly A, Searle G, Goldstone AP, Brooks DJ, Nicholas RS, Trigg W, Gunn RN, Sharp DJ. Kinetic analysis of the translocator protein positron emission tomography ligand [18F]GE-180 in the human brain. *Eur J Nucl Med Mol Imaging.* 2016;43(12):2201-2210.

3) Sridharan S*, **Raffel J***, Nandoskar A, Record C, Brooks DJ, Owen D, Sharp D, Muraro PA, Gunn R, Nicholas R. Confirmation of specific binding of the 18-kDa Translocator Protein (TSPO) radioligand [18F]GE-180: a blocking study using XBD173 in multiple sclerosis normal appearing white and grey matter. *Mol Imaging Biol.* 2019;21(5):935-944
(*joint first authors)

4) **Raffel J**, Wallace A, Gveric D, Reynolds R, Friede T, Nicholas R. Patient-reported outcomes and survival in multiple sclerosis: A 10-year retrospective cohort study using the Multiple Sclerosis Impact Scale-29. *PLOS Medicine*. 2017;14(7):e1002346.

Raffel J, Gafson AR, Dahdaleh S, Malik O, Jones B, Nicholas R. Inflammatory activity on natalizumab predicts short-term but not long-term disability in multiple sclerosis. *PLOS One*. 2017;12(1):E0169546.

PLOS ONE

RESEARCH ARTICLE

Inflammatory Activity on Natalizumab Predicts Short-Term but Not Long-Term Disability in Multiple Sclerosis

Joel Raffel*☯, Arie R. Gafson☯, Samer Dahdaleh, Omar Malik, Brynmor Jones, Richard Nicholas

Department of Medicine, Imperial College London, London, United Kingdom

☯ These authors contributed equally to this work.
* joelraffel@doctors.org.uk

Check for updates

OPEN ACCESS

Citation: Raffel J, Gafson AR, Dahdaleh S, Malik O, Jones B, Nicholas R (2017) Inflammatory Activity on Natalizumab Predicts Short-Term but Not Long-Term Disability in Multiple Sclerosis. PLoS ONE 12 (1): e0169546. doi:10.1371/journal.pone.0169546

Editor: David R. Booth, Westmead Millennium Institute for Medical Research, AUSTRALIA

Received: July 4, 2016

Accepted: December 19, 2016

Published: January 12, 2017

Copyright: © 2017 Raffel et al. This is an open access article distributed under the terms of the Creative Commons Attribution License, which permits unrestricted use, distribution, and reproduction in any medium, provided the original author and source are credited.

Data Availability Statement: Data were analysed as part of a clinical audit, registered and ethically approved at Imperial College Healthcare NHS Trust, for which written informed consent was not required (Audit registration number 1987–2015). Anonymized clinical data are not available on a public repository since ethical approval was not granted by Imperial College Healthcare NHS Trust Research Office to share individual patient disease characteristics outside of their healthcare institution, since these may contain identifying or sensitive patient information. Interested research may send requests for access to these data to

Abstract

Background

In people with multiple sclerosis treated with interferon-beta or glatiramer acetate, new MRI lesions and relapses during the first year of treatment predict a poor prognosis.

Objective

To study this association in those receiving natalizumab.

Methods

Data were collected on relapses, new MRI activity, and Modified Rio Score after initiation of natalizumab in an observational cohort of 161 patients with high baseline disability. These were correlated with Expanded Disability Status Scale (EDSS) progression at years 1, 2, 3, and 3–7 after treatment initiation, versus pre-treatment baseline.

Results

46/161 patients had a relapse in the first year and 44/161 had EDSS progression by year 2. Relapses and Modified Rio Score in the first year of treatment predicted EDSS progression at year 1 and 2 after treatment initiation. However, this effect disappeared with longer follow-up. Paradoxically, there was a trend towards inflammatory activity on treatment (first year Modified Rio Score, relapses, and MRI activity) predicting a *lower* risk of EDSS progression by years 3–7, although this did not reach statistical significance. Those with and without EDSS progression did not differ in baseline age, EDSS, or pre-treatment relapse rate. Relapses in year 0–1 predicted further relapses in years 1–3.

Conclusions

Breakthrough inflammatory activity after natalizumab treatment is predictive of short-term outcome measures of relapses or EDSS progression, but does not predict longer term EDSS progression, in this cohort with high baseline disability.

Richard Nicholas (richard.nicholas@imperial.nhs.uk).

Funding: Dr. Richard Nicholas is supported by the National Institute for Health Research. The authors received no specific funding for this work.

Competing Interests: This study received no specific funding or sponsorship. Dr. Raffel, Dr. Gafson, Dr. Dahdaleh, and Dr. Jones declare that there is no conflict of interest and report no disclosures. Dr. Malik has received travel grants to educational meetings from Biogen Idec and honoraria from Biogen Idec, which have been used exclusively for clinical research, outside the submitted work. Dr. Nicholas has received grants, personal fees and non-financial support from Novartis, grants, personal fees and non-financial support from Biogen Idec, personal fees from Genzyme, personal fees from Roche, outside the submitted work. This does not alter our adherence to PLOS ONE policies on sharing data and materials.

Introduction

In recent years, a number of new treatments have emerged for patients with relapsing multiple sclerosis (RMS).[1] Their development was underpinned by targeting MRI activity in phase 2 studies, leading to phase 3 studies which demonstrated reductions in relapse frequency and a variable effect on time to disability progression. The principal argument for their long term use is that treatments that target inflammatory activity probably improve long term disability outcomes, at least at a population level.[2, 3]

These principles have been extended in the pursuit of personalised medicine in multiple sclerosis (MS), where it is hypothesised that on-treatment breakthrough inflammatory activity can be used to predict poor long-term disability outcomes at an individual level.[4] This is supported by observational studies on therapies interferon-beta and glatiramer acetate, where early on-treatment relapses, MRI activity, and Kurtzke Expanded Disability Status Scale (EDSS) disability progression have been shown to predict poor medium-term clinical outcomes of relapses and/or EDSS progression in individuals.[5–11] For example, Rio and colleagues showed that combined scores of MRI lesions, relapses, and/or EDSS progression after interferon-beta initiation predicted further EDSS progression at two years.[9] Similarly, combined scores of MRI lesions and relapses after glatiramer acetate predict "clinical activity" (defined as relapses or EDSS progression) after 2 years.[6] Most of these studies are limited in that their follow-up periods were between 2–3 years.[6–11] Their applicability to other therapies such as teriflunomide, dimethyl fumarate, fingolimod, natalizumab, and alemtuzumab is also uncertain. If on-treatment breakthrough inflammatory activity does predict poor long-term disability outcomes, the next step would be to evaluate whether switching treatments can improve long-term prognosis, as proposed by the no evidence of disease activity (NEDA) approach.[12] However, for the treating physician, it is currently unclear whether on-treatment inflammatory breakthrough activity should trigger a change in medication, or not.

Natalizumab is a highly active therapy that is widely used in patients with RMS. It is effective in reducing relapses, MRI activity, and time to EDSS progression with a higher efficacy than interferon-beta.[13, 14] The objective of this observational study was to evaluate whether early relapses or MRI activity after starting natalizumab treatment predicts EDSS progression at later time points, in a cohort with high baseline disability.

Patients and Methods

Data were collected from an observational cohort of 204 patients initiating natalizumab between March 2007 and October 2010 at Imperial College Healthcare NHS Trust, with up to 7 years of follow-up. Data on relapse rate and EDSS were prospectively documented at routine 6-monthly clinic visits. EDSS data were collected until December 2014. MRI was routinely performed before treatment and at one year. Data were retrospectively collated for the purpose of this study. Patients were excluded if they had less than three years follow-up, or were treated with natalizumab for less than one year.

Data were analysed as part of a clinical audit, registered and ethically approved at Imperial College Healthcare NHS Trust, for which written informed consent was not required (Audit registration number 1987–2015). Anonymised clinical data are not available on a public repository since ethical approval was not granted by Imperial College Healthcare NHS Trust Research Office to share individual patient disease characteristics outside of their healthcare institution, since these may contain identifying or sensitive patient information. Requests for data may be sent to richard.nicholas@imperial.nhs.uk.

Early markers of inflammatory disease activity

Relapses were defined as an acute worsening of function lasting at least 48 hours, in the absence of fever or infection. MRI activity was defined as the presence of 1 active lesion (either new or enlarging T2 lesions) relative to a baseline MRI scan. A combined score of MRI and relapse activity was also applied to this first year after natalizumab therapy (Modified Rio Score–Table 1), which employs more stringent criteria to define new MRI activity.[7]

Disease progression

Disability progression was defined as an increase of 1 EDSS point in those with EDSS <5.5, or an increase of 0.5 EDSS point in those with EDSS ≥ 5.5. EDSS progression was confirmed over 6 months at repeat clinic visits. Patients were labelled as disability progression responders and non-responders after 1 year of treatment (Year 1 EDSS Progression) by comparing EDSS captured after 1 year with pre-natalizumab EDSS. This was repeated after 2 years, 3 years, and 3–7 years, by comparing the latest available EDSS rating (up to 7 years after treatment initiation) with pre-natalizumab EDSS.

Statistical analysis

Demographic data are presented as mean +/- standard deviation (SD). Difference between means was assessed using unpaired Student's t-test, after testing for normality of the data. To investigate the association between early markers of disease activity and disability progression data were analysed in Kaplan-Meier curves using Log-Rank test and Cox regression, and also in 2x2 contingency tables using Fisher's exact test with odds ratios (OR) and 95% confidence intervals (CI) calculated. Chi-squared test for trend was used for 3x2 contingency tables of the Modified Rio Score and for analysis of change in categorical data over time. Corrections for multiple comparisons were not made, since comparisons were complementary and a consistency of results was apparent between different groups.[15, 16] For the purpose of displaying results in graphical format, results were converted to percentages. A logical regression multivariable model was also used to investigate for multivariate associations that predict disability outcomes. SPSS and R statistical package were used for these analyses.

Results

Demographics

During the study period, 204 patients started natalizumab treatment. Subjects were excluded from analysis if they had discontinued natalizumab within 1 year (n = 16), if there were less than 3 years of clinical follow-up data (n = 20), or if there were insufficient clinical or radiological data (n = 7), leaving 161 patients for analysis. Of these, 127 received natalizumab

Table 1. Modified Rio Score[7].

Modified Rio Score scoring criteria		
Criterion	**Change over 1st year**	**Score**
MRI	$\leq$ 4 new T2 lesions	0
	> 4 new T2 lesions	1
Relapse	No relapses	0
	1 relapse	1
	$\geq$ 2 relapses	2
Score = MRI criterion + relapse criterion		

doi:10.1371/journal.pone.0169546.t001

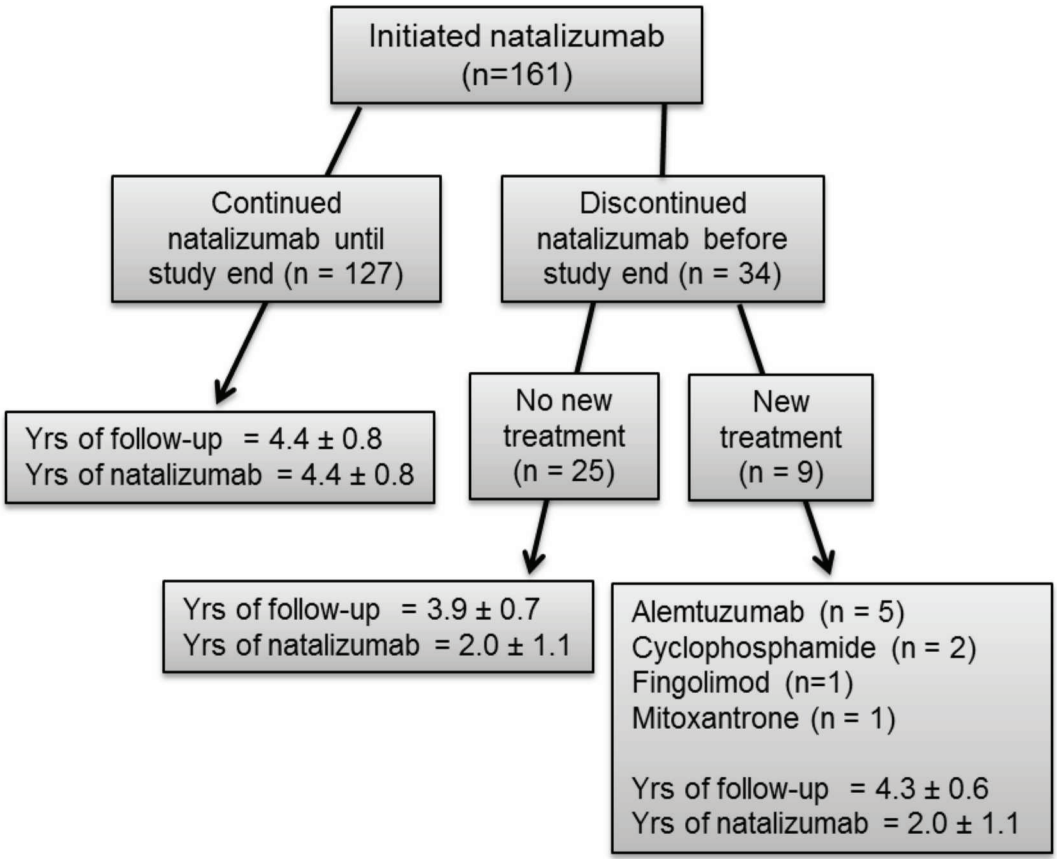


Fig 1. 161 participants were included in all analyses. The treatment pathway, and mean follow-up time, is detailed in the figure.

doi:10.1371/journal.pone.0169546.g001

throughout the study period, 9 stopped natalizumab after 1+ year of treatment and switched to a new disease modifying medication, and 25 stopped natalizumab after 1+ year of treatment but did not receive new disease modifying medication (Fig 1). No differences existed in demographic, clinical and MRI data between those included in and excluded from the study. There were no differences between Year 3–7 EDSS Progression Responder and Year 3–7 EDSS Progression Non-Responder cohorts, other than an expected difference in most recent EDSS (Table 2). Logistic regression multivariable analysis that included age, sex, disease duration, number of previous treatments, pre-natalizumab relapse rate, and pre-natalizumab EDSS confirmed that none of these baseline measures predicted response to treatment.

Markers of inflammatory disease do not affect disability progression survival analysis

46 of 161 patients had a relapse in the first year, and 28 of 161 had new MRI activity. Modified Rio score was 1 in 34 patients, and 2 in 16 patients. Markers of inflammatory disease in the first year (Modified Rio Score, relapses, MRI activity) and second year (relapses) had no significant effect on disability progression plotted as a survival analysis (Mod Rio Score year 0–1: risk ratio (RR) 1.15, log-rank p = 0.74, Cox regression p = 0.44; Relapses year 0–1: RR 1.3, log-rank p = 0.31, Cox regression p = 0.31; MRI activity year 0–1: RR 0.64, log-rank p = 0.21, Cox regression p = 0.24; Relapses year 1–2: RR 1.17, log-rank p = 0.51, Cox regression p = 0.51;

Table 2. Characteristics of study cohort, presented as mean ± SD. Percentages are rounded to the nearest integer, and may not add to 100%.

	Full Cohort	Year 3–7 EDSS Progression Responders	Year 3–7 EDSS Progression Non-Responders
Sample Number	161	101	60
Mean Age (Years)	40.6 ± 10.2	39.7 ± 10.8	42.1 ± 9.1
Sex			
Female	101 (63%)	67 (66%)	34 (57%)
Male	60 (37%)	34 (34%)	26 (43%)
Disease Duration (years)	8.9 ± 6.1	8.7 ± 6.0	9.4 ± 6.2
Number of previous treatments			
0	42 (26%)	30 (30%)	12 (20%)
1	89 (55%)	52 (51%)	37 (62%)
2	21 (13%)	14 (14%)	7 (12%)
3	8 (5%)	4 (4%)	4 (7%)
4	1 (1%)	1 (1%)	0
Relapses 2 years prior to natalizumab	3.0 ± 1.3	3.0 ± 1.3	2.9 ± 1.2
Pre natalizumab EDSS	4.2 ± 1.8	4.1 ± 1.9	4.4 ± 1.6
Most recent EDSS	4.5 ± 2.0	3.7 ± 2.0	5.8 ± 1.4 ****
Years of follow-up after natalizumab	4.3 ± 0.8	4.3 ± 0.8	4.3 ± 0.9

When divided into Year 3–7 EDSS Progression Responders and Non-Responders, there were no significant differences between characteristics, other than 'most recent EDSS' (**** = p<0.0001).

doi:10.1371/journal.pone.0169546.t002

Fig 2A–2D). Those with low Modified Rio Scores, and without relapses in year 0–1, appeared to have lower risk of disability progression in the first two years, but this effect disappeared with longer follow-up (Fig 2A and 2B).

Modified Rio Score predicts short-term but not medium-term disability progression

A limitation of Kaplan-Meier curves is that events (in this case disability progression) are treated as irreversible, which is inappropriate given that EDSS can improve with treatment. In addition, it was observed that curves converge and cross in both the Modified Rio Score and relapses survival analyses (Fig 2A and 2B), suggesting that any association between inflammatory biomarkers and disability progression may change over time. Therefore, contingency tables were used to investigate the relationship between inflammatory biomarkers and EDSS progression at specific time points of years 1, 2, 3, and 3–7.

Modified Rio Score in the first year of treatment predicted EDSS progression at year 1 and 2 (Year 1: 15/111 vs 9/34 vs 5/16 EDSS progression for those with Mod Rio Score of 0, 1, 2 respectively. Mod Rio Score 1, Odds Ratio (OR) 2.3, 95% Confidence Interval (CI) 0.9–5.9; Mod Rio Score 2, OR 2.9, CI 0.9–9.6; $p<0.05$. Year 2: 25/111 vs 12/34 vs 7/16 EDSS progression for those with Mod Rio Score of 0, 1, 2 respectively. Mod Rio Score 1, OR 1.9, CI 0.8–4.3; Mod Rio Score 2, OR 2.7, CI 0.9–7.9; $p<0.05$; Fig 3A and 3B). However, it did not predict EDSS progression at year 3, or year 3–7 (Year 3: 35/111 vs 12/34 vs 6/16 EDSS progression for those with Mod Rio Score of 0, 1, 2 respectively. Mod Rio Score 1, OR 1.2, CI 0.4–2.7; Mod Rio Score 2, OR 1.3, CI 0.4–3.9; $p = 0.57$; Year 3–7: 45/111 vs 12/34 vs 3/16 EDSS progression for those with Mod Rio Score of 0, 1, 2 respectively. Mod Rio Score 1, OR 0.8, CI 0.4–1.8; Mod Rio Score 2, OR 0.3, CI 0.1–1.3; $p = 0.11$; Fig 3C and 3D). If anything, there was a paradoxical trend towards *lower* Modified Rio Score predicting EDSS progression in years 3–7, although this was not statistically significant (Fig 3D). This shift over time in the polarity of the predictive value of

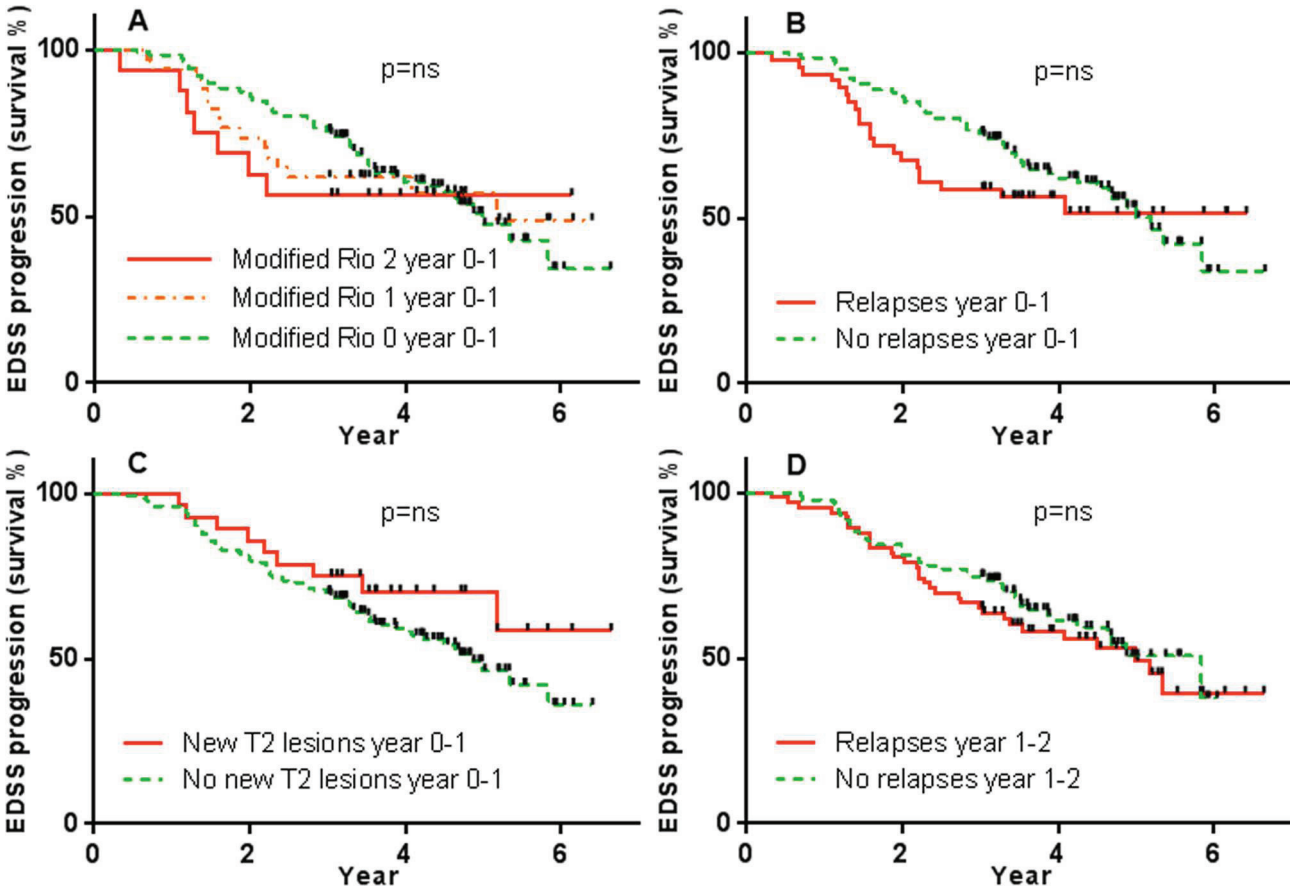


Fig 2. On-treatment inflammatory disease activity does not affect overall disability survival analysis. First year after natalizumab initiation Modified Rio Score (A), relapses (B), and MRI activity (C), and second year after natalizumab initiation relapses (D), versus survival from EDSS progression over time. Black markers on survival lines represent the duration of follow-up data for those participants who have not undergone EDSS progression (i.e. the time of subject censorship in survival analysis).

doi:10.1371/journal.pone.0169546.g002

Modified Rio Score on disability was caused by year-on-year increases in the proportion of non-responders within the Mod Rio Score 0 group ($p<0.0001$), versus no significant year-on-year change in the proportion of non-responders within the Mod Rio Score 1–2 group ($p = 0.90$).

Relapses and MRI activity predict short-term but not medium-term disability progression

Similar trends were observed when studying on-treatment relapses and MRI activity in isolation. Relapses in the first year of treatment predicted EDSS progression at year 1 and 2 (Year 1: 16/115 vs 13/48 EDSS progression for those without and with relapses respectively. OR 2.4, CI 1.1–5.6, $p<0.05$. Year 2: 26/115 vs 18/48 EDSS progression for those without and with relapses respectively. OR 2.2, CI 1.1–4.6, $p<0.05$; Fig 3E and 3F). However, they did not predict EDSS progression at year 3, or years 3–7 (Year 3: 36/115 vs 17/48 EDSS progression for those without and with relapses respectively. OR 1.3, CI 0.6–2.6, $p = 0.58$. Year 3–7: 46/115 vs 14/48 EDSS progression for those without and with relapses respectively. OR 0.7, CI 0.3–1.4, $p = 0.28$; Fig 3G and 3H). If anything, there was a paradoxical trend towards *lack* of relapses predicting EDSS progression at years 3–7, although this was not statistically significant (Fig 3H). New MRI activity in the first year of treatment did not predict EDSS progression at any future time

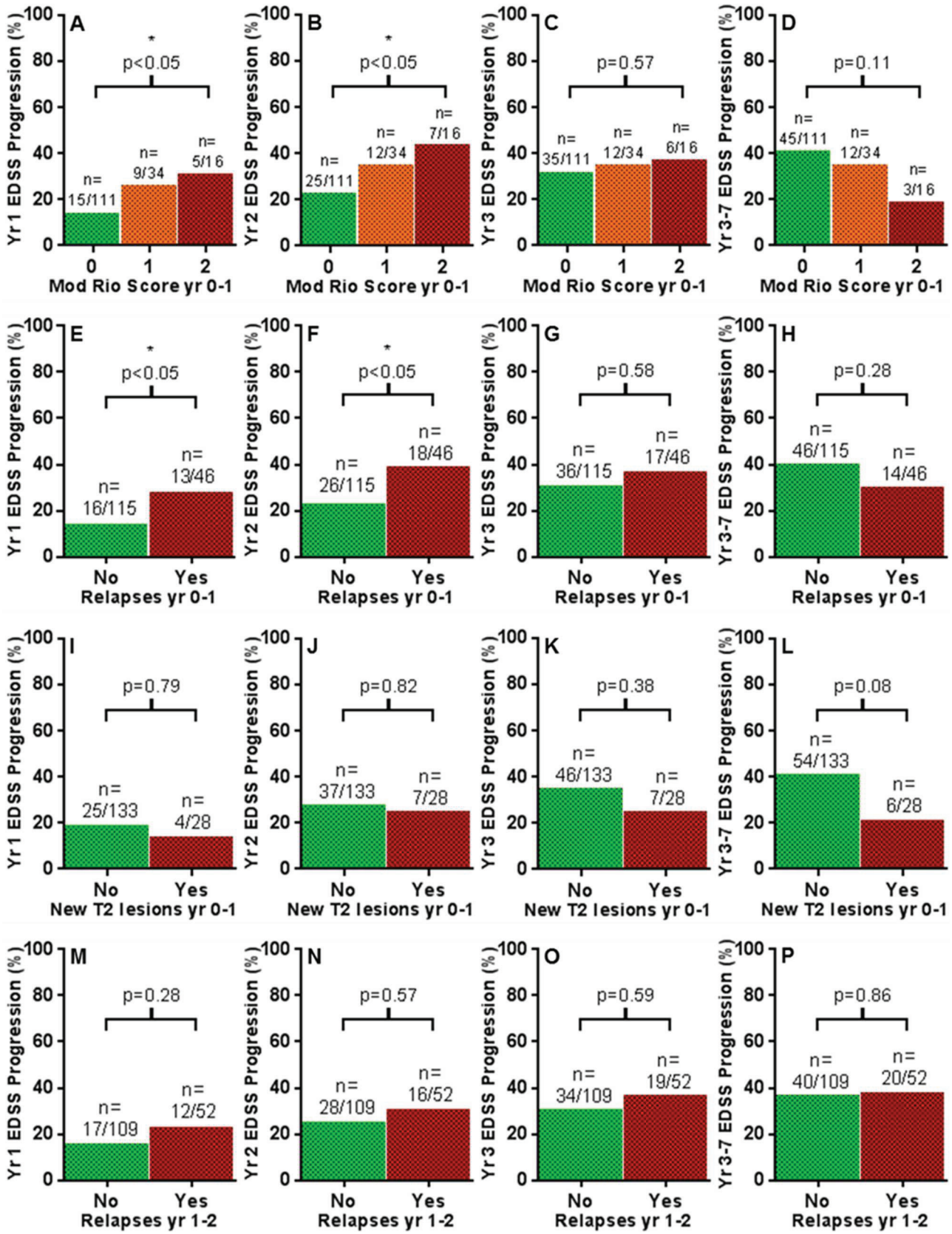

A
Yr 1 EDSS Progression (%)
*
p<0.05
n= 15/111
n= 9/34
n= 5/16
Mod Rio Score yr 0-1
B
Yr 2 EDSS Progression (%)
*
p<0.05
n= 25/111
n= 12/34
n= 7/16
Mod Rio Score yr 0-1
C
Yr 3 EDSS Progression (%)
p=0.57
n= 35/111
n= 12/34
n= 6/16
Mod Rio Score yr 0-1
D
Yr 3-7 EDSS Progression (%)
p=0.11
n= 45/111
n= 12/34
n= 3/16
Mod Rio Score yr 0-1
E
Yr 1 EDSS Progression (%)
*
p<0.05
n= 16/115
n= 13/46
No
Yes
Relapses yr 0-1
F
Yr 2 EDSS Progression (%)
*
p<0.05
n= 26/115
n= 18/46
No
Yes
Relapses yr 0-1
G
Yr 3 EDSS Progression (%)
p=0.58
n= 36/115
n= 17/46
No
Yes
Relapses yr 0-1
H
Yr 3-7 EDSS Progression (%)
p=0.28
n= 46/115
n= 14/46
No
Yes
Relapses yr 0-1
I
Yr 1 EDSS Progression (%)
p=0.79
n= 25/133
n= 4/28
No
Yes
New T2 lesions yr 0-1
J
Yr 2 EDSS Progression (%)
p=0.82
n= 37/133
n= 7/28
No
Yes
New T2 lesions yr 0-1
K
Yr 3 EDSS Progression (%)
p=0.38
n= 46/133
n= 7/28
No
Yes
New T2 lesions yr 0-1
L
Yr 3-7 EDSS Progression (%)
p=0.08
n= 54/133
n= 6/28
No
Yes
New T2 lesions yr 0-1
M
Yr 1 EDSS Progression (%)
p=0.28
n= 17/109
n= 12/52
No
Yes
Relapses yr 1-2
N
Yr 2 EDSS Progression (%)
p=0.57
n= 28/109
n= 16/52
No
Yes
Relapses yr 1-2
O
Yr 3 EDSS Progression (%)
p=0.59
n= 34/109
n= 19/52
No
Yes
Relapses yr 1-2
P
Yr 3-7 EDSS Progression (%)
p=0.86
n= 40/109
n= 20/52
No
Yes
Relapses yr 1-2

Fig 3. On-treatment inflammatory disease activity predicts short-term but not long-term disability outcomes. Early measures of on-treatment inflammatory disease in first year (A-L) and second year (M-P) after treatment initiation, versus percentage of future EDSS Progression in year 1 (A, E, I, M), year 2 (B, F, J, N), year 3 (C, G, K, O), and years 3–7 (D, H, L, P). * denotes p<0.05.

doi:10.1371/journal.pone.0169546.g003

point (Year 1: 25/113 vs 4/28 EDSS progression for those without and with new MRI activity respectively. OR 0.7, CI 0.2–2.3, p = 0.78 Year 2: 37/113 vs 7/28 EDSS progression for those without and with new MRI activity respectively. OR 0.86, CI 0.3–2.2, p = 0.82. Year 3: 46/113 vs 7/28 EDSS progression for those without and with new MRI activity respectively. OR 0.6, CI 0.2–1.6, p = 0.38. Year 3–7: 54/113 vs 6/28 EDSS progression for those without and with new MRI activity respectively. OR 0.4, CI 0.2–1.0, p = 0.08; Fig 3I–3L). Again, there was a paradoxical trend towards *lack* of new MRI activity predicting EDSS progression at years 3–7, although this was not statistically significant (Fig 3L). As before, this shift over time in the polarity of the predictive value of relapses and MRI activity on disability was caused by year-on-year increases in the proportion of non-responders within the 'no relapses group' ($p<0.0001$) and 'no new MRI activity group' ($p<0.0001$), versus no significant year-on-year change in the proportion of non-responders within the 'relapses group' (p = 0.89) and the 'new MRI activity group' (p = 0.54).

Similarly, the subgroup of patients with new gadolinium-enhancing MRI lesions in the first year of treatment (n = 14) had no difference in EDSS progression in future years (Year 1: 25/147 vs 4/14 EDSS progression for those without and with new gadolinium enhancing lesions respectively. OR 2.0, CI 0.6–6.7, p = 0.28. Year 2: 40/147 vs 4/14 EDSS progression for those without and with new gadolinium enhancing lesions respectively. OR 1.1, CI 0.3–3.6, p = 1.0. Year 3: 48/147 vs 4/14 EDSS progression for those without and with new gadolinium enhancing lesions respectively. OR 0.8, CI 0.2–2.8, p = 1.0.Year 3–7: 56/147 vs 4/14 EDSS progression for those without and with new gadolinium enhancing lesions respectively. OR 0.65, CI 0.2–2.2, p = 0.57). Relapses in the second year of treatment were also unable to predict EDSS progress at future time points (Year 1: 17/109 vs 12/52 EDSS progression for those without and with relapses respectively. OR 1.6, CI 0.7–3.7, p = 0.28. Year 2: 28/109 vs 16/52 EDSS progression for those without and with relapses respectively. OR 1.3, CI 0.6–2.7, p = 0.57. Year 3: 34/109 vs 19/52 EDSS progression for those without and with relapses respectively. OR 1.3, CI 0.6–2.5, p = 0.59. Year 3–7: 40/109 vs 20/52 EDSS progression for those without and with relapses respectively. OR 1.1, CI 0.5–2.1, p = 0.86; Fig 3M–3P).

Results are not affected by change in medication, baseline disability, or neutralising antibodies

As may be expected, patients with inflammatory activity on natalizumab treatment were more likely to switch to other disease modifying drugs, such as alemtuzumab, fingolimod, or cyclophosphamide. For example, 8/46 of those with relapses in year 0–1 switched to an alternative treatment at some point during the 3–7 year follow-up period of this study, versus 1/115 of those with no relapses. However, the trends observed in this study remained consistent with subgroup analyses after exclusion of those that switched to other medications (for example as represented in Fig 4). Trends also remained consistent with subgroup analysis restricted to those with baseline EDSS scores <4 (n = 68) or ≥ 4 (n = 93), and also after exclusion of those with neutralising antibodies (n = 6). There was no significant difference in mean follow-up time between those with different Modified Rio Scores, or indeed any of the other individual inflammatory measures.

Logistic regression multivariable model considered variables relating to demographics, disease history, and markers of inflammatory disease (age at natalizumab initiation, sex,

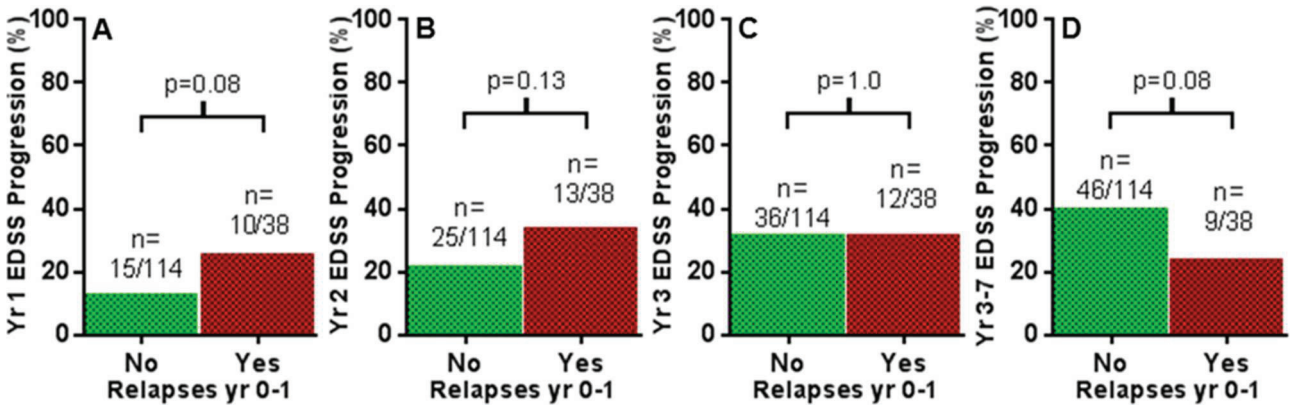


Fig 4. Results remain consistent after exclusion of those that switched to other treatment. After exclusion of patients who switched from natalizumab to other disease modifying treatment. On-treatment relapses in first year after treatment initiation versus percentage of future EDSS Progression in year 1 (A), year 2 (B), year 3 (C), and years 3–7 (D).

doi:10.1371/journal.pone.0169546.g004

pre-natalizumab relapse rate, pre-natalizumab MRI lesion count, pre-natalizumab MRI enhancing lesion count, number of previous treatments, post-natalizumab relapse rate, and post-natalizumab new MRI lesions), and found no further predictive relationships for disability outcomes (multiple r-squared: 0.051, p = 0.46).

Relapses in the first year of treatment with natalizumab predict further relapses

Relapses in year 0–1 of treatment were correlated with the risk of further relapses in years 1–3. 35 of 115 (30%) with no relapses in year 0–1 reported relapses in years 1–3. In contrast, 31 out of 46 (67%) with relapses in year 0–1 reported relapses in years 1–3 (OR 4.7, CI 2.3–9.8, $p<0.0001$).

Discussion

This is the first study to report on-treatment predictive measures of long term disability outcomes in a cohort of patients on natalizumab. We find that relapses and Modified Rio Score in the first year of natalizumab treatment predict year 1 and year 2 EDSS progression. However, this effect disappears after three years of follow-up. If anything, there is a consistent paradoxical trend towards on-treatment relapses, MRI activity, and high Modified Rio Score predicting *better* 3–7 year disability outcomes, versus pre-treatment baseline EDSS, although this did not reach statistical significance. This shift over time was driven by highly significant year-on-year increases in disability progression specifically in those *without* on-treatment inflammatory activity. In this group it was less likely for the EDSS to worsen in the first 1–2 years, but far more likely for the EDSS to worsen over each subsequent year. Results were consistent when restricted to those who remained on natalizumab throughout the follow-up period. Given this, our data suggests a disconnect between natalizumab's ability to suppress focal inflammatory activity underlying relapses and new T2 MRI lesions, and its putative effect on the progression of long-term disability.

Previous studies looking at predictive measures of treatment response have tended to focus on earlier generation MS treatments, namely interferons and glatiramer acetate. Like ours, these studies identified on-treatment MRI activity and relapses as medium-term ($\leq$3 years) prognostic markers of EDSS progression and/or further relapses.[5–11] However, the majority had limited follow up and thus conclusions on long term disability could not be made.[6–11]

It is possible that the predictive effect of relapses and MRI activity on short-term EDSS outcomes could reflect a predictive effect partly on relapse-mediated worsening of disability, rather than true progressive neurodegeneration. Related to this is a potential reporting bias, especially in studies based in the working neurology clinic, where it can be challenging to distinguish relapses from a true worsening of EDSS, and so both may be reported interdependently. This reporting bias decreases with long-term follow-up. In addition, we found that relapses in year 0–1 predict further relapses in years 1–3, in common with several of the above studies.[6, 7, 9, 11] Again, a patient reporting bias is likely to contribute to this association, and long-term disability progression should remain the preferred primary outcome. It would be of interest whether long-term follow-up data from the above studies would find results consistent with ours. Equally, it could be that the prognostic importance of relapses and MRI activity differs between interferon, glatiramer acetate, and natalizumab treatment.

Year 0–1 on-treatment MRI activity did not predict poor disability outcomes at any time point. This expands upon a previous post hoc analysis of randomized controlled trial data showing the clinical efficacy of natalizumab on year 0–2 relapses even in those with on-treatment MRI activity.[17] Of course, some new T2 lesions might have developed before natalizumab became effective, and future datasets should aim to "re-baseline" the patients with MRI scans performed 6 months after natalizumab initiation.[18] However, since gadolinium enhancing MRI also did not predict poor disability outcomes in our study, this suggests the lack of correlation between new MRI activity and long-term prognosis is real. Similarly, some relapses in years 0–1 may have developed before natalizumab became effective, but the data on year 1–2 relapses corroborates the finding of lack of predictive value of relapses on long-term disability.

Several caveats exist in this study, and must be considered. The cohort size is modest, and results should be replicated in larger cohorts. Our cohort had a high baseline EDSS (mean baseline EDSS 4.2) in comparison to interferon and glatiramer acetate studies (mean baseline EDSS 2 to 3), reflecting the fact that at the time of data collection, there were limited treatment options available for highly active relapsing-remitting and relapsing-progressive MS. Our cohort had poorer outcomes—46 of 161 patients had a relapse in the first year and 44/161 had EDSS progression by year 2—than previously described natalizumab cohorts with less baseline disability such as those in the pivotal randomised controlled trials.[13,14] Although some patients gained clear benefit from treatment it is likely that some patients within our cohort had a progressive component to their disease which was not responsive to treatment.[19, 20] Within this cohort, it could be that on-treatment breakthrough inflammatory activity is not a poor prognostic marker for long-term disability since it signifies that the patient does have an ongoing treatable focal inflammatory disease component, as opposed to others in the cohort who may have entered a predominantly irreversible neurodegenerative progressive stage of disease. That said, those with on-treatment inflammatory activity had equivalent baseline age and EDSS to those without on-treatment inflammatory activity in our cohort. In addition, results remained consistent when restricted to those with baseline EDSS <4. Another caveat arises in that follow-up time was variable, although always greater than 3 years. Kaplan-Meier curves tended to converge after this 3-year time point, bringing about the possibility that associations were affected by selection bias related to duration of follow-up, although this seems unlikely since follow-up duration was consistent between groups.

The observational nature of this study means we cannot speculate whether patients might have gained greater benefit from other treatments. Randomised controlled interventional studies are required to investigate whether those with breakthrough inflammatory activity would benefit from switching to other highly active treatments. Nevertheless, the data from this study argues that neither decrease in relapse rate, MRI activity, nor short-term stability of

EDSS can be assumed to equate to better long-term prognosis. This has far-reaching implications, from the treating physician assessing those with on-treatment clinical activity, to the design and interpretation of the clinical trial.

Acknowledgments

We thank the nurses, administrators, and patients at Imperial College Healthcare NHS Trust for their help and cooperation in collecting the data.

Author Contributions

Conceptualization: JR RN SD.

Formal analysis: JR AG.

Investigation: SD AG JR BJ.

Methodology: JR RN.

Resources: OM BJ.

Supervision: RN OM.

Writing – original draft: JR.

Writing – review & editing: JR AG RN.

References

1. Ransohoff RM, Hafler DA, Lucchinetti CF. Multiple sclerosis-a quiet revolution. Nat Rev Neurol. 2015; 11(3).
2. Sormani MP, Bonzano L, Roccatagliata L, Mancardi GL, Uccelli A, Bruzzi P. Surrogate endpoints for EDSS worsening in multiple sclerosis. A meta-analytic approach. Neurology. 2010; 75(4):302–9. doi: 10.1212/WNL.0b013e3181ea15aa PMID: 20574036
3. Goodin DS, Reder AT, Ebers GC, Cutter G, Kremenchutzky M, Oger J, et al. Survival in MS: a randomized cohort study 21 years after the start of the pivotal IFNbeta-1b trial. Neurology. 2012; 78(17):1315–22. PubMed Central PMCID: PMCPMC3335454. doi: 10.1212/WNL.0b013e3182535cf6 PMID: 22496198
4. Rio J, Comabella M, Montalban X. Multiple sclerosis: current treatment algorithms. Curr Opin Neurol. 2011; 24(3):230–7. doi: 10.1097/WCO.0b013e328346bf66 PMID: 21499098
5. Prosperini L, Gallo V, Petsas N, Borriello G, Pozzilli C. One-year MRI scan predicts clinical response to interferon beta in multiple sclerosis. European Journal of Neurology. 2009; 16(11):1202–9. doi: 10.1111/j.1468-1331.2009.02708.x PMID: 19538207
6. Rio J, Rovira A, Tintore M, Sastre-Garriga J, Castillo J, Auger C, et al. Evaluating the response to glatiramer acetate in relapsing-remitting multiple sclerosis (RRMS) patients. Mult Scler J. 2014; 20 (12):1602–8.
7. Sormani MP, Rio J, Tintore M, Signori A, Li D, Cornelisse P, et al. Scoring treatment response in patients with relapsing multiple sclerosis. Mult Scler J. 2013; 19(5):605–12.
8. Sormani MP, Li DK, Bruzzi P, Stubinski B, Cornelisse P, Rocak S, et al. Combined MRI lesions and relapses as a surrogate for disability in multiple sclerosis. Neurology. 2011; 77(18):1684–90. doi: 10.1212/WNL.0b013e31823648b9 PMID: 21975200
9. Rio J, Castillo J, Rovira A, Tintore M, Sastre-Garriga J, Horga A, et al. Measures in the first year of therapy predict the response to interferon beta in MS. Multiple sclerosis. 2009; 15(7):848–53. doi: 10.1177/1352458509104591 PMID: 19542263
10. Rio J, Rovira A, Tintore M, Huerga E, Nos C, Tellez N, et al. Relationship between MRI lesion activity and response to IFN-beta in relapsing-remitting multiple sclerosis patients. Multiple sclerosis. 2008; 14 (4):479–84. doi: 10.1177/1352458507085555 PMID: 18562504

11. Hyun JW, Kim SH, Jeong IH, Ahn SW, Huh SY, Park MS, et al. Utility of the rio score and modified rio score in korean patients with multiple sclerosis. PLoS One. 2015; 10(5):e0129243. PubMed Central PMCID: PMCPMC4444088. doi: 10.1371/journal.pone.0129243 PMID: 26010897

12. Imitola J, Racke MK. Is No Evidence of Disease Activity a Realistic Goal for Patients With Multiple Sclerosis? Jama Neurol. 2015; 72(2):145–7. doi: 10.1001/jamaneurol.2014.3860 PMID: 25531742

13. Polman CH, O'Connor PW, Havrdova E, Hutchinson M, Kappos L, Miller DH, et al. A randomized, placebo-controlled trial of natalizumab for relapsing multiple sclerosis. New Engl J Med. 2006; 354(9):899–910. doi: 10.1056/NEJMoa044397 PMID: 16510744

14. Rudick RA, Stuart WH, Calabresi PA, Confavreux C, Galetta SL, Radue EW, et al. Natalizumab plus interferon beta-1a for relapsing multiple sclerosis. New Engl J Med. 2006; 354(9):911–23. doi: 10.1056/NEJMoa044396 PMID: 16510745

15. Feise RJ. Do multiple outcome measures require p-value adjustment? BMC medical research methodology. 2002; 2:8. PubMed Central PMCID: PMC117123. doi: 10.1186/1471-2288-2-8 PMID: 12069695

16. Saville DJ. Multiple Comparison Procedures—the Practical Solution. Am Stat. 1990; 44(2):174–80.

17. Bates D, Bartholome E. Treatment effect of natalizumab on relapse outcomes in multiple sclerosis patients despite ongoing MRI activity. J Neurol Neurosurg Psychiatry. 2012; 83(1):55–60. doi: 10.1136/jnnp-2011-300279 PMID: 21865211

18. Dobson R, Rudick RA, Turner B, Schmierer K, Giovannoni G. Assessing treatment response to interferon-beta: is there a role for MRI? Neurology. 2014; 82(3):248–54. PubMed Central PMCID: PMCPMC3902760. doi: 10.1212/WNL.0000000000000036 PMID: 24336144

19. Leray E, Yaouanq J, Le Page E, Coustans M, Laplaud D, Oger J, et al. Evidence for a two-stage disability progression in multiple sclerosis. Brain: a journal of neurology. 2010; 133(Pt 7):1900–13. PubMed Central PMCID: PMCPMC2892936.

20. Feinstein A, Freeman J, Lo AC. Progressive multiple sclerosis 2 Treatment of progressive multiple sclerosis: what works, what does not, and what is needed. Lancet Neurol. 2015; 14(2):194–207. doi: 10.1016/S1474-4422(14)70231-5 PMID: 25772898

Feeney C, Scott G, Raffel J, Roberts S, Coello C, Jolly A, Searle G, Goldstone AP, Brooks DJ, Nicholas RS, Trigg W, Gunn RN, Sharp DJ. Kinetic analysis of the translocator protein positron emission tomography ligand [18F]GE-180 in the human brain. Eur J Nucl Med Mol Imaging. 2016;43(12):2201-2210.

Eur J Nucl Med Mol Imaging (2016) 43:2201–2210
DOI 10.1007/s00259-016-3444-z

ORIGINAL ARTICLE

Kinetic analysis of the translocator protein positron emission tomography ligand [^{18}F]GE-180 in the human brain

Claire Feeney[1,4] · Gregory Scott[1] · Joel Raffel[1] · S. Roberts[1] · Christopher Coello[1] · Amy Jolly[1] · Graham Searle[1] · A. P. Goldstone[1] · David J. Brooks[1,2] · Richard S. Nicholas[1] · William Trigg[3] · Roger N. Gunn[1] · David J. Sharp[1]

Received: 28 January 2016 / Accepted: 14 June 2016 / Published online: 28 June 2016
© The Author(s) 2016. This article is published with open access at Springerlink.com

Abstract
Purpose PET can image neuroinflammation by targeting the translocator protein (TSPO), which is upregulated in activated microglia. The high nonspecific binding of the first-generation TSPO radioligand [^{11}C]PK-11195 limits accurate quantification. [^{18}F]GE-180, a novel TSPO ligand, displays superior binding to [^{11}C]PK-11195 in vitro. Our objectives were to: (1) evaluate tracer characteristics of [^{18}F]GE-180 in the brains of healthy human subjects; and (2) investigate whether the TSPO Ala147Thr polymorphism influences outcome measures.
Methods Ten volunteers (five high-affinity binders, HABs, and five mixed-affinity binders, MABs) underwent a dynamic PET scan with arterial sampling after injection of [^{18}F]GE-180. Kinetic modelling of time–activity curves with one-tissue and two-tissue compartment models and Logan graphical analysis was applied to the data. The primary outcome measure was the total volume of distribution (V_T) across various regions of interest (ROIs). Secondary outcome measures were the standardized uptake values (SUV), the distribution volume and SUV ratios estimated using a pseudoreference region.
Results The two-tissue compartment model was the best model. The average regional delivery rate constant (K_1) was 0.01 mL cm^{-3} min^{-1} indicating low extraction across the blood–brain barrier (1 %). The estimated median V_T across all ROIs was also low, ranging from 0.16 mL cm^{-3} in the striatum to 0.38 mL cm^{-3} in the thalamus. There were no significant differences in V_T between HABs and MABs across all ROIs.
Conclusion A reversible two-tissue compartment model fitted the data well and determined that the tracer has a low first-pass extraction (approximately 1 %) and low V_T estimates in healthy individuals. There was no observable dependency on the rs6971 polymorphism as compared to other second-generation TSPO PET tracers. Investigation of [^{18}F]GE-180 in populations with neuroinflammatory disease is needed to determine its suitability for quantitative assessment of TSPO expression.

Keywords Positron emission tomography (PET) · GE180 · Translocator protein (TSPO) · Kinetic analysis · Quantification · Neuroinflammation

Introduction

The translocator protein (TSPO) is a mitochondrial transporter involved in varied intracellular processes, but its expression in the central nervous system (CNS) is relatively low under normal physiological conditions [1]. However, activation of microglial cells caused by inflammatory stimuli results in significant upregulation of TSPO expression [2]. TSPO quantification with PET provides a measure of intrinsic neuroinflammation in a variety of CNS diseases. Early PET studies used the isoquinoline [^{11}C]PK-11195 to measure TSPO

Electronic supplementary material The online version of this article (doi:10.1007/s00259-016-3444-z) contains supplementary material, which is available to authorized users.

✉ Claire Feeney
c.feeney@imperial.ac.uk

1 Division of Brain Sciences, Hammersmith Hospital Campus, Imperial College London, London, UK

2 Institute of Clinical Medicine, Aarhus University, Aarhus, Denmark

3 GE Healthcare Ltd, Amersham, UK

4 Computational, Cognitive and Clinical Neuroimaging Laboratory, Hammersmith Hospital, 3rd Floor, Burlington Danes Building, Du Cane Road, London W12 0NN, UK

binding and detected elevations across a range of conditions including multiple sclerosis [3], Huntington's disease [4], Alzheimer's disease [5, 6], traumatic brain injury [7] and ischaemic stroke [8]. However, the use of [^{11}C]PK-11195 is limited by a high nonspecific signal, making nonstandard approaches to data analysis necessary [9]. In addition, because ^{11}C has a half-life of 20.3 min, the use of [^{11}C]PK-11195 is restricted to locations with an on-site cyclotron.

A number of second-generation TSPO ligands have been developed recently with the promise of improved signal-to-noise ratio and greater specific binding. [^{18}F]GE-180 is a novel fluorinated radiotracer that binds to the TSPO with high affinity [10]. Developed from a series of tricyclic indoles, [^{18}F]GE-180 has demonstrated superior specific binding affinity to [^{11}C]PK-11195 in animal models of acute neuroinflammation [11] and stroke [12]. The ^{18}F radiolabel, with a half-life of 109.8 min, also makes [^{18}F]GE-180 more suitable than ^{11}C-based compounds for long-distance distribution, enabling widespread clinical use.

Other second-generation TSPO radiotracers (e.g. [^{11}C]PBR-28, [^{18}F]PBR-06, [^{11}C]-DAA1106, [^{11}C]-DPA713, [^{18}F] FEPPA) show binding affinities influenced by a TSPO polymorphism expressed by individuals and have been classified as high-affinity binders (HABs), mixed-affinity binders (MABs) and low-affinity binders (LABs) [13]. Expression of the TSPO Ala147Thr polymorphism results in MAB or LAB depending on whether one or two copies are present [14]. Here, we report a study in healthy subjects using [^{18}F]GE-180 PET imaging. The primary aim was to investigate tracer kinetics and quantification in healthy human subjects. The secondary aim was to investigate whether there were differences in binding between HABs and MABs.

Materials and methods

Human subjects

This study was approved by the Westminster Research Ethics Committee, London (13/LO/1596), the Riverside Research Ethics Committee (13/LO/1916), and the Administration of Radioactive Substances Advisory Committee (no. 631/336/30788). Research was conducted in accordance with the principles of the Declaration of Helsinki [15]. All subjects gave written, informed consent.

Ten healthy volunteers (seven men), mean age 41 ± 9 years (range 28 – 56 years), mean weight 81.8 ± 13 kg, were included in the study. A screening assessment was carried out that included full medical and drug history, blood pressure, height, weight, Allen's test for patency of the ulnar anastomosis, and the Structured Clinical Interview for DSM disorders (SCID). Blood samples were taken for analysis of full blood count, renal profile, clotting screen and TSPO genotyping. Exclusion criteria included pregnancy, a history of prior or current psychiatric or neurological disease, abuse of alcohol or drugs and contraindication to arterial line placement.

TSPO genotyping

DNA was extracted using a Qiagen QIAmp DNA blood mini kit. TSPO genotyping of the c.439A > G (p.Thr147A1a) (SNP rs6971) was performed using a TaqMan allelic discrimination assay. LABs (one subject) were excluded from the imaging component of the study. During the study design it was felt that on ethical and economical grounds LABs should not be exposed to this novel tracer and instead that the focus should be on MABs and HABs. Of the ten subjects eligible for imaging, five were HABs and five were MABs.

Synthesis of [^{18}F]GE-180

[^{18}F]-Fluorine was produced by the ^{18}O(p,n)^{18}F nuclear reaction on a GE PETtrace 8 cyclotron (The Grove Centre, Amersham, UK). All radiochemistry was performed on a GE FASTlab synthesizer with single-use cassettes. The average synthesis time was 43 mins, radiochemical yield was 43 % and purity was greater than 95 % [16]. The radiotracer was manufactured by GE Healthcare (The Grove Centre, Amersham, UK), transported to Hammersmith Hospital, London, and used within 8 h of manufacture.

Positron emission tomography scanning and image reconstruction

All subjects were scanned at the Clinical Imaging Facility, Imperial College London, Hammersmith Hospital. Prior to PET scanning, an arterial cannula was inserted under local anaesthesia (2 % lidocaine) into the radial artery to allow arterial blood sampling. An antecubital venous cannula was inserted for radiotracer administration.

PET studies were performed on a Biograph 6 (six-slice CT) scanner after administration of 182 ± 3.1 MBq via intravenous bolus injection over 10 s followed by a 10-mL saline flush. A low-dose CT scan preceded the PET acquisition to allow correction for tissue attenuation. Emission data were then acquired over 90 min in list mode and reconstructed as 24 temporal frames (6 × 15, 3 × 60, 5 × 120, 5 × 300, 5 × 600 s) using filtered back-projection (matrix size 168 × 168, zoom 2.6, 5-mm gaussian filter, pixel size 1.56 × 1.56, slice thickness 3 mm) with and without attenuation correction. Standard corrections for scatter, decay and random counts were applied.

Whole-blood, plasma activity and parent fraction of [^{18}F] GE-180

Arterial blood activity was measured every second for the first 15 min of the 90-min scan using an automated blood sampling system (ABSS Allog, Mariefred, Sweden) connected to the subject via a 1.5 m × 1.0 mm diameter polytetrafluoroethylene line (blood withdrawal rate 2.5 ml/min). In addition, blood samples (10 mL) were collected manually from the radial artery at 0, 5, 10, 15, 30, 50, 70 and 90 min to assay whole-blood and plasma activity. Plasma was obtained by centrifugation for 3 min at 1,800 *g*. Activity in whole blood and plasma was measured in a CAPRAC-t well counter over 10 – 60 s. The first 15 min of continuous whole-blood activity was combined with the activity from discrete samples to generate the whole-blood activity curve for use in data modelling. The continuous plasma-to-blood ratio was estimated using a constant model and a total plasma activity curve was obtained by correcting the whole-blood curve for this partition between plasma and blood.

The parent fraction of [^{18}F]GE-180 was measured by high-performance liquid chromatography (Agilent 1,100 and 1,260 series) of discrete plasma samples (3.5 mL). The parent fraction was fitted to a single exponential plus a constant model. The total plasma activity was multiplied by this parent fraction and then smoothed post peak by fitting to a triexponential function to generate an arterial parent plasma input function. A delay correction of up to +30 s was applied to the input function prior to fitting the kinetic modelling. This was performed to account for delay in the 1.5-m tube (28.3 s) and delay between the radial artery and the brain.

Magnetic resonance imaging

To provide additional anatomical information to aid analysis of the PET data, each subject underwent a structural T1-weighted MRI scan on a Siemens Verio 3-T scanner (matrix size 256 × 256, voxel size 1 × 1 × 1 mm , TR 9.63 ms, TE 4.74 ms, flip angle 9°).

Data analysis

A high level overview of the data analysis is provided in Fig. 1. We used the PET data analysis and kinetic modelling toolkit, MIAKAT™ (www.miakat.org), which incorporates software from SPM5 (Wellcome Trust Centre for Neuroimaging) and FSL (FMRIB, University of Oxford) [17]. The brain was initially extracted from the T1-weighted MR images. The CIC neuroanatomical atlas [18] was nonlinearly registered to the individual's extracted brain in order to generate a personalized set of anatomically parcellated regions [18]. Frame-by-frame motion correction of the dynamic (without attenuation correction) PET data was performed using mutual information coregistration of the individual frames to a reference frame. An average motion-corrected PET image was generated and used for coregistration with the T1-weighted MR image. Finally, regional tissue time–activity curves (TACs) were generated for each region of interest (ROI) defined from the CIC atlas that had been transformed into each individual's image space.

Datasets were analysed with a one-tissue compartment (1TC) model and a two-tissue compartment (2TC) model and the Logan graphical method, using the metabolite-corrected plasma input function as previously described [19] with a fixed 5 % blood volume correction. The primary outcome measures were the radioligand delivery rate constant (K_1; mL cm^{-3} min^{-1}), total distribution volume (V_T: mL cm^{-3}), and standardized uptake values (SUV). The SUV ratio (SUVR) and distribution volume ratio (DVR) were estimated using the cortical grey matter as a pseudo reference region. This region was chosen as there is no true reference region for TSPO, but the cortical grey matter has been used as a reference in previous work as healthy brain usually shows low TSPO expression in this region [20].

Time stability analysis

To investigate the stability of V_T over different scan durations, a time stability analysis was performed by analysing data for total time windows that ranged between 40 and 90 min in 10-min increments.

Statistical analysis

The Akaike information criterion (AIC) was used to select the most appropriate compartment model [21], where lower AIC was indicative of a more parsimonious model. To compare characteristics between the genetic groups (HAB/MAB), Fisher's exact test (gender) and the Mann Whitney *U* test (age, weight, injected dose) were used. To evaluate differences in TACs for blood data between the genetic groups, a repeated measures analysis of variance (ANOVA) was used with time as the within-subjects factor and genotype as the between-subjects factor. A repeated measures ANOVA was also used to compare outcome measures across multiple ROIs, where ROI was used as the within-subjects factor.

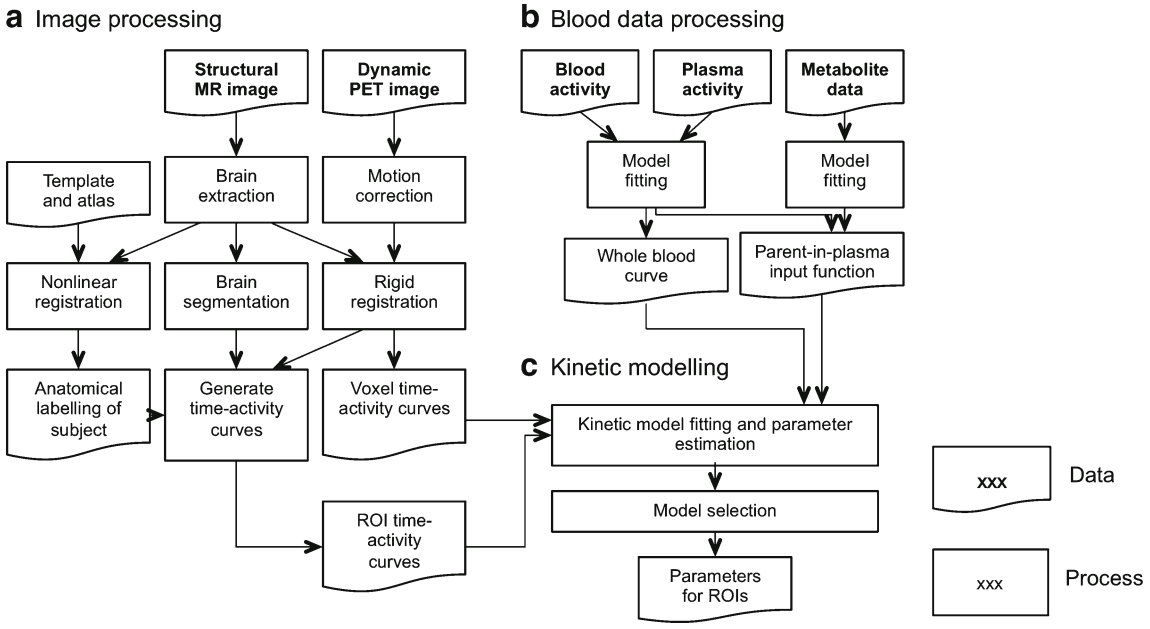


Fig. 1 Overview of data analysis. The MIAKAT™ analysis toolkit was used for image processing (**a**), blood data processing (**b**) and kinetic modelling (**c**) of the PET data

Results

Injection of [^{18}F]GE-180 caused no pharmacological effects based on patient reports, blood pressure, pulse, respiration rate and oxygen saturation after radioligand administration. There were no significant differences in gender, age or weight between HABs and MABs. With regard to correlations between age and the principal outcome measure, there were no significant correlations between age and V_T in either HABs and MABs in any of the ROIs studied (Spearman's rho = −0.3 – 0.7 $p = 0.188$ – 0.873 in HABs; Spearman's rho = 0.1 – 0.8, $p = 0.104$ – 0.94 in MABs). There were also no significant relationships between age and outcome measures when added as a covariate in the repeated measures ANOVA. Demographic data are provided in Supplementary Table 1.

Plasma data

In plasma, the concentration of [^{18}F]GE-180 peaked at about 45 s and then showed a rapid decrease (Fig. 2a). The fraction of unchanged [^{18}F]GE-180 over time is shown in Fig. 2b. The parent compound accounted for 65.0 – 81.7 % (range across subjects) of the total concentration in plasma at 30 min, and 57.3 – 78.3 % at 90 min. Three polar radioactive metabolites were identified over the course of the 90 min scanning window (<10 % of parent compound). The plasma-to-blood ratio remained constant at about 1.69 (Fig. 2c) across subjects. There were no significant differences in profiles of plasma over blood ($F(1,48) = 0.407$, $p = 0.541$), parent fraction ($F(1,48) = 0.871$, $p = 0.378$) or parent in plasma between genetic groups ($F(1,48) = 0.130$, $p = 0.728$). There was no interaction of genotype with time for any of these profiles ($p > 0.204$). The parent in plasma profiles for HABs and MABs are shown in Supplementary Fig. 1.

Tissue data

The concentration of the ligand in the brain peaked at around 1 min and then showed rapid washout in all subjects. Group-averaged tissue TACs for the frontal grey matter and thalamus are shown in Fig. 3a, b. A 60 – 90-min SUV image in a representative MAB subject is shown in Fig. 3c. Overall, there was low uptake of the tracer in brain with images being dominated by signal from blood vessels. There were no significant differences in SUV curves between genetic groups ($F(1,48) = 1.396$, $p = 0.271$). There was no interaction of genotype with time ($P = 0.684$).

Kinetic analysis

The results of the kinetic modelling are shown in Table 1. The 2TC model was superior to the 1TC model as judged by a

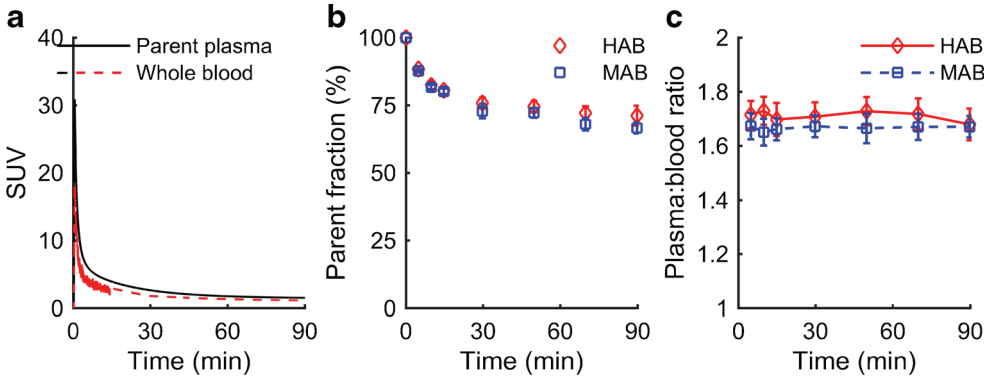


Fig. 2 Blood data. **a** Whole blood (*red*) and parent in plasma (*black*) curves for one subject. **b** The fraction of unchanged parent compound over time for high-affinity binders (*HAB*, *red*) and mixed-affinity binders (*MAB*, *blue*). **c** Plasma-to-blood ratio over time for HABs and MABs. Values are plotted in **b** and **c** as means ± standard error of the mean

lower AIC in all ROIs except the striatum. Example model fits for the 1TC and 2TC models are shown in Fig. 4a in a representative MAB subject. The first 10 min of Fig. 4a and Fig. 4c are shown in more detail in Supplementary Fig. 2. The 2TC model generally showed a good fit to the data except for an initial small mismatch in the blood volume peak, which was considered not to have affected V_T estimates. When we included the 2TC-fit model, it did not outperform the 2TC-fix based on the AIC. Blood volume estimates ranged from 6.3 % to 10.5 % (mean 8.4 %) across all ROIs. Therefore, the 2TC-fix was selected as the model to use for further analysis and gave average rate constants (across all regions and subjects) of $K_1 = 0.013$ mL cm^{-3} min^{-1}, $k_2 = 0.229$ min^{-1}, $k_3 = 0.035$ min^{-1} and $k_4 = 0.010$ min^{-1}, resulting in $V_T = 0.311$ mL cm^{-3} (Table 1).

K_1 was low across all ROIs in all subjects, indicating low extraction across the blood–brain barrier (BBB). This is consistent with the low tissue uptake observed in the images and the predominance of the vasculature structures. There was no significant effect of genetic group on any of the four rate

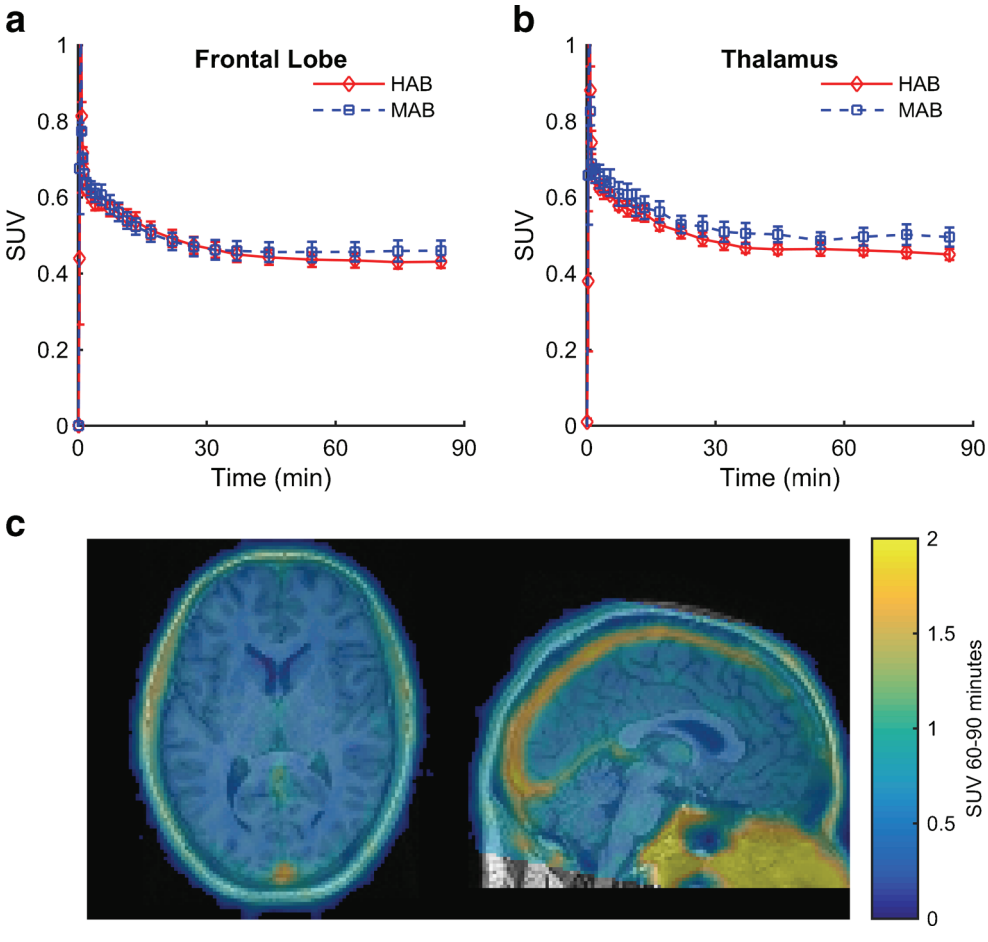


Fig. 3 Imaging data. Time–activity curves (TACs) are shown for high-affinity binders (*HAB*) and mixed-affinity binders (*MAB*) in the frontal grey matter (**a**) and thalamus (**b**). Standardized uptake values (SUV) are plotted as mean ± standard error of the mean. **c** SUV image calculated from the 60 – 90-min PET frames superimposed on the coregistered T1-weighted MR image in a representative MAB subject

Table 1 Parameter estimates and model fits

Model	Region	K_1 (mL/min)	k_2 (/min)	k_3 (/min)	k_4 (/min)	V_T (mL/cm^3)	Distribution volume ratio	AIC wins[a]
1TC	Frontal lobe	0.00472 (0.0041 – 0.006)	0.0271 (0.023 – 0.028)			0.171 (0.15 – 0.22)	0.939 (0.94 – 0.95)	2/10
	Parietal lobe	0.00513 (0.004 – 0.0061)	0.027 (0.024 – 0.028)			0.19 (0.16 – 0.22)	0.969 (0.96 – 1)	1/10
	Temporal lobe	0.00514 (0.0048 – 0.006)	0.0266 (0.025 – 0.028)			0.182 (0.17 – 0.24)	1.04 (1 – 1)	0/10
	Occipital lobe	0.00621 (0.0057 – 0.0074)	0.03 (0.025 – 0.032)			0.214 (0.19 – 0.25)	1.12 (1.1 – 1.2)	0/10
	Thalamus	0.00555 (0.0046 – 0.0058)	0.0261 (0.024 – 0.028)			0.182 (0.17 – 0.24)	1.03 (0.96 – 1.1)	0/10
	Striatum	0.00358 (0.003 – 0.0046)	0.0241 (0.021 – 0.025)			0.155 (0.14 – 0.2)	0.826 (0.78 – 0.89)	8/10
	Cerebellum	0.00656 (0.0054 – 0.0076)	0.0339 (0.034 – 0.034)			0.178 (0.16 – 0.22)	0.968 (0.91 – 1)	0/10
2TC	Frontal lobe	0.0102 (0.0089 – 0.013)	0.195 (0.15 – 1.6)	0.0301 (0.024 – 0.15)	0.00653 (0.004 – 0.017)	0.346 (0.26 – 0.5)	0.984 (0.96 – 1.2)	8/10
	Parietal lobe	0.0116 (0.011 – 0.014)	0.192 (0.15 – 0.25)	0.0334 (0.025 – 0.039)	0.00873 (0.0045 – 0.014)	0.33 (0.31 – 0.42)	1.01 (0.98 – 1.1)	9/10
	Temporal lobe	0.0143 (0.012 – 0.032)	0.217 (0.16 – 1.3)	0.0348 (0.03 – 0.15)	0.00927 (0.0063 – 0.016)	0.306 (0.27 – 0.42)	0.958 (0.93 – 1)	10/10
	Occipital lobe	0.0238 (0.019 – 0.031)	0.385 (0.2 – 0.62)	0.0395 (0.036 – 0.054)	0.0101 (0.0062 – 0.014)	0.35 (0.3 – 0.52)	1.07 (0.97 – 1.1)	10/10
	Thalamus	0.0118 (0.011 – 0.014)	0.16 (0.14 – 0.2)	0.0315 (0.026 – 0.042)	0.00881 (0.0062 – 0.012)	0.376 (0.28 – 0.41)	0.922 (0.81 – 1.1)	10/10
	Striatum	0.00413 (0.0033 – 0.0088)	1.14 (0.66 – 1.7)	4.89 (0.62 – 9.1)	0.14 (0.027 – 0.21)	0.155 (0.14 – 0.22)	0.451 (0.41 – 0.71)	2/10
	Cerebellum	0.0224 (0.016 – 1.3)	0.319 (0.23 – 78)	0.0331 (0.029 – 0.091)	0.0113 (0.0084 – 0.018)	0.281 (0.25 – 0.33)	0.916 (0.69 – 0.98)	10/10
Logan	Frontal lobe					0.265 (0.23 – 0.33)	0.931 (0.92 – 0.97)	
	Parietal lobe					0.284 (0.23 – 0.35)	0.996 (0.93 – 1)	
	Temporal lobe					0.312 (0.24 – 0.36)	1.01 (0.95 – 1.1)	
	Occipital lobe					0.34 (0.3 – 0.39)	1.14 (1.1 – 1.2)	
	Thalamus					0.3 (0.26 – 0.31)	0.991 (0.98 – 1)	
	Striatum					0.25 (0.21 – 0.29)	0.844 (0.7 – 0.92)	
	Cerebellum					0.29 (0.24 – 0.3)	0.99 (0.91 – 1)	

Data are presented as medians (interquartile ranges)

[a] For the 1TC model versus the 2TC model, the data shown are the proportions of the ten subjects for whom the model was the more parsimonious (defined as having the lower AIC)

constants. The Logan graphical method was also used to estimate the V_T in each ROI (Table 1). A representative plot is shown in Fig. 4b. Pooled V_T estimates from the 2TC model were positively correlated with V_T from the Logan method (Pearson's $r = 0.630$, $p < 0.0001$; regression equation $V_T(\text{Logan}) = 0.3 \times V_T(2\text{TC}) + 0.19$). The tissue TAC minus the whole-blood radioactivity curve demonstrated that approximately 20 % of the activity in a typical ROI came from blood (Fig. 4c).

Time stability analysis and outcome measures

The time stability analysis of the 2TC model demonstrated an increasing V_T for each successive time window analysed (shown for two ROIs in Fig. 4d). A comparison of six outcome measures for a number of ROIs is shown in Fig. 5. For all six outcome measures, no significant effect of genetic group was found ($p > 0.186$), nor was there any interaction between genetic group and ROI ($p = 0.468$).

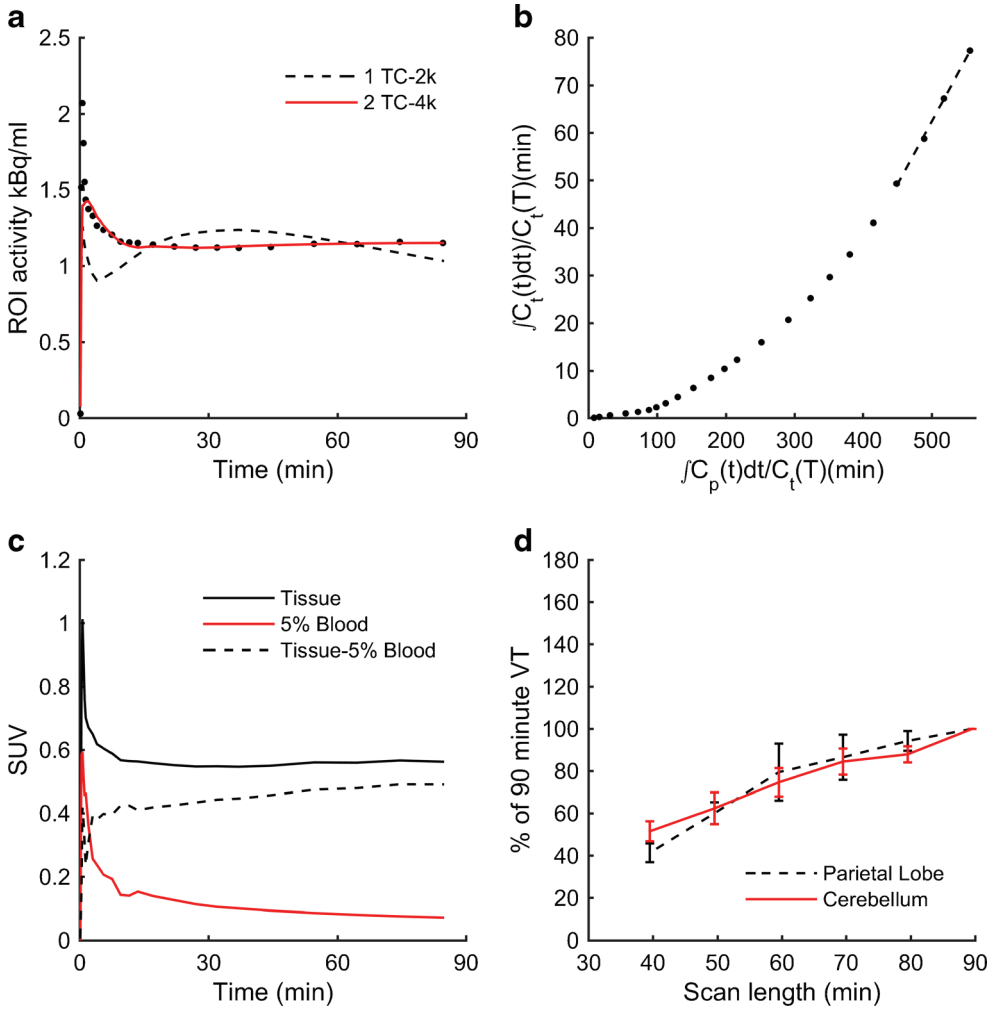


Fig. 4 Kinetic modelling and time stability analysis. **a** Model fits are shown for one-tissue compartment model (reversible 1TC, *dashed line*) and two-tissue compartment model (reversible 2TC, *red line*) against a time–activity curve (*black dots*) for the parietal lobe. **b** Logan plot (*black dashed line* the most linear portion of the curve) for the same time–activity curve as in **a**. **c** Parietal lobe time–activity curve (*solid line*), 5 % whole-blood activity curve (*red line*) and the curve of the difference between the two curves (*dashed line*) highlights the significant contribution of blood signal to the time–activity curve. **d** Estimates of two-tissue compartment model V_T calculated for 40 – 90-min scan windows in 10-min increments plotted as the absolute percentage difference compared to the final 90-min V_T for the parietal lobe and cerebellum grey matter regions of interest. The values plotted are means ± standard error of the mean

Discussion

Here we describe the characterization and quantification of the novel TSPO tracer [^{18}F]GE-180 for the first time in the normal healthy human brain. We generated arterial parent plasma and whole-blood input functions and fitted brain TACs to 1TC and 2TC kinetic models and Logan graphical analysis to generate outcome measures across regions and individuals. The following key outcome measures were generated from the analysis: K_1, V_T, SUV, DVR and SUVR with the cortical grey matter as a pseudo reference region. In addition, we investigated whether the TSPO Ala147Thr polymorphism in the TSPO binding site influenced these outcome measures [14, 22].

There was consistent and stable metabolism of [^{18}F]GE-180 parent compound across all individuals. There was no difference in blood or plasma activity between the two genotypes and there were only moderate levels of detectable metabolites in all individuals with 70 % of the intact parent tracer remaining at 90 min. SUV images across all individuals demonstrated low uptake of the tracer in brain tissue with significant tracer activity apparent in the blood compartments of the brain. The low brain uptake could reduce the signal-to-noise ratio for this tracer and might mean that variation in the activity within the blood across the groups could have biased results. In addition, the low uptake might make the tracer more susceptible to showing increased uptake when there is BBB breakdown.

Analysis of the tracer compartment models showed that the reversible 2TC model provided the best overall fit in the majority of cases. There was a small discrepancy in the model fit at the initial sharp peak of the curve, i.e. <5 min of data acquisition. It is possible that this may be due to increased dispersion of [^{18}F]GE-180 in the vascular bed, although this is difficult to quantify precisely. In addition, the 1.5-m line that was used from the radial artery to the arterial blood detection machine may have affected the model fit. However, this discrepancy should not significantly affect the estimation of V_T as this is based on the integral of the impulse response function (i.e. integral/area under the curve of plasma input function) [23]. K_1 could be affected by dispersion but would still remain

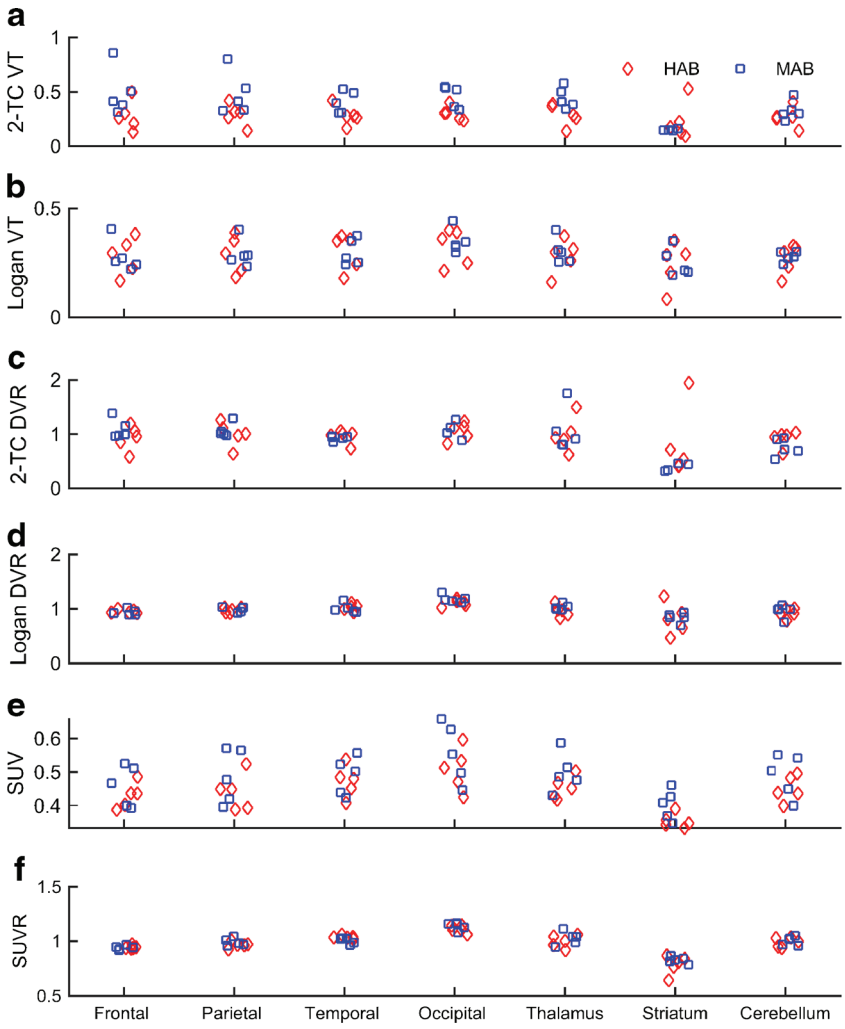


Fig. 5 Outcome measures. Six outcome measures for seven regions of interest (*red* high-affinity binders, *blue* mixed-affinity binders). **a** Two-tissue compartment model volume of distribution (*2-TC VT*). **b** Volume of distribution estimated using Logan plot (*Logan VT*). **c** Distribution volume ratio from the two-tissue compartment model using cortical grey matter as a reference region (*2-TC DVR*). **d** Distribution volume ratio estimated using Logan plot and cortical grey matter as a reference region (*Logan DVR*). **e** 60 – 90 min standardized uptake values (**e** *SUV*). **f** 60 – 90 min standardized uptake value ratios (**f** *SUVR*) using cortical grey matter as a reference region

small after any correction and therefore the interpretation of low brain delivery of this tracer is still valid.

Using the 2TC model, the initial rate constant, K_1, was consistently low, suggesting a low extraction fraction and delivery into brain tissue. Theoretically, there could be a number of reasons for this. First, the low K_1 could be due to low lipophilicity. However, preclinical work has suggested that this tracer is relatively lipophilic (log*D* at pH 7.4 is 2.95), making this unlikely. Second, [^{18}F]GE-180 could be a substrate for xenobiotic pumps at the BBB such as the three major ABC transporters, p-glycoprotein (ABCB1), multidrug resistance protein 1 (ABCC1) and mitoxantrone resistance protein (ABCG2), as can be seen with other tracers with low BBB penetration [24]. Third, the low K_1 could be due to increased plasma protein binding, although the relationship here is complex and high plasma protein binding does not always lead to low brain penetration. Most molecules to a greater or lesser extent bind to human serum albumin and some tracers also bind to alpha1-acid glycoprotein [25]. However, in the case of [^{18}F]GE-180, the binding affinity to these or other plasma proteins may be considerable. A limitation of this study was that the protein binding of [^{18}F]GE-180 was not measured. However, in vitro work suggests that in humans the plasma free fraction is approximately 3 %.

The median volume of distribution of [^{18}F]GE-180 using the 2TC model across all subjects and brain regions ranged from 0.16 to 0.38 mL cm^{-3}. There was little variability across brain regions. V_T estimates were lower than those observed for some other second-generation TSPO tracers (e.g. 4.1 ± 1.6 mL cm^{-3} for [^{11}C]-PBR-28 in grey matter [26], and 0.72 – 1.06 mL cm^{-3} for [^{11}C]PK-11195 [27]).

Our time stability analysis demonstrated that V_T did not reach a stable level but continuously increased over the 90-min scanning window. This might have led to underestimation of V_T. A scan time of 90 min was originally selected based on preclinical studies and on consideration of what would be acceptable to the individual subjects. However, our results suggest that a longer scanning duration might give a more 'stable' V_T estimate. This ongoing increase in V_T could have been caused by the accumulation of radiometabolites in the brain. However, only modest levels of metabolites were detected in the blood, and earlier preclinical work demonstrated

very low penetration of any metabolite into the brain with 94 % parent at 60 min [28]. Metabolites have not formally been identified, but all those observed in this study were more polar than the parent. It is believed that the two main routes of metabolism are *O*-demethylation and hydroxylation of the aliphatic ring [28]. Other metabolites could be a combination of the two processes or hydroxylation at different sites. The question of accumulation of metabolites in the brain is most relevant when brain uptake is high, which was not the case here. It is also worth noting that these time stability results are consistent with those from other TSPO tracers which also do not achieve a stable estimate within a 2-h scanning window, e.g. [^{11}C]PBR28 [19].

No evidence of an effect of TSPO genotype on any of our outcome measures was found. No differences in K_1, V_T, DVR, SUV or SUVR between MABs and HABs were found. This was an unexpected finding, as in vitro work with cold GE-180 displacing [^{3}H]PK11195 has shown a binding affinity of 15:1 between HABs and LABs (D. Owen, personal communication). Although we did not acquire PET scans in LABs, we would still have expected to see differences in the outcome measures between HABs and MABs. Our expectation was that MABs would show an intermediate binding relative to that in HABs, i.e. around 50 % of the binding in HABs [13]. The fact that we did not observe such a difference in vivo may have been a consequence of the low uptake seen with this tracer. Genotype effects may be found in other groups, for example older individuals or diseased individuals in whom we may expect microglial TSPO expression to be higher. We did consider the effect that increasing age of the subjects could have had on TSPO binding, as has been shown previously [29], but we did not find any correlations between age and V_T in any of the ROIs.

In summary, we report the first PET studies of [^{18}F]GE-180 in humans. Administration of the tracer was safe and the scan was tolerated well by all subjects. A reversible 2TC model fitted the data well and determined that the tracer has a low first-pass extraction (about 1 %) and low V_T estimates in our healthy subjects. There was no observable dependency on the rs6971 polymorphism as compared to other second-generation TSPO PET tracers. A low first-pass extraction combined with a tissue signal with a relatively large blood component suggests similarities to [^{11}C]PK-11195 in vivo. However, more work with [^{18}F]GE-180 in humans would be informative and should include studies in patients with neuroinflammatory conditions to assess signal in the presence of upregulated TSPO, studies in subjects of various ages and a competition study to more clearly delineate specific binding.

Acknowledgments We thank all the subjects who participated in the study. GE Healthcare provided [^{18}F]GE-180 free of charge.

Author contributions statement C.F. contributed to acquisition of data and analysis of data, and drafted the article. G.Scott contributed to analysis of data, and drafted the article. J.R. contributed to acquisition of data and analysis of data. and drafted the article. S.R. contributed to acquisition of data. and revised the article. C.C. contributed to analysis and interpretation of the data, and revised the article. A.J. contributed to analysis of data and revised the article. G.Searle contributed to analysis of data and revised the article. D.B. revised the article. R.N. revised the article. W.T. revised the article. R.G. contributed to analysis and interpretation of data, and revised the article. D.J.S. designed the study, contributed to analysis of the data and revised the article. All authors approved the manuscript.

Compliance with ethical standards

Funding D.J.S. has a National Institute of Health Research Professorship (RP-011-048). C.F. has an MRC Clinical Research Fellowship and G.Scott has a Wellcome Trust and GlaxoSmithKline Clinical Research Fellowship. The work was also supported by the National Institute of Health Imperial College Biomedical Research Centre, a grant to R.S.N. from GE Healthcare Ltd with support from Fast Forward LLC (National Multiple Sclerosis Society) and GE Healthcare.

Conflicts of interest W.T. is an employee of GE Healthcare. J.R. has received funding for his salary from GE Healthcare Ltd with support from Fast Forward LLC (National Multiple Sclerosis Society). All other authors declare no conflicts of interest.

Ethical approval All procedures performed in studies involving human subjects were in accordance with the ethical standards of the institutional research committee and with the principles of the 1964 Declaration of Helsinki and its later amendments or comparable ethical standards.

Informed consent Informed consent was obtained from all individual subjects included in the study.

Open Access This article is distributed under the terms of the Creative Commons Attribution 4.0 International License (http://creativecommons.org/licenses/by/4.0/), which permits unrestricted use, distribution, and reproduction in any medium, provided you give appropriate credit to the original author(s) and the source, provide a link to the Creative Commons license, and indicate if changes were made.

References

1. Cosenza-Nashat M, Zhao ML, Suh HS, Morgan J, Natividad R, Morgello S, et al. Expression of the translocator protein of 18 kDa by microglia, macrophages and astrocytes based on immunohistochemical localization in abnormal human brain. Neuropathol Appl Neurobiol. 2009;35(3):306–28.
2. Chen MK, Guilarte TR. Translocator protein 18 kDa (TSPO): molecular sensor of brain injury and repair. Pharmacol Ther. 2008;118(1):1–17.
3. Banati RB, Newcombe J, Gunn RN, Cagnin A, Turkheimer F, Heppner F, et al. The peripheral benzodiazepine binding site in the brain in multiple sclerosis: quantitative in vivo imaging of microglia as a measure of disease activity. Brain J Neurol. 2000;123(Pt 11):2321–37.
4. Pavese N, Gerhard A, Tai YF, Ho AK, Turkheimer F, Barker RA, et al. Microglial activation correlates with severity in Huntington disease: a clinical and PET study. Neurology. 2006;66(11):1638–43.
5. Cagnin A, Brooks DJ, Kennedy AM, Gunn RN, Myers R, Turkheimer FE, et al. In-vivo measurement of activated microglia in dementia. Lancet. 2001;358(9280):461–7.

6. Edison P, Archer HA, Gerhard A, Hinz R, Pavese N, Turkheimer FE, et al. Microglia, amyloid, and cognition in Alzheimer's disease: an [11C](R)PK11195-PET and [11C]PIB-PET study. Neurobiol Dis. 2008;32(3):412–9.
7. Ramlackhansingh AF, Brooks DJ, Greenwood RJ, Bose SK, Turkheimer FE, Kinnunen KM, et al. Inflammation after trauma: microglial activation and traumatic brain injury. Ann Neurol. 2011;70(3):374–83.
8. Gerhard A, Schwarz J, Myers R, Wise R, Banati RB. Evolution of microglial activation in patients after ischemic stroke: a [11C](R)-PK11195 PET study. Neuroimage. 2005;24(2):591–5.
9. Kropholler MA, Boellaard R, Schuitemaker A, Folkersma H, van Berckel BN, Lammertsma AA. Evaluation of reference tissue models for the analysis of [11C](R)-PK11195 studies. J Cereb Blood Flow Metab. 2006;26(11):1431–41.
10. Wadsworth H, Jones PA, Chau WF, Durrant C, Fouladi N, Passmore J, et al. [18F]GE-180: a novel fluorine-18 labelled PET tracer for imaging translocator protein 18 kDa (TSPO). Bioorg Med Chem Lett. 2012;22(3):1308–13.
11. Dickens AM, Vainio S, Marjamaki P, Johansson J, Lehtiniemi P, Rokka J, et al. Detection of microglial activation in an acute model of neuroinflammation using PET and radiotracers 11C-(R)-PK11195 and 18F-GE-180. J Nucl Med. 2014;55(3):466–72.
12. Boutin H, Murray K, Pradillo J, Maroy R, Smigova A, Gerhard A, et al. 18F-GE-180: a novel TSPO radiotracer compared to 11C-R-PK11195 in a preclinical model of stroke. Eur J Nucl Med Mol Imaging. 2015;42(3):503–11.
13. Owen DR, Gunn RN, Rabiner EA, Bennacef I, Fujita M, Kreisl WC, et al. Mixed-affinity binding in humans with 18-kDa translocator protein ligands. J Nucl Med. 2011;52(1):24–32.
14. Owen DR, Yeo AJ, Gunn RN, Song K, Wadsworth G, Lewis A, et al. An 18-kDa translocator protein (TSPO) polymorphism explains differences in binding affinity of the PET radioligand PBR28. J Cereb Blood Flow Metab. 2012;32(1):1–5.
15. General Assembly of the World Medical Association. World Medical Association Declaration of Helsinki: ethical principles for medical research involving human subjects. J Am Coll Dent. 2014;81(3):14–8.
16. Wickstrom T, Clarke A, Gausemel I, Horn E, Jorgensen K, Khan I, et al. The development of an automated and GMP compliant FASTlab synthesis of [(18)F]GE-180; a radiotracer for imaging translocator protein (TSPO). J Labelled Comp Radiopharm. 2014;57(1):42–8.
17. Searle G, Reis Marques T, Plisson C, Natesan S, Howes O, Tzortzi A, et al. Kinetic analysis of [11C]-IMA107, a novel PET radiotracer for PDE10A. J Nucl Med Meeting Abstracts. 2014;55 Suppl 1:204.
18. Tziortzi AC, Searle GE, Tzimopoulou S, Salinas C, Beaver JD, Jenkinson M, et al. Imaging dopamine receptors in humans with [11C]-(+)-PHNO: dissection of D3 signal and anatomy. Neuroimage. 2011;54(1):264–77.
19. Fujita M, Imaizumi M, Zoghbi SS, Fujimura Y, Farris AG, Suhara T, et al. Kinetic analysis in healthy humans of a novel positron emission tomography radioligand to image the peripheral benzodiazepine receptor, a potential biomarker for inflammation. Neuroimage. 2008;40(1):43–52.
20. Owen DR, Guo Q, Kalk NJ, Colasanti A, Kalogiannopoulou D, Dimber R, et al. Determination of [(11)C]PBR28 binding potential in vivo: a first human TSPO blocking study. J Cereb Blood Flow Metab. 2014;34(6):989–94.
21. Akaike H. A new look at the statistical model identification. IEEE Trans Automat Contr. 1974;19(6):716–23.
22. Guo Q, Colasanti A, Owen DR, Onega M, Kamalakaran A, Bennacef I, et al. Quantification of the specific translocator protein signal of 18F-PBR111 in healthy humans: a genetic polymorphism effect on in vivo binding. J Nucl Med. 2013;54(11):1915–23.
23. Gunn RN, Gunn SR, Cunningham VJ. Positron emission tomography compartmental models. J Cereb Blood Flow Metab. 2001;21(6):635–52.
24. Toth M, Haggkvist J, Varrone A, Finnema SJ, Doorduin J, Tokunaga M, et al. ABC transporter-dependent brain uptake of the 5-HT1B receptor radioligand [(11)C]AZ10419369: a comparative PET study in mouse, rat, and guinea pig. EJNMMI Res. 2014;4(1):64.
25. Lockhart A, Davis B, Matthews JC, Rahmoune H, Hong G, Gee A, et al. The peripheral benzodiazepine receptor ligand PK11195 binds with high affinity to the acute phase reactant alpha1-acid glycoprotein: implications for the use of the ligand as a CNS inflammatory marker. Nucl Med Biol. 2003;30(2):199–206.
26. Park E, Gallezot JD, Delgadillo A, Liu S, Planeta B, Lin SF, et al. (11)C-PBR28 imaging in multiple sclerosis patients and healthy controls: test-retest reproducibility and focal visualization of active white matter areas. Eur J Nucl Med Mol Imaging. 2015;42(7):1081–92.
27. Jucaite A, Cselenyi Z, Arvidsson A, Ahlberg G, Julin P, Varnas K, et al. Kinetic analysis and test-retest variability of the radioligand [11C](R)-PK11195 binding to TSPO in the human brain – a PET study in control subjects. EJNMMI Res. 2012;2:15.
28. Chau WF, Black AM, Clarke A, Durrant C, Gausemel I, Khan I, et al. Exploration of the impact of stereochemistry on the identification of the novel translocator protein PET imaging agent [(18)F]GE-180. Nucl Med Biol. 2015;42:711–9
29. Schuitemaker A, van der Doef TF, Boellaard R, van der Flier WM, Yaqub M, Windhorst AD, et al. Microglial activation in healthy aging. Neurobiol Aging. 2012;33(6):1067–72.

Sridharan S*, Raffel J*, Nandoskar A, Record C, Brooks DJ, Owen D, Sharp D, Muraro PA, Gunn R, Nicholas R. Confirmation of specific binding of the 18-kDa Translocator Protein (TSPO) radioligand [18F]GE-180: a blocking study using XBD173 in multiple sclerosis normal appearing white and grey matter. Mol Imaging Biol. 2019;21(5):935-944

(*joint first authors)

MOLECULAR IMAGING AND BIOLOGY

Mol Imaging Biol (2019) 21:935–944
DOI: 10.1007/s11307-019-01323-8
© The Author(s), 2019
Published Online: 22 February 2019

WMIS World Molecular Imaging Society

Check for updates

RESEARCH ARTICLE

Confirmation of Specific Binding of the 18-kDa Translocator Protein (TSPO) Radioligand [^{18}F]GE-180: a Blocking Study Using XBD173 in Multiple Sclerosis Normal Appearing White and Grey Matter

Sujata Sridharan,[1] Joel Raffel,[1] Ashwini Nandoskar,[1] Chris Record,[1] David J. Brooks,[1,2,3] David Owen,[1] David Sharp,[1] Paolo A. Muraro,[1] Roger Gunn,[4] Richard Nicholas[1]

[1]*Division of Brain Sciences, Faculty of Medicine, Imperial College London, Hammersmith Hospital Campus, Burlington Danes Building, Du Cane Road, London, W12 0NN, UK*
[2]*Institute of Clinical Medicine, Aarhus University, Aarhus, Denmark*
[3]*Institute of Neuroscience, Newcastle upon Tyne University, Newcastle upon Tyne, UK*
[4]*Invicro Ltd., London, UK*

Abstract

Purpose: Measurements of non-displaceable binding (V_{ND}) of positron emission tomography (PET) ligands are not often made *in vivo* in humans because they require ligands to displace binding to target receptors and there are few readily available, safe ones to use. A technique to measure V_{ND} for ligands for the 18-kDa translocator protein (TSPO) has recently been developed which compares the total volume of distribution (V_T) before and after administration of the TSPO ligand XBD173. Here, we used XBD173 with an occupancy plot to quantify V_{ND} for two TSPO radiotracers, [^{18}F]GE-180 and [^{11}C]PBR28, in cohorts of people with multiple sclerosis (MS). Additionally, we compared plots of subjects carrying high (HAB) or mixed binding (MAB) affinity polymorphisms of TSPO to estimate V_{ND} without receptor blockade.

Procedures: Twelve people with MS underwent baseline MRI and 90-min dynamic [^{18}F]GE-180 PET or [^{11}C]PBR28 PET ($n = 6$; three HAB, three MAB each). Arterial blood sampling was used to generate plasma input functions for the two-tissue compartment model. V_{ND} was calculated using two independent methods: the occupancy plot (by modelling the differences in signal post XBD173) and the polymorphism plot (by modelling the differences in signal across presence and absence of rs6971 genotypes).

Results: Whole brain V_T (mean ± standard deviation) was 0.29 ± 0.17 ml/cm^3 for [^{18}F]GE-180 and 5.01 ± 1.88 ml/cm^3 for [^{11}C]PBR28. Using the occupancy and polymorphism plots respectively, V_{ND} for [^{18}F]GE-180 was 0.11 ml/cm^3 (95 % CI = 0.02, 0.16) and 0.20 ml/cm^3 (0.16, 0.34), accounting for, on average, 55 % of V_T in the whole brain. For [^{11}C]PBR28, these values were 3.81 ml/cm^3 (3.02, 4.21) and 3.49 ml/cm^3 (1.38, 4.27), accounting for 67 % of average whole brain V_T.

Sujata Sridharan and Joel Raffel are joint first authors.

Correspondence to: Sujata Sridharan; *e-mail:* s.sridharan@imperial.ac.uk

Conclusions: Although V_T for [18F]GE-180 is low, indicating low brain penetration, half the signal shown by MS subjects reflected specific TSPO binding. V_T for [11C]PBR28 was higher and two thirds of the binding was non-specific. No brain ROIs were devoid of specific signal, further confirming that true reference tissue approaches are potentially problematic for estimating TSPO levels.

Key words: PET, Occupancy plot, Polymorphism plot, Multiple sclerosis, [18F]GE-180, [11C]PBR28, XBD173

Introduction

Several positron emission tomography (PET) ligands exist for the 18-kDa translocator protein (TSPO), which can be upregulated in the mitochondria of activated microglia when the central nervous system becomes inflamed (see [1] for review). Currently, it is unclear, in humans, what proportion of the observed *in vivo* PET signal represents specific TSPO binding and what proportion is merely non-displaceable binding. This is a particular problem with TSPO imaging as (1) the binding of a large majority of TSPO ligands is affected by carriage of a single nucleotide polymorphism (SNP rs6971) and (2) affinity thus varies according to whether participants are homozygotic (high or low affinity binders, HABs/LABs) or heterozygotic (mixed affinity binders, MABs). This results in increased tracer-specific variability across cohorts [2]. TSPO is known to be expressed ubiquitously throughout the human brain, meaning that there is no suitable reference region (free of specific binding) which would allow the non-displaceable proportion of the signal to be estimated *in vivo* (see [3] for overview). Assuming that the fraction of non-displaceable binding is negligible can dramatically affect the interpretation of results. It is therefore important to investigate the proportion of binding that is specific for each TSPO tracer [4, 5].

Approaches recently described by Owen et al. [6] and Guo et al. [7] can be used to estimate the non-displaceable component of the total volume of distribution (V_{ND}) *in vivo*. In short, for the TSPO ligand of interest, the total volume of distribution, V_T, is calculated both before and after blockade with the TSPO ligand XBD173. V_{ND} is derived from the *x*-intercept of the graph of $V_T^{baseline}$ against $V_T^{baseline}-V_T^{block}$ (see 'Materials and Methods'). In addition, use of a polymorphism plot (Guo, et al. [8]), which assumes that MABs express an equal percentage of high and low affinity binding sites [6, 9], allows V_{ND} to be derived from the *x*-intercept of V_T^{HAB} against $V_T^{HAB}-V_T^{MAB}$ (see 'Materials and Methods').

One recently developed ligand, [18F]GE-180, has exhibited a higher signal to background ratio than (R)-[11C]PK11195 in several preclinical models [10–12]. However, in human studies, it has shown unexpectedly low brain penetration [13–15]. Additionally, *in vitro* data shows that binding of [18F]GE-180 to TSPO is sensitive to the presence of the rs6971 SNP [2, 9, 16]; however, in these *in vivo* human studies, the expected genotype dependence of signals was not observed [13, 14]. This phenomenon may be due to poor extraction of [18F]GE-180 over the blood–brain barrier (BBB) and/or the action of active efflux pumps such as P-glycoprotein. Given these unexpected results, we wished to clarify the proportion of [18F]GE-180 uptake detected with PET in the human brain that is non-displaceable. A recent blocking study in healthy control subjects confirmed the presence of specific binding throughout the human brain with [11C]PBR28 [6]. Here, we describe a similar blocking study to investigate whether (and what proportion of) [18F]GE-180 and [11C]PBR28 PET signal is specific to TSPO binding in people with multiple sclerosis (MS).

Materials and Methods

Participants

Twelve people with clinically definite MS according to revised 2010 MacDonald criteria were recruited from the Imperial College Healthcare NHS Trust. The participants were aged between 20 and 50 years old and provided written informed consent, under ethics reviewed by the London Riverside Research Ethics Committee (REC reference 14/LO/0343 [18F]GE-180-scanned participants, 13/LO/1916 [11C]PBR28-scanned participants).

Participants attended a screening visit, including clinical ratings with the expanded disability status scale (EDSS) [17] and the collection of blood, to establish TSPO SNP genotype. Predicted LABs were excluded. Participants returned for a baseline visit where they underwent MRI and a 90-min dynamic [18F]GE-180 or [11C]PBR28 PET scan. One week later [18F]GE-180, or on the afternoon of the same day [11C]PBR28, participants returned for a 'post-blockade' scan; they were administered a 90-mg oral dose of XBD173 2 h prior to a repeat PET scan with the same tracer and dose as previously administered. The dose of 90 mg was selected based on that previously calculated by Owen et al. in a blocking study using [11C]PBR28 to achieve at least 75 % XBD173 occupancy in adult participants [6].

Arterial Plasma Measurement

Participants had radial artery cannulation and blood was withdrawn continuously at a target rate of 2.5 ml min^{-1} from the start of each scan for the first 15 min. In addition, discrete blood samples were drawn at 0, 5, 10, 15, 30, 50, 70 and 90 min ([18F]GE-180) or 0, 5, 10, 15, 20, 25, 30, 40, 50, 60, 70, 80 and 90 min ([11C]PBR28) for metabolite analysis. For [18F]GE-180, tracer concentrations in whole blood and plasma were measured in a well counter and radiometabolite analysis performed using two high performance liquid chromatography (HPLC) systems (Agilent 1260 Infinity and Agilent 110 Series) in isocratic mode. Briefly, samples were spun down to obtain plasma, which was then added to HPLC-grade acetonitrile to precipitate proteins. After centrifugation, the samples were rotary evaporated and analytes collected and reconstituted in 7 % ethanol solution and filtered in 15-mm syringe filters with a nylon membrane of pore size 0.2 μm. For [11C]PBR28, methods described by Owen et al. [6] were used to determine the parent fraction of tracer in plasma and whole blood.

Scanning Protocol

All participants scanned with [18F]GE-180 underwent MR scans on a 3-T Siemens Magnetom MR B19 scanner, including T1 magnetisation prepared rapid gradient echo (MPRAGE) sequences. [18F]GE-180 was synthesised, as previously described, on a FastLab™ platform [18]. A low-dose CT scan was performed for attenuation correction immediately prior to a 90-min dynamic PET scan on a Siemens Biograph 6 with a field of view of 168 × 168 × 148 mm^3. The tracer was injected as an intravenous bolus over the course of 30 s with a target dose of 185 MBq. List-mode data were histogrammed into 24 frames (6 × 15 s, 3 × 60 s, 5 × 120 s, 5 × 300 s and 5 × 600 s) and reconstructed using filtered back projection (FBP) with a ramp filter. Reconstructed voxel size and spatial resolution were 1.57 × 1.57 × 1.92 and ~5 mm, respectively. For participants scanned with [11C]PBR28, MR scans were performed on a Siemens Magnetom Trio scanner, while PET scans were also performed on a Siemens Biograph 6, with list-mode data histogrammed into 26 frames (8 × 15 s, 3 × 60 s, 5 × 120 s, 5 × 300 s and 5 × 600 s) and reconstructed using FBP with a 5-mm Gaussian filter. For [18F]GE-180 scans, the tracer was injected 30 s after scan start time (two fewer frames in the reconstruction).

Image Analysis

PET images underwent frame-to-frame realignment and were coregistered with T1 MRI in PMOD (v3.6, PMOD Technologies Ltd., Switzerland). Coregistrations were quality checked manually. MRI was used to segment the brain into 83 regions using the Hammers atlas [19]. These regions were inspected manually for overlap and edited where necessary to minimise spillover from large-vessel vascular activity. Respective smaller ROIs were then combined to create final bilateral ROIs as follows: frontal, temporal, parietal and occipital lobes (FL, TL, PL, OL), striatum, putamen, thalamus, cerebellum, corpus callosum, brainstem, whole brain (WB) and normal appearing white matter (NAWM). Lesions were defined semi-automatically on MRI using a local thresholding technique implemented in in-house software (BioMedIA group, Department of Computing, Imperial College London). T1, T2 fluid attenuated inversion recovery (FLAIR), double inversion recovery (DIR) and phase sensitive inversion recovery (PSIR) sequences were used to maximise sensitivity of lesion identification. All ROIs excluded lesions.

Kinetic Analysis

All kinetic analysis was performed in PMOD. Calibrated continuous and discrete blood data were corrected for decay and the parent fraction of tracer in plasma was calculated for each discrete sample. Plasma over blood (POB) ratios were calculated and the parent fraction of tracer in plasma fitted to a Watabe parent fraction model [20] of the form $f_{\text{parent}}(t) = f_{\text{p}} \cdot \left\{ \frac{1}{1-\left(\frac{A^B}{u^B+C}\right)} \right\}$, where f_{p} is the free fraction of parent tracer and A, B, C and u are constants. This was multiplied with the continuous whole blood data to produce a metabolite-corrected arterial plasma input function. V_{T} was calculated from the unconstrained two-tissue compartment model as previously described [13, 14].

Calculating the Component of Non-Displaceable Binding

Three methods were used to determine the non-displaceable (V_{ND}) and displaceable (V_{S}) components of the total volume of distribution (V_{T}). Of these methods, two were independent: the occupancy plot (methods 1a and 1b) and the polymorphism plot (method 2).

Method 1a: Occupancy Plot with Individual V_{ND}

The occupancy plot is an adaptation of the Lassen plot described by Cunningham et al. [4]. Given that $V_{\text{T}}^{\text{baseline}} = V_{\text{S}} + V_{\text{ND}}$ (baseline condition) and $V_{\text{T}}^{\text{block}} = V_{\text{S}}\left(1-Occ_{\text{drug}}\right) + V_{\text{ND}}$ (block condition), it follows that $V_{\text{T}}^{\text{baseline}} - V_{\text{T}}^{\text{block}} = Occ_{\text{drug}} \cdot \left(V_{\text{T}}^{\text{baseline}} - V_{\text{ND}}\right)$. Thus, plotting $V_{\text{T}}^{\text{baseline}}$ against $V_{\text{T}}^{\text{baseline}} - V_{\text{T}}^{\text{block}}$ allows derivation of V_{ND} (x-intercept) and the occupancy of XBD173 (slope). This method assumes that V_{ND} is the same at pre and post-block time points and that the fractional occupancy of XBD173

does not change across the brain. Method 1a plots these data for each individual participant.

Method 1b: Occupancy Plot with Constrained V_{ND}

In order to calculate a group V_{ND}, data from individual participants were plotted as described in method 1a, with the x-intercept forced to a best fit for all participants. This was done by constraining the x-intercept (V_{ND}) to be equal (for all participants) on a group level, using a linear regression implemented in Matlab (R2018a, The MathWorks, Inc., MA, USA).

Method 2: Polymorphism Plot

The polymorphism plot, described by Guo et al. [7], does not require pharmacological blockade. Instead, it relies upon the assumption that MABs express 50 % HAB and 50 % LAB binding sites [6, 9]. Thus, similarly to methods 1a and 1b, $V_T^{HAB} - V_T^{MAB} = \Delta\left(V_T^{HAB} - V_{ND}\right)$, where Δ is a constant $\left(\frac{BP_{ND}^{HAB} - BP_{ND}^{MAB}}{BP_{ND}^{HAB}}\right)$ relating to the non-displaceable binding potential, BP_{ND}, for HABs and LABs, respectively. Again, a plot of V_T^{HAB} against $V_T^{HAB} - V_T^{MAB}$ thus gives V_{ND} as the x-intercept.

Statistics

Linear regressions were generated in Matlab (R2018a, The MathWorks, Inc., MA, USA) and V_T and V_{ND} results are expressed as mean ± standard deviation (SD). For each tracer, V_Ts in different ROIs were compared using repeated measures one-way ANOVA with a Tukey test for multiple comparisons. Statistical tests were performed in GraphPad Prism (v7, GraphPad Software, Inc., San Diego, CA, USA).

Results

Demographics

The mean age of participants scanned with [18F]GE-180 was 46.8 ± 9.1 years, mean age of onset was 36.2 ± 12.8 years and EDSS ranged between 3.5 and 7.5. For [11C]PBR28, mean age was 40.5 ± 9.0 years (unpaired t test: $p = 0.25$, not significant, ns, compared to [18F]GE-180), mean age of onset was 35.4 ± 6.2 years ($p = 0.78$, ns compared to [18F]GE-180) and EDSS ranged between 1 and 6.5 ($p = 0.13$, ns compared to [18F]GE-180). All participants had been treated with disease-modifying therapy. Participant demographics are summarised in Table 1.

Visual Assessment of PET Reveals Blockade of TSPO

Sixty- to 90-min sum PET images were generated for all participants. There was little obvious visual difference in sum PET images pre- and post-block (*e.g.*, participants F and H, Figs. 1 and 2, right hand side) for participants scanned with [18F]GE-180 but a small decrease was evident with [11C]PBR28. V_Ts were then generated for all participants in all Hammers atlas ROIs and visualised as a heat map (left hand side, Figs. 1 and 2). In contrast to sum PET images, there were clear visual differences between pre- and post-block V_Ts with both tracers.

[18F]GE-180 Binds Specifically to TSPO

Mean whole brain baseline V_T was 0.29 ± 0.17 ml/cm^3 for [18F]GE-180 and 5.31 ± 1.53 for [11C]PBR28. There were no significant differences in V_T between any ROIs for [18F]GE-180. For [11C]PBR28, the putamen was elevated over NAWM ($p = 0.03$).

Blockade with XBD173 confirmed that both [18F]GE-180 and [11C]PBR28 exhibit specific binding in the MS brain. Of the

Table 1.. Summary of participant demographics for those scanned with [18F]GE-180 and [11C]PBR28

Tracer	Participant	HAB/MAB	Sex	Age/age at onset (years)	EDSS	Previous DMTs; current DMT
[18F]GE-180	A	HAB	M	43/32	6.5	GA; GA
	B	MAB	M	53/36	4.0	IVIG, natalizumab; IVIG
	C	MAB	F	60/47	3.5	Alemtuzumab; alemtuzumab
	D	HAB	F	33/20	5.5	IB-1a/1b, natalizumab, alemtuzumab, AHSCT; natalizumab
	E	MAB	F	46/38	6.0	IB-1a, GA, fingolimod, natalizumab; alemtuzumab
	F	HAB	M	46/32	7.5	Natalizumab; AHSCT
[11C]PBR28	G	HAB	F	44/40	6.5	Natalizumab; natalizumab
	H	MAB	M	29/27	1.0	DF; DF
	I	MAB	F	39/30	6.5	Alemtuzumab, MSCT, natalizumab; MCTD
	J	MAB	F	56/44	4.0	Natalizumab, AHSCT, IB-1a; nil
	K	HAB	M	37/35.5	1.5	DF; nil
	L	HAB	M	38/36	1.5	DF; nil

HAB/MAB high/mixed affinity binder, *EDSS* (Kurtzke) expanded disability status scale, *DMT* disease modifying therapy, *GA* glatiramer acetate, *IVIG* intravenous immunoglobulin, *IB* interferon-beta, *AHSCT* autologous haematopoietic stem cell transplantation, *DF* dimethyl fumarate, *MSC* mesenchymal stem cell therapy, *MCTD* mixed connective tissue disease

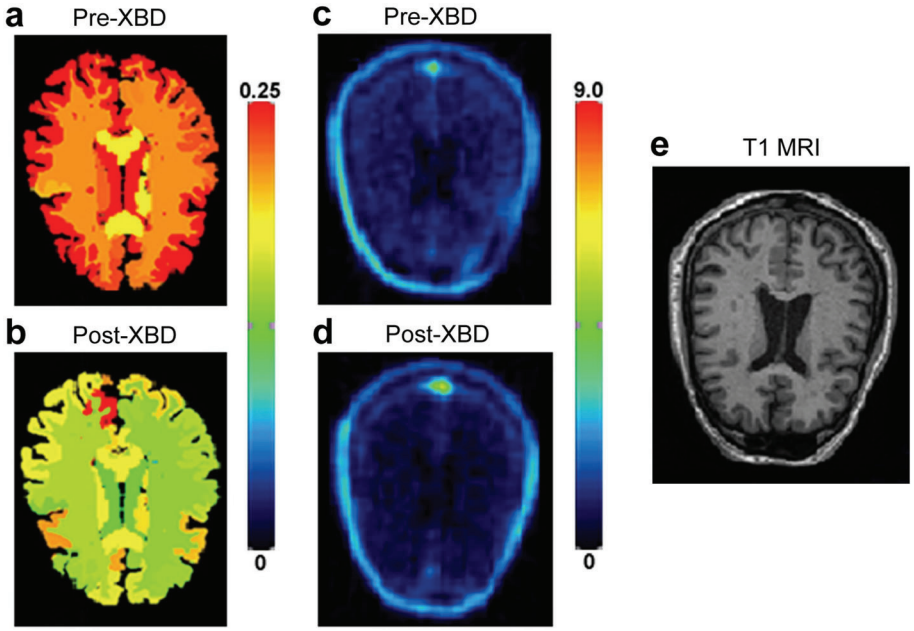


Fig. 1 Hammers atlas filled with V_T results in transverse view **a** pre- and **b** post-XBD173 administration, for participant F scanned with [**18**F]GE-180. V_T (ml/cm**3**) for each region is mapped onto the participant's regional atlas in patient space. Sum 60–90 min PET images (kBq ml^{-1}) for the same subject in transverse view **c** pre- and **d** post-XBD173 administration. **e** T1 MRI for same subject.

12 participants, one displayed no measureable occupancy and was excluded from further analyses (participant K, HAB scanned with [^{11}C]PBR28). Mean whole brain baseline V_T for the remaining [^{11}C]PBR28 participants was 5.43 ± 1.68 ml/cm^3. Method 1a, the unconstrained occupancy plot, gave a mean V_{ND} of 0.18 ± 0.05 ml/cm^3 for [^{18}F]GE-180 and 3.65 ± 1.79 ml/cm^3 for [^{11}C]PBR28. Method 1b, using an occupancy plot and constraining the *x*-intercept across participants, gave mean V_{ND}

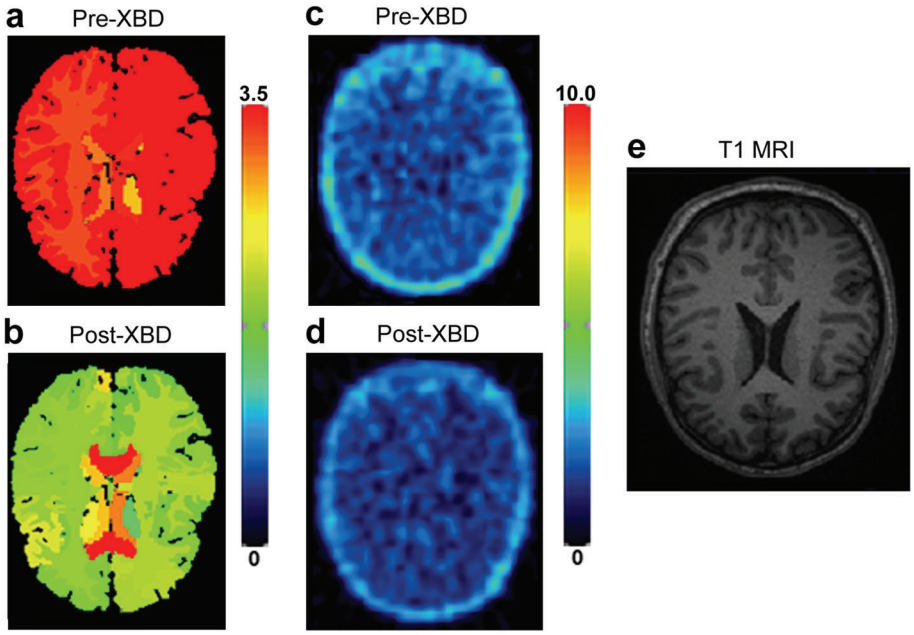


Fig. 2 Hammers atlas filled with V_T results in transverse view **a** pre- and **b** post-XBD173 administration, for participant H scanned with [**11**C]PBR28. V_T (ml/cm**3**) for each region is mapped onto the participant's regional atlas in patient space. Sum 60–90 min PET images (kBq ml^{-1}) for the same subject in transverse view **c** pre- and **d** post-XBD173 administration. **e** T1 MRI for same subject.

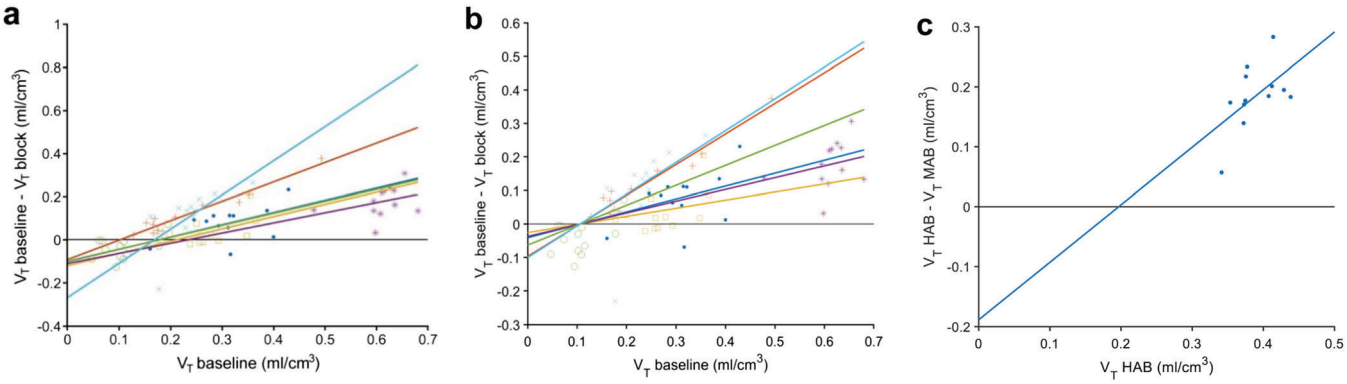


Fig. 3 **a** Individual linear regression with occupancy plot, **b** constrained *x*-intercept occupancy plot and **c** polymorphism plot, bottom for [**18**F]GE-180. V_{ND} is derived from the *x*-intercept. Different symbols indicate individual patients for **a** and **b**; each symbol represents a region of interest.

estimates of 0.11 and 3.81 ml/cm^3 respectively. Method 2, using a polymorphism plot, produced V_{ND} estimates of 0.20 and 3.49 ml/cm^3, respectively (Figs. 3 and 4). With V_{ND} estimates of 0.16 ± 0.05 ml/cm^3 (mean of the three methods) for [^{18}F]GE-180 and 3.65 ± 0.16 ml/cm^3 for [^{11}C]PBR28 and mean baseline whole brain V_T of 0.29 and 5.43 ml/cm^3, respectively, the specific binding ($V_S = V_T - V_{ND}$) accounted for 45 % of total V_T in the brain for [^{18}F]GE-180 (57 % HABs; 20 % MABs) and 33 % for [^{11}C]PBR28 (37 % HABs; 25 % MABs). The reduction in uptake for both tracers post-XBD173 administration is further highlighted in Fig. 5, where a clear decrease in V_T in the majority of ROIs is observed. Furthermore, BP_{ND} ($= \frac{V_T}{V_{ND}} - 1$) was used to calculate the mean HAB/MAB signal ratio for each tracer using these mean V_{ND} values. For [^{18}F]GE-180, this was 5.45 ± 3.29 ($p < 0.01$), while for [^{11}C]PBR28, the HAB/MAB ratio was 3.21 ± 1.27 ($p < 0.01$).

Specific Binding to TSPO Is Ubiquitous in the MS Brain

For [^{18}F]GE-180, V_S accounted for between 39 % (striatum) and 54 % (thalamus) of total binding in the selected ROIs (mean ± SD, 45 ± 5 %). For [^{11}C]PBR28, V_S accounted for between 6 % (striatum) and 43 % (brainstem) of total binding (29 ± 11 %). All other ROIs defined by the Hammers atlas, including the caudate and non-cortical GM, exhibited mean V_T between 0.25 and 0.56 ml/cm^3 and between 3.99 and 7.39 ml/cm^3, respectively. Thus, it follows that no ROIs were consistently devoid of specific TSPO binding, as measured by either tracer.

Discussion

This study was designed to quantify the non-specific binding (V_{ND}) of the TSPO PET tracers [^{18}F]GE-180 and [^{11}C]PBR28 in people with MS. We found that V_{ND} accounts for, on average, 55 and 67 % of the total binding of [^{18}F]GE-180 and [^{11}C]PBR28, respectively, indicating that the remaining 45 or 33 % are attributable to specific signal (V_S).

[^{18}F]GE-180 has shown high signal-to-noise ratios in preclinical studies [10–12, 21, 22] but unexpectedly low brain penetration in human healthy controls [13–15]. Recent studies have demonstrated markedly increased uptake of [^{18}F]GE-180 in people with glioblastoma [23] and in people

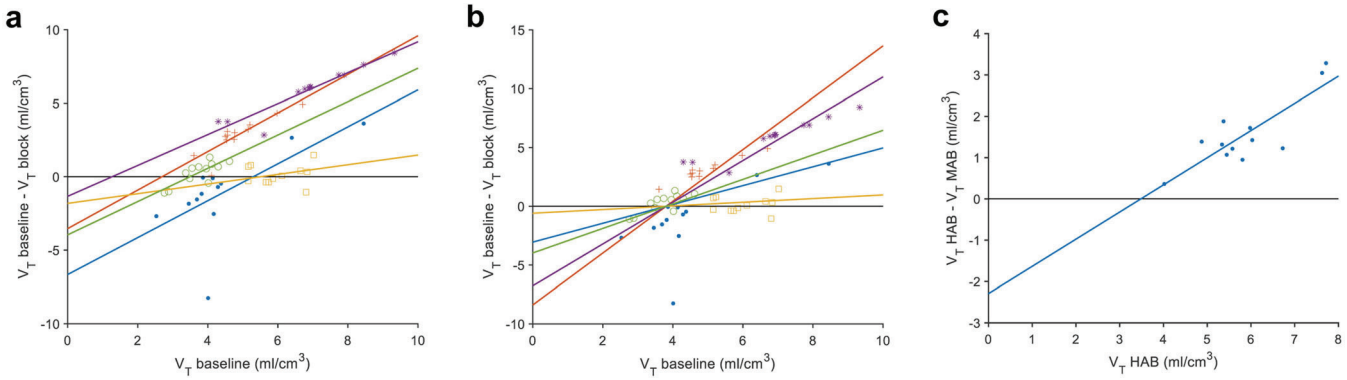


Fig. 4 **a** Individual linear regression with occupancy plot, **b** constrained *x*-intercept occupancy plot and **c** polymorphism plot, bottom for [**11**C]PBR28. V_{ND} is derived from the *x*-intercept. Different symbols indicate individual patients for **a** and **b**; each symbol represents a region of interest.

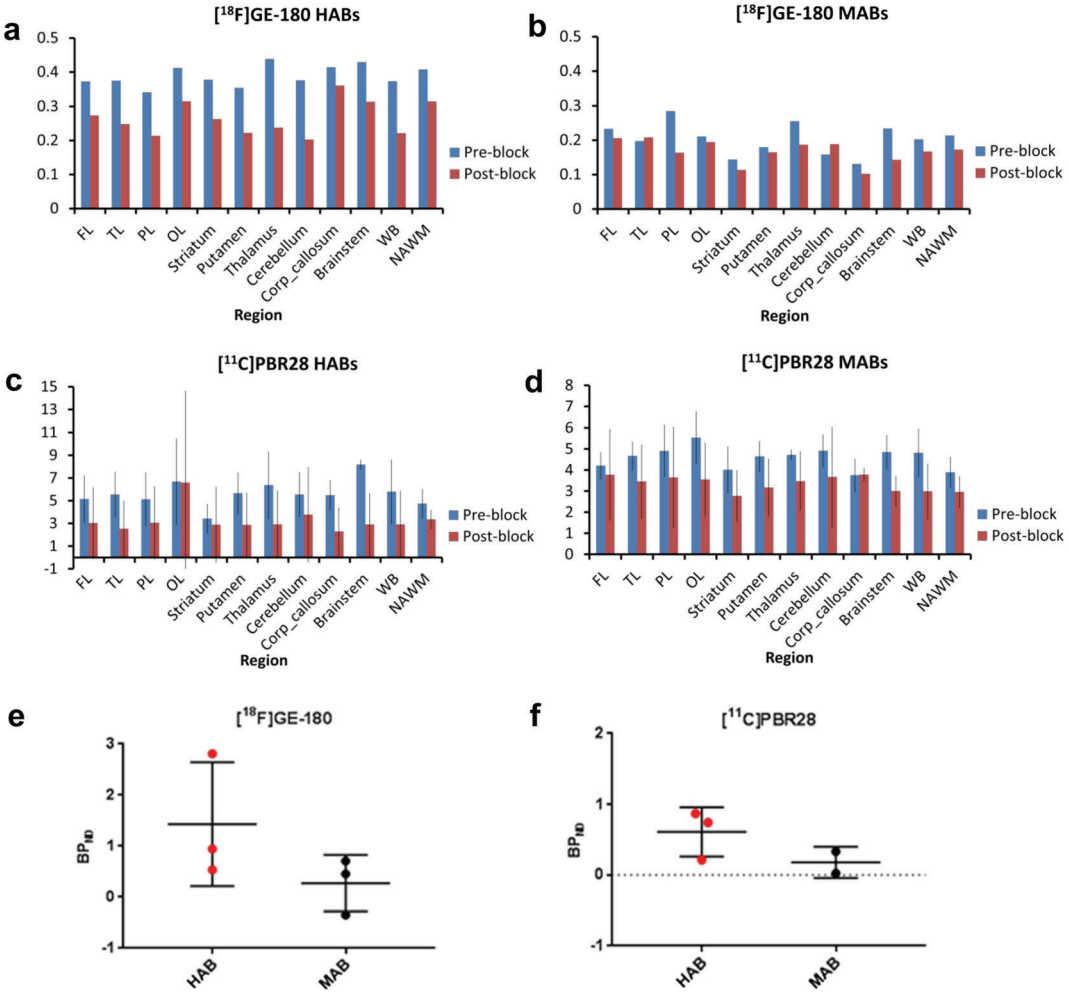


Fig. 5 Bar graph plots of average regional V_T pre- and post-blockade for HABs and MABs for **a** and **b**: [18F]GE-180; **c** and **d**: [11C]PBR28. **e** and **f**: HAB *vs.* MAB group V_T estimates for each tracer ($n = 6$ [18F]GE-180; $n = 5$ [11C]PBR28).

with relapsing-remitting MS [24], but questions remain as to whether this increase in signal represents specific binding or is merely due to non-specific signal in areas of blood–brain barrier breakdown. Another recent study which directly compared [18F]GE-180 with [11C]PBR28 in healthy controls who were scanned with both tracers (morning and afternoon) found up to 20 times lower volumes of distribution with the former compared to the latter [15] as well as difficulties with [18F]GE-180 quantification. To our knowledge, ours is the first study assessing non-displaceable binding of [18F]GE-180 and comparing both tracers in disease cohorts. Our results argue that, despite low brain penetration [13, 14], [18F]GE-180 does exhibit a specific signal in the MS brain and hence could be useful in conditions with pathologically increased levels of TSPO. We also performed gadolinium contrast-enhancing MRI in the cohort of participants scanned with [18F]GE-180 and observed no contrast enhancement (in lesion areas or otherwise), suggesting no extensive BBB breakdown. Although this observation does not exclude the possibility of micro-BBB breakdown, which could allow passage of [18F]GE-180 molecules, but not the larger gadolinium molecules, through the disrupted area, the finding does concur with that of Vomacka et al. [25]. The authors of this study also comment that (in their previous study [23]) areas with contrast enhancement in MR did not always correlate with increased [18F]GE-180 signal, indicating that signal increases in PET are likely to be related to TSPO expression rather than exclusively BBB breakdown. The results also have broader implications on how novel tracers should be validated and compared. While high absolute V_Ts are preferable in a tracer, it is crucial to understand what proportion of V_T is driven by V_{ND}. This can be achieved using a blocking study, which, given the lack of an appropriate receptor-free reference region in the brain, we suggest should be undertaken for all TSPO tracers undergoing clinical development.

Although the occupancy plot has been more commonly used in V_{ND} quantification [4], an alternative approach, relevant for TSPO tracers which are susceptible to the rs6971 SNP, is to create a polymorphism plot, which does not require pharmacological blockade and relies only on the assumption of equal expression of HAB and LAB sites. Our

V_{ND} results from both methods (including free and fixed-intercept occupancy plots) were in good agreement for both tracers, giving an average V_{ND} of 0.16 ± 0.05 ml/cm^3 for [^{18}F]GE-180 and 3.65 ± 0.16 ml/cm^3 for [^{11}C]PBR28. In this study, we also demonstrate that V_T is consistently greater than V_{ND} for both [^{18}F]GE-180 and [^{11}C]PBR28; in other words, no ROIs were devoid of specific TSPO binding. This finding fits with previous observations that reference tissue approaches may not be appropriate in TSPO PET studies [6].

[^{11}C]PBR28 has been validated with blocking experiments prior to our study, both in healthy controls [6, 26] and in a disease cohort [27]. [^{11}C]PBR28 is generally accepted as an effective TSPO tracer *in vivo* [28–32] although exhibits counterintuitively decreased V_T in subjects with neuroinflammation [29]. In Owen et al. [6], the V_{ND} of [^{11}C]PBR28 was 1.98 ml/cm^3 (~ 50 % of V_T), while Fujita et al. [26] reported an average V_T of 4.3 ml/cm^3 (in HABs) and a BP_{ND} of 1.2, giving a very similar V_{ND} of 1.98 ml/cm^3 (~ 45 % of V_T). In our study, V_{ND} for [^{11}C]PBR28 was 3.65. It is possible that this is a disease-specific difference, given that both the former studies were performed in healthy subjects; however, the sample size in our study was also small and the estimation of V_{ND} may therefore be subject to some biological variability. Nevertheless, the proportion of non-specific binding for [^{18}F]GE-180 is comparable to or even lower than that of [^{11}C]PBR28 (V_{ND} ~ 55 *vs.* ~69 %, respectively), although absolute V_Ts are lower [6, 27]. This result further indicates that [^{18}F]GE-180 is able to identify specific TSPO signal in the MS brain, in spite of low brain penetration. We also report respective HAB and MAB V_S of 57 and 20 % for [^{18}F]GE-180 and 37 and 25 % for [^{11}C]PBR28, although the group numbers ($n = 3$ for both [^{18}F]GE-180 groups and [^{11}C]PBR28 HABs, $n = 2$ for [^{11}C]PBR28 MABs) are too small to draw firm conclusions.

As has been pointed out previously, the brain penetration of [^{18}F]GE-180 is very low in humans [13–15]. Our findings also showed low values of V_T and K_1, indicating low extraction of the tracer across the blood−brain barrier (K_1 ~ 0.003 *vs.* 0.2 ml/cm^3/min for [^{11}C]PBR28; *i.e.*, ~ 60× lower). Zanotti-Fregonara and colleagues also noted difficulty in kinetic model fitting of [^{18}F]GE-180 data using the standard two-tissue compartment model with free blood volume parameter, which we used [15]. Here, however, we were able to fit the large majority of regions well, with R^2 comparable to those seen with [^{11}C]PBR28 (R^2 ~ 0.8) and standard errors on V_T estimates < 20 % for both tracers. It is possible that this is due to the larger, less noisy ROIs selected for analysis in our study compared to those used by Zanotti-Fregonara and colleagues. Also to be considered is the fact that our study involved (six) participants with MS, compared to the four healthy controls and single participant with amytrophic lateral sclerosis in the other study, which may have resulted in altered binding kinetics due to disease-specific pathology. Although a methodology considering large ROIs in a disease such as MS, with focal lesion-based pathology, may seem to limit the usefulness of a tracer, there is evidence that there is a global effect on TSPO PET signal in regions such as NAWM and normal appearing grey matter (see [33] for review), suggesting that [^{18}F]GE-180 need not be excluded from use based on this fact. Many recent studies using [^{11}C]PBR28 (and other tracers) have elected to use the 2TCM-1K kinetic model [34], which incorporates a parameter representing the endothelial fraction of binding of a TSPO tracer, for quantification [29]. The 2TCM-1K has been used with [^{18}F]GE-180 data [13] and has not shown a substantial advantage in terms of parsimony criteria (Akaike Information Criteria, AIC) compared to the 2TCM. Furthermore, [^{11}C]PBR28 datasets are often still analysed using the 2TCM, primarily for comparison with data from other tracers [15, 35, 36]. We also found good fits to [^{11}C]PBR28 data with the 2TCM; thus, here, we elected to use this model to analyse data from both tracers.

The *in vitro* HAB/LAB ratio of binding affinity for [^{11}C]PBR28 has been observed to be approximately 1:50 [9], while for [^{18}F]GE-180, this ratio is between 1:5 and 1:15 (personal communication, DRO, WT). *In vivo*, [^{11}C]PBR28-scanned MABs express approximately half the signal compared to HABs [6]. The slope of the polymorphism plot is equivalent to $\frac{BP_{ND}^{HAB} - BP_{ND}^{MAB}}{BP_{ND}^{HAB}}$. For [^{18}F]GE-180, our equivalent *in vivo* HAB/MAB ratio was found to be 5.43 ± 3.27 and the average slope was thus expected to be approximately 0.8, while for [^{11}C]PBR28, these values were 3.21 ± 1.27 and 0.7. Our results for the slopes of the polymorphism plots were 0.96 and 0.67 respectively and thus fell within one standard deviation of the predicted values. Previous studies using [^{18}F]GE-180 have been unable to detect consistent differences in tracer signal between HABs and MABs [13, 14, 24], indicating that brain penetration of the tracer is low, except where BBB breakdown may be present [24]. Contrary to these results, in our study, HABs exhibited approximately twice the total volume of distribution of MABs in selected ROIs at baseline. It is likely that the difference in our study is driven primarily by one HAB with particularly high signal (participant D) and one MAB with particularly low signal (participant E). Clearly there is considerable variability in population V_T and with the small sample size in our study ($n = 6$), we are unable to validate our findings with statistical tests. In addition, the difference in scan timing between the first and second (post-XBD173) scan varied for each tracer (half a day for [^{11}C]PBR28 and 1 week for [^{18}F]GE-180), which itself may have introduced some variability in PET signal. Thus, we suggest continuing binding status stratification of participants in future studies, where larger data pools may enable more reliable HAB/MAB binding ratio estimates.

Several caveats exist in this study. Firstly, the occupancy of XBD173 in the two cohorts (slopes in the occupancy plots) varied between 24 and 95 % (fixed-intercept plot) for [^{18}F]GE-180 and 16 and 220 % for [^{11}C]PBR28. Clearly, the occupancy of XBD173 cannot

exceed 100 %, and indeed, the dose administered was pre-calculated to give an expected approximate 75 % occupancy, allowing for participant weights and considering the dose-occupancy relationship described by Owen et al. [6] for [11C]PBR28. Of course, it should also be noted that these values were obtained from the fixed-intercept occupancy plot; for the free intercept plot, occupancies were within one standard deviation of the expected value. This point again highlights the large variability across cohorts and the fact that averaging results across participants, even within the same disease population, may not be a suitable approach. In addition, one participant scanned with [11C]PBR28 exhibited no substantial occupancy and was excluded from further analysis. This large inter-individual variability in occupancy was also seen in previous XBD173 blocking studies [6, 27], reflected in the variability in total signal reduction (V_T) between pre and post-block scans. Whether driven by biological variability or experimental noise, these results provide evidence that V_{ND} cannot necessarily be assumed to be the same across regions and a population. If there is indeed a biological spectrum of V_{ND} between individuals, this raises the interesting possibility that blocking scans should be included for all participants in all TSPO PET studies to optimally quantify V_S. This would have broad repercussions on TSPO PET study design, including cost, radiation exposure and participant discomfort. All neuro-PET tracers are, of course, better able to penetrate brain tissue when the BBB is disrupted. In the case of [18F]GE-180, which exhibits low penetration of the healthy BBB, this is particularly relevant. Although our cohorts were selected due to their clinically low or 'inactive' MRI, and although we investigated only lesion-free ROIs, we only performed contrast enhanced MRI to estimate BBB integrity in the [18F]GE-180 cohort, and no measure of micro-BBB disruption was performed. Lastly, although this study was performed in a cohort of people with MS, we have not investigated how V_T differs in MS lesions or how it correlates with clinical outcomes. This study was not powered to address these questions, since participants were not burdened with large lesion loads. Instead, these questions will be explored in follow-up studies.

Conclusion

In summary, pharmacological blockade with XBD173 demonstrates, for the first time *in vivo*, that [18F]GE-180 does bind specifically to TSPO in normal appearing white and grey matter, to an extent that is highly comparable to [11C]PBR28, in spite of the low extraction fraction of the former.

Acknowledgements. The authors wish to thank Dr. William Trigg (formerly GE Healthcare), Dr. Christopher Buckley and Ms. Joanne Stevens (GE Healthcare) and Professor Federico Turkheimer (King's College London) for their valuable advice during the analysis and write-up of this study.

Funding Information. This [18F]GE-180 arm of the study was funded by grants from GE Healthcare, FastForward and the MSTC, awarded to the Imperial College Trust. The [11C]PBR28 arm of the study was funded by an Imperial College BRC IMPETUS 2014 grant.

Compliance with Ethical Standards

Conflict of Interest

SS, RN and JR have received funding from GE Healthcare. JR is a current employee of the MHRA; work herein was completed while JR was employed by Imperial College.
PAM declares honoraria for speaking and travel support from Bayer, Biogen, Merck Serono and Novartis.
DJB holds consultancies with GE Healthcare and Biogen.
RG is an employee of Invicro, Ltd.
All other authors have no disclosures.

Open Access This article is distributed under the terms of the Creative Commons Attribution 4.0 International License (http://creativecommons.org/licenses/by/4.0/), which permits unrestricted use, distribution, and reproduction in any medium, provided you give appropriate credit to the original author(s) and the source, provide a link to the Creative Commons license, and indicate if changes were made.

Publisher's Note Springer Nature remains neutral with regard to jurisdictional claims in published maps and institutional affiliations.

References

1. Rupprecht R, Papadopoulos V, Rammes G, Baghai TC, Fan J, Akula N, Groyer G, Adams D, Schumacher M et al (2010) Translocator protein (18 kDa) (TSPO) as a therapeutic target for neurological and psychiatric disorders. Nat Rev Drug Discov 9:971–988
2. Owen DR, Yeo AJ, Gunn RN, Song K, Wadsworth G, Lewis A, Rhodes C, Pulford DJ, Bennacef I, Parker CA, StJean PL, Cardon LR, Mooser VE, Matthews PM, Rabiner EA, Rubio JP et al (2012) An 18-kDa translocator protein (TSPO) polymorphism explains differences in binding affinity of the PET radioligand PBR28. J Cereb Blood Flow Metab 32:1–5
3. Turkheimer FE, Rizzo G, Bloomfield PS, Howes O, Zanotti-Fregonara P, Bertoldo A, Veronese M et al (2015) The methodology of TSPO imaging with positron emission tomography. Biochem Soc Trans 43:586–592
4. Cunningham VJ, Rabiner EA, Slifstein M, Laruelle M, Gunn RN et al (2010) Measuring drug occupancy in the absence of a reference region: the Lassen plot re-visited. J Cereb Blood Flow Metab 30:46–50
5. Lassen NA, Bartenstein PA, Lammertsma AA, Prevett MC, Turton DR, Luthra SK, Osman S, Bloomfield PM, Jones T, Patsalos PN, O'Connell MT, Duncan JS, Andersen JV et al (1995) Benzodiazepine receptor quantification in vivo in humans using [11C] flumazenil and PET: application of the steady-state principle. J Cereb Blood Flow Metab 15:152–165
6. Owen DR, Guo Q, Kalk NJ, Colasanti A, Kalogiannopoulou D, Dimber R, Lewis YL, Libri V, Barletta J, Ramada-Magalhaes J, Kamalakaran A, Nutt DJ, Passchier J, Matthews PM, Gunn RN, Rabiner EA et al (2014) Determination of [11C]PBR28 binding potential in vivo: a first human TSPO blocking study. J Cereb Blood Flow Metab 34:989–994
7. Guo Q, Colasanti A, Owen DR, Onega M, Kamalakaran A, Bennacef I, Matthews PM, Rabiner EA, Turkheimer FE, Gunn RN et al (2013) Quantification of the specific translocator protein signal of 18F-PBR111 in healthy humans: a genetic polymorphism effect on in vivo binding. J Nucl Med 54:1915–1923
8. Guo Q, Owen DR, Rabiner EA, Turkheimer FE, Gunn RN (2014) A graphical method to compare the in vivo binding potential of PET radioligands in the absence of a reference region: application to

[11C]PBR28 and [18F]PBR111 for TSPO imaging. J Cereb Blood Flow Metab 34:1162–1168
9. Owen DR, Howell OW, Tang SP, Wells LA, Bennacef I, Bergstrom M, Gunn RN, Rabiner EA, Wilkins MR, Reynolds R, Matthews PM, Parker CA et al (2010) Two binding sites for [3H]PBR28 in human brain: implications for TSPO PET imaging of neuroinflammation. J Cereb Blood Flow Metab 30:1608–1618
10. Boutin H, Murray K, Pradillo J, Maroy R, Smigova A, Gerhard A, Jones PA, Trigg W et al (2015) 18F-GE-180: a novel TSPO radiotracer compared to 11C-R-PK11195 in a preclinical model of stroke. Eur J Nucl Med Mol Imaging 42:503–511
11. Dickens AM, Vainio S, Marjamaki P, Johansson J, Lehtiniemi P, Rokka J, Rinne J, Solin O, Haaparanta-Solin M, Jones PA, Trigg W, Anthony DC, Airas L et al (2014) Detection of microglial activation in an acute model of neuroinflammation using PET and radiotracers C-11-(R)-PK11195 and F-18-GE-180. J Nucl Med 55:466–472
12. James ML, Belichenko NP, Shuhendler AJ, Hoehne A, Andrews LE, Condon C, Nguyen TVV, Reiser V, Jones P, Trigg W, Rao J, Gambhir SS, Longo FM et al (2017) [18F]GE-180 PET detects reduced microglia activation after LM11A-31 therapy in a mouse model of Alzheimer's disease. Theranostics 7:1422–1436
13. Fan Z, Calsolaro V, Atkinson RA, Femminella GD, Waldman A, Buckley C, Trigg W, Brooks DJ, Hinz R, Edison P et al (2016) Flutriciclamide (18F-GE180) PET: first-in-human PET study of novel third-generation in vivo marker of human translocator protein. J Nucl Med 57:1753–1759
14. Feeney C, Scott G, Raffel J, Roberts S, Coello C, Jolly A, Searle G, Goldstone AP, Brooks DJ, Nicholas RS, Trigg W, Gunn RN, Sharp DJ et al (2016) Kinetic analysis of the translocator protein positron emission tomography ligand [18F]GE-180 in the human brain. Eur J Nucl Med Mol Imaging 43:2201–2210
15. Zanotti-Fregonara P, Pascual B, Rizzo G et al (2018) Head-to-head comparison of 11C-PBR28 and 18F-GE180 for the quantification of TSPO in the human brain. In J Nucl Med 59(8):1260–1266
16. Owen DRJ, Gunn RN, Rabiner EA, Bennacef I, Fujita M, Kreisl WC, Innis RB, Pike VW, Reynolds R, Matthews PM, Parker CA et al (2011) Mixed-affinity binding in humans with 18-kDa translocator protein ligands. J Nucl Med 52:24–32
17. Kurtzke JF (1983) Rating neurologic impairment in multiple sclerosis: an expanded disability status scale (EDSS). Neurology 33:1444–1452
18. Wadsworth H, Jones PA, Chau WF, Durrant C, Fouladi N, Passmore J, O'Shea D, Wynn D, Morisson-Iveson V, Ewan A, Thaning M, Mantzilas D, Gausemel I, Khan I, Black A, Avory M, Trigg W et al (2012) [18F]GE-180: a novel fluorine-18 labelled PET tracer for imaging translocator protein 18 kDa (TSPO). Bioorg Med Chem Lett 22:1308–1313
19. Hammers A, Allom R, Free SL et al (2002) Three-dimensional probabilistic atlas of the human brain. Neuroimage 16:S86–S86
20. Watabe H, Channing MA, Der MG et al (2000) Kinetic analysis of the 5-HT2A ligand [11C] MDL 100,907. J Cereb Blood Flow Metab 20:899–909
21. Sridharan S, Lepelletier FX, Trigg W, Banister S, Reekie T, Kassiou M, Gerhard A, Hinz R, Boutin H et al (2017) Comparative evaluation of three TSPO PET radiotracers in a LPS-induced model of mild neuroinflammation in rats. Mol Imaging Biol 19:77–89
22. Russmann V, Brendel M, Mille E, Helm-Vicidomini A, Beck R, Günther L, Lindner S, Rominger A, Keck M, Salvamoser JD, Albert NL, Bartenstein P, Potschka H et al (2017) Identification of brain regions predicting epileptogenesis by serial [18F]GE-180 positron emission tomography imaging of neuroinflammation in a rat model of temporal lobe epilepsy. Neuroimage Clin 15:35–44
23. Albert NL, Unterrainer M, Fleischmann DF, Lindner S, Vettermann F, Brunegraf A, Vomacka L, Brendel M, Wenter V, Wetzel C, Rupprecht R, Tonn JC, Belka C, Bartenstein P, Niyazi M et al (2017) TSPO PET for glioma imaging using the novel ligand 18F-GE-180: first results in patients with glioblastoma. Eur J Nucl Med Mol Imaging 44:2230–2238
24. Unterrainer M, Mahler C, Vomacka L, Lindner S, Havla J, Brendel M, Böning G, Ertl-Wagner B, Kümpfel T, Milenkovic VM, Rupprecht R, Kerschensteiner M, Bartenstein P, Albert NL et al (2018) TSPO PET with [(18)F]GE-180 sensitively detects focal neuroinflammation in patients with relapsing-remitting multiple sclerosis. Eur J Nucl Med Mol Imaging 45:1423–1431
25. Vomacka L, Albert NL, Lindner S, Unterrainer M, Mahler C, Brendel M, Ermoschkin L, Gosewisch A, Brunegraf A, Buckley C, Kümpfel T, Rupprecht R, Ziegler S, Kerschensteiner M, Bartenstein P, Böning G et al (2017) TSPO imaging using the novel PET ligand [18F]GE-180: quantification approaches in patients with multiple sclerosis. EJNMMI Res 7:89
26. Fujita M, Kobayashi M, Ikawa M, Gunn RN, Rabiner EA, Owen DR, Zoghbi SS, Haskali MB, Telu S, Pike VW, Innis RB et al (2017) Comparison of four 11C-labeled PET ligands to quantify translocator protein 18 kDa (TSPO) in human brain: (R)-PK11195, PBR28, DPA-713, and ER176-based on recent publications that measured specific-to-non-displaceable ratios. EJNMMI Res 7:84
27. Veronese M, Reis Marques T, Bloomfield PS, Rizzo G, Singh N, Jones D, Agushi E, Mosses D, Bertoldo A, Howes O, Roncaroli F, Turkheimer FE et al (2018) Kinetic modelling of [11C]PBR28 for 18 kDa translocator protein PET data: a validation study of vascular modelling in the brain using XBD173 and tissue analysis. J Cereb Blood Flow Metab 38:1227–1242
28. Albrecht D, Shcherbinin S, Wooten D et al (2016) Occipital lobe as a pseudo-reference region for [11C]PBR28 PET imaging: validation in chronic pain and amyotrophic lateral sclerosis cohorts. J Nucl Med 57:1814
29. Bloomfield PS, Selvaraj S, Veronese M, Rizzo G, Bertoldo A, Owen DR, Bloomfield MAP, Bonoldi I, Kalk N, Turkheimer F, McGuire P, de Paola V, Howes OD et al (2016) Microglial activity in people at ultra high risk of psychosis and in schizophrenia: an [11C]PBR28 PET brain imaging study. Am J Psychiatry 173:44–52
30. Datta G, Colasanti A, Kalk N, Owen D, Scott G, Rabiner EA, Gunn RN, Lingford-Hughes A, Malik O, Ciccarelli O, Nicholas R, Nei L, Battaglini M, Stefano ND, Matthews PM et al (2017) 11C-PBR28 and 18F-PBR111 detect white matter inflammatory heterogeneity in multiple sclerosis. J Nucl Med 58:1477–1482
31. Kreisl WC, Fujita M, Fujimura Y, Kimura N, Jenko KJ, Kannan P, Hong J, Morse CL, Zoghbi SS, Gladding RL, Jacobson S, Oh U, Pike VW, Innis RB et al (2010) Comparison of [11C]-(R)-PK 11195 and [11C]PBR28, two radioligands for translocator protein (18 kDa) in human and monkey: implications for positron emission tomographic imaging of this inflammation biomarker. Neuroimage 49:2924–2932
32. Park E, Gallezot JD, Delgadillo A, Liu S, Planeta B, Lin SF, O'Connor KC, Lim K, Lee JY, Chastre A, Chen MK, Seneca N, Leppert D, Huang Y, Carson RE, Pelletier D et al (2015) 11C-PBR28 imaging in multiple sclerosis patients and healthy controls: test-retest reproducibility and focal visualization of active white matter areas. Eur J Nucl Med Mol Imaging 42:1081–1092
33. Airas L, Nylund M, Rissanen E (2018) Evaluation of microglial activation in multiple sclerosis patients using positron emission tomography. Front Neurol 9:181
34. Rizzo G, Veronese M, Tonietto M, Zanotti-Fregonara P, Turkheimer FE, Bertoldo A et al (2014) Kinetic modeling without accounting for the vascular component impairs the quantification of [11C]PBR28 brain PET data. J Cereb Blood Flow Metab 34:1060–1069
35. Collste K, Forsberg A, Varrone A, Amini N, Aeinehband S, Yakushev I, Halldin C, Farde L, Cervenka S et al (2016) Test-retest reproducibility of [C-11]PBR28 binding to TSPO in healthy control subjects. Eur J Nucl Med Mol Imaging 43:173–183
36. Collste K, Plaven-Sigray P, Fatouros-Bergman H et al (2017) Lower levels of the glial cell marker TSPO in drug-naive first-episode psychosis patients as measured using PET and [11C]PBR28. Mol Psychiatry 22:850–856

Raffel J, Wallace A, Gveric D, Reynolds R, Friede T, Nicholas R. Patient-reported outcomes and survival in multiple sclerosis: A 10-year retrospective cohort study using the Multiple Sclerosis Impact Scale-29. PLOS Medicine. 2017;14(7):e1002346.

PLOS | MEDICINE

RESEARCH ARTICLE

Patient-reported outcomes and survival in multiple sclerosis: A 10-year retrospective cohort study using the Multiple Sclerosis Impact Scale–29

Joel Raffel[1,2☯], Alison Wallace[1☯], Djordje Gveric[1], Richard Reynolds[1], Tim Friede[3], Richard Nicholas[1,2*]

1 Division of Brain Sciences, Faculty of Medicine, Imperial College London, London, United Kingdom, **2** Imperial College Healthcare NHS Trust, London, United Kingdom, **3** Department of Medical Statistics, University Medical Center Göttingen, Göttingen, Germany

☯ These authors contributed equally to this work.
* r.nicholas@imperial.ac.uk

Check for updates

OPEN ACCESS

Citation: Raffel J, Wallace A, Gveric D, Reynolds R, Friede T, Nicholas R (2017) Patient-reported outcomes and survival in multiple sclerosis: A 10-year retrospective cohort study using the Multiple Sclerosis Impact Scale–29. PLoS Med 14(7): e1002346. https://doi.org/10.1371/journal.pmed.1002346

Academic Editor: Sanjay Basu, Stanford University, UNITED STATES

Received: January 10, 2017

Accepted: June 7, 2017

Published: July 10, 2017

Copyright: © 2017 Raffel et al. This is an open access article distributed under the terms of the Creative Commons Attribution License, which permits unrestricted use, distribution, and reproduction in any medium, provided the original author and source are credited.

Data Availability Statement: There is an ethical restriction for transferring the dataset. The MSSTB has ethical approval to collect and store clinical and pathological data, and to make data freely available to any interested research group for academic purposes (Wales Research Ethics Committee 3–08/MRE09/31+5). These data are available only on request to the MSSTB, and submissions must be approved by the MSSTB Review Panel prior to transfer. Interested researchers can contact the

Abstract

Background

There is increasing emphasis on using patient-reported outcomes (PROs) to complement traditional clinical outcomes in medical research, including in multiple sclerosis (MS). Research, particularly in oncology and heart failure, has shown that PROs can be prognostic of hard clinical endpoints such as survival time (time from study entry until death). However, unlike in oncology or cardiology, it is unknown whether PROs are associated with survival time in neurological diseases. The Multiple Sclerosis Impact Scale–29 (MSIS-29) is a PRO sensitive to short-term change in MS, with questions covering both physical and psychological quality of life. This study aimed to investigate whether MSIS-29 scores can be prognostic for survival time in MS, using a large observational cohort of people with MS.

Methods and findings

From 15 July 2004 onwards, MSIS-29 questionnaires were completed by people with MS registered with the MS Society Tissue Bank ($n = 2,126$, repeated 1 year later with $n = 872$ of the original respondents). By 2014, 264 participants (12.4%) had died. Higher baseline MSIS-29 physical (MSIS-29-PHYS) score was associated with reduced survival time (subgroup with highest scores versus subgroup with lowest scores: hazard ratio [HR] 5.7, 95% CI 3.1–10.5, $p < 0.001$). Higher baseline MSIS-29 psychological score was also associated with reduced survival time (subgroup with highest scores versus subgroup with lowest scores: HR 2.8, 95% CI 1.8–4.4, $p < 0.001$). In those with high baseline MSIS-29 scores, mortality risk was even greater if the MSIS-29 score worsened over 1 year (HR 2.3, 95% CI 1.2–4.4, $p = 0.02$). MSIS-29-PHYS scores were associated with survival time independent of age, sex, and patient-reported Expanded Disability Status Scale score in a Cox regression analysis (per 1-SD increase in MSIS-29-PHYS score: HR 1.8, 95% CI 1.1–2.9, $p = 0.03$). A limitation of the study is that this cohort had high baseline age and disability levels;

MSSTB (ukmstissuebank@imperial.ac.uk) at Imperial College London.

Funding: RN is supported by the National Institute for Health Research (NIHR) Biomedical Research Centre Funding Scheme at Imperial College. RN has received a grant from the UK MS/PD society for the MS Society Tissue Bank. The funders had no role in study design, data collection and analysis, decision to publish, or preparation of the manuscript.

Competing interests: I have read the journal's policy and the authors of this manuscript have the following competing interests. TF is a Section Editor with PLOS ONE. TF reports personal fees for consultancies (including data monitoring committees) from Novartis, Bayer, Biogen, AstraZeneca, Janssen, Grünenthal, Pharmalog, SGS and Roche, all outside the submitted work. RN has received grants, personal fees and non-financial support from Novartis, grants, personal fees and non-financial support from Biogen Idec, personal fees from Genzyme, personal fees from Roche, outside the submitted work.

Abbreviations: 95% CI, 95% confidence interval; df, degrees of freedom; EDSS, Expanded Disability Status Scale; HR, hazard ratio; MS, multiple sclerosis; MSIS-29, Multiple Sclerosis Impact Scale–29; MSIS-29-PHYS, MSIS-29 physical; MSIS-29-PSYCH, MSIS-29 psychological; MSSTB, MS Society Tissue Bank; prEDSS, patient-reported Expanded Disability Status Scale; PRO, patient-reported outcome; SD, standard deviation.

the prognostic value of MSIS-29 for survival time at earlier disease stages requires further investigation.

Conclusions

This study reports that PROs can be prognostic for hard clinical outcomes in neurological disease, and supports PROs as a meaningful clinical outcome for use in research and clinical settings.

Author summary

Why was this study done?

- Patient-reported outcomes (PROs) are questionnaires completed by people with a given condition, to help capture the impact of disease or treatment on the individual.
- PROs have many uses, e.g., to screen for symptoms, assess treatment response, and enhance doctor–patient communication.
- However, they are still underused in neurological conditions, in part because it is not clear if PROs relate to 'hard clinical outcomes' like disability or mortality.
- The Multiple Sclerosis Impact Scale–29 (MSIS-29) questionnaire is a PRO that assesses quality of life in people with multiple sclerosis (MS).
- Our study aimed to investigate whether MSIS-29 score is associated with the future risk of death in a large cohort of people with MS.

What did the researchers do and find?

- MSIS-29 questionnaires were completed by 2,126 people with MS in the UK. The questionnaire was repeated 1 year later in 872 people.
- Of the 2,126 participants, 264 died over 10 years of follow-up.
- We found that the MSIS-29 scores of participants were associated with their risk of 10-year mortality, even after adjusting for known risk factors for mortality such as age, sex, and baseline disability score.
- The subgroup with the highest MSIS-29 physical scores (indicating the poorest physical quality of life) had a 5.7 times greater risk of death than the subgroup with the lowest scores. Mortality risk was even higher in those for whom the MSIS-29 score worsened over 1 year.

What do these findings mean?

- To our knowledge, this is the first study to associate PROs with risk of mortality in neurological disease.
- This study shows that how a person with MS answers the MSIS-29 questions is important and relates to how well they may do in terms of health in the future.

- A limitation of the study is that participants with early disease and minimal disability were underrepresented.
- To improve neurological care, we must incorporate PROs into automated electronic systems to serve both routine clinical care and large-scale data collection. This will allow us to address key issues such as comparing the effectiveness of treatment options and tailoring treatment options to an individual's needs.

Introduction

Patient-reported outcomes (PROs) are defined as 'any report of the status of a patient's health condition that comes directly from the patient, without interpretation of the patient's response by a clinician or anyone else' [1]. They can offer significant advantages over assessment by a physician: they better capture the impact of disease on the person; they are often easier and cheaper to administer; and they can often be completed from the home environment, potentially allowing for long-term, geographically diverse, and large-scale observational and interventional studies [2]. They can also enhance routine clinical care in areas such as symptom screening, monitoring treatment response, care coordination, care systems assessment, and improving communication in the doctor–patient clinical encounter [3–6].

PROs are increasingly being used to complement traditional outcome measures in disciplines such as oncology, cardiology, and neurology. The increasing use of PROs in interventional trials is partly driven by the need for pharmaceutical companies to justify labelling and promotional claims in post-licensing marketing [1,7]. However, research and clinical practice, particularly in oncology, have led the way in proving that PROs can offer more than this: it is now well established in oncology that PROs are associated with hard clinical endpoints such as survival time (time from study entry until death) and can add prognostic value to the more traditional physician-reported outcome measures [8–10]. PROs are also well established as prognostic for survival time in heart failure [11–13]. However, such associations are more difficult to study in neurological research, in part because it is rarer for the clinical endpoint of trials in neurological disease to be survival.

The Multiple Sclerosis Impact Scale–29 (MSIS-29) is a PRO that attempts to assess both physical and psychological quality of life in multiple sclerosis (MS) [14]. It has the advantage of being self-reported and can be distributed by post. It could potentially be utilised in progressive MS trials, as it appears sensitive to clinically relevant change over short time frames [15]. This is in contrast to the traditional physician-assessed Expanded Disability Status Scale (EDSS), which is the primary outcome favoured in most MS trials despite several well-documented limitations, including poor interrater and intrarater reliability and a limited sensitivity to change over the time frame of 2–3 years, especially in progressive MS [16–20]. Though small studies have correlated MSIS-29 score with EDSS score, it is unknown how the MSIS-29 is linked to robust clinical endpoints such as survival time [21,22]. Indeed, to our knowledge, no PROs have been associated with survival in MS or any other neurological disease.

This study aimed to investigate whether MSIS-29 scores can be prognostic for survival time (time from MSIS-29 completion to death) in MS, using a large observational cohort of people with MS from the MS Society Tissue Bank (MSSTB). The primary study hypothesis was that MSIS-29 scores are associated with survival time in MS.

Methods

Study population

Since 1998, the MSSTB has operated a nationwide community-based scheme for people with MS and non-MS controls in the UK to donate their brain and spinal cord after death, by providing written consent while alive (ethics approval in 1998: London Multicentre Research Ethics Committee—MREC/02/2/39; then in 2008: Wales Research Ethics Committee 3–08/MRE09/31; then in 2013: Wales Research Ethics Committee 3–08/MRE09/31+5) [23]. This cohort is a unique population in that the participants are followed from registration to death, with eventual pathological confirmation [23]. On 15 July 2004, MSIS-29 questionnaires were sent out to all registered donors. For those who completed a MSIS-29 questionnaire at this time, a second MSIS-29 questionnaire was sent out 1 year later, to measure change in MSIS-29. In addition, since 15 July 2004, all new registered donors have been sent a MSIS-29 questionnaire at the time of registration, as well as a 'patient-reported EDSS' (prEDSS) [24,25]. This study included people with MS registered in the MSSTB up until 1 January 2014 who had completed at least 1 MSIS-29 questionnaire. Data were stored in the MSSTB facility at Imperial College London and were analysed in 2015–2016.

Outcome measures

The MSIS-29 consists of 29 questions answered on a 5-point Likert scale, giving 2 scores: the MSIS-29 physical (MSIS-29-PHYS) score (questions 1–20; therefore score range 20–100) and the MSIS-29 psychological (MSIS-29-PSYCH) score (questions 21–29; therefore score range 9–45) [14,26]. Imputation was used to address questionnaires returned with missing data using the following rule: if greater than 66% of questions had been answered within MSIS-29-PHYS or within MSIS-29-PSYCH, missing answers were imputed using the mean of the answered questions from the MSIS-29-PHYS or MSIS-29-PSYCH of that individual participant [27]. Otherwise, all data from that MSIS-29-PHYS or MSIS-29-PSYCH were excluded. The EDSS is a physician-reported gold standard for categorising disability in MS. The minimum score of 0 represents no impairment, 7 represents restriction to wheelchair, and the maximum score of 10 represents death. The prEDSS uses the same scale and can be completed without physician input, with good correlation [24]. A description of how to request access to the MSIS-29 questionnaire and the prEDSS questionnaire is available in S1 Appendix. Ten-year data on mortality were collected up until 1 June 2014. Survival time was defined using date of first MSIS-29 questionnaire as the entry point, date of death as the endpoint, and date of study completion (1 June 2014) as the censorship date for those still alive.

Baseline MSIS-29 scores were categorised into 5 equally spaced subgroups as follows: MSIS-29-PHYS scores—20–35, 36–51, 52–68, 69–84, 85–100; MSIS-29-PSYCH scores—9–16, 17–23, 24–30, 31–37, 38–45. In addition, for those with a repeat MSIS-29 questionnaire 1 year after baseline, the following subgroups were used: Subgroup 1—initial MSIS-29-PHYS score 20–84, no worsening after 1 year; Subgroup 2—initial MSIS-29-PHYS score 20–84, worsening after 1 year ($\geq$1 point); Subgroup 3—initial MSIS-29-PHYS score 85–100, no worsening after 1 year; and Subgroup 4—initial MSIS-29-PHYS score 85–100, worsening after 1 year ($\geq$1 point).

Statistical analysis

We did not preregister or publish a detailed analysis plan for this study. The statistical analysis is described below. Details on the history of this study and changes to the analysis plan are provided in S2 Appendix, while an early project outline is provided in S3 Appendix.

Population demographics are presented as mean (standard deviation [SD]) and frequency (percentage) for continuous and categorical variables, respectively. Differences between continuous variables were tested with the unpaired Student's *t*-test, or one-way analysis of variance (ANOVA) when more than 2 groups, while differences between categorical data were tested with the chi-square test. To assess whether MSIS-29-PHYS score, MSIS-29-PSYCH score, prEDSS score, and change in MSIS-29-PHYS score are associated with mortality, survival times were modelled using Cox proportional hazard models where the hazard ratios (HRs) for the respective instruments were adjusted for age and sex. The HRs are presented with 95% confidence intervals (95% CIs) and *p*-values testing the null hypothesis of the HRs being equal to 1. Survival curves within the subgroups were estimated using Kaplan–Meier estimators. Correlations between the 3 PRO scales (MSIS-29-PHYS, MSIS-29-PSYCH, and prEDSS) were estimated using rank-based Spearman correlations, which are reported with *p*-values testing the null hypothesis of no correlation. To investigate whether MSIS-29-PHYS and MSIS-29-PSYCH scores are associated with survival independent of prEDSS score, survival times were modelled using a Cox regression with prEDSS score, MSIS-29-PHYS score, MSIS-29-PSYCH score, age, and sex as independent variables. The SAS 9.4 platform was used for all statistical analysis.

Results

Population demographics

In all, 2,914 people with MS were enrolled in the MSSTB over the study period. 2,126 participants completed the MSIS-29 questionnaire for inclusion in this study (participation rate 73.0%). Of these, 2,119 participants completed both the MSIS-29-PHYS and MSIS-29-PSYCH questionnaire, and 7 participants completed only the MSIS-29-PHYS questionnaire. Data were imputed for 273 participants. A prEDSS assessment was available at the same time as the MSIS-29 assessment in 630 participants, and a repeat MSIS-29 questionnaire was completed 1 year after baseline by 872 participants. Differences in baseline characteristics between those included and those not included in the study, those with and without imputed data, those with and without prEDSS data, and those with and without longitudinal MSIS-29 data are presented in Table 1.

Median follow-up time was 9 years, while 865 participants had the maximum 10 years of follow-up. Up until 1 June 2014, 264 (12.4%) of the total group had died. The mean population age at MSIS-29 assessment was 54 (SD 11.9) years, with a disease length of 18.5 (SD 15.0) years, and 1,630 (76.7%) were female. At baseline, mean MSIS-29-PHYS score was 62 (SD 20.5), mean MSIS-29-PSYCH score was 23.6 (SD 8.7), and mean prEDSS score was 5.7 (SD 2.2).

A higher MSIS-29-PHYS score is associated with reduced survival time

Cox regression models demonstrated that higher MSIS-29-PHYS score was associated with reduced survival time independently of age and sex (Wald chi-square, [degrees of freedom (df) = 4, n = 2,126] = 98.5, $p < 0.001$; Fig 1A). Older age at first MSIS-29 completion (Wald chi-square [df = 1, n = 2,126] = 88.6, $p < 0.001$) and male sex (Wald chi-square [df = 1, n = 2,126] = 24.8, $p < 0.001$) were also associated with reduced survival time in the model. HRs for death were greater, and reduced survival times were observed, with higher MSIS-29-PHYS score, using the ranges 20–35, 36–51, 52–68, 69–84, and 85–100 (Fig 1B). The HR for death was 5.7 in the subgroup with MSIS-29-PHYS score 85–100 compared with the subgroup with MSIS-29-PHYS score 20–35 (HR 5.7, 95% CI 3.1–10.5, $p < 0.001$). Those with higher MSIS-29-PHYS scores were more likely to be male (chi-square [df = 4, n = 2,126] = 25.2, $p < 0.001$)

Table 1. Differences in baseline characteristics between those included and those not included in the study, those with and without imputed data, those with and without prEDSS data, and those with and without longitudinal MSIS-29 data.

Characteristic	*n*	Male sex	Age	Disease duration	Baseline MSIS-29-PHYS	Baseline MSIS-29-PSYCH
Included in the study						
Yes	2,126	496 (23.3%)	54.0 (11.9)	18.5 (15.0)	62.0 (20.5)	23.6 (8.7)
No	788	182 (23.1%)	55.8 (13.3)	18.4 (11.3)	n/a	n/a
p-Value		0.894	**<0.001**	0.827		
Imputed data						
No	1,853	439 (23.7%)	53.5 (11.7)	17.9 (14.5)	61.4 (20.5)	23.6 (8.8)
Yes	273	57 (20.9%)	57.4 (12.9)	23.3 (16.8)	65.8 (20.4)	23.3 (8.6)
p-Value		0.305	**<0.001**	**<0.001**	**0.001**	0.484
prEDSS completed						
Yes	630	152 (24.1%)	50.9 (12.3)	16.9 (17.0)	62.1 (20.4)	23.8 (8.7)
No	1,496	344 (23.0%)	55.2 (11.5)	19.2 (13.9)	61.9 (20.6)	23.5 (8.7)
p-Value		0.573	**<0.001**	**<0.001**	0.909	0.457
1-year repeat MSIS-29 completed						
Yes	872	188 (21.6%)	55.1 (11.1)	18.2 (13.4)	60.6 (19.5)	23.0 (8.3)
No	1,254	308 (24.6%)	53.1 (12.4)	18.8 (15.9)	63.0 (21.1)	24.0 (9.0)
p-Value		0.107	**<0.001**	0.407	**0.008**	**0.007**

Data are presented as n (percent) or mean (SD). Differences between categorical data (sex) were tested with the chi-square test. Differences between continuous data (age, disease duration, MSIS-29-PHYS, MSIS-29-PSYCH) were tested with the unpaired Student's t-test. Significant p-values are highlighted in bold.

MSIS-29, Multiple Sclerosis Impact Scale–29; MSIS-29-PHYS, MSIS-29 physical; MSIS-29-PSYCH, MSIS-29 psychological; n/a, not applicable; prEDSS, patient-reported Expanded Disability Status Scale.

https://doi.org/10.1371/journal.pmed.1002346.t001

and had older age (F[df = 4, n = 2,121] = 16.1, $p < 0.001$) and longer disease duration (F[df = 4, n = 2,121] = 4.1, $p < 0.01$; Table 2).

A higher MSIS-29-PSYCH score is associated with reduced survival time

Similarly, Cox regression models demonstrated that higher MSIS-29-PSYCH score was associated with reduced survival time independently of age and sex (Wald chi-square [df = 4, n = 2,119] = 19.2, $p < 0.001$; Fig 2A), although the effect was less pronounced than with MSIS-29-PHYS. HRs for death were greater, and reduced survival times were observed, with higher MSIS-29-PSYCH score, using the ranges 9–16, 17–23, 24–30, 31–37, and 38–45 (Fig 2B). The HR for death was 2.8 in the subgroup with MSIS-29-PSYCH score 38–45 compared with the subgroup with MSIS-29-PHYS score 9–16 (HR 2.8, 95% CI 1.8–4.4, $p < 0.001$). In contrast to MSIS-29-PHYS score, higher MSIS-29-PSYCH score was not associated with male sex or longer disease duration and was associated with younger age (F[df = 4, n = 2,114] = 5.5, $p < 0.001$; Table 2).

MSIS-29-PHYS score is correlated with prEDSS score but is independently associated with survival time

There was a strong correlation between the MSIS-29-PHYS and MSIS-29-PSYCH scores (r [df = 2,117] = 0.54, $p < 0.001$). There was a strong correlation between the MSIS-29-PHYS score and the prEDSS score (r[df = 628] = 0.52, $p < 0.001$) and a weak correlation between the MSIS-29-PSYCH score and the prEDSS score (r[df = 623] = 0.19, $p < 0.001$). To determine

A

Parameter		Hazard Ratio	95% Hazard Ratio Confidence Limits		p-value	p-value factor
MSIS-29-PHYS score (compared to 20-35)	36-51	0.995	0.486	2.038	0.989	<0.001
	52-68	1.853	0.998	3.438	0.051	
	69-84	2.140	1.155	3.966	0.016	
	85-100	5.728	3.131	10.479	<0.001	
Age	per year	1.051	1.041	1.063		<0.001
Sex	male vs. female	1.906	1.479	2.457		<0.001

B

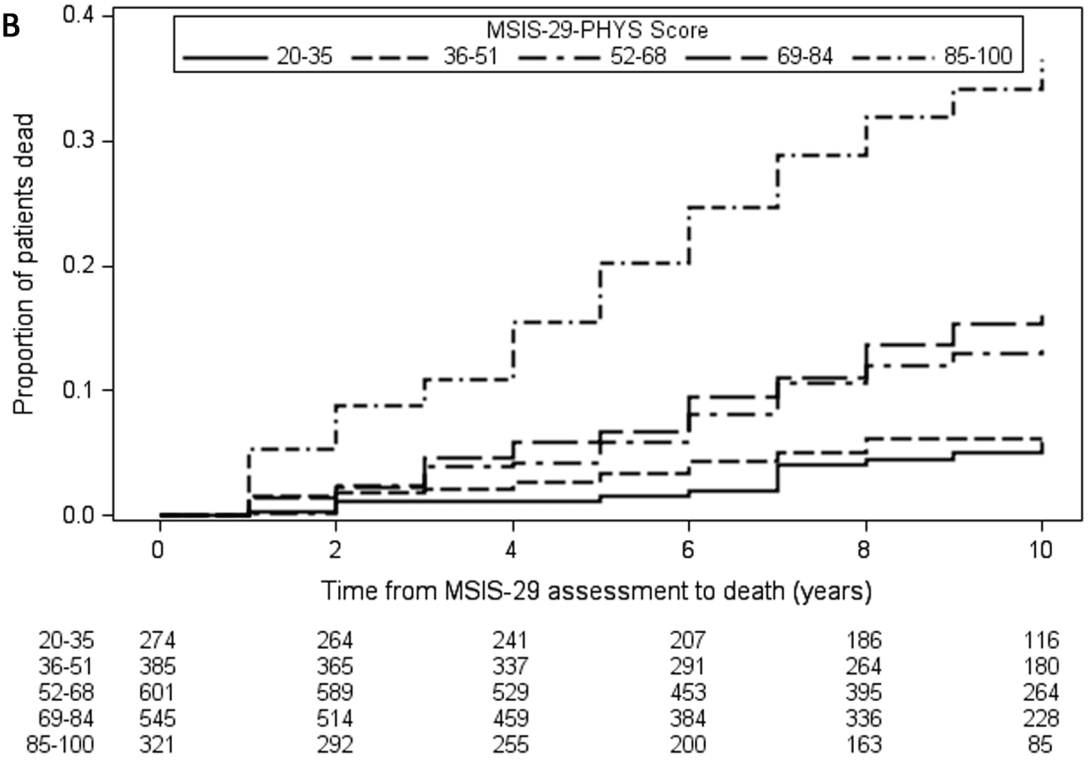


Fig 1. Higher MSIS-29-PHYS scores are associated with reduced survival time. (A) Table: Higher MSIS-29-PHYS score was associated with reduced survival time (greater hazard ratio for death), as were older age at first MSIS-29 completion and male sex. (B) Kaplan–Meier failure curves (n = 2,126). Note that Kaplan–Meier curves do not account for the effect of age and sex on survival time. MSIS-29, Multiple Sclerosis Impact Scale–29; MSIS-29-PHYS, MSIS-29 physical.

https://doi.org/10.1371/journal.pmed.1002346.g001

whether the MSIS-29-PHYS and MSIS-29-PSYCH scores were associated with survival time independently of prEDSS score, all measures were included in a Cox regression model, along with age and sex, in the limited number of participants who completed all 3 measures (n = 625; Table 3). Reduced survival time was associated with older age at baseline (per year: HR 1.07, 95% CI 1.04–1.10, $p < 0.001$), a higher prEDSS score (per 1 SD [2.2]: HR 2.0, 95% CI 1.0–3.7, $p < 0.05$), and a higher MSIS-29-PHYS score (per 1 SD [20.3]: HR 1.8, 95% CI 1.1–2.9, $p < 0.05$).

Table 2. Variation in characteristics between those with different baseline MSIS-29 scores.

Characteristic	*n*	Male sex	Age	Disease duration	Baseline MSIS-29-PHYS	Baseline MSIS-29-PSYCH
MSIS-29-PHYS score						
20–35	274	44 (16.1%)	49.1 (11.1)	15.8 (14.0)	27.5 (4.7)	14.6 (5.0)
36–51	385	70 (18.2%)	53.0 (11.8)	17.4 (15.5)	44.0 (4.5)	19.8 (6.6)
52–68	601	146 (24.3%)	54.9 (12.0)	19.0 (15.1)	60.6 (4.8)	23.6 (7.2)
69–84	545	137 (25.1%)	55.4 (12.1)	19.5 (15.5)	76.0 (4.6)	26.7 (7.9)
85–100	321	99 (30.8%)	55.1 (11.2)	19.7 (13.2)	92.0 (4.9)	30.5 (9.0)
p-Value		**<0.001**	**<0.001**	**0.003**	**<0.001**	**<0.001**
MSIS-29-PSYCH score						
9–16	525	115 (21.9%)	55.3 (12.0)	19.8 (15.6)	46.8 (20.0)	12.9 (2.2)
17–23	598	143 (23.9%)	54.6 (12.1)	18.9 (15.0)	59.2 (17.6)	20.1 (2.0)
24–30	512	124 (24.2%)	53.6 (11.7)	17.9 (14.8)	67.2 (16.4)	26.7 (2.0)
31–37	326	83 (25.5%)	52.4 (11.8)	18.0 (14.9)	74.0 (14.7)	33.7 (2.0)
38–45	158	30 (19.0%)	51.4 (11.2)	16.2 (12.4)	82.1 (14.7)	40.8 (2.3)
p-Value		0.834	**<0.001**	0.053	**<0.001**	**<0.001**

Data are presented as n (percent) or mean (SD). Differences between categorical data (sex) were tested with the chi-square test. Differences between continuous data (age, disease duration, MSIS-29-PHYS, MSIS-29-PSYCH) were tested with one-way analysis of variance (ANOVA). Significant p-values are highlighted in bold.

MSIS-29, Multiple Sclerosis Impact Scale–29; MSIS-29-PHYS, MSIS-29 physical; MSIS-29-PSYCH, MSIS-29 psychological.

https://doi.org/10.1371/journal.pmed.1002346.t002

Worsening in the MSIS-29-PHYS score over 1 year is associated with reduced survival time

The MSIS-29 questionnaire was repeated after 1 year in a subgroup ($n = 872$) of those who had originally completed the MSIS-29 in 2004. Comparing MSIS-29-PHYS stable/improving score participants with MSIS-29-PHYS worsening score participants (change in MSIS-29-PHYS ≤ 0 versus > 0), there was no statistically significant difference in mortality (Cox regression adjusted for age and sex: $n = 872$, HR = 1.2, 95% CI 0.9–1.2, $p = 0.28$). However, in the subgroup of participants whose initial MSIS-29-PHYS score was 85–100, a longitudinal worsening of MSIS-29-PHYS score was associated with reduced survival time (HR = 2.3, 95% CI 1.2–4.4, $p = 0.016$; Fig 3). This was not apparent in the subgroup with initial MSIS-29-PHYS score 20–84 (HR = 1.3, 95% CI 0.8–2.0, $p = 0.24$; Fig 3). Fig 3B shows the survival curves for the 4 subgroups.

Discussion

This study reports that higher MSIS-29 score is associated with reduced survival time in a large observational cohort of people with MS. MSIS-29-PHYS and MSIS-29-PSYCH scores were both associated with survival time, although MSIS-29-PHYS score has stronger prognostic value, and associates with survival time independently of age, sex, and prEDSS score in a Cox regression model. In addition, in the subgroup with initial MSIS-29-PHYS score 85–100, a 1-year longitudinal worsening of MSIS-29-PHYS score is associated with an even worse prognosis. This finding shows that how a person with MS answers these questions is important and relates to how well they may do in terms of health in the future. To our knowledge, this is the first study to associate PROs with survival outcomes in any neurological disease.

This study benefitted from the MSSTB cohort in several ways. We believe this is the largest cohort with reported MSIS-29 results to date, other than 1 web-based cohort [28,29], and the MSSTB has by far the longest follow-up after MSIS-29 completion (up to 10 years, median 9

A

Parameter		Hazard Ratio	95% Hazard Ratio Confidence Limits		p-value	p-value factor
MSIS-29-PSYCH score (compared to 9-16)	17-23	1.475	1.036	2.101	0.031	<0.001
	24-30	1.441	0.995	2.087	0.053	
	31-37	1.474	0.965	2.250	0.073	
	38-45	2.789	1.762	4.414	<0.001	
Age	per year	1.057	1.046	1.068		<0.001
Sex	male vs. female	2.110	1.638	2.716		<0.001

B

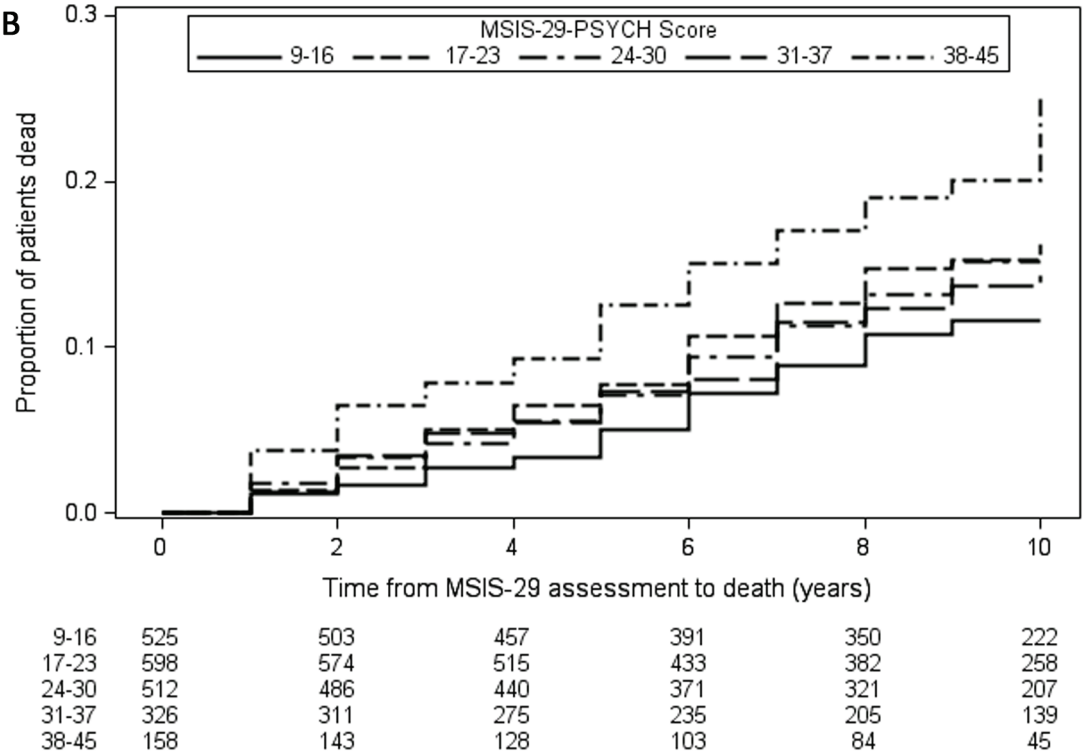


Fig 2. Higher MSIS-29-PSYCH scores are associated with reduced survival time. (A) Table: Higher MSIS-29-PSYCH score was associated with reduced survival time (greater hazard ratio for death), as were older age at first MSIS-29 completion and male sex. (B) Kaplan–Meier failure curves (n = 2,119). Note that Kaplan–Meier curves do not account for the effect of age and sex on survival time. MSIS-29, Multiple Sclerosis Impact Scale–29; MSIS-29-PSYCH, MSIS-29 psychological.

https://doi.org/10.1371/journal.pmed.1002346.g002

years). This cohort had 264 deaths within the study period. This number of deaths allowed the prognostic value of MSIS-29 scores for survival time to be studied.

One should consider the external validity of this cohort's results to the general MS population. The MSSTB recruitment strategy is based entirely in the community, relying upon community-based presentations and a quarterly magazine, *MS Matters*, distributed to approximately 30,000 members of the Multiple Sclerosis Society of Great Britain and Northern Ireland [30]. Moreover, the MSSTB population has previously been shown to be representative of the UK MS population in terms of disease characteristics and clinical milestones over the course of

Table 3. Reduced survival time (greater hazard ratio for death) was associated with older age, higher prEDSS score, and higher MSIS-29-PHYS score in the limited cohort with prEDSS score available (n = 625).

Parameter	Hazard ratio	95% hazard ratio confidence limits		*p*-Value
		Lower	Upper	
prEDSS, per 1 SD (2.2)	1.952	1.025	3.718	0.042
MSIS-29-PHYS, per 1 SD (20.3)	1.762	1.057	2.938	0.030
MSIS-29-PSYCH, per 1 SD (8.7)	0.905	0.631	1.297	0.587
Age, per year	1.070	1.042	1.099	<0.001
Sex, male versus female	1.237	0.622	2.459	0.544

MSIS-29, Multiple Sclerosis Impact Scale–29; MSIS-29-PHYS, MSIS-29 physical; MSIS-29-PSYCH, MSIS-29 psychological; prEDSS, patient-reported Expanded Disability Status Scale.

https://doi.org/10.1371/journal.pmed.1002346.t003

the disease [23]. The spread of MSIS-29 scores in this study was comparable with that reported in other large cohort studies [28,29]. In addition, factors that are known to associate with reduced survival, such as male sex, older age at baseline, and higher prEDSS score, were also found to associate with reduced survival time in this cohort, along with MSIS-29 score [31–33]. However, at the time of enrolment into the MSSTB, participants are often late in their disease course, as evidenced by this study's mean disease duration of 18.5 years and mean prEDSS score of 5.7 at baseline MSIS-29 questionnaire. Therefore, this study likely underrepresents those with earlier disease and less disability, and it is uncertain how MSIS-29 scores and their prognostic value for mortality will vary in this group. One might hypothesize that those with earlier disease would have lower MSIS-29 scores and increased survival times, on average [29].

There are several other limitations to this study. Only a limited cohort completed the prEDSS questionnaire (n = 630), and only a limited cohort completed a longitudinal MSIS-29 (n = 872), mostly because of changes to the study protocol over time. Also, this study used a prEDSS rather than the traditional physician-reported EDSS, although these have previously been shown to correlate well [24]. Data on disease subtype, relapses, and disease-modifying therapy were not available for this study, and could influence the relationship between MSIS-29 score and survival time. Like most clinical outcome measures, PROs are susceptible to random measurement error, and hence regression dilution bias likely causes a decrease in the prognostic value of MSIS-29 for mortality [34]. However, previous studies have reported the test–retest reliability of MSIS-29-PHYS and MSIS-29-PSYCH to be high (intraclass correlation coefficients of 0.94 and 0.87, respectively), and so this effect is likely minimal [14].

In MS research, PROs such as MSIS-29 offer several advantages over traditional physician-assessed outcome measures such as the EDSS [2]. Interrater EDSS variability is high [17,35]. The EDSS also has a limited sensitivity to change over the 2- to 3-year time scale of clinical trials [36,37]. This is especially true in progressive MS, where the EDSS often does not capture changes in arm function or subtle changes in mobility [38]. MSIS-29 can be more responsive to clinically relevant change over short time frames [15,39]. PROs including MSIS-29 can also be sent to large cohorts of people with MS, and completed by post or online [29]. PROs could therefore enable large cohort studies, which would otherwise be financially unfeasible, such as comparative clinical effectiveness research. PROs validated against hard clinical endpoints could also be incorporated into patient registries to help address key questions in personalised medicine relating to prognosis, predicting response to treatment, and assessing response to treatment. These are increasingly important issues in MS and other neurological diseases like epilepsy, stroke, Parkinson disease, and spasticity, where a range of therapies are now available but questions remain regarding how to treat the individual.

A

Parameter		Hazard Ratio	95% Hazard Ratio Confidence Limits		p-value	p-value factor
MSIS-29-PHYS subgroup (compared to subgroup 1)	subgroup 2	1.289	0.843	1.972	0.241	<0.001
	subgroup 3	2.577	1.469	4.519	0.001	
	subgroup 4	5.839	3.213	10.611	<0.001	
Age	per year	1.055	1.038	1.071		<0.001
Sex	male vs. female	2.238	1.557	3.218		<0.001

B

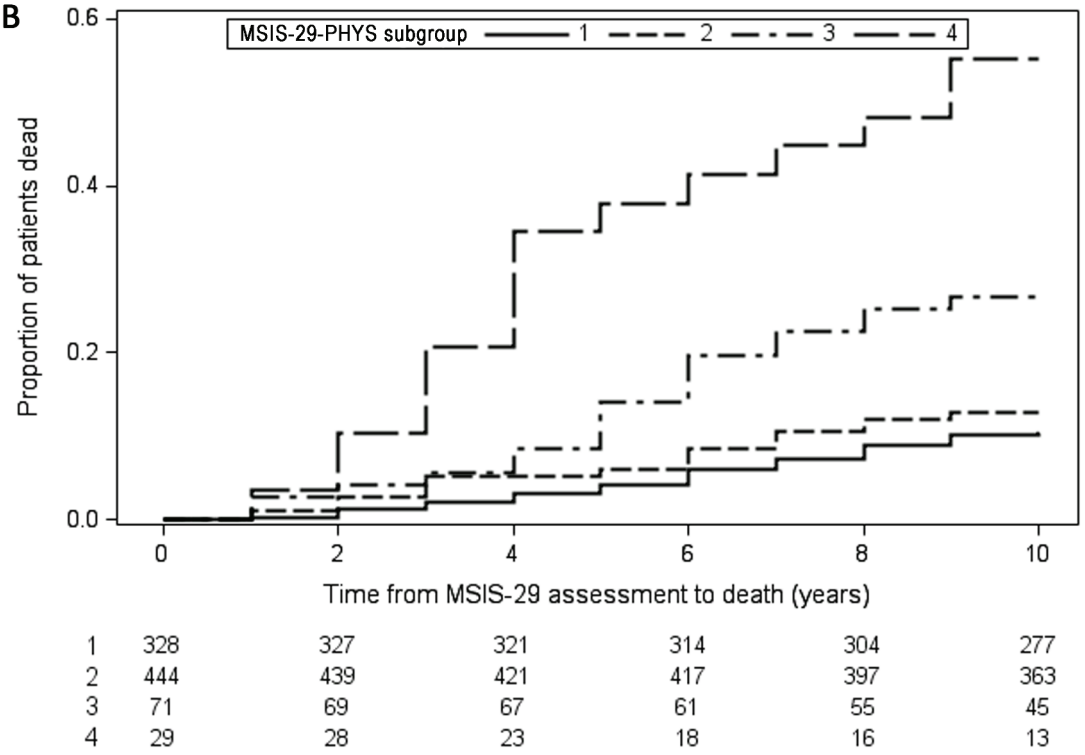


Fig 3. Longitudinally worsening MSIS-29-PHYS scores are associated with reduced survival time. Four subgroups are presented in this figure: Subgroup 1—initial MSIS-29-PHYS score 20–84, no worsening after 1 year (solid line); Subgroup 2—initial MSIS-29-PHYS score 20–84, worsening after 1 year (short-dashed line); Subgroup 3—initial MSIS-29-PHYS score 85–100, no worsening after 1 year (dot-dashed line); Subgroup 4—initial MSIS-29-PHYS score 85–100, worsening after 1 year (long-dashed line). (A) Table: Subgroups 1 and 2 had no statistically significant difference in survival time (HR = 1.289, 95% CI 0.843–1.972, p = 0.241). Subgroup 4 had reduced survival time compared with subgroup 3 (HR = 2.266, 95% CI 1.163–4.413, p = 0.016). p < 0.001 for differences between the 4 subgroups. (B) Kaplan–Meier failure curves (n = 872). Note that Kaplan–Meier curves do not account for the effect of age and sex on survival time. HR, hazard ratio; MSIS-29, Multiple Sclerosis Impact Scale–29; MSIS-29-PHYS, MSIS-29 physical.

https://doi.org/10.1371/journal.pmed.1002346.g003

Outside of the research setting, PROs can benefit individual patients directly if they are utilized in routine clinical practice. Oncology has again led the way, where PROs are routinely used to enhance patient care [5]. PROs can help screen for changes in physical or psychological symptoms, and identify unmet health, care, and support needs. They can be used as a decision aid when devising or evaluating treatment plans [40]. Patients and doctors can have differing views on which outcomes matter most, and the effective use of PROs can help refocus care

goals to the views of the individual patient [41,42]. This might also empower patients towards improved self-management of their condition [43]. When assessed in a randomised controlled trial, PROs enhanced doctor–patient communication and improved patient health-related quality of life and emotional well-being [4].

On a healthcare provision level, PROs can also be used to audit quality of care within a service or to compare quality of care between services [44]. PROs are often now incorporated into automated electronic systems for data collection, with high user compliance [45,46]. As well as providing direct benefit to patients, these systems can also feed into patient registries to help address research questions.

Further research questions emerge from this study. With this study having shown that MSIS-29 score is associated with death, similar methods could be used to investigate whether MSIS-29 score is associated with disability outcomes, such as time until wheelchair use. The effect of disease-modifying treatment on MSIS-29 and long-term clinical endpoints needs further attention, to assess whether MSIS-29 scores could be used as a surrogate for response to treatment. Multiple variables, including other PROs collected at multiple time points, could be incorporated into more complex models to better predict outcomes in large cohorts.

PROs will continue to be used in interventional studies, in part to satisfy labelling and promotional claims in post-licensing marketing [1,7]. This study argues that the MSIS-29 questionnaire can offer more than this, since its association with hard clinical endpoints supports its use as a meaningful clinical outcome to inform care decision-making. In oncology, PROs are now established as influential and clinically relevant measures, and it is accepted that the classic clinical endpoints do not fully capture the benefits, risks, and costs of treatment [8–10]. MS and neurology research will continue to rely upon clinical trials, as well as 'big data' gathered from clinical registries. The careful incorporation of PROs can enrich such datasets and allow the investigation of research questions beyond what traditional physician-based assessments can offer.

Supporting information

S1 Appendix. Description of how to request access to the MSIS-29 questionnaire and prEDSS questionnaire, and a copy of the MSIS-29 questionnaire.
(DOCX)

S2 Appendix. Description of the analysis plan, and historical changes made to the study.
(DOCX)

S3 Appendix. Imperial College London medical student BSc project outlines 2013–14, with a description of MSIS-29 project.
(PDF)

Acknowledgments

Clinical data were supplied by the MSSTB, funded by the Multiple Sclerosis Society of Great Britain and Northern Ireland, registered charity 207495.

We wish to thank the donors registered with the MSSTB for their consent and participation.

Author Contributions

Conceptualization: JR AW TF RN.

Data curation: DG RR RN.

Formal analysis: JR AW TF RN.

Investigation: JR AW DG.

Methodology: JR TF RN.

Supervision: RN.

Visualization: JR TF RN.

Writing – original draft: JR AW RN.

Writing – review & editing: JR RR DG TF RN.

References

1. US Department of Health and Human Services, Food and Drug Administration, Center for Drug Evaluation and Research, Center for Biologics Evaluation and Research, Center for Devices and Radiological Health. Guidance for industry. Patient-reported outcome measures: use in medical product development to support labeling claims. Silver Spring (Maryland): Food and Drug Administration; 2009. Available from: https://www.fda.gov/downloads/Drugs/. . ./Guidances/UCM193282.pdf. Accessed 2017 Jun 14.
2. Fayers P, Machin D. Quality of life: the assessment, analysis and interpretation of patient-reported outcomes. Hoboken (New Jersey): John Wiley & Sons; 2013.
3. Hilarius DL, Kloeg PH, Gundy CM, Aaronson NK. Use of health-related quality-of-life assessments in daily clinical oncology nursing practice—a community hospital-based intervention study. Cancer. 2008;113(3):628–37. https://doi.org/10.1002/cncr.23623 PMID: 18543317
4. Velikova G, Booth L, Smith AB, Brown PM, Lynch P, Brown JM, et al. Measuring quality of life in routine oncology practice improves communication and patient well-being: a randomized controlled trial. J Clin Oncol. 2004;22(4):714–24. https://doi.org/10.1200/JCO.2004.06.078 PMID: 14966096
5. Howell D, Molloy S, Wilkinson K, Green E, Orchard K, Wang K, et al. Patient-reported outcomes in routine cancer clinical practice: a scoping review of use, impact on health outcomes, and implementation factors. Ann Oncol. 2015;26(9):1846–58. https://doi.org/10.1093/annonc/mdv181 PMID: 25888610
6. Snyder CF, Aaronson NK, Choucair AK, Elliott TE, Greenhalgh J, Halyard MY, et al. Implementing patient-reported outcomes assessment in clinical practice: a review of the options and considerations. Qual Life Res. 2012;21(8):1305–14. https://doi.org/10.1007/s11136-011-0054-x PMID: 22048932
7. McLeod LD, Coon CD, Martin SA, Fehnel SE, Hays RD. Interpreting patient-reported outcome results: US FDA guidance and emerging methods. Expert Rev Pharmacoecon Outcomes Res. 2011;11(2):163–9. https://doi.org/10.1586/erp.11.12 PMID: 21476818
8. Secord AA, Coleman RL, Havrilesky LJ, Abernethy AP, Samsa GP, Cella D. Patient-reported outcomes as end points and outcome indicators in solid tumours. Nat Rev Clin Oncol. 2015;12(6):358–70. https://doi.org/10.1038/nrclinonc.2015.29 PMID: 25754949
9. Lipscomb J, Gotay CC, Snyder CF. Patient-reported outcomes in cancer: a review of recent research and policy initiatives. CA Cancer J Clin. 2007;57(5):278–300. https://doi.org/10.3322/CA.57.5.278 PMID: 17855485
10. Gotay CC, Kawamoto CT, Bottomley A, Efficace F. The prognostic significance of patient-reported outcomes in cancer clinical trials. J Clin Oncol. 2008;26(8):1355–63. https://doi.org/10.1200/JCO.2007.13.3439 PMID: 18227528
11. Kosiborod M, Soto GE, Jones PG, Krumholz HM, Weintraub WS, Deedwania P, et al. Identifying heart failure patients at high risk for near-term cardiovascular events with serial health status assessments. Circulation. 2007;115(15):1975–81. https://doi.org/10.1161/CIRCULATIONAHA.106.670901 PMID: 17420346
12. Tate CW, Robertson AD, Zolty R, Shakar SF, Lindenfeld J, Wolfel EE, et al. Quality of life and prognosis in heart failure: results of the Beta-Blocker Evaluation of Survival Trial (BEST). J Card Fail. 2007;13(9):732–7. https://doi.org/10.1016/j.cardfail.2007.07.001 PMID: 17996821
13. Heidenreich PA, Spertus JA, Jones PG, Weintraub WS, Rumsfeld JS, Rathore SS, et al. Health status identifies heart failure outpatients at risk for hospitalization or death. J Am Coll Cardiol. 2006;47(4):752–6. https://doi.org/10.1016/j.jacc.2005.11.021 PMID: 16487840
14. Hobart J, Lamping D, Fitzpatrick R, Riazi A, Thompson A. The Multiple Sclerosis Impact Scale (MSIS-29)—a new patient-based outcome measure. Brain. 2001;124:962–73. PMID: 11335698

15. Bosma LVAE, Sonder JM, Kragt JJ, Polman CH, Uitdehaag BMJ. Detecting clinically-relevant changes in progressive multiple sclerosis. Mult Scler. 2015;21(2):171–9. https://doi.org/10.1177/1352458514540969 PMID: 25013153

16. Kurtzke JF. Rating neurologic impairment in multiple sclerosis: an expanded disability status scale (EDSS). Neurology. 1983;33(11):1444–52. PMID: 6685237

17. Noseworthy JH, Vandervoort MK, Wong CJ, Ebers GC. Interrater variability with the Expanded Disability Status Scale (EDSS) and Functional Systems (FS) in a multiple sclerosis clinical trial. Neurology. 1990;40(6):971–5. PMID: 2189084

18. Hobart J, Freeman J, Thompson A. Kurtzke scales revisited: the application of psychometric methods to clinical intuition. Brain. 2000;123:1027–40. PMID: 10775547

19. Cohen JA, Reingold SC, Polman CH, Wolinsky JS, International Advisory Committee on Clinical Trials in Multiple Sclerosis. Disability outcome measures in multiple sclerosis clinical trials: current status and future prospects. Lancet Neurol. 2012;11(5):467–76. https://doi.org/10.1016/S1474-4422(12)70059-5 PMID: 22516081

20. European Medicines Agency. Guideline on clinical investigation of medicinal products for the treatment of multiple sclerosis. London: European Medicines Agency; 2015. Available from: http://www.ema.europa.eu/docs/en_GB/document_library/Scientific_guideline/2015/03/WC500185161.pdf. Accessed 2017 Jun 14.

21. Hoogervorst ELJ, Zwemmer JNP, Jelles B, Polman CH, Uitdehaag BMJ. Multiple Sclerosis Impact Scale (MSIS-29): relation to established measures of impairment and disability. Mult Scler. 2004;10(5):569–74. https://doi.org/10.1191/1352458504ms1078oa PMID: 15471375

22. McGuigan C, Hutchinson M. The multiple sclerosis impact scale (MSIS-29) is a reliable and sensitive measure. J Neurol Neurosurg Psychiatry. 2004;75(2):266–9. PMID: 14742602

23. Reynolds R, Roncaroli F, Nicholas R, Radotra B, Gveric D, Howell O. The neuropathological basis of clinical progression in multiple sclerosis. Acta Neuropathol. 2011;122(2):155–70. https://doi.org/10.1007/s00401-011-0840-0 PMID: 21626034

24. Collins CD, Ivry B, Bowen JD, Cheng EM, Dobson R, Goodin DS, et al. A comparative analysis of Patient-Reported Expanded Disability Status Scale tools. Mult Scler. 2016;22(10):1349–58. https://doi.org/10.1177/1352458515616205 PMID: 26564998

25. Lechner-Scott J, Kappos L, Hofman M, Polman CH, Ronner H, Montalban X, et al. Can the expanded disability status scale be assessed by telephone? Mult Scler. 2003;9(2):154–9. https://doi.org/10.1191/1352458503ms884oa PMID: 12708811

26. Ramp M, Khan F, Misajon RA, Pallant JF. Rasch analysis of the Multiple Sclerosis Impact Scale (MSIS-29). Health Qual Life Outcomes. 2009;7:58. https://doi.org/10.1186/1477-7525-7-58 PMID: 19545445

27. Sterne JAC, White IR, Carlin JB, Spratt M, Royston P, Kenward MG, et al. Multiple imputation for missing data in epidemiological and clinical research: potential and pitfalls. BMJ. 2009;339:b2393. https://doi.org/10.1136/bmj.b2393

28. Jones KH, Jones PA, Middleton RM, Ford DV, Lockhart-Jones H, Tuite-Dalton K, et al. Physical disability, anxiety and depression in people with MS: an internet-based survey via the UK MS Register. PLoS ONE. 2014;9(8):e104604. https://doi.org/10.1371/journal.pone.0104604

29. Jones KH, Ford DV, Jones PA, John A, Middleton RM, Lockhart-Jones H, et al. The physical and psychological impact of multiple sclerosis using the MSIS-29 via the web portal of the UK MS Register. PLoS ONE. 2013;8(1):e55422. https://doi.org/10.1371/journal.pone.0055422 PMID: 23383186

30. MS Society. MS Matters—your MS magazine. Available from: https://www.mssociety.org.uk/get-involved/membership/ms-matters-magazine. Accessed 2017 Apr 30.

31. Weinshenker BG. Natural history of multiple sclerosis. Ann Neurol. 1994;36(Suppl):S6–11. https://doi.org/10.1002/ana.410360704

32. Kingwell E, van der Kop M, Zhao Y, Shirani A, Zhu F, Oger J, et al. Relative mortality and survival in multiple sclerosis: findings from British Columbia, Canada. J Neurol Neurosurg Psychiatry. 2012;83(1):61–6. https://doi.org/10.1136/jnnp-2011-300616 PMID: 21865212

33. Levic ZM, Dujmovic I, Pekmezovic T, Jarebinski M, Marinkovic J, Stojsavljevic N, et al. Prognostic factors for survival in multiple sclerosis. Mult Scler. 1999;5(3):171–8. https://doi.org/10.1177/135245859900500306 PMID: 10408717

34. Hutcheon JA, Chiolero A, Hanley JA. Random measurement error and regression dilution bias. BMJ. 2010;340:c2289. https://doi.org/10.1136/bmj.c2289 PMID: 20573762

35. Verdiertaillefer MH, Zuber M, Lyoncaen O, Clanet M, Gout O, Louis C, et al. Observer disagreement in rating neurologic impairment in multiple-sclerosis—facts and consequences. Eur Neurol. 1991;31(2):117–9. https://doi.org/10.1159/000116658 PMID: 2044616

36. van Winsen LML, Kragt JJ, Hoogervorst ELJ, Polman CH, Uitdehaag BMJ. Outcome measurement in multiple sclerosis: detection of clinically relevant improvement. Mult Scler. 2010;16(5):604–10. https://doi.org/10.1177/1352458509359922 PMID: 20086019

37. Kragt JJ, Thompson AJ, Montalban X, Tintore M, Rio J, Polman CH, et al. Responsiveness and predictive value of EDSS and MSFC in primary progressive MS. Neurology. 2008;70(13):1084–91.

38. Ontaneda D, Fox RJ, Chataway J. Clinical trials in progressive multiple sclerosis: lessons learned and future perspectives. Lancet Neurol. 2015;14(2):208–23. https://doi.org/10.1016/S1474-4422(14)70264-9 PMID: 25772899

39. Hobart JC, Riazi A, Lamping DL, Fitzpatrick R, Thompson AJ. How responsive is the Multiple Sclerosis Impact Scale (MSIS-29)? A comparison with some other self report scales. J Neurol Neurosurg Psychiatry. 2005;76(11):1539–43. https://doi.org/10.1136/jnnp.2005.064584 PMID: 16227547

40. Greenhalgh J. The applications of PROs in clinical practice: what are they, do they work, and why? Qual Life Res. 2009;18(1):115–23. https://doi.org/10.1007/s11136-008-9430-6 PMID: 19105048

41. Marshall S, Haywood K, Fitzpatrick R. Impact of patient-reported outcome measures on routine practice: a structured review. J Eval Clin Pract. 2006;12(5):559–68. https://doi.org/10.1111/j.1365-2753.2006.00650.x PMID: 16987118

42. Rothwell PM, McDowell Z, Wong CK, Dorman PJ. Doctors and patients don't agree: Cross sectional study of patient's and doctors' perceptions and assessments of disability in multiple sclerosis. BMJ. 1997;314(7094):1580–3. PMID: 9169401

43. Stimson GV. Obeying doctor's orders: a view from the other side. Soc Sci Med. 1974;8(2):97–104. PMID: 4821252

44. Devlin NJ, Appleby J. Getting the most out of PROMS: putting health outcomes at the heart of NHS decision-making. London: The King's Fund; 2010. Available from: https://www.kingsfund.org.uk/publications/getting-most-out-proms. Accessed 2017 Apr 6.

45. Wright EP, Selby PJ, Crawford M, Gillibrand A, Johnston C, Perren TJ, et al. Feasibility and compliance of automated measurement of quality of life in oncology practice. J Clin Oncol. 2003;21(2):374–82. https://doi.org/10.1200/JCO.2003.11.044 PMID: 12525532

46. Jensen RE, Snyder CF, Abernathy AP, Basch E, Potosky AL, Roberts AC, et al. Review of electronic patient-reported outcomes systems used in cancer clinical care. J Oncol Pract. 2014;10(4):e215–22. https://doi.org/10.1200/JOP.2013.001067 PMID: 24301843

Appendix B

List of publications by the thesis author related to work conducted during clinical fellowship but not otherwise discussed in thesis

Additional publications by the thesis author related to work conducted during clinical fellowship but not otherwise discussed in thesis:

1) Nicholas RS, Han E, **Raffel J**, Chataway J, Friede T. Over three decades study populations in progressive multiple sclerosis have become older and more disabled, but have lower on-trial progression rates: A systematic review and meta-analysis of 43 randomised placebo-controlled trials. *Multiple Sclerosis Journal.* 2019;25(11):1462-1471.
   https://www.ncbi.nlm.nih.gov/pubmed/30141723
2) Kamourieh S, Gananandan K, **Raffel J**, Nicholas R. Natalizumab Granule Cell Neuronopathy: FDG-PET in diagnosis and immune reconstitution with G-CSF. *Neuroimmunology and Neuroinflammation*. 2017;4(5):e384.
   https://www.ncbi.nlm.nih.gov/pubmed/28761903
3) Puentes F, van der Star B, Lidster K, Boomkamp S, Kipp M, Boon L, Bosca I, **Raffel J**, Gnanapavan S, van der Valk P, Barnett SC, Baker D, Amor S. Neurofilament Light as an immune target for pathogenic antibodies. *Immunology*. 2017;152(4):580-588.
   https://www.ncbi.nlm.nih.gov/pubmed/28718500
4) Nandoskar A, **Raffel J**, Scalfari AS, Friede T, Nicholas RS. Pharmacological approaches to the management of secondary progressive multiple sclerosis. *Drugs*. 2017;77(8):885-910. Review.
   https://www.ncbi.nlm.nih.gov/pubmed/28429241
5) **Raffel J**, Sridharan S, Nicholas R. [11C]PBR28 PET in multiple sclerosis: neuroinflammation or otherwise? *Annals of Neurology.* 2017;81:323-324.
   https://www.ncbi.nlm.nih.gov/pubmed/28019656
6) **Raffel J**, Wakerley B, Nicholas R. Multiple sclerosis. *Medicine*. 2016; 44(9):537–541
   https://www.medicinejournal.co.uk/article/S1357-3039(16)30108-6/fulltext
7) Martin J*, **Raffel J***, Nicholas R. Progressive dwindling in multiple sclerosis: An opportunity to improve care. *PLOS One.* 2016;11(7):e0159210
   (*joint first authors)
   https://www.ncbi.nlm.nih.gov/pubmed/27441557
8) **Raffel J**, Gafson AR; Malik O; Nicholas R. Anti-JC virus antibody titres increase over time with natalizumab treatment. *Multiple Sclerosis Journal.* 2015;21(14):1833-8.
   https://www.ncbi.nlm.nih.gov/pubmed/26449743
9) Amor S, van der Star BJ, Bosca I, **Raffel J**, Gnanapavan S, Watchorn J, Kuhle J, Giovannoni G, Baker D, Malaspina A, Puentes F. Neurofilament light antibodies in serum reflect response to natalizumab treatment in multiple sclerosis. *Multiple Sclerosis Journal.* 2014;20(10):1355-62
   https://www.ncbi.nlm.nih.gov/pubmed/24515731
10) **Raffel J**, Dobson R, Gafson A, Mattoscio M, Muraro P, Giovannoni G. Multiple sclerosis therapy and Epstein-Barr virus antibody titres. *Mult Scler Relat Disord*. 2014;3:372-4
    https://www.ncbi.nlm.nih.gov/pubmed/25876475
11) **Raffel JB**, Malik O, Nicholas R. Assessing dalfampridine efficacy in the physician's office. *Multiple Sclerosis Journal*. 2014;20(1):24-6
    https://www.ncbi.nlm.nih.gov/pubmed/23727943

Appendix C

Permissions to reproduce, in this thesis, publications of the thesis author, and published figures from third party copyright works

Permissions to reproduce, in this thesis, publications of the thesis author

1) **Raffel J**, Gafson AR, Dahdaleh S, Malik O, Jones B, Nicholas R. Inflammatory activity on natalizumab predicts short-term but not long-term disability in multiple sclerosis. *PLOS One*. 2017;12(1):e0169546.

Text taken from publisher's website relating to permission to reproduce publications:

Copyright: *© 2017 Raffel et al. This is an open access article distributed under the terms of the Creative Commons Attribution License, which permits unrestricted use, distribution, and reproduction in any medium, provided the original author and source are credited.*

2) Feeney C, Scott G, **Raffel J**, Roberts S, Coello C, Jolly A, Searle G, Goldstone AP, Brooks DJ, Nicholas RS, Trigg W, Gunn RN, Sharp DJ. Kinetic analysis of the translocator protein positron emission tomography ligand [18F]GE-180 in the human brain. *Eur J Nucl Med Mol Imaging.* 2016;43(12):2201-2210.

Text taken from publisher's website relating to permission to reproduce publications:

This article is distributed under the terms of the Creative Commons Attribution 4.0 International License (http://creativecommons.org/licenses/by/4.0/), which permits unrestricted use, distribution, and reproduction in any medium, provided you give appropriate credit to the original author(s) and the source, provide a link to the Creative Commons license, and indicate if changes were made.

3) Sridharan S*, **Raffel J***, Nandoskar A, Record C, Brooks DJ, Owen D, Sharp D, Muraro PA, Gunn R, Nicholas R. Confirmation of specific binding of the 18-kDa Translocator Protein (TSPO) radioligand [18F]GE-180: a blocking study using XBD173 in multiple sclerosis normal appearing white and grey matter. *Mol Imaging Biol.* 2019;21(5):935-944

(*joint first authors)

Text taken from publisher's website relating to permission to reproduce publications:

© The Author(s) 2019 ***Open Access*** *This article is distributed under the terms of the Creative Commons Attribution 4.0 International License (http://creativecommons.org/licenses/by/4.0/), which permits unrestricted use, distribution, and reproduction in any medium, provided you give appropriate credit to the original author(s) and the source, provide a link to the Creative Commons license, and indicate if changes were made.*

4) **Raffel J**, Wallace A, Gveric D, Reynolds R, Friede T, Nicholas R. Patient-reported outcomes and survival in multiple sclerosis: A 10-year retrospective cohort study using the Multiple Sclerosis Impact Scale-29. *PLOS Medicine*. 2017;14(7):e1002346.

Text taken from publisher's website relating to permission to reproduce publications:

Copyright © 2017 Raffel et al This is an open access article distributed under the terms of the Creative Commons Attribution License, which permits unrestricted use, distribution, and reproduction in any medium, provided the original author and source are credited.

Permissions to reproduce, in this thesis, published figures from third party copyright works

Figure 1

Figure 1: The typical course of relapsing-remitting and secondary progressive multiple sclerosis. Adapted from Compston and Coles, 2008.20Adapted from:

Compston A, Coles A. Multiple sclerosis. Lancet. 2008;372(9648):1502-17. doi: 10.1016/S0140-6736(08)61620-7. PubMed PMID: 18970977.

Agreement between Dr. Joel Raffel ("You") and Elsevier ("Elsevier") consisting of license details and the terms and conditions provided by Elsevier and Copyright Clearance Center:

License Number: 4697770019375
License date: Oct 28, 2019
Licensed Content Publisher: Elsevier
Licensed Content Publication: The Lancet
Licensed Content Title: Multiple sclerosis
Licensed Content Author: Alastair Compston,Alasdair Coles
Licensed Content Date: 25–31 October 2008
Licensed Content Volume: 372
Licensed Content Issue: 9648
Licensed Content Pages: 16
Type of Use: reuse in a thesis/dissertation
Portion: figures/tables/illustrations
Number of figures/tables/illustrations: 1
Format: both print and electronic
Are you the author of this Elsevier article? No
Will you be translating? No
Original figure numbers: Figure 4
Title of your thesis/dissertation: Assessing Disease Activity in Multiple Sclerosis: Biomarkers and Clinical Measures
Expected completion date: Dec 2019
Estimated size (number of pages): 304

Figure 2

Figure 1: The typical course of relapsing-remitting and secondary progressive multiple sclerosis. Adapted from Compston and Coles, 2008.[20]Adapted from:

Hauser SL, Oksenberg JR. The neurobiology of multiple sclerosis: Genes, inflammation, and neurodegeneration. Neuron. 2006;52(1):61-76. doi: DOI 10.1016/j.neuron.2006.09.011. PubMed PMID: WOS:000241408100005.

Agreement between Dr. Joel Raffel ("You") and Elsevier ("Elsevier") consisting of license details and the terms and conditions provided by Elsevier and Copyright Clearance Center:

License Number: 4697760968608
License date: Oct 28, 2019
Licensed Content Publisher: Elsevier
Licensed Content Publication: Neuron
Licensed Content Title: The Neurobiology of Multiple Sclerosis: Genes, Inflammation, and Neurodegeneration
Licensed Content Author: Stephen L. Hauser,Jorge R. Oksenberg
Licensed Content Date: Oct 5, 2006
Licensed Content Volume:52
Licensed Content Issue: 1
Licensed Content Pages: 16
Type of Use: reuse in a thesis/dissertation
Portion: figures/tables/illustrations
Number of figures/tables/illustrations: 1
Format: both print and electronic
Are you the author of this Elsevier article? No
Will you be translating? No
Original figure numbers: Figure 2
Title of your thesis/dissertation: Assessing Disease Activity in Multiple Sclerosis: Biomarkers and Clinical Measures
Expected completion date: Dec 2019
Estimated size (number of pages): 304

Figure 17

Figure 1: The typical course of relapsing-remitting and secondary progressive multiple sclerosis. Adapted from Compston and Coles, 2008.[20]Adapted from:

Feeney C, Scott G, Raffel J, Roberts S, Coello C, Jolly A, Searle G, Goldstone AP, Brooks DJ, Nicholas RS, Trigg W, Gunn RN, Sharp DJ. Kinetic analysis of the translocator protein positron emission tomography ligand [(18)F]GE-180 in the human brain. Eur J Nucl Med Mol Imaging. 2016;43(12):2201-10. Epub 2016/06/29. doi: 10.1007/s00259-016-3444-z. PubMed PMID: 27349244.

Text taken from publisher's website relating to permission to reproduce figure:

This article is distributed under the terms of the Creative Commons Attribution 4.0 International License (http://creativecommons.org/licenses/by/4.0/), which permits unrestricted use, distribution, and reproduction in any medium, provided you give appropriate credit to the original author(s) and the source, provide a link to the Creative Commons license, and indicate if changes were made.

Figure 27

Figure 1: The typical course of relapsing-remitting and secondary progressive multiple sclerosis. Adapted from Compston and Coles, 2008.[20]Adapted from:

Cole JH, Leech R, Sharp DJ, Alzheimer's Disease Neuroimaging I. Prediction of brain age suggests accelerated atrophy after traumatic brain injury. Annals of neurology. 2015;77(4):571-81. Epub 2015/01/28. doi: 10.1002/ana.24367. PubMed PMID: 25623048.

Text taken from publisher's website relating to permission to reproduce figure:

© 2015 The Authors Annals of Neurology published by Wiley Periodicals, Inc. on behalf of American Neurological Association. This is an open access article under the terms of the Creative Commons Attribution-NonCommercial License, which permits use, distribution and reproduction in any medium, provided the original work is properly cited and is not used for commercial purposes.

Figure 28

Figure 1: The typical course of relapsing-remitting and secondary progressive multiple sclerosis. Adapted from Compston and Coles, 2008.[20]Adapted from:

Cole JH, Ritchie SJ, Bastin ME, Valdes Hernandez MC, Munoz Maniega S, Royle N, Corley J, Pattie A, Harris SE, Zhang Q, Wray NR, Redmond P, Marioni RE, Starr JM, Cox SR, Wardlaw JM, Sharp DJ, Deary IJ. Brain age predicts mortality. Mol Psychiatry. 2017. doi: 10.1038/mp.2017.62. PubMed PMID: 28439103.

Text taken from publisher's website relating to permission to reproduce figure:

This is an open access article distributed under the terms of the Creative Commons CC BY license, which permits unrestricted use, distribution, and reproduction in any medium, provided the original work is properly cited. You are not required to obtain permission to reuse this article.

Figure 29

Figure 1: The typical course of relapsing-remitting and secondary progressive multiple sclerosis. Adapted from Compston and Coles, 2008.[20]Adapted from:

Cole JH, Leech R, Sharp DJ, Alzheimer's Disease Neuroimaging I. Prediction of brain age suggests accelerated atrophy after traumatic brain injury. Annals of neurology. 2015;77(4):571-81. Epub 2015/01/28. doi: 10.1002/ana.24367. PubMed PMID: 25623048.

Text taken from publisher's website relating to permission to reproduce figure:

© 2015 The Authors Annals of Neurology published by Wiley Periodicals, Inc. on behalf of American Neurological Association. This is an open access article under the terms of the Creative Commons Attribution-NonCommercial License, which permits use, distribution and reproduction in any medium, provided the original work is properly cited and is not used for commercial purposes.

and

Cole JH, Ritchie SJ, Bastin ME, Valdes Hernandez MC, Munoz Maniega S, Royle N, Corley J, Pattie A, Harris SE, Zhang Q, Wray NR, Redmond P, Marioni RE, Starr JM, Cox SR,

Wardlaw JM, Sharp DJ, Deary IJ. Brain age predicts mortality. Mol Psychiatry. 2017. doi: 10.1038/mp.2017.62. PubMed PMID: 28439103.

Text taken from publisher's website relating to permission to reproduce figure:

This is an open access article distributed under the terms of the Creative Commons CC BY license, which permits unrestricted use, distribution, and reproduction in any medium, provided the original work is properly cited. You are not required to obtain permission to reuse this article.